COBALT-CLUSTER MEDIATED PROPARGYL CATION AND RADICAL REARRANGEMENTS

ALKYNE-COBALT-CLUSTERS:

SYNTHESES, STRUCTURES AND REARRANGEMENTS OF METAL-STABILIZED PROPARGYL CATIONS AND RADICALS

By

JOHN H. KALDIS, B.Sc.

A Thesis

Submitted to the School of Graduate Studies

In Partial Fulfillment of the Requirements

for the Degree

Doctor of Philosophy

McMaster University

DOCTOR OF PHILOSOPHY (2003) McMaster University

(Chemistry) Hamilton, Ontario

TITLE: Alkyne-Cobalt-Clusters: Syntheses, Structures and Rearrangements of Metal-Stabilized Propargyl Cations and Radicals

AUTHOR: John H. Kaldis, B.Sc. (University of Western Ontario)

SUPERVISOR: Dr. Michael J. McGlinchey

NUMBER OF PAGES: xv, 192

Abstract

Cobalt-clusters are versatile reagents in organometallic chemistry. Their ability to protect an alkyne allows one to selectively manipulate a ligand without undergoing a competitive reaction from the alkyne. Cobalt-clusters geometrically modify linear alkynes to 136-145° degrees, thereby allowing for some non-traditional alkynyl chemistry to occur. In particular, the focus of this dissertation lies upon the chemistry of cobalt-complexed propargyl alkynols, the ability of cobalt to stabilize neighbouring cations generated from these alcohols, and the chemistry that can be accomplished by altering the steric and electronic effects. We have chosen to study the possibility of inducing migration of various substituents from one terminus of the cobalt-complexed alkyne to the alcoholic site of the propargyl group via protonation of the desired complex. While examining various silanes, and altering the propargyl alcohol itself, we have considered both steric and electronic effects, thereby determining the idealized conditions for such transfers to occur. Furthermore, in our attempts to successfully apply these migrations to several systems, we have acquired a diverse synthetic knowledge of propargyl cobalt-clusters and their intricate reactivity.

An examination of the potential for allyl migrations in norbornyl derivatives revealed several fascinating transformations. Upon protonation with HBF_4, [(2-*endo*-allyldimethylsilyl)ethynylborneol]$Co_2(CO)_6$, **63**, suffers elimination of water or propene, to yield [(2-allyldimethylsilyl)ethynylborn-2-ene]$Co_2(CO)_6$, **68**, [(2-*endo*-dimethylfluorosilyl)ethynylborneol]$Co_2(CO)_6$, **69**, respectively, and, surprisingly, the tricobalt complex (2-norbornylidene)$CHCCo_3(CO)_9$, **70**. In contrast, protonation of the

terminal alkyne (2-*endo*-ethynylborneol)$Co_2(CO)_6$, **76**, an anticipated precursor to **70**, led instead to (2-ethynyl-2-bornene)$Co_2(CO)_6$, **78**, and the ring-opened species (2-ethynyl-4-isopropyl-1-methylcyclohexa-1,3-diene)$Co_2(CO)_6$, **79**. However, conversion of **76** to **70** was achievable upon prolonged heating at reflux in acetone, thereby also affording the corresponding alcohol, [2-(2-hydroxybornyl)]$CH_2CCo_3(CO)_9$, **77**. A mechanistic rationale is offered for the formation of $RCH_2CCo_3(CO)_9$ clusters upon protonation of alkyne complexes of the type $(RC{\equiv}CH)Co_2(CO)_6$.

Our interest in acid-promoted rearrangements in cobalt-clusters led us to novel propargyl radical chemistry induced by using particular solvents. The protonation of (1,1-diphenyl-2-propyn-1-ol)$Co_2(CO)_6$, **108**, with HBF_4 in dichloromethane generates the expected metal-stabilized propargyl cation, and also rearranges to give the tricobalt cluster $Ph_2C{=}CH\text{-}CCo_3(CO)_9$, **33**. In contrast, use of THF as solvent affords the radical $(Co_2(CO)_6)[HC{\equiv}C\text{-}CPh_2{\cdot}]$, which dimerizes at the methyne position; subsequent cyclization and carbonylation yields 2,5-bis-(diphenylmethylene)cyclopent-3-en-1-one, **112**.

Furthermore, use of a fluorenyl substituent, instead of the diphenyl analogue, has uncovered a route to transition-metal peroxides of general synthetic potential. Treatment of benzyl- or vinyl-dimethylsilylethynylfluoren-9-ol[$Co_2(CO)_6$], **53** and **54**, respectively, with HBF_4 in diethyl ether or THF has afforded the very first known bimetallic transition metal peroxides, **124** and **125**.

Finally, the ability of cobalt-clusters to alter the geometry of cycloalkanes has been investigated. Treatment of 1-[axial]-(trimethylsilylethynyl)cyclohexan-1-ol, **129**, with dicobalt octacarbonyl results in a conformational ring flip such that the bulky

dicobalt-alkyne cluster moiety now occupies the favored equatorial site. However, when a 4-tert-butyl substituent is present, the coordinated alkynyl group retains its original axial or equatorial position.

Complexation of *trans*-[diaxial]-1,4-bis(triphenylsilylethynyl)cyclohexan-1,4-diol, **142**, brings about a chair-to-chair conformational inversion such that both cluster fragments now occupy equatorial sites. In contrast, *cis*-1,4-bis-(triphenylsilylethynyl)cyclohexan-1,4-diol, **143**, reacts with $Co_2(CO)_8$ to yield the twist-boat conformer, **145**, in which the two axial hydroxy substituents exhibit intra-molecular hydrogen bonding. Likewise, the corresponding reaction of *cis*-1,4-bis(trimethylsilylethynyl)cyclohexan-1,4-diol, **147**, with $Co_2(CO)_8$ leads to a twist-boat, **149**, but, in this case, the molecules are linked through intermolecular hydrogen bonds. The importance of X-ray crystallography in the unambiguous determination of molecular conformations has been emphasized.

Acknowledgements

My sincere gratitude is extended to my supervisor Dr. Michael J. McGlinchey. MJM I am greatly indebted to you for selfless time commitments to our vast chemistry and non-chemistry (soccer) discussions. Thank you for instilling a great deal of knowledge in me, and allowing me to grow as a scientist. Your true passion for chemistry has made it both easy and enjoyable to work with you over the last several years. Although I may never attain the chemical knowledge you possess, I am almost certain that I would stop your penalty kick in the World Cup final.

Dr. Michael A. Brook and Dr. Alex D. Bain, my committee members, I wish to thank you for your insight, guidance, and suggestions during my thesis work. You both have been very patient and understanding with regards to committee meetings and meeting thesis deadlines.

Dr. Jim F. Britten, whom I have easily taken up a year of his life with countless crystallography problems and questions. Thank you for all the late nights spent on my disordered molecules, and more importantly, for becoming a tremendous friend in the process. It has indeed been a pleasure learning from and working with you.

Thank you to Dr. Don Hughes, Brian Sayer, Dr. Kirk Green, Mike Malott, George Timmins, and Tadek Olech for their time and assistance on numerous occasions.

To all the ladies I've encountered in the chemistry office, and who have always gone out of their way to help: Carol Dada, Josie Petrie, Barbara DeJean, Tammy Fehr, Marilyn McIntyre, Nancy Kolenski, the little things you ladies have done are immeasurable.

I have been fortunate to be surrounded by some incredible people in the MJM lab, from the moment of my arrival to the day of my departure, these people have truly been a pleasure to work with: Ralph Ruffolo, Jamie Dunn, Mark Stradiotto, Hari Gupta, Pippa Lock, Nada Reginato, Laura Harrington, Nicole Deschamps, Sonya Balduzzi, Yannick Ortin, Frank Ogini, and Stacey Brydges.

There are many people who have been part of my pleasant experience at McMaster, far too many to mention here. I wish to especially thank Bernie Pointner and Tom Bajorek, who have definitely contributed to many good experiences at McMaster, and have never been ones to deter from *discussing chemistry* over a pint.

Since athletics, have been a large part of my McMaster experience, I must thank all past and present members of the morning basketball crew, the weekend road hockey gang, *200 Toes of Fury*, and to *the Anal. Chems*; I will never forget our run to the Phoenix Cup in the summer of 2001.

Finally, thank you to my parents, Bob and Noula, for giving me the opportunity that they never had, and allowing me to pursue all my goals, while never doubting me; and to my brother, Angelo, for listening to all my stories, and sharing in our joy of science. You all have always been there for me, and your love and support has kept life in perspective; words cannot do justice to how I feel about you.

Table of Contents

Chapter Two: Cobalt-Mediated Migrations

Chapter Three: Tricobalt Clusters

List of Figures

List of Tables

Chapter One: Introduction

1.1 Organometallics

1.1.1 General

Organometallic chemistry is generally defined as the discipline dealing with compounds that contain a direct bond between a metal atom and one or more carbon atoms.[1] This includes covalently bonded systems, such as tetraethyl lead, $Pb(C_2H_5)_4$, ionic systems typified by sodium cyclopentadienide, $Na^+C_5H_5^-$, and π-dative complexes such as ferrocene, $Fe(C_5H_5)_2$. There are however, numerous exceptions to this definition, as cyanides and carbides, e.g. $K_3Fe(CN)_6$ and Cr_3C_2, respectively, are not considered organometallic species. Many chemists also regard complexes consisting of an organic group attached through a carbon to an atom that is less electronegative than carbon to be organometallic. This would include the metalloids of the Periodic Table, such as boron, silicon and arsenic, yet would exclude the lighter halogens and chalcogens. Therefore, many silicon complexes and boron species, such as carboranes, are technically considered organometallics, but for the purpose of this thesis, the focus will primarily involve the initial definition provided above.

1.1.2 History

It is arguable that L.C. Cadet, a French chemist, synthesized the first known documented organometallic compound in 1760.[2] While attempting to prepare invisible

ink, he accidentally generated dicacodyl, a vile odoured liquid, using cobalt minerals containing arsine salts, as shown in Equation 1.1.

$$As_2O_3 + CH_3COOK \rightarrow [(CH_3)_2As]_2O + \text{other products} \qquad \textbf{Equation 1.1}$$

However it was not until 1848 when R.W. Bunsen, renowned for his invention of the Bunsen burner, identified and characterized dicacodyl, in the course of his investigations of alkarsines of the type $R_2As\text{-}AsR_2$.[3] Although Cadet and Bunsen prepared the first organometallic complexes, it is widely acknowledged that the true pioneer of the field of organometallic chemistry is Edward Frankland, one of Bunsen's protégés, who also detected the presence of helium in the atmosphere of the sun. While attempting to form ethyl radicals by treating organohalides with zinc metal, Frankland prepared the first organo-zinc compound, diethylzinc, as in Equation 1.2, and later synthesized the first alkyl-mercury by treating sodium amalgam with a methyl halide as shown in Equation 1.3.[4] These findings subsequently led to similar compounds, initially formulated as SnC_2H_5 and $CoCrCH_3$, which served as important reagents for organic chemistry prior to the discovery of Grignard reagents in 1899.[4]

$$ZnI_2 + 2Et^{\bullet} \not\longleftarrow 2EtI + 2Zn \longrightarrow ZnEt_2 + ZnI_2 \qquad \textbf{Equation 1.2}$$

$$2CH_3X + 2Na + Hg \longrightarrow Hg(CH_3)_2 + NaX \qquad \textbf{Equation 1.3}$$

The first reported organometallic complex that contained a transition metal was prepared by W.C. Zeise in 1827.[5] He prepared $K[PtCl_3(C_2H_4)]\cdot H_2O$, now known to be a square planar complex, by refluxing platinum tetrachloride with aqueous ethanol, and subsequently treating the solution with HCl and KCl, as shown in Scheme 1.1.[5]

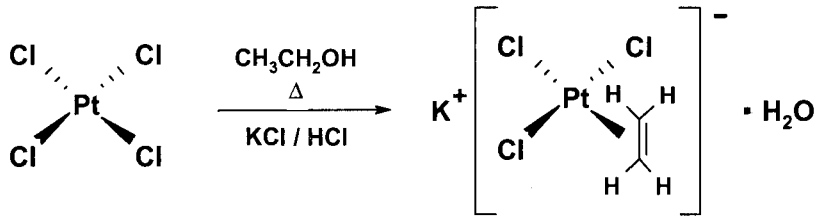

Scheme 1.1: The preparation of Zeise's salt.

One might have thought that this groundbreaking revelation by Zeise would have led to a plethora of organometallic chemistry. However, it was not until the end of the nineteenth century that Ludwig Mond prepared the first metal carbonyls, $Ni(CO)_4$ and $Fe(CO)_5$;[6] numerous subsequent advances in the field, such as bis(arene)chromium sandwich complexes[7] and the biggest breakthrough of all, namely ferrocene, recognized independently by Sir Geoffrey Wilkinson and by Ernst O. Fischer,[8] have been discussed in a series of historical vignettes in the American Chemical Society journal *Organometallics*.[7c,9]

In 1927 N.V. Sidgwick first proposed a numerical method for calculating potentially stable organo-transition metal compounds.[10] This was the Effective Atomic Number (EAN) rule, by which he extended the octet theory of G.N. Lewis,[11] and used it to rationalize coordination compounds. The EAN, or 18-Electron Rule, states that a stable complex, with the electronic configuration of the next highest noble gas, is obtained when the sum of the transition metal *d*-electrons, electrons donated from the ligand, and the overall charge of the complex equals 18.

1.1.3 Metal Carbonyl Complexes

The widespread occurrence of carbon monoxide as a ligand prompts a brief discussion of the bonding model used to explain how a relatively non-basic ligand interacts with a metal in a low oxidation state. As depicted in Figure 1.1, the highest occupied molecular orbital (HOMO) in CO is weakly antibonding and is comprised of a lone pair of electrons heavily localized on carbon. These electrons can be donated to a vacant metal orbital and, as a result, strengthen the carbon-oxygen bond. Concomitantly, the electron-rich metal compensates by donating electron density from a filled *d*-orbital of appropriate symmetry into the vacant π*-orbital of carbon monoxide. This dative π-back-bonding markedly weakens the carbon-oxygen bond and is conveniently monitored by infrared spectroscopy. Carbon monoxide is considered to possess a triple bond and exhibits a ν_{CO} stretch at 2143 cm^{-1}.[12] In $Cr(CO)_6$ this value decreases to 2000 cm^{-1}, but the effect of charge on the metal is clearly demonstrated by the observation that a very electron-rich metal is capable of a high degree of π-back-donation; typically the 18-electron metal anion $V(CO)_6^-$ has a ν_{CO} stretch at 1860 cm^{-1}.[12] In contrast, the isoelectronic cationic system $Mn(CO)_6^+$ absorbs at 2090 cm^{-1}.[12] Moreover, carbonyl infrared spectra can provide a subtle probe for the presence of metal-stabilized carbocationic ligands.

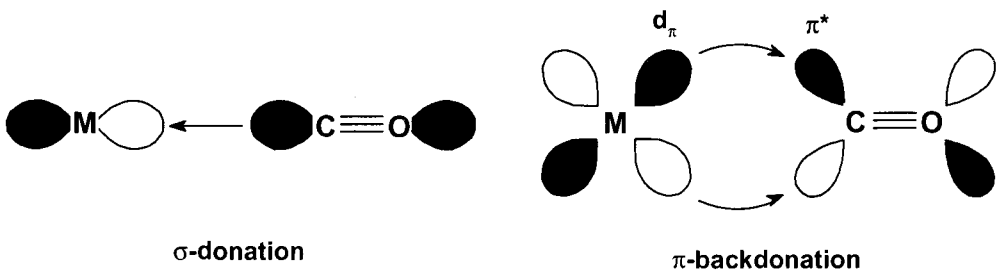

Figure 1.1 Synergic bonding in metal carbonyls.

1.2 Cobalt

Since much of this thesis deals with the organometallic chemistry of cobalt, a brief outline of the physical and chemical properties of this important element is presented hereafter. Cobalt is the 27th element of the Periodic Table, found in Group 9 and Period 4. It is a d-block transition metal with the electronic configuration of [Ar]$4s^2 3d^7$, a coordination number of 6, and common oxidation states of +2 and +3. Cobalt-59, the only naturally occurring isotope of cobalt, is paramagnetic, with spin quantum number I = 7/2, and has melting and boiling points of 1493 °C and 3100 °C, respectively.[13]

The name cobalt is derived from *kobald*, the German word for goblin or evil spirit, and *cobalos*, the Greek word for mine. It is a hard, bluish-white metal, resembling iron and nickel in appearance, and may be traced as far back as 1300 B.C. to early civilizations of Egypt and Mesopotamia, where certain cobalt-containing minerals were valued for their ability to provide deep blue colouration in glass.[14] The first documented discovery of cobalt was in 1739 by a Swedish chemist, Georg Brandt, who was attempting to prove that this colouration in glass was due to an unknown element, and not (as was commonly believed at the time) bismuth, an element often found in the same locations as cobalt. However, it was only about 1780, when Bergman and coworkers examined the properties of cobalt, that its elemental character was established.[14]

Although cobalt is not an extremely abundant element, it has a diverse area of occurrence, including rocks, seawater, coal, meteorites, soil, plants and animals. Cobalt generally occurs in compounds with arsenic, oxygen and sulfur, and its primary ores are cobaltite (CoAsS), erythrite ($Co_3(AsO_4)_2$), and smaltite ($CoAs_2$). The principal ore

deposits are found in Zaire, Morocco, and Canada, where it is usually recovered as a by-product from mining and refinement of nickel, silver, lead, copper and iron.[13] Isolation usually is initiated by treatment with sulphuric acid, which leaves metallic copper as a residue and dissolves out iron, cobalt, and nickel as the sulphates.[20] Iron is obtained by precipitation with lime (CaO) while cobalt is produced as the hydroxide by precipitation with sodium hypochlorite (Equation 1.4).[13] The trihydroxide, $Co(OH)_3$, is heated to form the oxide and reduced with either charcoal (Equation 1.5), aluminum (the Goldschmidt process)[15], or hydrogen to form pure cobalt metal.

$$2Co^{2+}(aq) + NaOCl(aq) + 4OH^-(aq) + H_2O \rightarrow 2Co(OH)_3(s) + NaCl(aq) \quad \textbf{Equation 1.4}$$

$$2Co(OH)_3\ (\Delta) \rightarrow Co_2O_3 + 3H_2O$$

$$2Co_2O_3 + 3C \rightarrow Co + 3CO_2 \quad \textbf{Equation 1.5}$$

Cobalt is used in electroplating to provide an attractive surface that is oxidatively resistant, yet is more commercially applicable in the form of alloys. Alnico, an alloy comprised of aluminum, nickel and cobalt is used to make powerful permanent magnets, while Stellite alloys, containing cobalt, chromium and tungsten, are used to make high-speed, high temperature cutting tools and dyes.[13] Cobalt is also used to make alloys for jet engines and gas turbines, magnetic steels and some types of stainless steels. It is also important to human nutrition as it is an essential part of vitamin B_{12}.

Although cobalt-59 is the only naturally occurring form of cobalt, there are ten known isotopes of cobalt, including radioactive cobalt-60, which is by far the most extensively investigated artificially produced isotope of cobalt. It is an important source of gamma radiation, and is used considerably as a medical tracer, and a radiotherapeutic

agent to treat some forms of cancer. This radioisotope, which has gamma ray emissions 25 times greater than that of radium, is prepared by neutron bombardment, and is also invaluable industrially for detecting flaws in metal parts.[16] Interestingly, Leo Szilard, an American nuclear physicist, identified cobalt-60 as a potential 'doomsday device' that was capable of eradicating life on earth. It was theorized that a dirty radioactive cobalt bomb, similar to a hydrogen bomb, upon impact could transmute cobalt into cobalt-60, which with its half-life of 5.26 years would survive long enough to allow airborne particles to settle to the earth, thereby making it impractical to hide in shelters from the fallout.[17]

1.3 Cobalt Carbonyls: Structures and Reactivity

1.3.1 Octacarbonyldicobalt

Octacarbonyldicobalt is an orange-red, air- and temperature-sensitive, crystalline solid, that is of great importance as a precursor for the formation of tetranuclear dicobalt complexes upon treatment with alkynes. It will decompose to the purple cobalt(II) oxide or carbonate with prolonged exposure to air; thermal degradation at temperatures of 50 °C or above, thereby initially affording dodecarbonyltetracobalt, and ultimately cobalt metal. One of the most common early preparations of octacarbonyldicobalt involved the reaction of carbon monoxide and hydrogen gases with cobalt(II) acetate in acetic acid (Equation 1.6).[18] At present, it is readily prepared commercially by combining cobalt metal and carbon monoxide gas under regulated thermal and barometric conditions (Equation 1.7).

$$2Co(OCOCH_3)_2 + 8CO(g) + 2H_2(g) \xrightarrow{CH_3COOH} Co_2(CO)_8 + 4CH_3COOH \quad \textbf{Equation 1.6}$$

$$2Co(s) + 8CO(g) \xrightarrow[30\text{-}40\ atm]{150°C} Co_2(CO)_8 \quad \textbf{Equation 1.7}$$

The solid-state analysis of octacarbonyldicobalt revealed a C_{2v} symmetric structure with square pyramidal geometry at the metal, comprised of three terminal and two bridging carbonyl ligands, **1a**.[19] From solution infrared spectroscopy, Noack and Bohr[20] identified a second, non-bridged isomeric species, **1b**, with D_{3d} symmetry, as shown in Figure 1.2. Interestingly, Noack used infrared spectroscopy to investigate the doubly bridged form **1a**, and its unbridged counterpart **1b** in pentane solution, and found that the unbridged species was slightly more prevalent at room temperature, while at lower temperatures the bridged isomer was significantly more abundant.[20] The existence of a third isomer, **1c**, of D_{2d} symmetry, was later revealed by both infrared[21] and Raman[22] spectroscopy. Recently, Aullón has demonstrated the sequential transformation in solution from **1a**→**1c** and **1c**→**1b**, and devised a mechanistic interpretation, noting from DFT calculations,[23] that **1c** is the slightly more energetically favoured isomer. Incidentally, these structural assignments have also permitted a comparison with the structures of the remaining group 9 metal carbonyls without the aid of crystallographic evidence, as infrared data for $Rh_2(CO)_8$ are indicative of the bridged form,[24] while $Ir_2(CO)_8$ exists as the all-terminal isomer.[25]

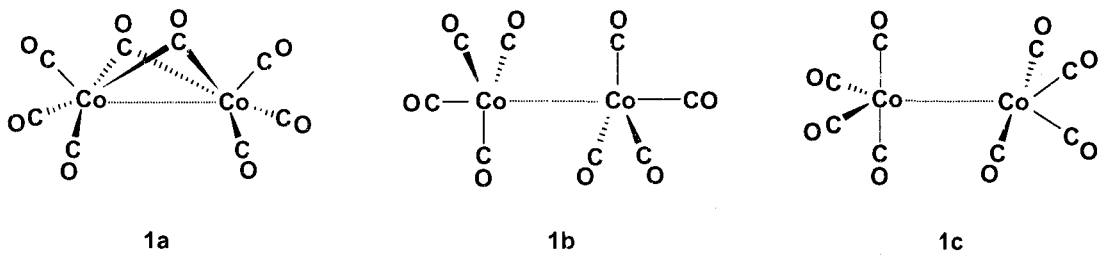

Figure 1.2 The three known isomers of octacarbonyldicobalt.

Octacarbonyldicobalt will react readily with an alkyne in most organic solvents, displacing two bridged carbonyl ligands, and affording a tetranuclear cluster of general formula (RCCR′)[$Co_2(CO)_6$], as shown in Equation 1.8.[26]

$$RC{\equiv}CR' + Co_2(CO)_6 \rightarrow (RCCR')[Co_2(CO)_6] + 2CO(g) \quad \textbf{Equation 1.8}$$

The acetylene and propynyl cobalt-alkyne derivatives were originally prepared in 1954,[27] however, structural evidence for a cobalt complexed alkyne was not available until 1959, in the form of the diphenylacetylene analogue, (PhC≡CPh)[$Co_2(CO)_6$].[28] The hexa-coordinate nature of each cobalt atom with distorted octahedral geometry was clearly illustrated, while the alkyne carbons were situated above and perpendicular to the cobalt atoms with an approximate tetrahedral geometry. Typical alkynyl carbon-carbon and carbon-cobalt bond lengths in such systems are 1.34 Å and 1.98 Å, respectively.

1.3.2 Reactions of Cobalt-Alkyne Complexes

Since their discovery, many novel cobalt-alkyne complexes have been prepared,[29] and now serve several important roles in organometallic chemistry, the most common of which is as a protecting group for the alkyne.[30] By protecting this functionality, one may control the chemistry of the organic molecule of interest by preventing a competitive reaction involving the alkyne itself, thus allowing one to selectively manipulate other groups within the ligand. This may even be a direct result of the modification of the R-C≡C-R′ linkage. The alkyne, normally a linear substituent in unconstrained organic systems, will bend such that each R-C≡C angle falls in the range of 136-145° when complexed to form the metal cluster. As will become apparent subsequently, this

deviation from linearity can facilitate numerous reactions, and even introduce additional ones which otherwise would not occur.

The substituents of the coordinated alkyne can be modified while retaining the cobalt-alkyne bond. An effective illustration of this is presented in Scheme 1.2, where oct-1-en-4-yne, **2**, is treated with dicobalt octacarbonyl to protect the alkyne; subsequent addition of BH_3 in the presence of oxygen, and final removal of the cobalt moiety, affords the functionalized alkyne, oct-4-yn-1-ol, **3**.[30a]

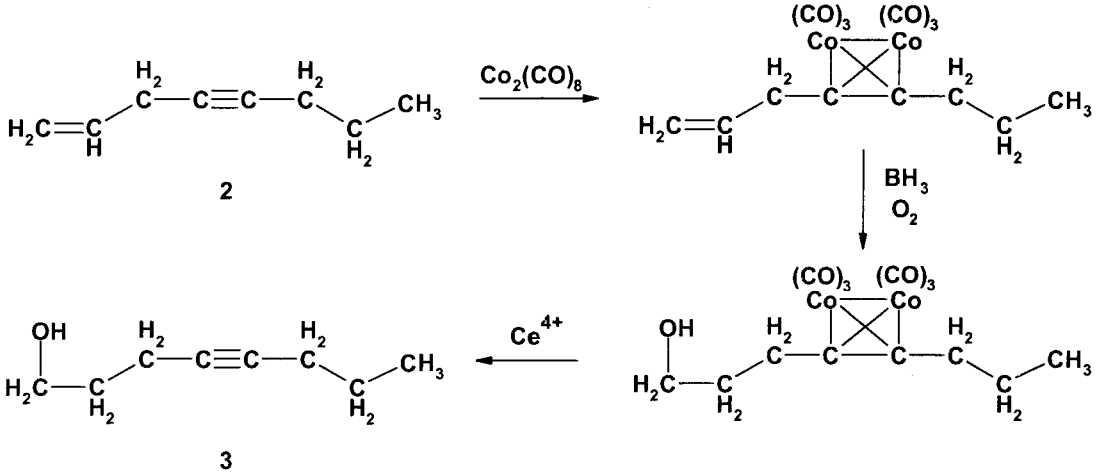

Scheme 1.2 Functionalization of a hexacarbonyldicobalt protected octyne.

Electrophilic substitution reactions on complexed π-bonded organic ligands are also conveniently achievable. For example, a Friedel-Crafts acylation, which is not normally viable for the free ligand, may be accomplished on diphenylacetylene, **4**, when complexed to dicobalt hexacarbonyl, as shown in Scheme 1.3.[31] Interestingly, the complexed diphenylacetylene species has also been used as a catalyst for the polymerization of vinyl chloride.

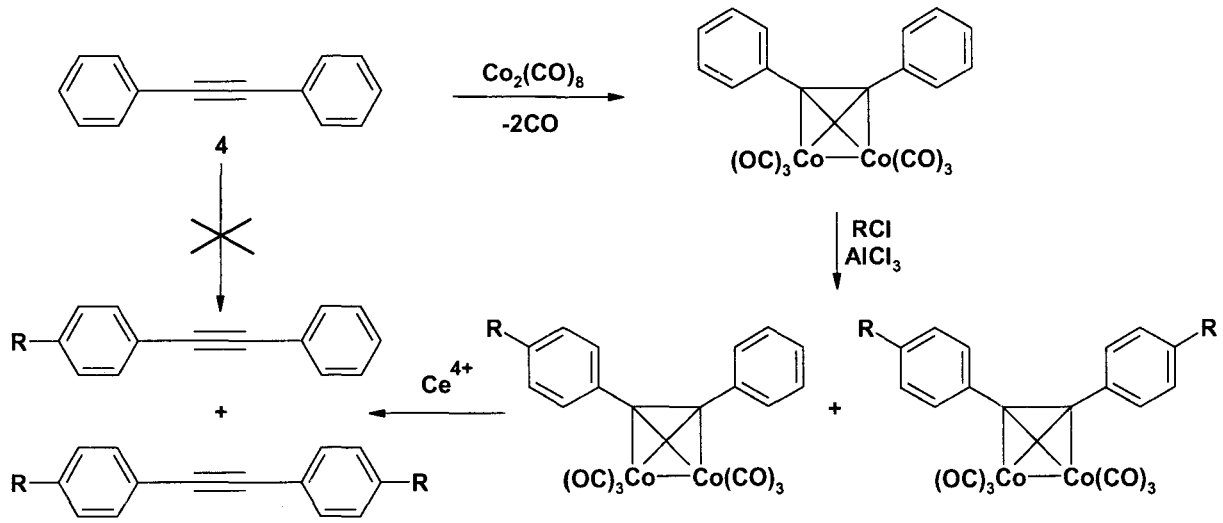

Scheme 1.3 Friedel Crafts acylation of dicobalt-complexed diphenylacetylene.

At ambient temperatures, alkyne-hexacarbonyldicobalt clusters will readily undergo exchange reactions with more electronegatively-substituted alkynes, as shown in Equation 1.9.[32]

$$RC{\equiv}CR[Co_2(CO)_6] + R'C{\equiv}CR' \rightleftharpoons R'C{\equiv}CR'[Co_2(CO)_6] + RC{\equiv}CR \quad \textbf{Equation 1.9}$$

The increase in stability of these clusters is directly proportional to the increase in π-back-donation from the cobalt filled *d*-orbitals to the π* orbitals of the alkyne derivative, thereby strengthening the alkyne-cobalt bond. A hierarchy of substituents effecting ligand displacement has been established:[30a]

$$(CF_3)_2 > (CO_2Me)_2 > Ph_2 > Me, Ph > Me_2 > H, Ph = H, Me > H_2 > (CH_2NEt_2)_2$$

Other reactions involving cobalt-alkynes include the rearrangement of alkyne-dicobalt hexacarbonyl complexes to alkylidyne-nonacarbonyltricobalt species in the presence of an acidic medium; this rearrangement will be discussed further in Chapter 3.

Finally, the chemistry of (propargylic alcohol)$Co_2(CO)_6$ complexes, which is a major component of this thesis, will be addressed in considerable detail later in this chapter.

1.4 The Isolobal Analogy

Isolobality is a term used to describe two molecular fragments whose frontier orbitals are similar in number, symmetry properties, approximate energy and extent in space, and number of electrons.[33] This relationship, represented pictorially as a double-headed arrow above half an orbital, ⟷, may be used to rationalize the replacement of one substituent by a molecular fragment that can be chemically quite different. As such, the isolobal analogy provides an important connection between organic and organometallic chemistry. This is exemplified by the notional transformation of an organic tetrahedrane into a tetrahedral organometallic cluster through progressive substitution of three (CR) vertices by $[Co(CO)_3]$ fragments, as shown in Figure 1.3.

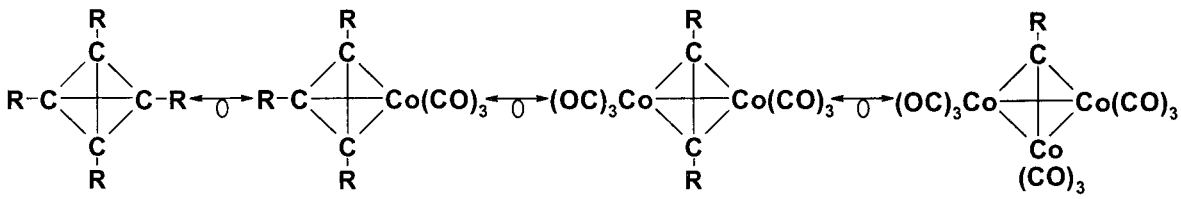

Figure 1.3 Progressive isolobal substitution of CR vertices with $[Co(CO)_3]$ fragments.

This concept may be further applied to numerous organic, inorganic and organometallic fragments, including established isolobal correlations such as: BH ⟷ $Fe(CO)_3$, CH ⟷ $(C_5H_5)Mo(CO)_2$, CH_2 ⟷ $Fe(CO)_4$, and CH_3 ⟷ $Mn(CO)_5$. However, this relationship does not guarantee that substitution of any isolobal fragments will always generate a kinetically stable molecule. This may be clearly demonstrated

upon substituting the two CH_2 fragments in ethylene with two isolobal $Fe(CO)_4$ fragments to form the coordinatively unsaturated $Fe_2(CO)_8$, **5**, which is not a stable entity and instead is found as nonacarbonyldiiron, **6**, which is more akin to cyclopropanone (see Figure 1.4).[33]

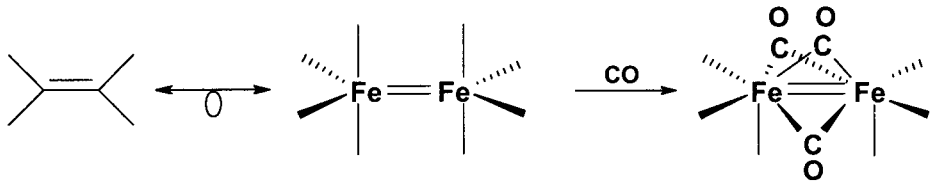

5 **6**

Figure 1.4 Isolobal replacement of ethylene by iron carbonyl fragments.

1.5 Carbocation Stabilization

1.5.1 General

Carbocations are species bearing a formal positive charge on a carbon atom. The cationic carbon is sp^2 hybridized with trigonal planar geometry, and can be visualized as possessing an empty *p* orbital perpendicular to the plane containing the three substituents, as illustrated in Figure 1.5 for the methyl cation, **7**.[34] Carbocations may be considered hypovalent species, such that there are only three shared pairs of electrons around carbon, instead of the usual four. As a result, carbocations are normally very unstable and highly reactive species, unless generated in a superacid medium such that the counter-ion is exceedingly non-nucleophilic. This latter area has been eloquently reviewed by Olah subsequent to his award of the Nobel Prize in 1994.[35] As such, carbocations are acknowledged as short-lived intermediates in an enormous number of organic reactions, including nucleophilic substitutions, addition to alkanes, aromatic substitutions, polymerizations, and reactions of carbonyl compounds, carboxylic acids and other

derivatives. Fundamentally, there are two types of carbocations: classical (trivalent) and non-classical (penta-coordinate or greater). Classical carbocations (*carbenium* ions) are of the general type $[CRR'R'']^+$, where the substituents can be hydrogen, alkyl, aryl, halogen, alkoxy, etc., as depicted for the methyl cation in Figure 1.5. In contrast, non-classical cations (*carbonium* ions) are exemplified by the CH_5^+ ion, which is commonly encountered in mass spectrometry. The 2-norbornyl cation, **8**, also shown in Figure 1.5, was the focal point of one of the fiercest debates ever in organic chemistry, which has since been resolved, garnering it recognition as the first non-classical carbocation.[36]

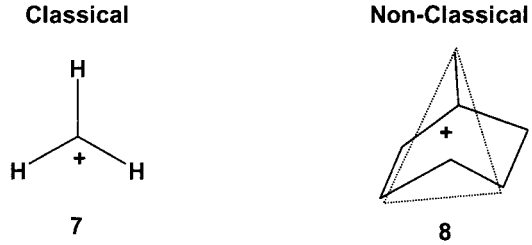

Figure 1.5 The classical methyl, **7**, and non-classical 2-norbornyl, **8**, cations.

Since then, several other cations have been classified as non-classical, including the 7-norbornenyl, **9**, and 7-norbornadienyl, **10**, cations,[37] whereby the overlap between the vacant *p*-orbital at the C(7) position and the filled π-orbital of the alkene alleviates the electron deficiency at C(7) and leads to charge delocalization (Figure 1.6).

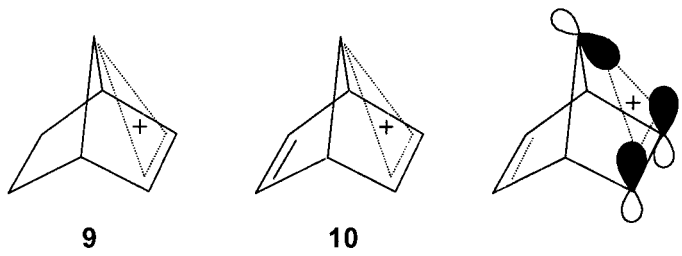

Figure 1.6 The 7-norbornenyl, **9**, and 7-norbornadienyl, **10**, cations.

Traditionally, carbocations have been generated by two common methods:[38]

1) Heterolytic cleavage with loss of a molecular entity capable of accepting a negative charge, such as a halide, via an S_N1 or ionization process (Equation 1.10)
2) Addition of a positively charged species (electrophile) to a neutral, unsaturated molecule (Equation 1.11)

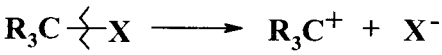

Equation 1.10

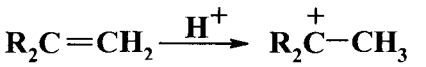

Equation 1.11

However, another method, which is an extension of Equation 1.10, and is of greater relevance to the work discussed herein, involves the reversible addition of an acid to an alcohol functionality, with subsequent heterolysis and loss of water. (Equation 1.12).

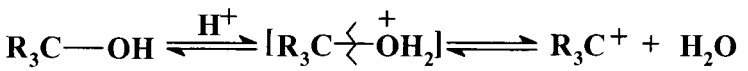

Equation 1.12

Since carbocations are Lewis acids, and therefore very electrophilic; extending their lifetime is of tremendous interest in organic chemistry in order to observe the potential reactivity of these species, and to increase the possibility of novel reactions and rearrangements. The two primary methods of prolonging the existence of carbocations involve the introduction of electronic and/or steric effects through neighbouring ligands.

1.5.2 Electronic Effects

The lifetimes of carbocations vary with structure, and generally become more stable as their degree of substitution increases, in the order of H_3C^+ (methyl) < RH_2C^+

(primary) < R_2HC^+ (secondary) < R_3C^+ (tertiary). In particular, the lifetime of these species will increase with the ability of the substituents attached to the positively charged carbon to provide electron density to the electron-deficient centre. An effective illustration of this involves comparison of the methyl and ethyl cations in Figure 1.7. In the methyl cation, all three hydrogen atoms are situated so that the hydrogen *s*-orbitals used in bonding to the central carbon are unable to overlap with the vacant p-orbital of the sp^2 hybridized carbon. In contrast, the ethyl cation can adopt three orientations such that one of the adjacent C-H bonds may align with the empty *p*-orbital of the cationic center, thereby providing a means for transfer of electron density, and an increase in stability by 36 kcal/mol.[39]

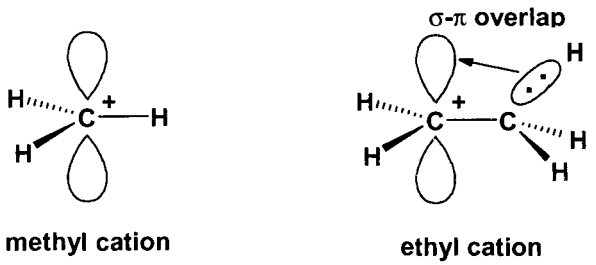

Figure 1.7 Comparison of the methyl and ethyl cations.

This trend arises from extended orbital overlap, and more specifically, from overlap involving a vacant *p*-type orbital of the cation with a filled σ-bond orbital one atom removed from the cation. This phenomenon is referred to as hyperconjugation, and may be extended to include carbocations bearing alkyl groups in place of any or all of the hydrogens. Hyperconjugation requires an idealized geometry for non-orthogonal orbital overlap between the substituent and the adjacent carbocationic centre, whereby non-bonding, lone pair electrons are contributed more readily than π-bonded pairs, which are in turn more readily shared than sigma-bonded pairs.

Cation stabilization is not limited to simple alkyl groups, as other atoms can be involved in an even more efficient manner. This may be exemplified by the hydrolysis of 2,2'-dichlorodiethyl sulfide, **11**, the notorious Mustard Gas discharged in World War I, shown in Scheme 1.4. Species with a full positive charge localized on a primary carbon would be extremely unfavorable intermediates in chemical reactions; however, the introduction of an electron-rich functionality, such as a sulfur atom, can provide anchimeric assistance by alleviating some of the developing positive charge on an adjacent primary carbon atom through electron donation from a lone pair with concomitant charge delocalization onto the sulfur atom. [40]

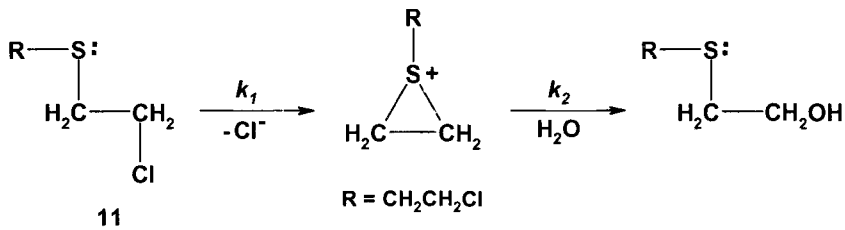

Scheme 1.4 The Hydrolysis of Mustard Gas.

The stability of a carbocation may also be influenced by the availability of resonance interactions. Groups that have a conjugated π system will aid in alleviating the positive charge through delocalization, and therefore substantially increase the stability of the cation. This may perhaps be best exemplified through the classical triphenylmethyl cation, whereby numerous canonical structures, some of which are shown in Figure 1.8 may be drawn to demonstrate the delocalization of the cation throughout the π system of all three phenyl rings. It is worth noting that charge delocalization can occur not only through π-bonds but may also be effected by lone pairs on adjacent heteroatoms.

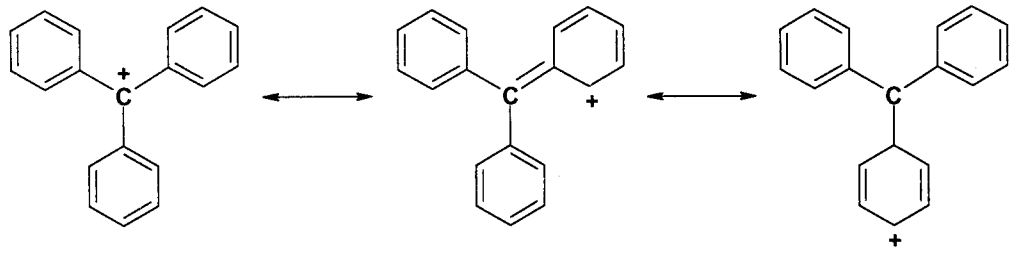

Figure 1.8 Resonance contributors of the triphenylmethyl cation.

1.5.3 Steric Effects

Steric protection from attack by a nucleophile is nicely illustrated by the t-butyl cation depicted in Figure 1.9. The t-butyl cation is hyperconjugatively stabilized by nine possible interactions with adjacent C-H bonds, which have afforded sufficient stability to allow for its isolation as a salt,[41,42] and crystallographic characterization.[42] Moreover, as the central carbon is transformed from a tetrahedral environment into a trigonal geometry, there is a release of steric strain as the carbocation is generated. Thermodynamic considerations reveal that formation of the t-butyl cation requires 83 kcal/mol less energy than does the methyl cation from the corresponding hydrocarbon precursor.[43]

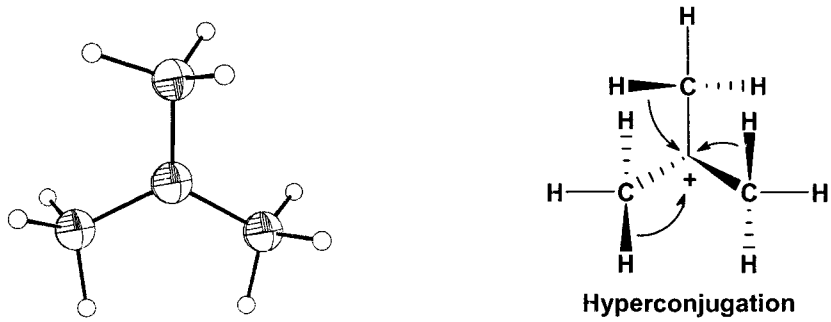

Figure 1.9 Molecular structure of the t-butyl cation, and its hyperconjugative stability.

1.6 Cobalt Alkynes-Bimetallic Cobalt Clusters

1.6.1 Metal-Stabilized Propargyl Cations

More recently, a novel approach toward stabilizing carbocations by using transition metal clusters has been studied extensively,[44] and the effects exerted by metal clusters on the reactivity of various molecular entities have been of particular interest within the McGlinchey group. Bimetallic and trimetallic clusters are known to stabilize carbocations in the α-position by delocalizing the positive charge through a metal centre onto the coordinated ligands. More specifically, metal cluster-stabilized propargyl cations have been a recent focal point, whereby propargyl alcohols, complexed by a dimetallic fragment, are treated with an acidic reagent, thus generating a cation which is stabilized by the adjacent metal fragment, as illustrated in Scheme 1.5. Nicholas initiated this work over a decade ago,[45] and since then many research groups have accomplished intricate studies in this area.[46]

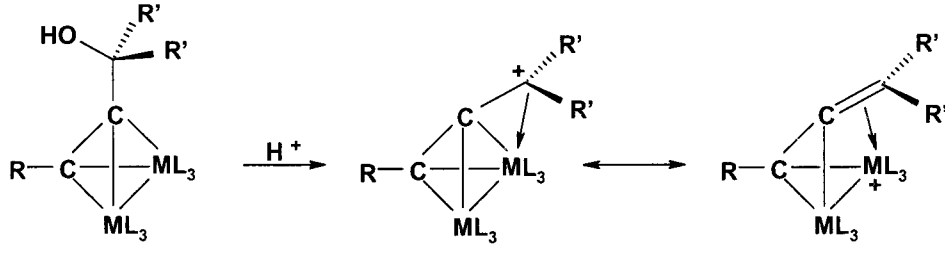

Scheme 1.5 The ability of a metal to stabilize an adjacent carbocation in bimetallic systems.

Hoffmann has conducted several EHMO calculations on dicobalt complexes,[47] indicating that the cationic intermediate may be best represented as a bent structure, **12a**, allowing overlap between the vacant p_z orbital of the methylene carbon with the filled cobalt d_{z^2} orbital, as opposed to an upright structure, **12b**, where the cation is localized on the sp^2-hybridized CR_2 carbon, shown in Figure 1.10.

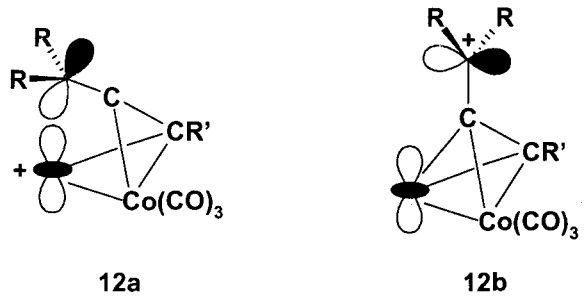

12a 12b

Figure 1.10 Orbital representation of a metal-stabilized cationic intermediate.

In fact, Hoffmann calculated a difference of 17.5 kcal/mol in energy between the two structures. This result is in accord with a subsequent calculation on the closely related alkyne, $[FeCo(CO)_6(HC{\equiv}C\text{-}CH_2)]$, wherein it was suggested that replacement of the charged $[Co(CO)_3]^+$ moiety with an $Fe(CO)_3$ fragment, rendering the molecule neutral, provides an excellent model for the dicobalt cation.[48] Furthermore, this isolobal substitution, which generates stable, isoelectronic analogues, has facilitated both the isolation and crystallization of several related mixed iron-cobalt clusters, which clearly demonstrate the proximal nature of the methylene carbon to the $Fe(CO)_3$ vertex, as shown in Figure 1.11.[48,49]

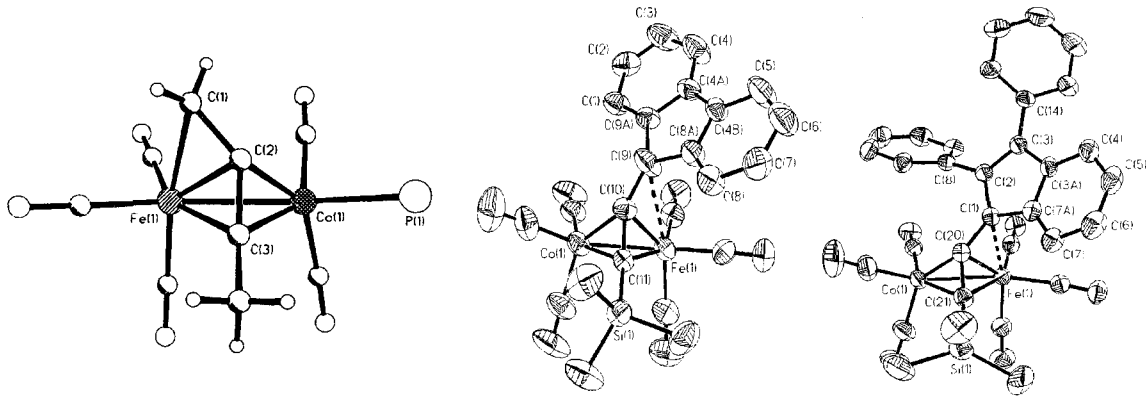

Figure 1.11 X-ray structures of $(MeC{\equiv}CCH_2)[(OC)_3FeCo(CO)_2PPh_3]$[48], $[FeCo(CO)_6(TMS\text{-}C{=}C{=}fluorenyl)]$[49], and $[FeCo(CO)_6(TMS\text{-}C{=}C{=}diphenylindenyl)]$[49].

1.6.2 NMR Evidence of a Fluxional Process

Experimental evidence obtained from variable-temperature NMR data provides convincing evidence for the bent geometry characteristic of cobalt stabilized propargyl cations. Nicholas[50] has demonstrated that $[(HC{\equiv}C\text{-}CMe_2)Co_2(CO)_6]^+$ exhibits two distinct methyl resonances in its ^{13}C NMR spectrum at 233 K. Dunn and coworkers[49] have confirmed this phenomenon by illustrating the inequivalence of the fluorenyl and diphenylindenyl carbons in each of the dicobalt cation analogues of $[FeCo(CO)_6$(TMS-C=C=fluorenyl)] and $[FeCo(CO)_6$(TMS-C=C=diphenylindenyl)], in the course of low temperature NMR investigations.[49]

Furthermore, Mislow[51] and Nicholas[52] were the first to speculate that a fluxional process must be occurring in tricobalt- and dicobalt-stabilized cations, whereby the cationic carbon of the ligand migrates between metal vertices. Subsequently, Schreiber and coworkers established the existence of two fluxional processes, and proposed a mechanism to explain the dynamic behaviour.[53] By investigating a complex bearing diasterotopic labels, Schrieber concluded that upon protonation, ligand migration occurs from one cobalt vertex to the other via: (i) a low-energy (~10 kcal/mol) antarafacial migration, resulting in enantiomerization, or (ii) a slightly higher energy (~13 kcal/mol) syn/anti interconversion involving either 180° rotation about the formal double bond or suprafacial migration, causing diastereomerization of the propargylic site, as shown in Figure 1.12. The difference in energy may be attributed to charge localization on the carbon atom, due to poor orbital overlap in the rotated transition state for the suprafacial migration process, versus better charge delocalization in the upright transition state for

the antarafacial migration process, which maintains partial orbital overlap between the empty carbon p_z and filled cobalt d_z^2 oribitals.[53]

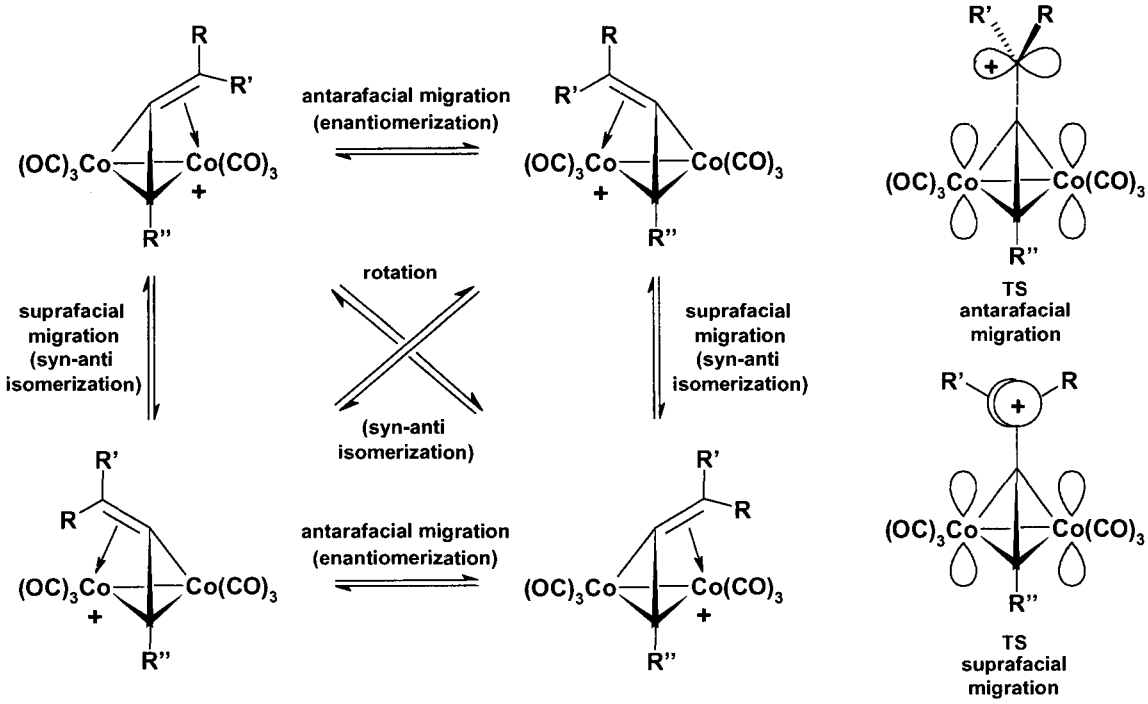

Figure 1.12 Proposed mechanism of fluxional processes involved in stabilization of propargyl cations by hexacarbonyldicobalt.

Recently, Schmalz[54] has verified Schrieber's proposal by identifying both transition states through hybrid density functional calculations (B3LYP). More interestingly, Schmalz has also investigated the potential for a dicobalt-alkyne species to stabilize a dicationic complex. Natural bond order (NBO) calculations on the simplest possibility, $[(CH_2C{\equiv}C\text{-}CH_2)Co_2(CO)_6]^{2+}$, **13**, indicated that the cobalt cluster could indeed compensate both cationic charges, with two different structural representations: a *cisoid* structure, **13a**, where both methylene groups lean toward the same cobalt atom, and a more energetically favoured (9.5 kcal/mol relative to **13a**) *transoid* species, **13b**, whereby the methylenes are bent toward different cobalt atoms, as shown in Figure

1.13.[54] It is noteworthy that the isolobal di-iron analogue, $[CH_2=C=C=CH_2]Fe_2(CO)_6$, has been previously prepared, whereby both $[Co(CO)_3]^+$ fragments are substituted by neutral $Fe(CO)_3$ entities.[55]

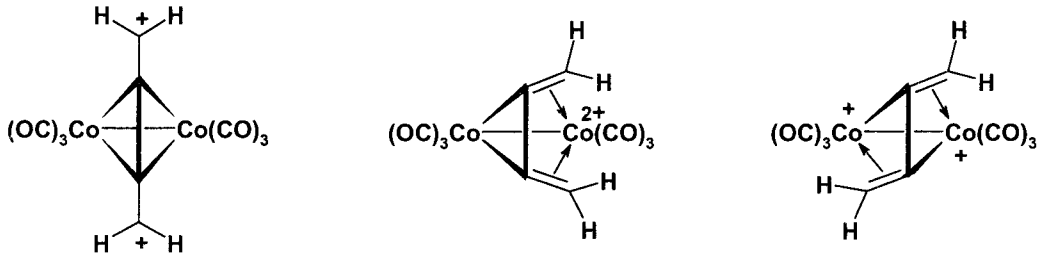

13 13a 13b

cisoid *transoid*

Figure 1.13 The potential for hexacarbonyldicobalt to stabilize two propargyl cations.

1.6.3 Alkyne-Dicobalt Cluster Cations

In light of the ability for cobalt to provide stability to carbocations in cobalt complexed alkynes, one might suspect that the presence of two such moieties would increase the possibility of preparing a cation sufficiently stable to be characterized by X-ray crystallography. In 1998 Melikyan's group[56] became the first (and thus far only group) to successfully prepare and crystallize a cobalt-stabilized propargyl cationic species, **14**, as shown in Figure 1.14. The crystal structure reveals a trigonal planar geometry at the cationic carbon, C-13, which is preferentially bent up to 0.38 Å towards one of the neighbouring cobalts in each individual cluster, thus substantiating previous NMR evidence that cobalt assists in alleviating the positive charge in propargyl cations. Even though the crystals were not of outstanding quality, as the counter-ion was disordered, the data collected were weak ($2.9° > 2\theta > 35°$), and the atoms were only isotropically refined with an agreement factor, R_1, of greater than ten percent, this was

still an exceedingly meritorious achievement. Furthermore, one must consider the packing effects induced by the sterically encumbered molecule, which may have influenced the positioning of the cobalt atoms; therefore it is difficult to quantify the amount of electronic assistance offered to the cationic centre.

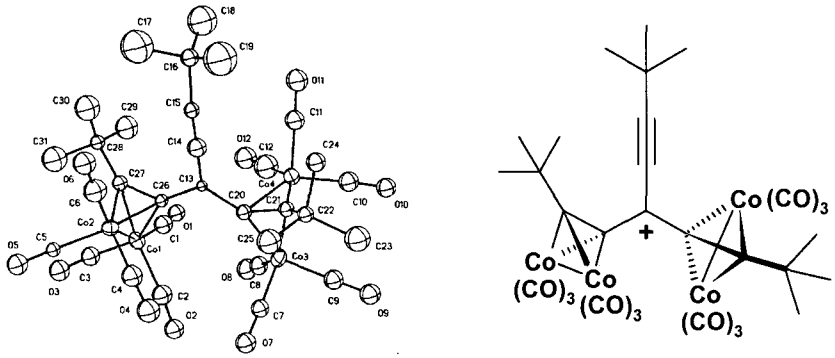

Figure 1.14 The first structurally characterized cobalt-stabilized propargyl cation, **14**.

One should emphasise that cationic stabilization has not been restricted merely to cobalt centred clusters. In fact, a hierarchy has been established regarding the stabilizing abilities of a series of transition metal moieties towards propargylic carbocations. In homometallic clusters, the ordering is: $[Cp_2Mo_2(CO)_4(HC{\equiv}C\text{-}CH_2)]^+ > [\text{ferrocenyl-}CH_2]^+ > [Co_2(CO)_6(HC{\equiv}C\text{-}CH_2)]^+$,[57] and for individual vertices in heterometallic clusters: $Ru(CO)_3 > Fe(CO)_3 > CpW(CO)_2 > PPh_3Co(CO)_2 > Co(CO)_3$.[46c,58]

The chemistry of (propargyl)dicobalt cations has rapidly expanded over the past several years, and several comprehensive reviews have appeared that describe their diverse applications in organic, biological and natural product syntheses.[59]

The most widely employed synthetic applications of cobalt-clustered propargyl cation chemistry have been derived from the remarkable reaction pioneered by K.M. Nicholas.[45a] The reaction entails generation of a cobalt-stabilized propargyl cation

through addition of a protic or Lewis acid to an alcohol precursor, and subsequent exclusive addition of a desired nucleophile to the propargylic site. Enols, certain arenes, thiols, phosphines, amines, sulfonamides, and oxygen-centered functionalities containing alcohol, hydroxy and alkoxy groups, have proven to be efficient nucleophiles. Theoretically, the importance of this reaction lies in the retention of stereochemistry during the course of the nucleophilic addition. In effect, the reaction occurs by a double inversion process whereby, following protonation of the alcohol precursor, the cobalt displaces the leaving group (water), and exo attack by the incoming nucleophile results in retention of the original stereochemistry. Subsequent facile removal of the cobalt moiety by use of $(NH_4)_2Ce(NO_3)_6$,[60] $Fe(NO_3)_3$,[30a] Me_3NO,[61] or more recently $(H_2NCH_2)_2$[62] affords a novel free alkyne, as shown in Scheme 1.6. This method has even been used in biological transformations, and in the synthesis of biologically active molecules such as enediynes,[63] (+)-begamide E,[64] blastinomycine,[65] cyclocolorenone,[66] and tetrapyrroles,[67] and intermediates of insect pheromones,[68] vitamin A derivatives,[69] and carotenes.[69]

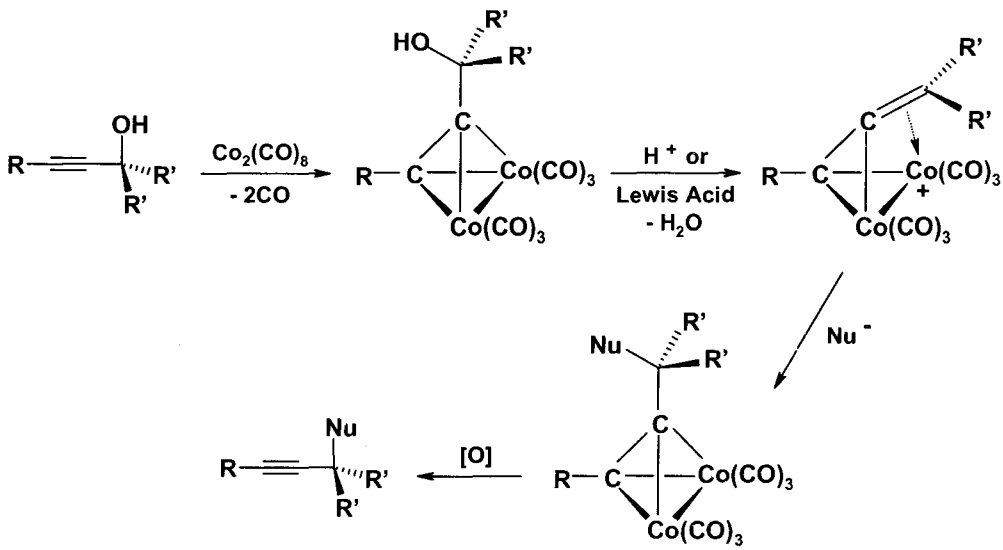

Scheme 1.6 The Nicholas Reaction.

Furthermore, use of a cobalt-complexed 1,3-enyne instead of an alcohol permits dual substitution of the ligand through initial addition of an electrophile, followed by the nucleophile, thus generating an α,β-functionalized propargylic alkyne.[70] (Scheme 1.7)

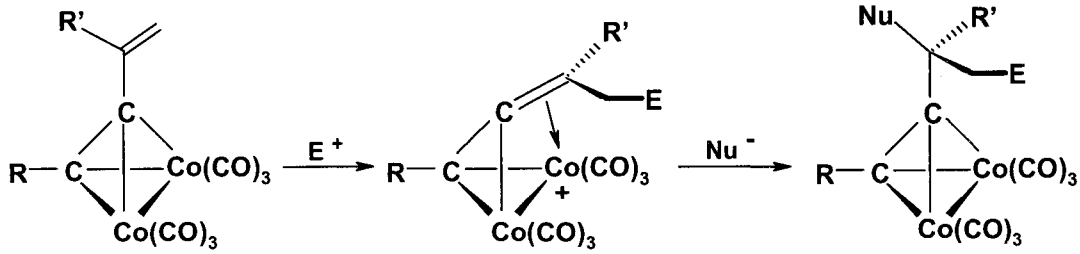

Scheme 1.7 Generation of α,β-functionalized propargylic alkyne from a cobalt-complexed 1,3-enyne.

Several reactions involving transient propargyl cations take advantage of the bend angle resulting from complexation of the metal to the linear alkyne: these include intra-molecular alkylations/cyclizations, and Pauson-Khand[71] reactions which afford cobalt-free 2-cyclopenten-1-ones derived from an alkyne, an alkene, and carbon monoxide provided by the cobalt carbonyl. Schreiber[72] has elegantly exemplified these concepts by addition of boron trifluoride etherate to a cobalt-complexed diallyl acetal, inducing exclusive *endo*-cyclization and subsequently a Pauson-Khand[71] type rearrangement upon heating to generate the tricyclic species, **15**, as depicted in Scheme 1.8.

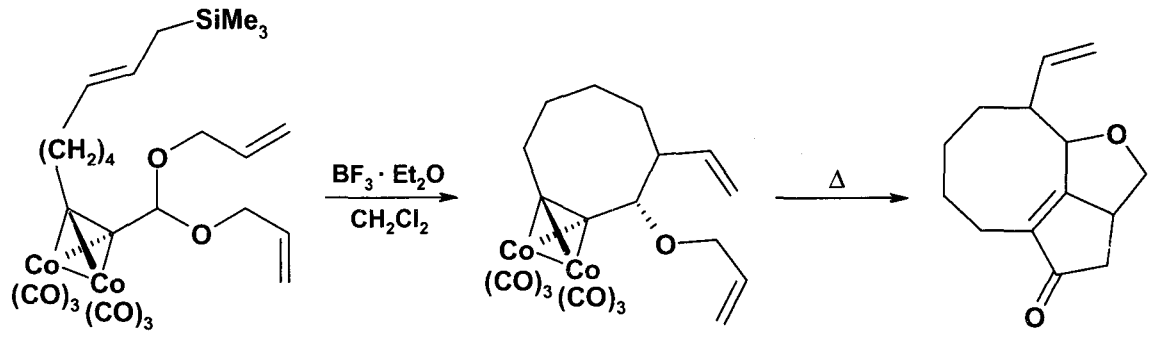

15

Scheme 1.8 Cobalt-cluster mediated intramolecular cyclization with a subsequent Pauson-Khand rearrangement.

Moreover, the bend angle induced upon complexation to form cobalt clusters has been exploited in terms of developing migration reactions mediated by propargyl cations. This topic will be comprehensively examined in Chapter 2. In addition, recent attention has been focussed on cobalt-cluster stabilized propargyl radicals generated from these cations. This fledgling field has enormous potential, and some preliminary studies are presented in Chapter 4.

1.7 Thesis Objectives

It is of considerable interest to observe how well-established organic reactions can be modified in a controlled manner when conducted in the proximity of a transition metal. By complexing a transition metal to a free organic ligand, one may contrast the difference in products obtained from a specific reaction with those expected from its organic precursor under similar conditions. In fact, by altering the geometry, as well as the electronic and steric character of the organic ligand, transition metal analogues generate many products that are otherwise unattainable from direct organic reactions. Moreover, in many cases removal of the transition metal moiety is facile, thus allowing the isolation of novel organic products.

In this thesis, the focus has been on the syntheses, structures and dynamics of cobalt-stabilized cationic systems. The particular areas studied include: the migrations of allyl silanes (Chapter Two), terpenoid cations that are susceptible to Wagner-Meerwein rearrangements (Chapter Three), mechanistic implications into the formation of tricobalt clusters from their dicobalt acetylenic precursors (Chapter Three), the conversion of propargyl cations into the corresponding radical species (Chapter Four), and the structural variability of sterically hindered alkyne cluster complexes (Chapter Five). Although the standard spectroscopic and spectrometric techniques (NMR, IR, mass spectrometry, etc.) are extensively employed, a specific emphasis has been placed on X-ray crystallography as the ultimate method of structure determination.

Chapter Two: Cobalt-Cluster Mediated Migrations

2.1 Background

2.1.1 Cyclizations

As mentioned in the Introductory Chapter, cobalt-cluster-assisted intramolecular cyclizations have become a prominent area of interest in cobalt-stabilized cation chemistry. The approximate 40° angle distortion resulting from complexing dicobalt hexacarbonyl to otherwise linear alkynes facilitates conjoining of the alkyne termini to produce molecules with varying ring sizes. This has been accomplished using alcohol, ether, and epoxide terminal functionalities through treatment of the specified complex with a Lewis acid, thereby affording 5-9 membered cyclic ethers.[59a] However, recently, considerable attention has been focused on the construction of cycloalkynes comprised only of carbon, utilizing the advantageous bend angle provided by cobalt complexes.

This research was initiated by Schreiber and coworkers who studied a cobalt-complexed alkyne bearing terminal methoxy methylene and alkynylsilane groups, **16**. Addition of $BF_3{\cdot}Et_2O$ to the metal-complexed silane was thought to create a metal-stabilized cationic intermediate, **17**, thus prompting intramolecular electrophilic attack upon the alkene.[72] The intermediate so generated contains a hyperconjugatively stabilized β-silyl cation, **18**, resulting from σ-donation of electron density from the α-carbon-silicon bond into the empty p-orbital of the carbocation. Subsequent nucleophilic

attack by a fluoride ion at the silicon centre brings about elimination of Me_3SiF, and affords the cyclic product, **19** (Scheme 2.1).

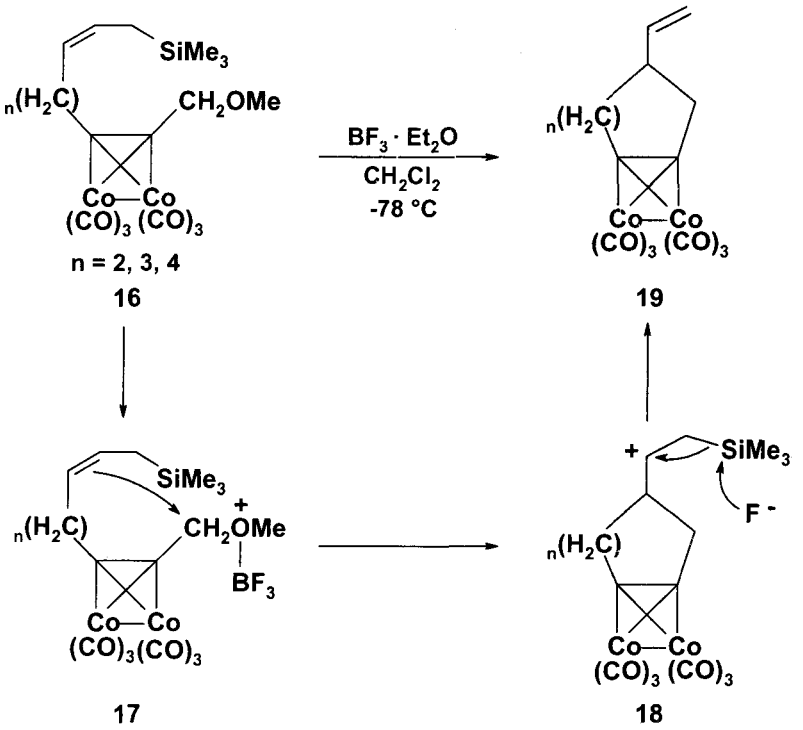

Scheme 2.1 Intramolecular cyclizations facilitated by cobalt bend-angle.

Free five-, six- and seven-membered cyclic alkynes have only been observed in low temperature matrices, or as transient intermediates in trapping and isotopic labeling experiments.[73] Since cyclooctyne is the only uncomplexed alkyne that has been prepared and isolated,[74] recent attention has been drawn to the development of routes to cobalt-complexed small-ring alkynes. Magnus[75] has successfully prepared the smallest known cobalt complexed ring system, a cyclohexenyne, while Chisholm[76] has reported an example of both a ditungsten cyclohexyne and cycloheptyne complex. In a more general approach, Green *et al.*[77] have adapted Schreiber's synthesis and prepared several seven-membered cyclic systems with β-silyl stabilized intermediates, starting from cobalt

clusters with appropriate allylsilane and propargylic acetate functions, and subsequently adding a Lewis Acid, as shown in Scheme 2.2. Furthermore, the Green group has prepared similar cycloheptenyne dicobalt clusters in an efficient manner by using [4 + 3] cycloadditions of allylsilanes or allystannanes to suitable dicobalt clusters, also shown in Scheme 2.2.[78] In this vein, a very recent report is noted, whereby cobalt cation mediated cyclizations have been used to prepare pyrones and benzofuranones.[79]

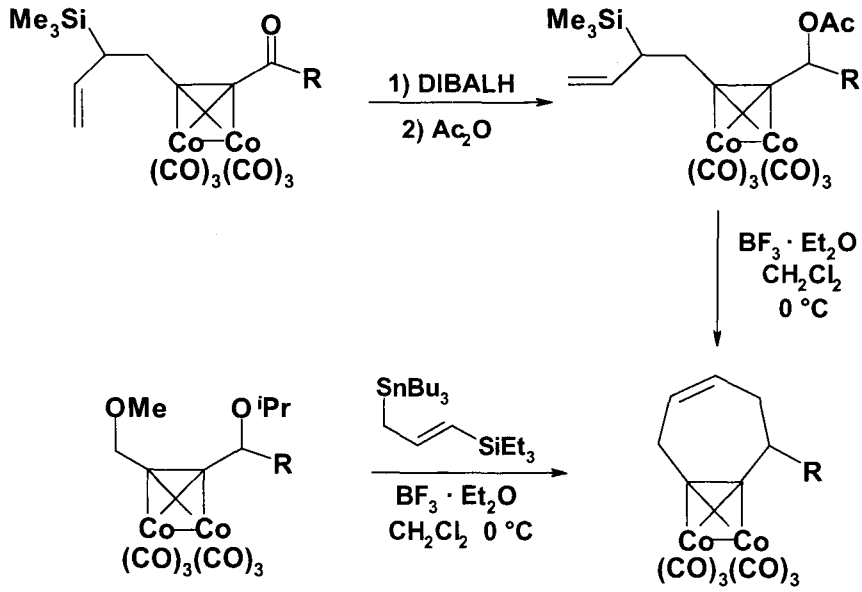

Scheme 2.2 Formation of cycloheptyl hexacarbonyldicobalt derivatives.

2.1.2 Allyl Migrations

In the course of attempts to generate a silicon analogue of a metal-stabilized propargyl cation, Ruffolo *et al.*[80] observed a novel migration reaction related to Schrieber's work, that once again proceeded with the assistance of a β-silyl stabilized cation. Ruffolo used an alkyne-dicobalt cluster bearing propargyl alcohol and allylsilyl substituents, **20**. The group's intention was to compare the susceptibility toward

protonation of the allyl and propargyl groups.[80] The use of HBF_4 as the proton source led to an exciting new revelation: the allyl group had migrated from the silicon across the alkyne bridge to the propargyl carbon in the bimetallic cluster (Scheme 2.3). The product was identified using 2D NMR techniques, whereby a ^{1}H-^{13}C correlation between the propargyl carbon and the geminal methylene protons of the allyl was clearly evident in the Heteronuclear Multiple Bond Correlation (HMBC) NMR spectrum. Further confirmation was provided by the observation of a 251 Hz doublet in the ^{29}Si NMR spectrum, indicating that a fluorine atom was directly bonded to silicon. However, repeated attempts to obtain X-ray quality single crystals appropriate for a crystallographic analysis proved unsuccessful.

It became evident that protonation on the alcohol was favoured, initially affording a cobalt cluster stabilized propargyl cation, **21**. It was hypothesized that the allyl substituent then positioned itself for intramolecular electrophilic attack by the cationic center, thus producing a seven-membered cyclic intermediate containing a hyperconjugatively stabilized β-silyl cation, **22**. This is unquestionably a short-lived intermediate, as the affinity for formation of a silicon-fluoride bond is greater than the potential stability provided for the β-silyl cation by the metal cluster; hence, the ring opens to produce **23**. It is worth noting that this is different from Schreiber's system (Scheme 2.1), whereby the silicon is now a constituent of the seven-membered ring intermediate, and internal elimination results in ring opening. The formation of the fluorine-silicon bond was believed to be the thermodynamic driving force for the allyl migration, which was also evident upon protonation of the analogous isopropenyl system (Scheme 2.3).[80]

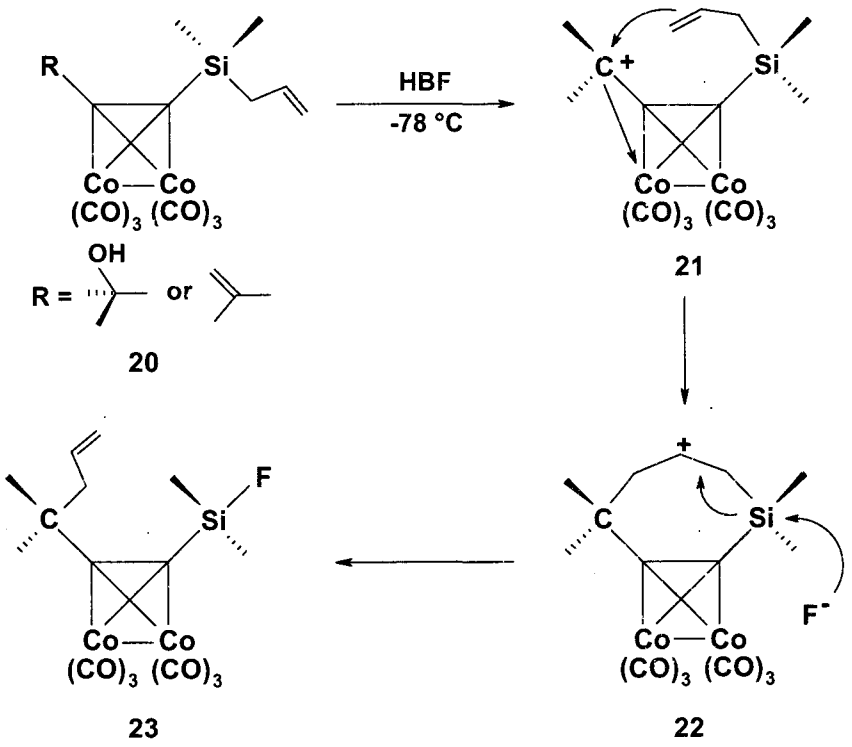

Scheme 2.3 Allyl transfer via a seven-membered ring intermediate.

2.2 Results and Discussion - Allylsilanes

In light of the efficiency of migration of an allyl substituent from a silyl terminus to a propargylic site, efforts were made to determine whether the allyl transfer reaction was exclusive to the isopropyl system. By replacing the propargyl alcohol, but retaining the allylsilane, the effectiveness of the allyl transfer with different metal-stabilized intermediate cations can be investigated, while probing steric limitations and electronic influences afforded by various substituents.

2.2.1 Ferrocenyl Derivative

Since a very effective method of synthesizing allylsilanes has been developed, several experiments were conducted in order to determine the efficiency of allyl transfers

in bulkier systems. Ideally, one would prefer ligands in which simple elimination of the alcohol could be avoided, thereby ensuring that any possible migration or rearrangement is not disfavored because of competing pathways available to the cationic intermediate. An excellent possibility would appear to involve the ferrocenyl system, **24**, whereby the sandwich moieties not only provide steric bulk in the environment of the alcohol, but also offer further stabilization of the initially generated carbocation by delocalizing the positive charge onto the iron atom, **25**, as seen in Scheme 2.4.

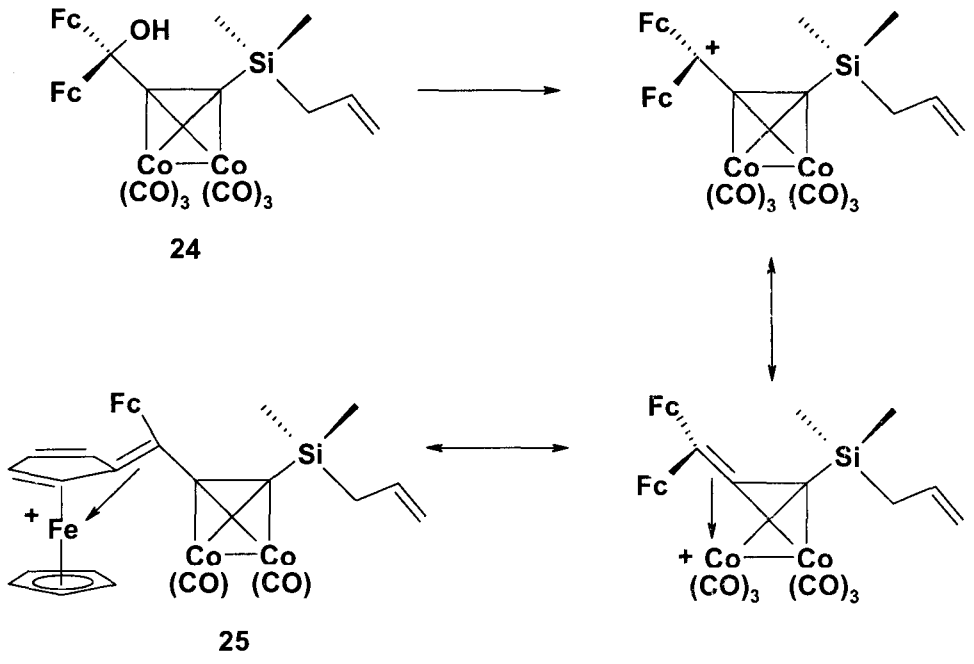

Scheme 2.4 Resonance forms of a diferrocene substituted propargyl cation.

Since diferrocenyl ketone, **26**, is not readily available, it was synthesized using a slightly modified literature procedure,[81] in a Friedel-Crafts type combination of ferrocene and oxalyl chloride in dichloromethane at -78 °C as illustrated in Scheme 2.5.

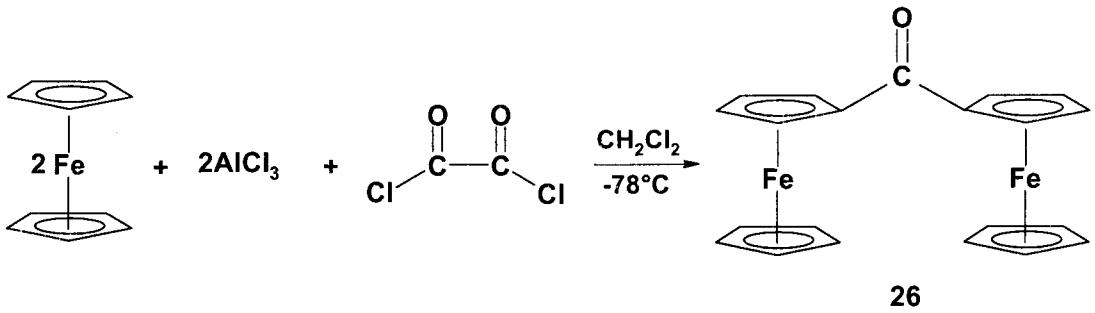

26

Scheme 2.5 Synthesis of diferrocenyl ketone.

Even though formation of the ketone was successful, addition of the alkyne was attempted numerous times, yet proved to be fairly ineffective, as less than 10% of the desired diferrocenyl-alkynol was recovered. This contrasts with a literature report where it has been claimed that the alkyne was previously prepared analogously in 76% yield.[82] Apparently, the steric crowding associated with formation of the tertiary alcohol is greater than was originally envisaged and resulted in unsatisfactory yields. Therefore, considering the difficulty in generating sufficient diferrocenyl-alkynol in the initial reaction, and since several more steps were required to obtain the cobalt-complexed allylsilane precursor, **24**, it seemed impractical to pursue this objective.

2.2.2 Di-t-butyl Derivative

However, these observations did not dissuade us from our intention of determining the generality of allyl migrations as several other readily available, sterically encumbered ketones were considered, notably 2,2,4,4-tetramethyl-3-pentanone. Treatment of trimethylsilylacetylene with *n*-butyllithium, followed by addition of the ketone afforded the di-t-butylalkynol, **27**. Cleavage of the trimethylsilyl group was accomplished with the use of tetrabutylammonium fluoride, thus generating **28**, as shown

in Scheme 2.6. Before continuing with the synthesis of the allylsilane, a small amount of the terminal alkyne, **28**, was treated with octacarbonyldicobalt to determine whether generation of a di-t-butyl cobalt-alkyne complex was sterically feasible. Thin-layer chromatography suggested that the dinuclear species, **29**, was indeed formed, yet quickly decomposed and regenerated the uncomplexed ligand, **28**, rendering its isolation futile.

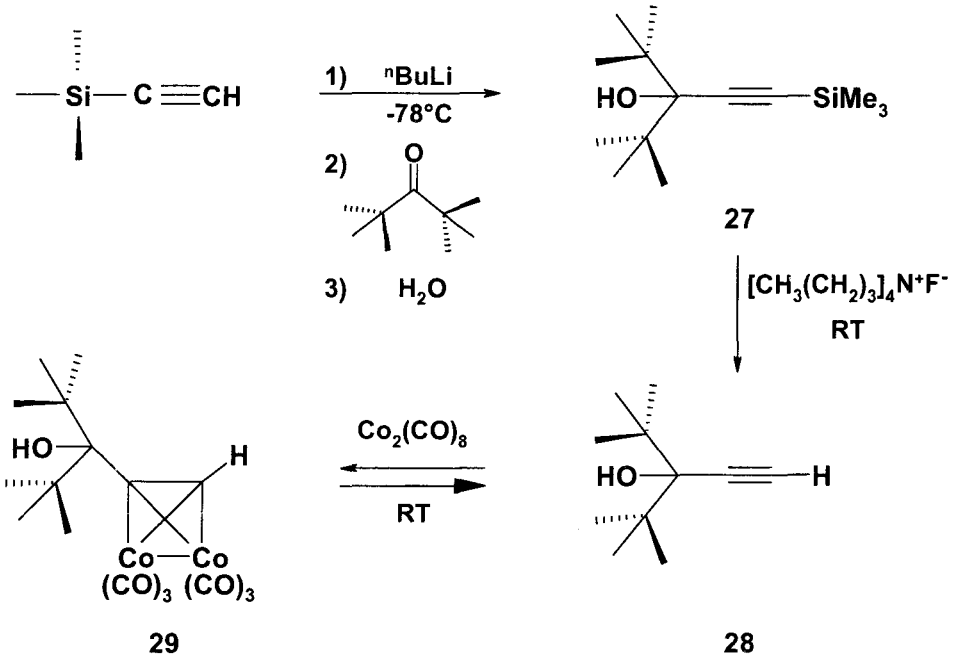

Scheme 2.6 Attempted synthesis of **29**.

A semi-empirical molecular model calculation using Hyperchem[83] at the PM3 level of theory, shown in Figure 2.1, suggests that there is the potential for substantial steric interference between the t-butyl groups and the carbonyls on cobalt, which may have reduced the stability of **29**.

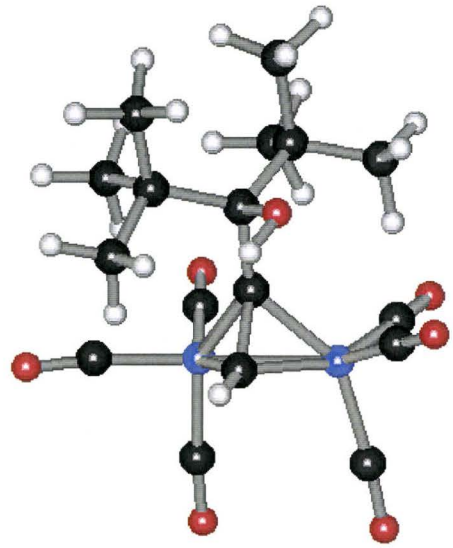

Figure 2.1 Hyperchem model of **29**.[83]

It is interesting that several tri-t-butyl systems are known to exist, as discussed earlier in section 1.5.3, yet replacement of one t-butyl functionality with a cobalt-complexed alkyne renders the compound unstable, which implies that the cobalt cluster is a bulkier substituent. However, from work to be discussed in Chapter 5, it will become evident that the t-butyl group is in fact more sterically demanding in cyclohexyl systems, and therefore in all probability, the existence of tri-t-butyl systems may be attributable to the symmetrical nature of each molecule, whereas the irregularity of the cobalt complex may have rendered **29** unstable. A thorough search of the literature revealed that although several 1,1-disubstituted t-butyl propargyl systems exist,[84] only monosubstituted t-butyl analogues have been successfully complexed with octacarbonyldicobalt.[85]

2.2.3 Diphenyl Derivative

Our attention remained focused on developing comparable bulky alkynols that could not undergo simple elimination yet enabled allyl migrations. The selection of the diphenyl ketone precursor pertained to its ability to provide some steric resistance, while concurrently allowing for flexibility of the propargylic site, in comparison to the di-t-butyl system, which has greater three dimensional constraints. Furthermore, the excellent stabilizing capabilities offered to the initial cation formed upon protonation, by both the cobalt complex and through resonance interactions with the phenyl groups, as illustrated in Scheme 2.7, made this an obvious choice. It was anticipated that the prolonged lifetime of the cationic intermediate would increase the probability of the allyl group migrating from silicon.

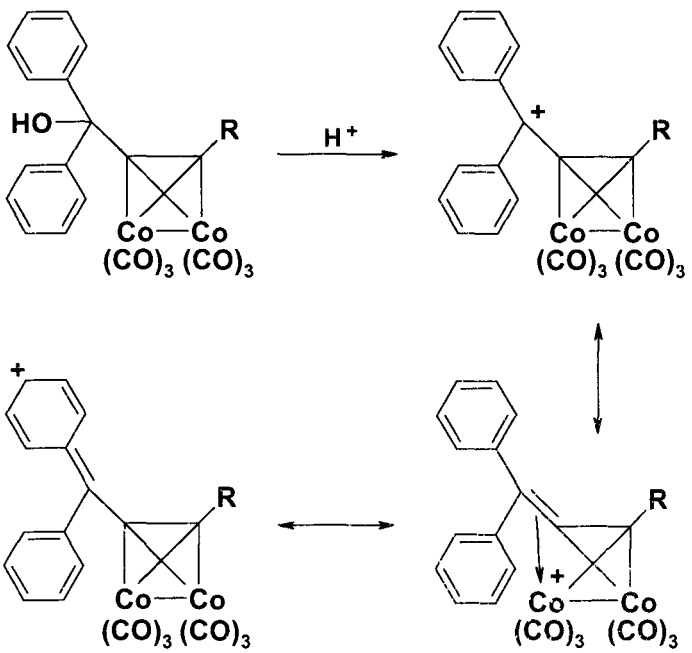

Scheme 2.7 Resonance contributors of a cobalt-complexed propargyl diphenyl cation.

The diphenyl analogue, was readily synthesized in a manner similar to that attempted for the di-t-butyl system, by treating benzophenone with trimethylsilylacetylide, and deprotecting the alkyne with tetrabutylammonium fluoride, to produce the terminal alkyne, **30**. Deprotonation of **30** with two equivalents of *n*-butyllithium, and addition of allyldimethylchlorosilane furnished the desired alkyne, **31**, which was subsequently allowed to react with octacarbonyldicobalt to yield the cluster **32**, as depicted in Scheme 2.8.

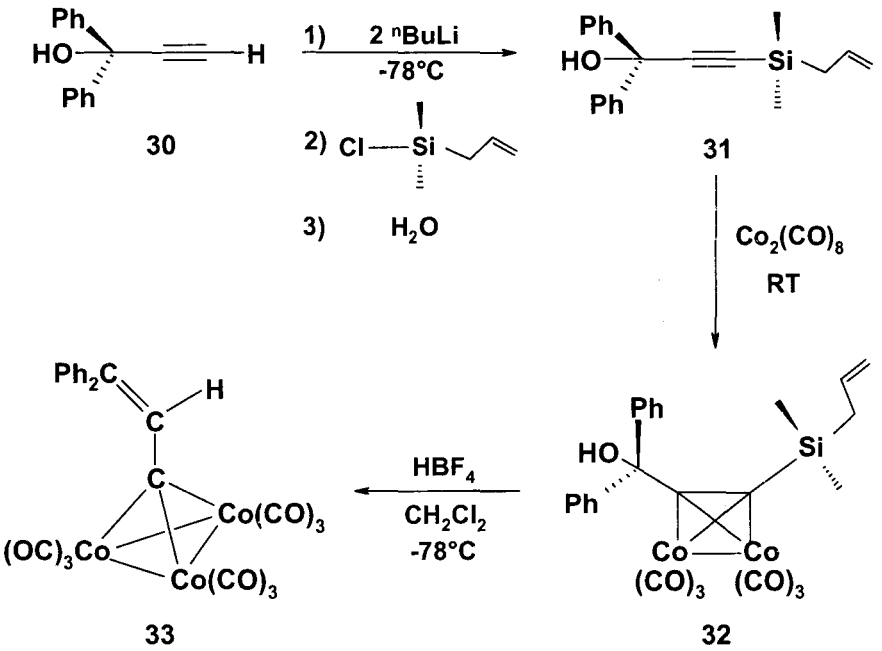

Scheme 2.8 Synthesis and protonation of **32**.

However, to our surprise, addition of 1.5 equivalents of HBF_4 to the silyl cluster, **32**, in dichloromethane, afforded the tricobalt cluster, **33**, as the only isolable product, as shown in Scheme 2.8. Formation of such a trinuclear species, and the mechanistic implications for tricobalt clusters, will be addressed in more detail in Chapter 3. In

contrast, repetition of this reaction in tetrahydrofuran produced the hydrogen abstraction, radical product, **34**, seen in Scheme 2.9. Formation of radical species upon protonation of cobalt clusters in tetrahydrofuran is a recent development in propargyl cation chemistry, and will be discussed further in Chapter 4. Several other unresolvable fractions were observed during chromatographic separation of the products of both reactions. These included the expected "propene-elimination" product, $[Ph_2C(OH)CCSiMe_2F]Co_2(CO)_6$, which could not be isolated because of binding to the column, yet was identified by the characteristic ^{19}F splittings of the methyl resonances in the NMR spectra of the crude product. However, the allyl migration product was, at best, a minor constituent.

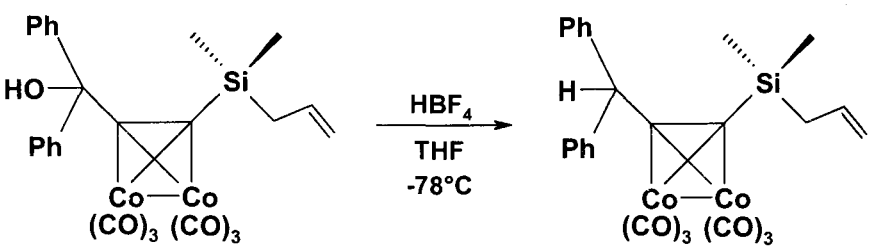

32 **34**

Scheme 2.9 Formation of hydrogen abstraction product, **34**, in THF.

The question now arises as to why there was no evidence for an allyl migration. Although, intuitively one might suggest that electronic effects induced by the phenyl substituents posed a greater problem, in that the stability of the initially generated cation, **35**, was perhaps far more significant than that offered by the intermediate β-silyl cation, **36**, required for migration (Scheme 2.10), Nicholas has demonstrated that the simple unsubstituted propargyl cation is in fact more stable than **35**.[52a] This implies that even with the rotational flexibility offered by the phenyl substituents, the steric encumbrance is still great enough to prevent allyl migration in this system.

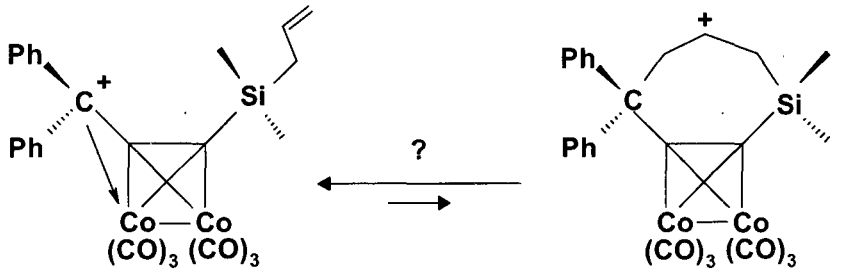

35 36

Scheme 2.10 Contrast of the stability provided by the phenyl substituents versus silicon.

Although one must conclude that an allyl migration was not viable in this system, the steric limitation for the addition of octacarbonyl dicobalt to a disubstituted propargylic alkynol has been noted, and apparently lies between the di-t-butyl and diphenyl substituents.

2.2.4 Fluorenyl Derivative

Suspecting that the diphenyl cation, **35**, discussed above is too sterically demanding to allow for interaction with the allylsilyl functionality at the other terminus of the coordinated alkyne, we chose to investigate the analogous fluorenyl system, which is comparable in terms of bearing two phenyl rings, yet is constrained to maintain planarity. Moreover, the fluorene system introduces an intriguing electronic effect in that the longevity of the cation is directly attributable to the stabilization provided by the cobalt cluster. In the absence of a metal the cation would be an anti-aromatic 12π system, with a somewhat reduced stability relative to **35**, which may in turn encourage migration of the allyl group. Furthermore, elimination upon protonation is not possible, and the planarity of the ligand should provide some steric relief in comparison to the diphenyl analogue.

The fluorenyl-allylsilane, **37**, was prepared analogously to its diphenyl counterpart and, after treatment with octacarbonyldicobalt, afforded 9-[(allyldimethylsilyl)ethynyl]-9H-fluoren-9-ol[$Co_2(CO)_6$], **38**. Protonation of **38** afforded a single product, as was evident from thin layer chromatography with a 1:1 mixture of dichloromethane and hexanes, and proved to be the desired allyl migration adduct, **39**, shown in Scheme 2.11. The product **38** was identified by NMR, as the proton and carbon chemical shifts of the allyl functionality were noticeably different from those of the starting material, **38**. Single crystals of **39** were successfully obtained for X-ray diffraction data collection, and used to develop the molecular model depicted in Figure 2.2, unambiguously verifying migration of the allyl fragment from silicon to C9. During purification of **39** by column chromatography, the development of a second product became apparent and, after isolation, was identified from its NMR and mass spectra as the silanol, **40**, which had also undergone an allyl migration.

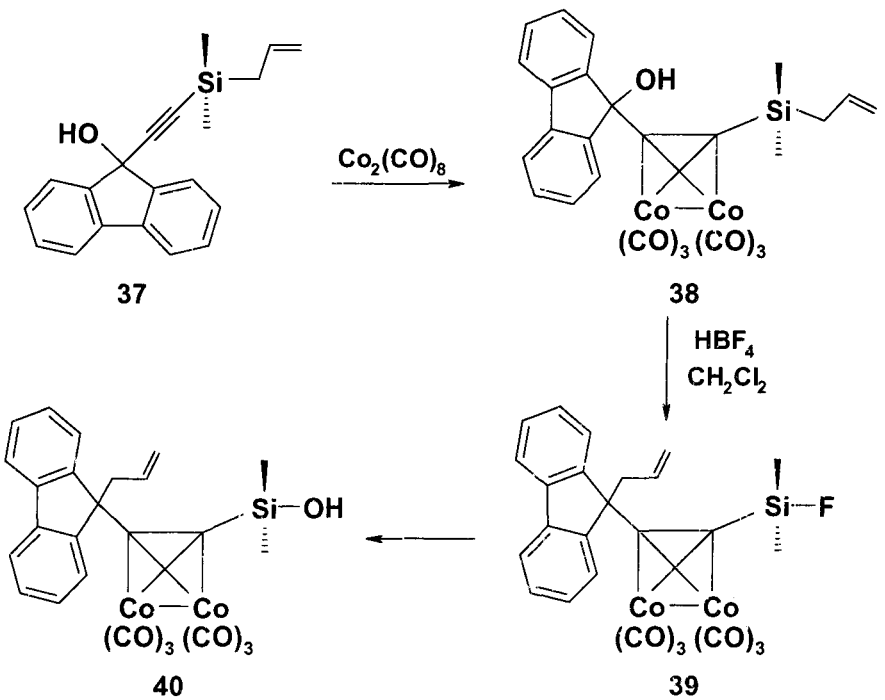

Scheme 2.11 Formation of allyl migration products in the fluorenyl system.

In retrospect, it is evident that the silanol **40** was generated from **39** during chromatographic separation, whereby the initial product suffers some decomposition and is also partially hydrolysed through interaction with the silica gel. The eventual result is the acquisition of the fluorosilane, **39**, and the silanol, **40**, in overall yields of 60% and 20%, respectively.

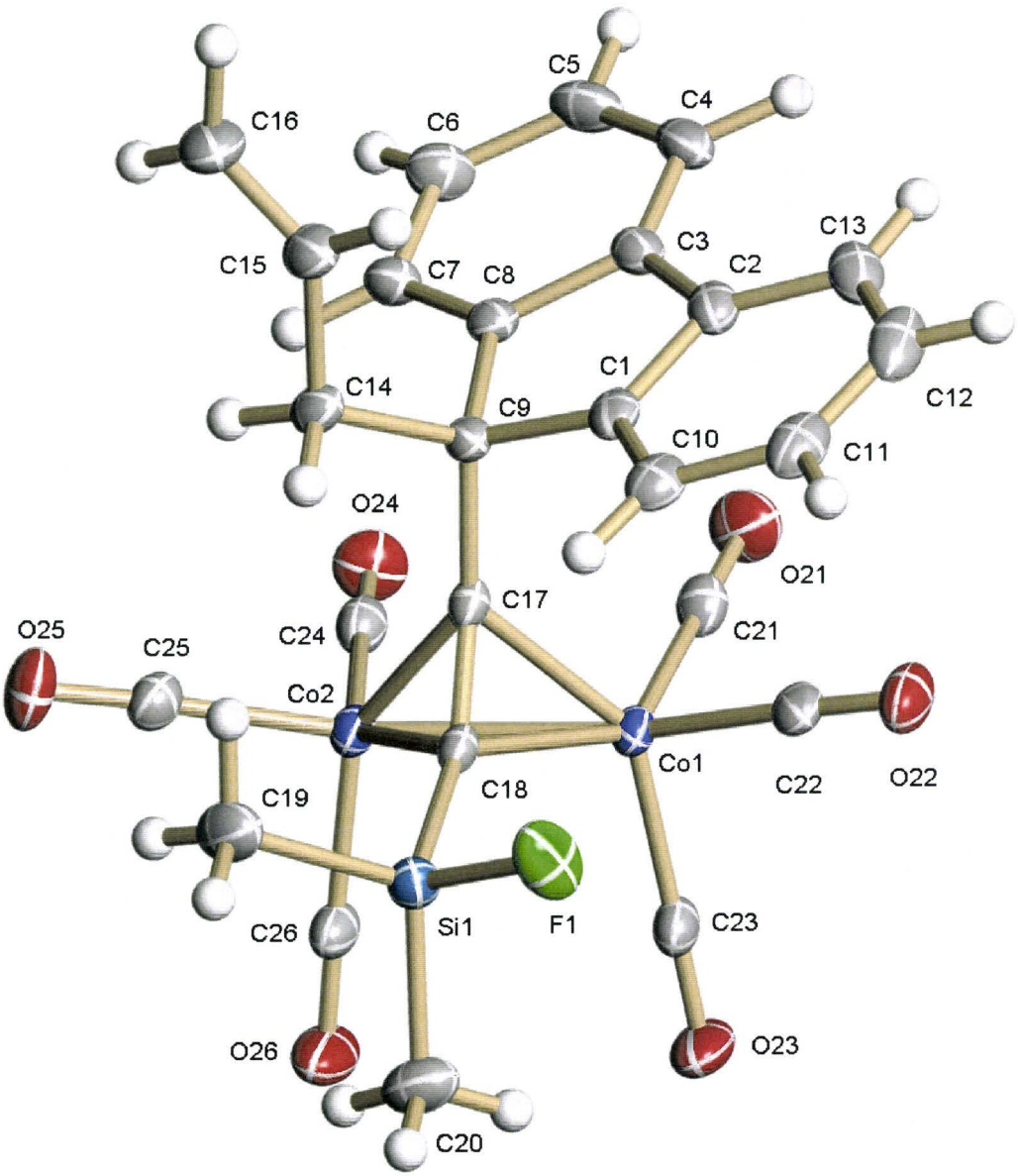

Figure 2.2 Molecular structure of the ally migration product **39** with 30% thermal probability ellipsoids.

One can now see that, since allyl migration was the predominant pathway in this system, such rearrangements are eminently viable when (a) steric constraints are minimized, and (b) simple elimination is averted. Furthermore, removal of the cobalt carbonyl cluster, and also the silyl protecting group, would appear to indicate a novel and convenient method of preparing alkynes bearing substituents attached to a quaternary centre, which could be used in subsequent organic syntheses.

Upon further purification of the allylsilane, **37**, several other minor inseparable fractions were observed, including a diallydisilane, a β-hydroxy functionalized silane, and a tertiary alcohol; these products were only isolable as the corresponding cluster complexes **41**, **42**, and **43**, shown in Figure 2.3, after treatment of the mixture with octacarbonyldicobalt.

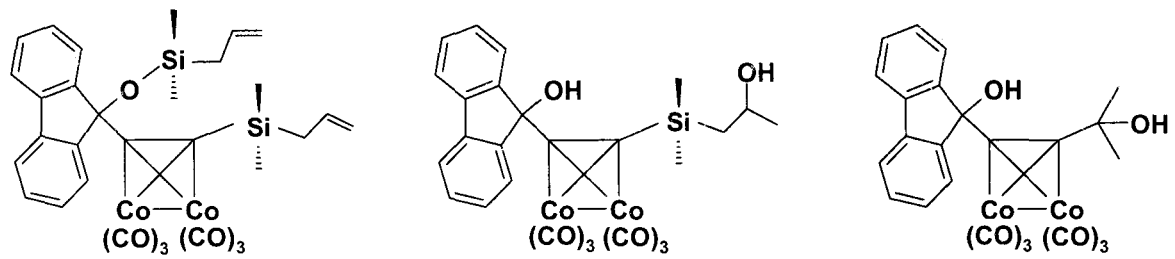

41 **42** **43**

Figure 2.3 Products isolated after treatment of minor fraction obtained from formation of **37**, with octacarbonyldicobalt.

Whether these products arose directly from generation of the allylsilane, or rearrangement upon chromatographic separation, remains debatable. However, it is thought that the siloxane, **41**, was generated upon reaction of excess allyldimethylcholorosilane with the dianion formed from addition of two equivalents of *n*-butyllithium to 9-ethynyl-9H-fluoren-9-ol.

The β-hydroxysilane, **42**, is believed to have arisen during chromatographic purification of the originally targeted uncomplexed allylsilane, **37**. The silica gel column, known to be slightly acidic,[86] presumably promoted protonation at the methylene terminus of the allyl group, thus generating a β-silyl stabilized cation, which then underwent nucleophilic attack by water, and upon treatment with octacarbonyldicobalt gave the observed product **42**. Although the NMR and mass spectra alluded to molecule **42**, its identity was only confirmed upon a single crystal X-ray diffraction study, which revealed the structure that appears in Figure 2.4a.

The excellent crystallinity of this compound appears to have been enhanced by the strong intra- and intermolecular hydrogen bonding evident within the crystal structure, as illustrated in Figure 2.4b. Two crystallographically unrelated molecules are found in the unit cell, for which the four hydroxy groups adopt a slightly distorted square planar arrangement, and deviate merely 0.2 Å from planarity. Donor-acceptor statistics for all hydrogen bonds are listed in Table 2.1. The hydrogen bonding within this species undoubtedly contributed to its stability, and permitted its isolation. The corresponding hydroxysilane may not be favoured in the diphenyl system, **32**, because of rotational interference engendered by the rings.

(a)

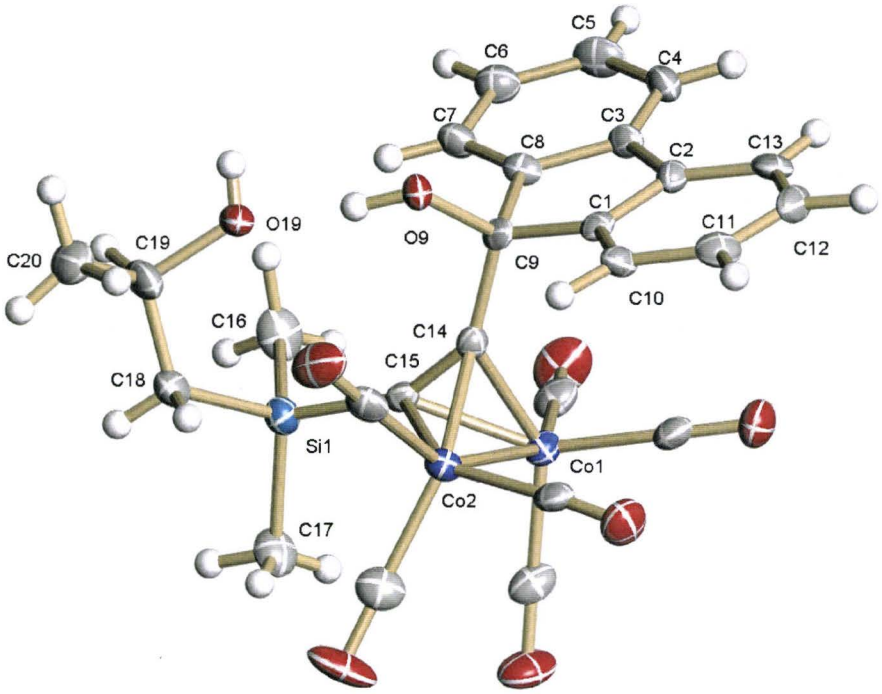

(b)

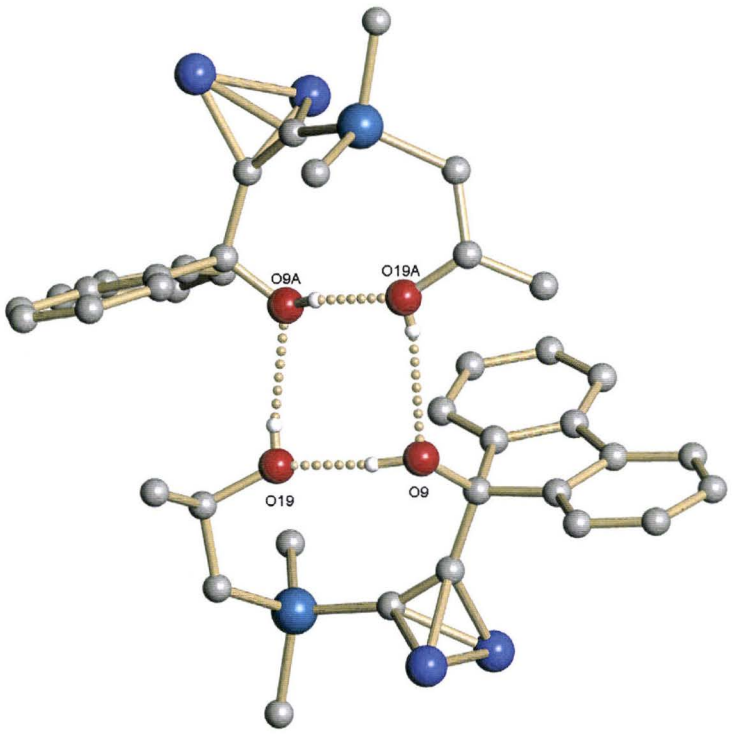

Figure 2.4 (a) Molecular structure of **42**, with 30% thermal probability ellipsoids. (b) Asymmetric unit, showing intra- and intermolecular hydrogen bonding, whereby irrelevant hydrogens and carbonyl groups have been removed for clarity.

Table 2.1: Intra- and Intermolecular Hydrogen Bonds in **49**.

D-H····A	D····H	H····A	D····A	D-H····A angle
O9-H····O19	0.87(4) Å	1.90(4) Å	2.732(6) Å	161(4)°
O9A-H····O19A	0.84 Å	1.91 Å	2.691(7) Å	154°
O19-H····O9A	0.72(5) Å	2.03(5) Å	2.740(8) Å	170(7)°
O19A-H····O9	0.63(7) Å	2.22(7) Å	2.835(8) Å	166(10)°

With respect to the other unexpected product, **43**, our initial thought was that it may have arisen through reaction of the fluorenyl-alkynyl anion, generated *in situ*, with any traces of acetone left from cleaning the glassware prior to conducting the experiment. However, repetition of this reaction, taking meticulous care to avoid any possibility of contamination by acetone, still afforded small quantities of the product, which was unambiguously identified X-ray crystallographically, as shown in Figure 2.5. As with the hydroxysilane, **42**, hydrogen bonding is a prominent feature of the crystal structure; however, unlike **42**, it is only manifested intramolecularly.

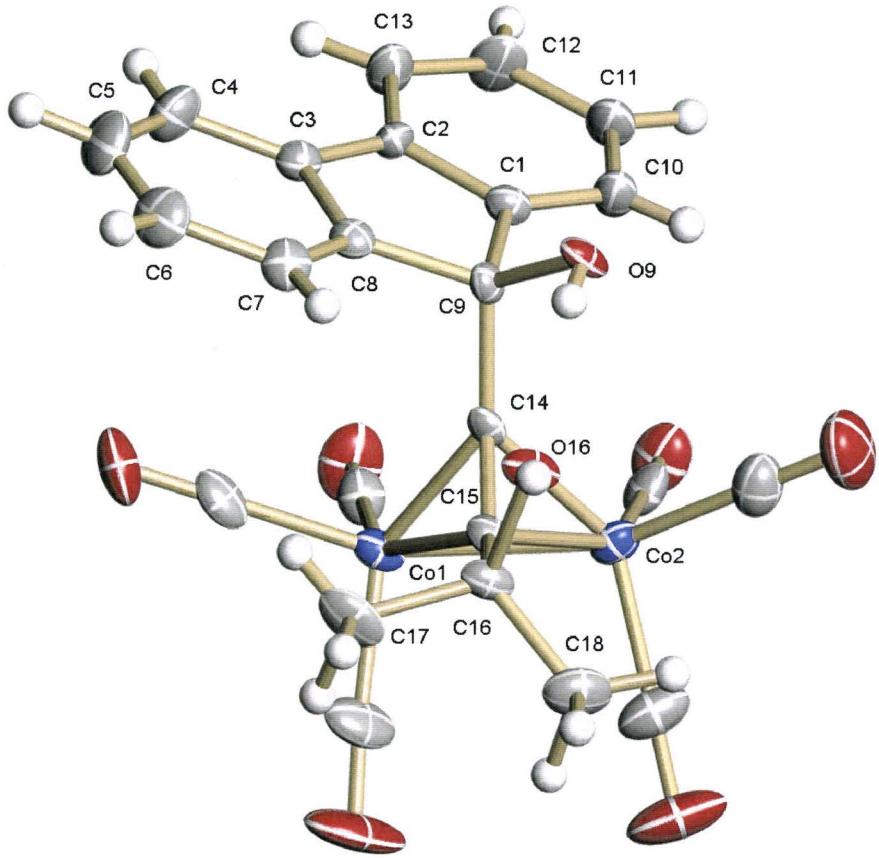

Figure 2.5 Molecular structure of **43**, with 30 % thermal probability ellipsoids. The intramolecular hydrogen bond contact between O9-O16 is 2.790 Å.

One cannot overlook the possibility that the three-carbon unit originated from the allyl substituent attached to the silane. It is not immediately evident how the allyl functionality migrates to the alkynyl terminus with concomitant cleavage of the dimethylsilyl fragment, however, it is suspected that a fluorenyl dimerization process is involved, and mechanistic investigations are ongoing.

2.3 Alternative Migratory Groups

Since the electronic and steric criteria for allyl migrations in cobalt clusters had been established, our objectives turned toward the investigation of other systems with the

potential to undergo analogous rearrangements. By retaining the propargyl alcohol functionality and altering the allylsilane, the idea was that these migrations might not be restricted to allyl groups, and therefore, the analogous vinylic and benzylic silanes were studied.

2.3.1 Vinylsilane

The vinylsilane was chosen because it has one carbon less in its chain, which would entail a much smaller, five-membered ring intermediate, **44**, (Scheme 2.12) – *assuming an intramolecular rather than an intermolecular process* – as opposed to the normal seven-membered ring invoked for the allyl migration.

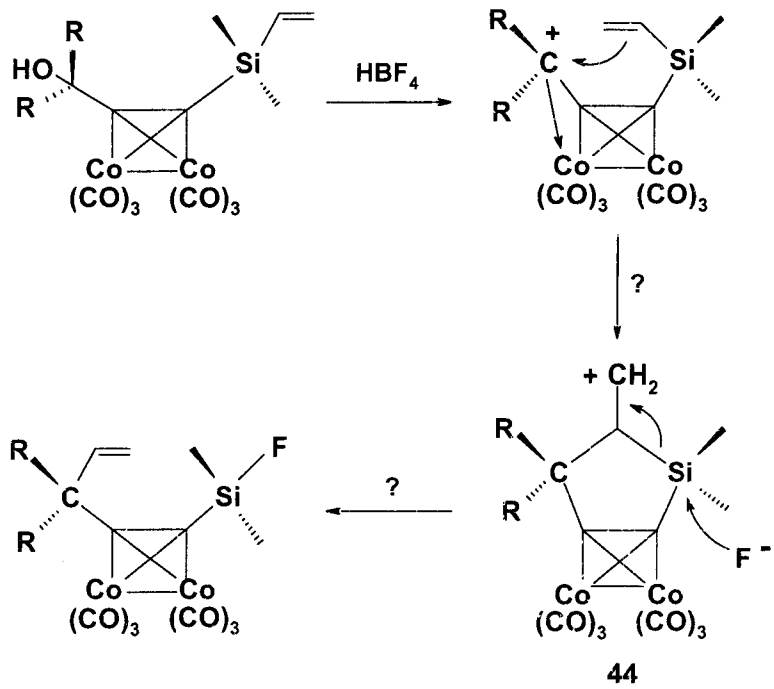

Scheme 2.12 Hypothesized route to a vinyl migration.

Although there are no examples of stable five-membered rings containing an alkyne functionality, even when complexed, it was hypothesized that the presence of a larger silicon atom might reduce the ring strain, whilst alleviating some of the developing charge on the primary carbocation, thereby making the cobalt-complexed silacyclopentyne, **44**, an achievable intermediate. In fact a Hyperchem[83] calculation at the PM3 level for the dimethyl substituted system, which proved so successful for allyl migrations, reveals that the externally eliminated analogue of **44**, might be a feasible 5-membered ring intermediate, as illustrated in Figure 2.6.

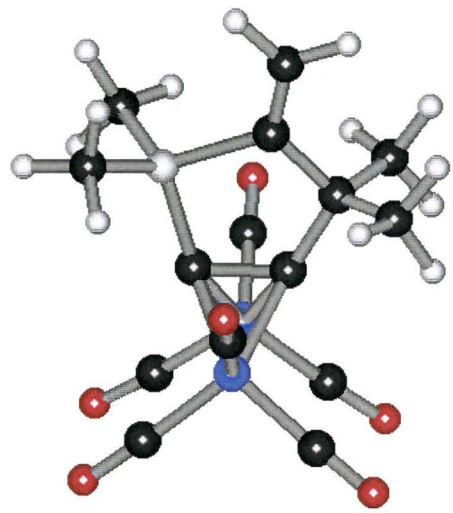

Figure 2.6 Hyperchem model of a possible 5-membered ring cobalt-cluster species.[83]

Two equivalents of nBuLi were allowed to react with a solution of 2-methyl-3-butyn-2-ol in anhydrous diethyl ether over a period of four hours, at which point vinyldimethylchlorosilane was added to the dilithiated intermediate to produce the ethynyl-vinylsilane, **45**. The alkyne was isolated after column chromatography with a 1:1 mixture of dichloromethane/hexanes as eluent; subsequent treatment with a solution of dicobalt octacarbonyl in THF yielded the cobalt-complexed vinylsilane, **46**, that was

purified chromatographically. However, protonation using HBF_4 afforded the elimination product, **47**, exclusively, indicating that vinyl migration was not a viable process (Scheme 2.13). Reprotonation of **46** did not afford any new products.

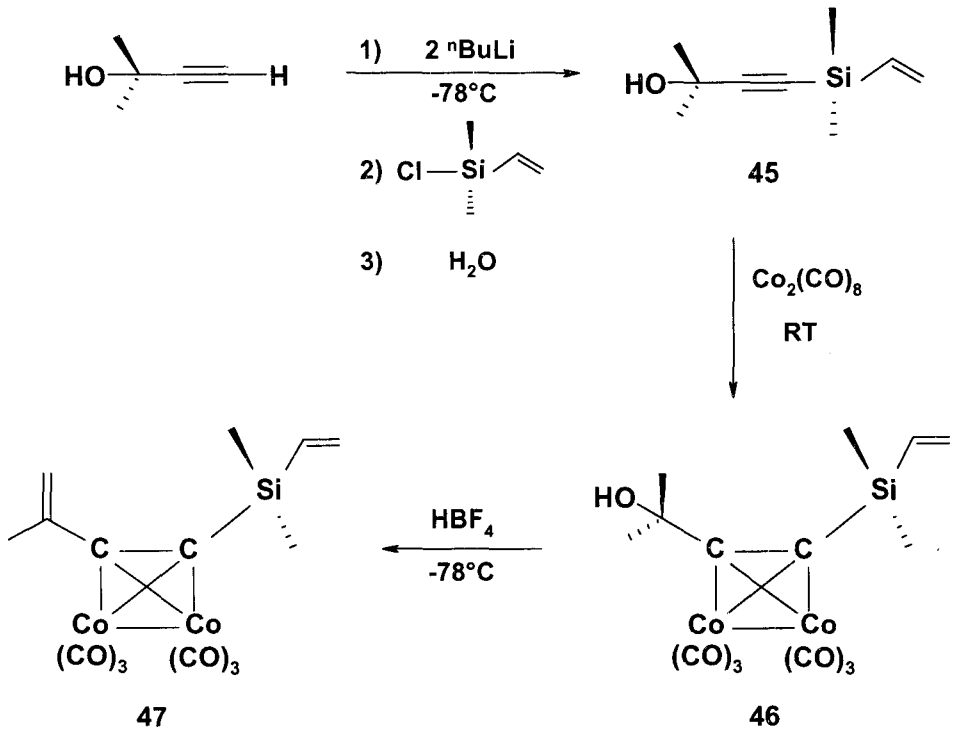

Scheme 2.13 Elimination product, **47**, obtained upon attempted vinyl migration.

One may surmise that formation of the metal-stabilized propargyl cation occurred, but that either ring strain prevented the formation of the five-membered ring intermediate or, more likely, the β-silicon was unable to provide sufficiently enhanced stability for the primary cation.

2.3.2 Benzylsilane

The benzyl substituent was chosen because of its similarity to the allyl group, in that the benzyl moiety actually contains an allyl subsystem. The objective was to

determine whether the thermodynamic driving force provided by the formation of a silicon-fluorine bond was great enough to induce a benzyl migration. In order for this to happen, the aromatic character of the phenyl ring would have to be lost, albeit temporarily, as illustrated in Scheme 2.14. Thus, the initial result of rearrangement, would be an energetically disfavoured methylene-cyclohexadiene, **48,** that should rapidly rearomatize to generate an ortho-tolyl substituent, **49**.

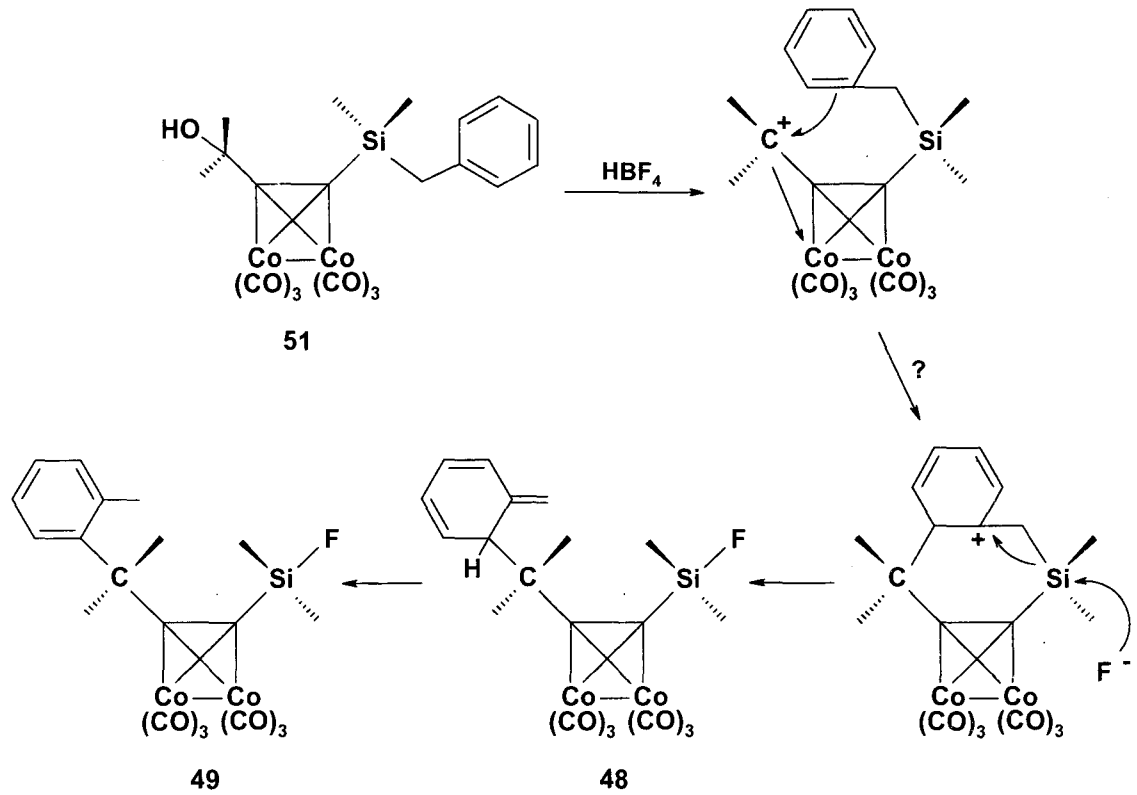

Scheme 2.14 Hypothesized benzyl migration overcoming aromaticity and rearomatizing.

The benzylsilane, **50**, was prepared analogously to the vinylsilane, and reaction with dicobalt octacarbonyl produced the metal-complexed benzylsilane, **51**. Not surprisingly, perhaps, protonation with HBF_4 did not result in a benzyl migration, but instead furnished the elimination product, **52**, exclusively (Scheme 2.15). Therefore, one

may conclude that the stability provided by the aromatic ring exceeds the thermodynamic driving force provided by the formation of a silicon-fluorine bond. Once again, elimination of water from the isopropyl alcohol was favoured over rearrangement involving the substituent bonded to silicon.

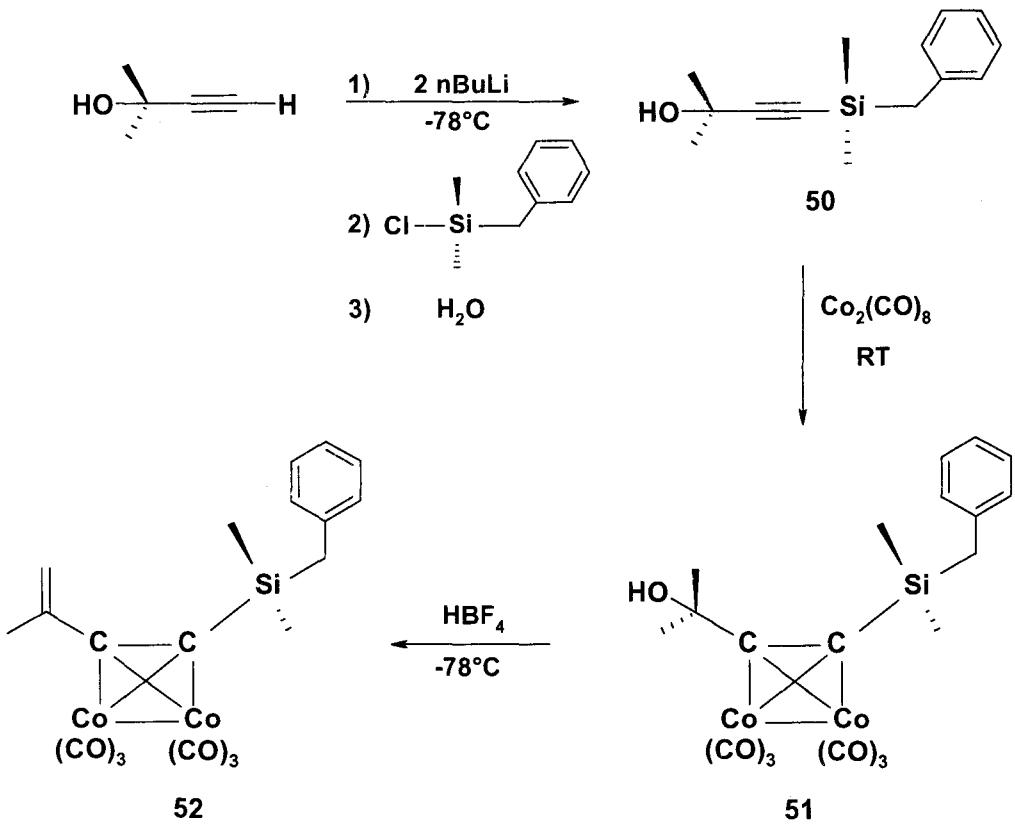

Scheme 2.15 Elimination product, **52**, obtained upon attempted benzyl migration.

2.3.3 Fluorenyl Analogues

To avoid the competing side-reaction of elimination, and to enhance the possibility of bringing about a vinyl or benzyl migration while maintaining minimal steric interference, the fluorenyl analogues of **46** and **51**, *i.e.* **53** and **54**, shown in Figure 2.6, were synthesized.

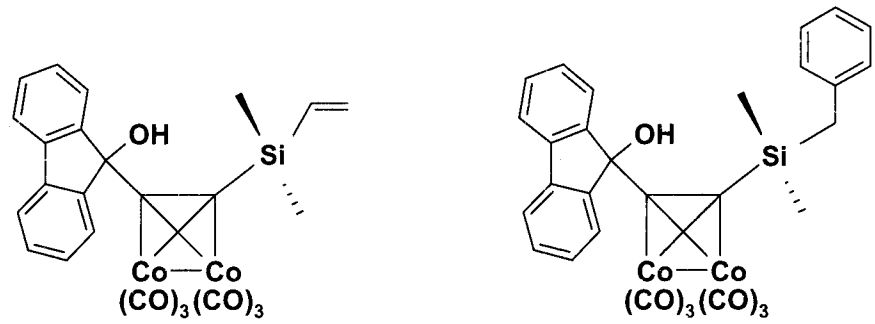

53 54

Figure 2.7 Potential migratory ligands.

However, protonation reactions in a variety of solvents did not yield any migration products, and instead afforded some intriguing radical derivatives, which will be described in Chapter 4. Evidently, one may conclude that vinyl and benzyl migrations are not possible in these simple systems, owing to their inability to stabilize any viable intermediates.

2.4 Summary

Therefore, it has become apparent that allyl migrations from one cobalt-complexed alkynyl terminus to the other are attainable when conditions are optimized to include sterically non-demanding functionalized propargyl alcohols, and to prevent simple elimination upon protonation of the alcohol. Seven-membered, and likely larger, cyclic intermediates appear to be feasible for this transfer, however preliminary calculations suggest that smaller silicon-containing ring intermediates may be possible under appropriate conditions.

Chapter Three: Tricobalt Clusters

3.1 Borneol and Fenchol

In light of our inability to induce vinyl or benzyl groups to undergo migrations analogous to those already found for allyl substituents, efforts were refocused on application of the allyl transfer reaction to other systems. By altering the organic moiety, while retaining the allylsilane, the generality of the allyl transfer reaction was investigated in the complementary borneol and fenchol systems.

3.1.1 Background

It has long been known that uncomplexed borneol and fenchol alkynes are susceptible to extensive Wagner-Meerwein type rearrangements upon protonation.[87] The transformation of 2-ethynylborneol, **55**, to 4-ethynylborneol, **57**, exemplifies this occurrence, as illustrated in Scheme 3.1. Initial protonation and isomerization of **55**, affords **56**, which can undergo a methyl shift (Nametkin rearrangement) and further rearrangement to yield **57** after quenching.[88]

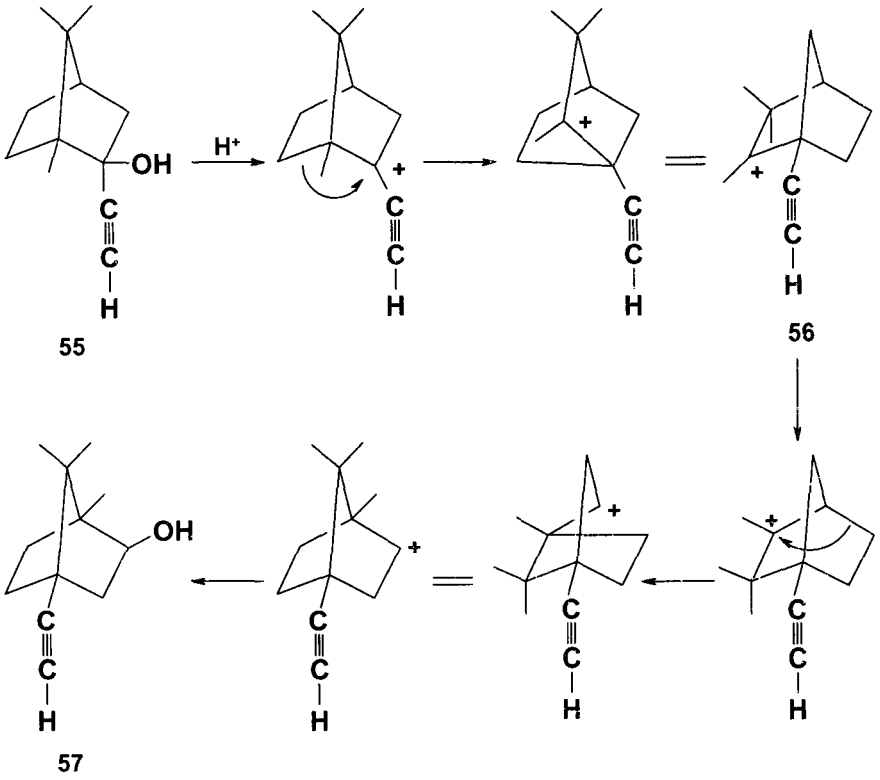

Scheme 3.1. Conversion of 2-ethynylborneol to 4-ethynylborneol via a Wagner-Meerwein rearrangement.

3.1.2 Introduction

It has been previously demonstrated in this laboratory that attaching a metal cluster to the *endo* position as in the 2-*endo*-propynylborneol hexacarbonyldicobalt derivatives, **58a**, will prevent this particular rearrangement in bornyl systems. Protonation of the bornyl cluster **58a,** at -78 °C, did not afford a Wagner-Meerwein rearrangement product, but instead yielded the cobalt-stabilized 2-bornyl cation, **59a**, that was identified by NMR spectroscopy.[89] More compellingly, replacement of a tricarbonylcobalt moiety by an isolobal (cyclopentadienyl)dicarbonylmolybdenum vertex, as in **58b**, afforded the corresponding molybdenum-stabilized cation, **59b**, which has been characterized by X-ray crystallography.[90] Conversely, the analogous fenchyl-

dicobalt cluster cation, **61a**, immediately undergoes a Wagner-Meerwein rearrangement to **62**, while the corresponding fenchyl-molybdenum cation, **61b**, is considerably more stable and has been structurally characterized (Scheme 3.2).[91]

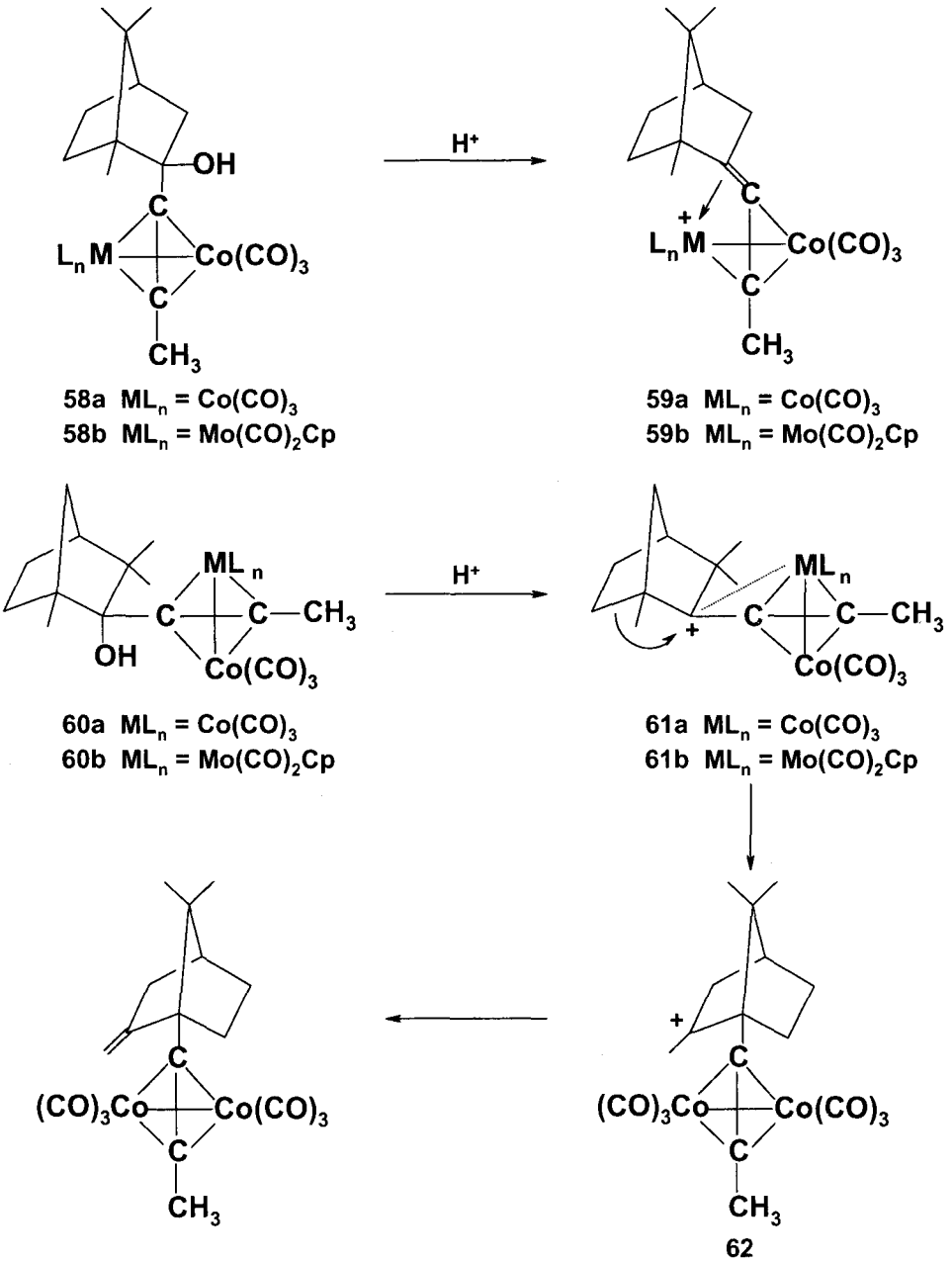

Scheme 3.2 Cationic clusters derived from borneol and fenchol.

3.1.3 Objective

Our original goal was to investigate the stereochemical requirements for this general reaction by incorporating the allyl-alkynylsilane within a rigid terpenoid skeleton. In particular, we were intrigued by the potential migration of an allyl group from an *endo* site to the *exo* face of a bornyl system (i.e., **63** → **64**), and vice versa (i.e., **65** → **66**) for the fenchyl analogue, as depicted in Scheme 3.3.

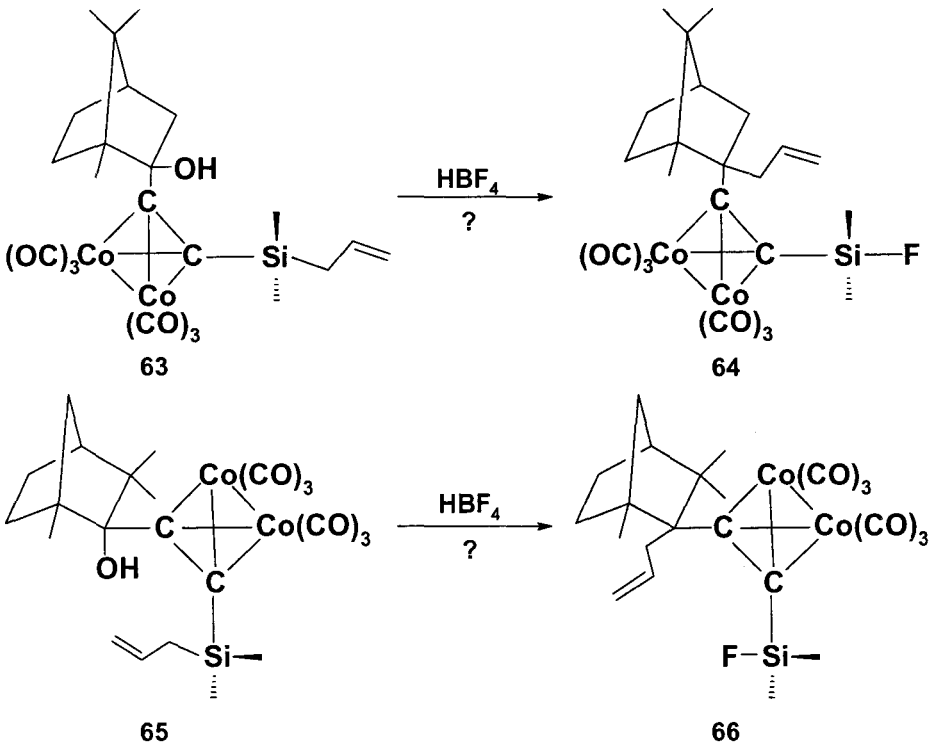

Scheme 3.3 Proposed allyl migrations in the bornyl and fenchyl systems.

Even though the potential for elimination upon protonation in the bornyl case was acknowledged, the belief was that some migration product might still be observed, even if it was necessary to reprotonate the alkene.

3.2 Results and Discussion

3.2.1 Borneol and Fenchol Allylsilanes

In the expectation that alkynyl anions would attack camphor from the *endo* face,[92] and fenchone from the *exo* face,[93] these ketones were each treated with trimethylsilylethynyllithium, at -78 °C. Removal of the TMS functionality with tetra-*n*-butylammonium fluoride and incorporation of the allyldimethylsilyl group affording **67** proved successful, as shown in Scheme 3.4 for the bornyl system.

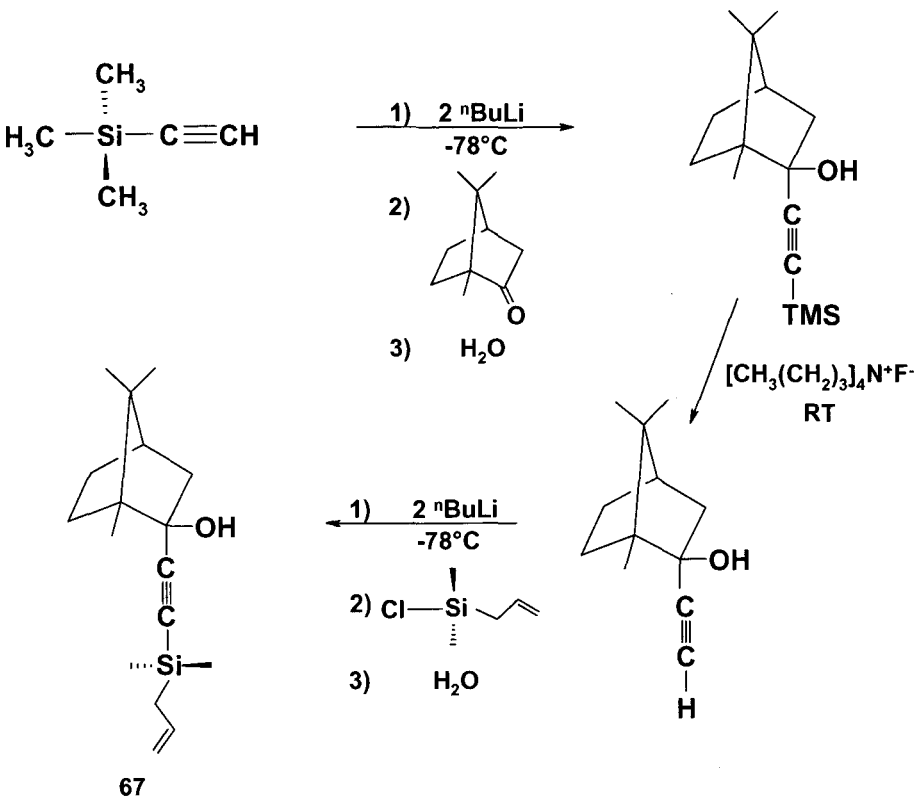

Scheme 3.4 Synthetic route to (2-*endo*-allyldimethylsilyl)ethynylborneol, **67**.

Addition of octacarbonyldicobalt to the appropriate alkynyl-allylsilanes afforded **63** and **65**, respectively, which were each treated with HBF_4 in ether at -78 °C and the products examined after chromatographic separation. It was immediately evident that the fenchyl system had yielded a multitude of products, each in very low yield. The ^1H NMR

and mass spectra of these materials indicated that the anticipated allyl transfer product was, at best, a minor constituent among many others. We therefore chose to focus our efforts on the more tractable bornyl system.

As shown in Scheme 3.5, when the *exo* alcohol **63** was treated with an equimolar quantity of HBF_4 in ether at -78 °C, the 2-alkynyl-2-bornene, **68**, and the fluorosilane, **69**, were formed.[94] However, when HBF_4 was added in excess and the reaction mixture allowed to warm to room temperature over a twelve-hour period, chromatographic separation yielded a third isolable product, the tricobalt cluster, **70**, involving an exocyclic elimination, as revealed by its 2-D ^1H-^1H COSY and ^1H-^{13}C shift-correlated NMR spectra. There was no evidence for production of the allyl migration product **64**.

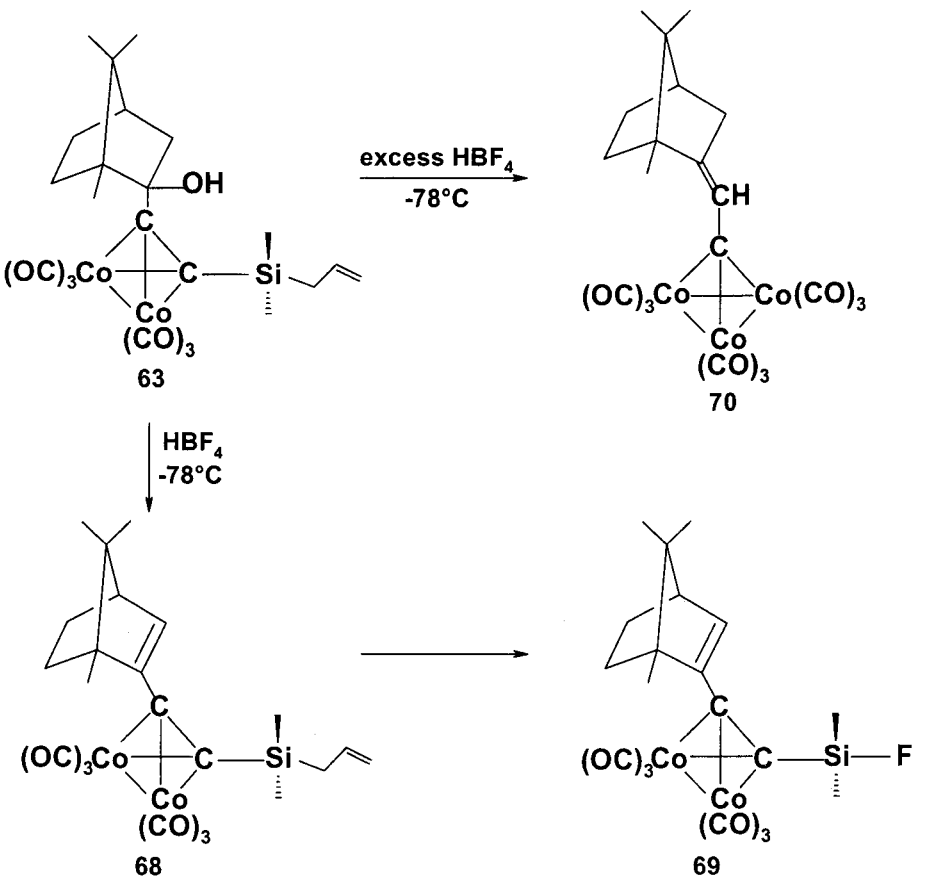

Scheme 3.5 Products derived from the protonation of **63**.

Routes to **68** and **69** may be readily envisaged; the former simply arises from elimination of water from the starting alcohol, while the latter results from protonation of the allyl group in **68** to generate a β-silyl cation with subsequent elimination of propene and concomitant formation of a silicon-fluorine bond.

Although it has long been known that terminal alkyne-dicobalt complexes of the type $(RC{\equiv}CH)Co_2(CO)_6$ can rearrange under acidic conditions to yield alkylidyne clusters $RCH_2\text{-}CCo_3(CO)_9$,[95-97] the mechanism of this transformation has never been elucidated, and will be addressed later in this chapter. Therefore, formation of the tricobalt cluster, **70**, which was analogous to the diphenyl tricobalt cluster, **33**, previously observed, implies the intermediacy of a terminal alkyne complex via cleavage of the allyldimethylsilyl functionality.

Interestingly, protonation of [(2-*endo*-trimethylsilyl)ethynylborneol]$Co_2(CO)_6$, yields only the elimination product, [(2-trimethylsilyl)ethynylborn-2-ene]$Co_2(CO)_6$, with no evidence for cleavage of the trimethylsilyl moiety, or formation of a trinuclear cluster.[94] This suggests that the presence of a thermodynamically favoured Si-F bond prompts cleavage of the silyl moiety, since fluorine is electron withdrawing, and perhaps weakens the opposing alkyne-silicon bond, thereby increasing its lability in comparison to the trimethylsilyl substituent.

3.2.2 Trimethylsilyl Allylsilane

In light of the apparent facile cleavage of the allyldimethylsilyl moiety from **63**, the closely analogous cluster $[Me_3Si\text{-}C{\equiv}C\text{-}SiMe_2(allyl)]Co_2(CO)_6$, **71**, was protonated with HBF_4 in ether at -78 °C, and yielded $[Me_3Si\text{-}C{\equiv}C\text{-}SiMe_2F]Co_2(CO)_6$, **72**, and

$[Me_3Si\text{-}C{\equiv}C\text{-}SiMe_2OH]Co_2(CO)_6$, **73** (Scheme 3.6); the latter compound is not evident as an initial product, and is apparently formed during chromatography on the silica column. After chromatographic purification, **72** was reprotonated in ether at -78 °C and afforded exclusively the terminal alkyne cluster **74**, verifying cleavage of the fluorodimethylsilyl functionality. It is worth noting that Knox and coworkers have demonstrated that protonation of similar mono- and di-silyl substituted molybdenum-alkynyl clusters readily leads to desilylation.[98] However, the greater tendency towards dissociation of the fluorosilane relative to the trimethylsilane, implies that the electron withdrawing character of fluorine significantly weakens the opposing silicon-carbon bond, thereby affording it more susceptible to cleavage than a TMS group. Further protonation of **74** did not produce the expected tricobalt species, $Me_3Si\text{-}CH_2\text{-}CCo_3(CO)_9$, **75**; however, when **74** was heated at reflux in acetone over a 36 hour period, **75** was produced.[94]

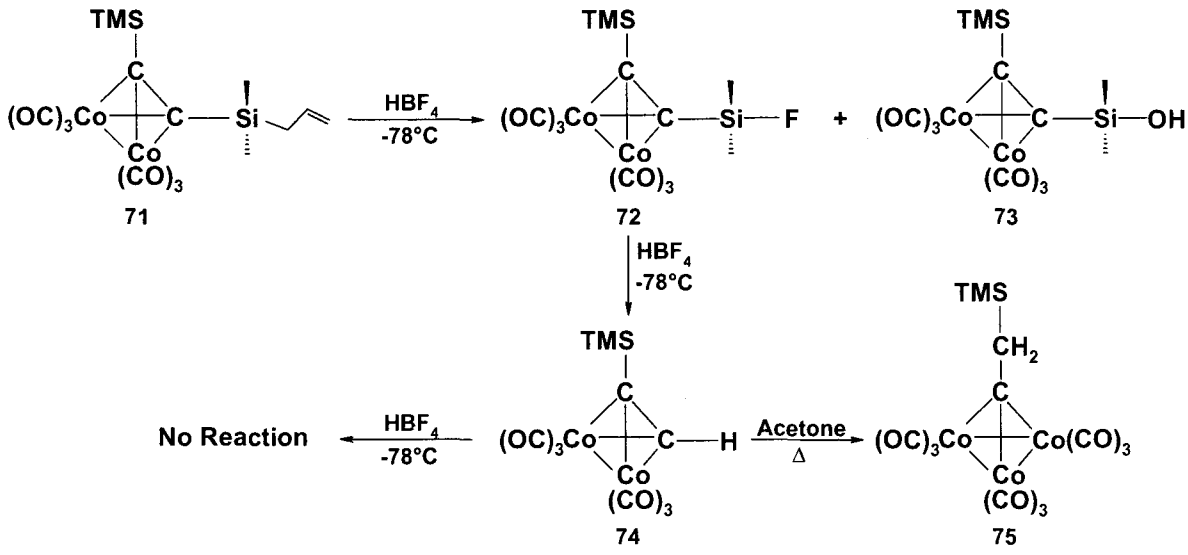

Scheme 3.6 Products derived from the protonation of **71**.

3.2.3 Cobalt-Mediated Ethynylborneol Rearrangements

Concluding that either **63** or **69** can suffer desilylation under acidic conditions, we chose to study the behavior of (2-*endo*-ethynylborneol)$Co_2(CO)_6$, **76**, to investigate the susceptibility of both the alkyne and hydroxyl sites towards protonation, under various conditions. Initially **76** was heated in refluxing acetone for 36 hours, thereby generating two tricobalt clusters: the previously prepared **70**, and its corresponding alcohol **77**, the structure of which was definitively established by X-ray crystallography.[94] A slight rotational disorder of the borneol function around the conjoining methylene unit of the tricobalt cluster prevented anisotropic refinement of the ligand. However, the *endo* positioning of the cluster in **77** is clearly evident in Figure 3.1. In contrast, duplication of this reaction in diethyl ether merely resulted in re-isolation of the starting material, **76**. It is perhaps somewhat surprising that such rearrangements have been shown to occur in acetone, and one cannot entirely eliminate the possibility that traces of an acidic impurity, present within the solvent, served as the protonating species.

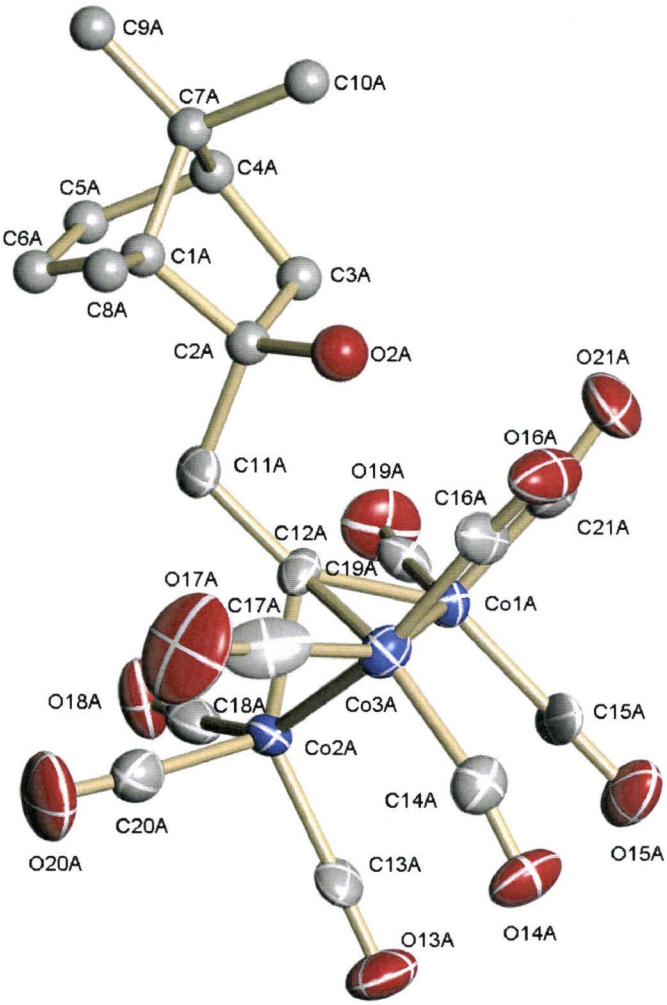

Figure 3.1. X-ray crystal structure of **77** showing the atom numbering system, with hydrogen atoms omitted for clarity.

Additionally, treatment of the (2-*endo*-ethynylborneol)$Co_2(CO)_6$ complex, **76**, with HBF_4 in ether at -78 °C, and chromatographic separation of the mixture after warming to room temperature, furnished two major products: the 2-alkynyl-2-bornene complex, **78**, and a second complex, **79**, isomeric with **78**, as shown in Scheme 3.7.[94] A third product, obtained in minimal yield, appears to have undergone ring-opening and a carbonyl insertion, but currently remains unidentified.

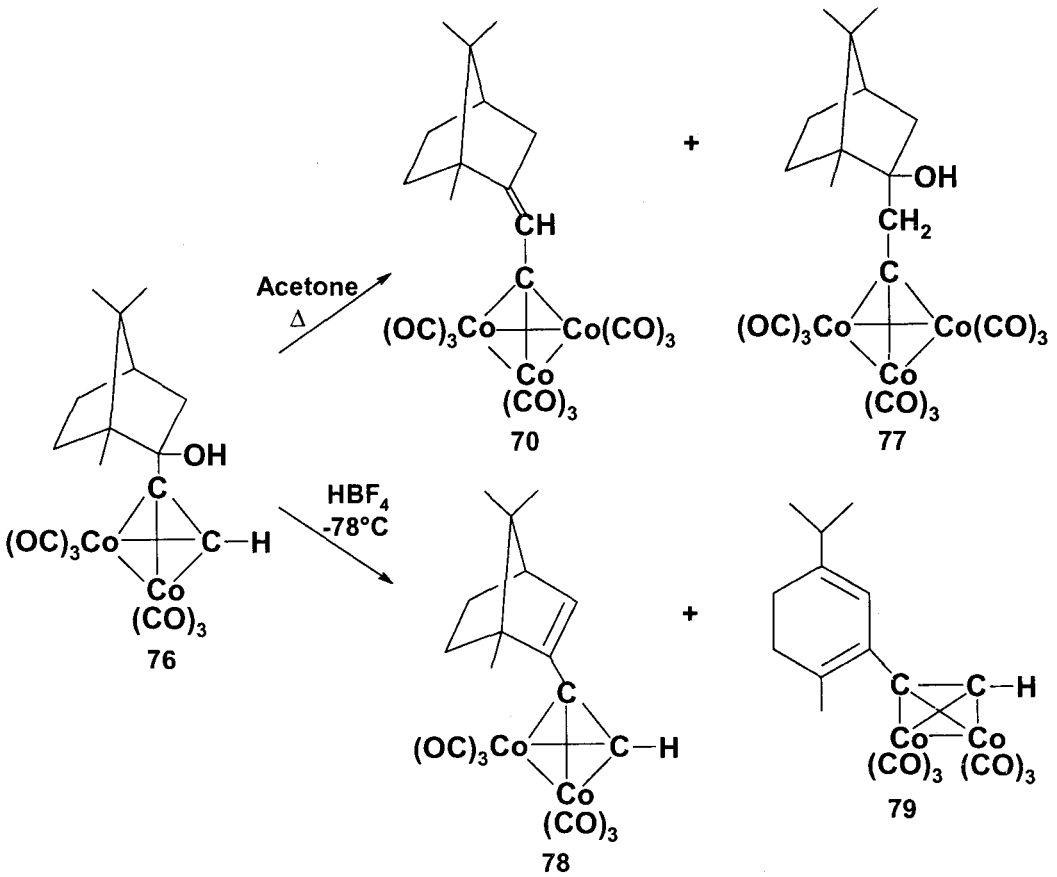

Scheme 3.7 Products derived from the protonation of **76**.

The identification of **79** relies on its mass and NMR spectra. The presence of the $(HC{\equiv}C)Co_2(CO)_6$ moiety is evident from the characteristic loss of six carbonyls in the mass spectrum, while the isopropyl group is readily observable in the ^1H and ^{13}C NMR spectra, and was confirmed by ^1H-^1H COSY and ^1H-^{13}C shift-correlated experiments. These latter data also established that the methylene groups were adjacent; moreover, one pair of methylene protons exhibited a long-range correlation to the ring carbon bearing the isopropyl substituent. The final assignment as the 2-ethynyl-4-isopropyl-1-methylcyclohexa-1,3-diene complex, **79**, is unambiguous,[99] and a mechanistic rationale appears in Scheme 3.8.[94]

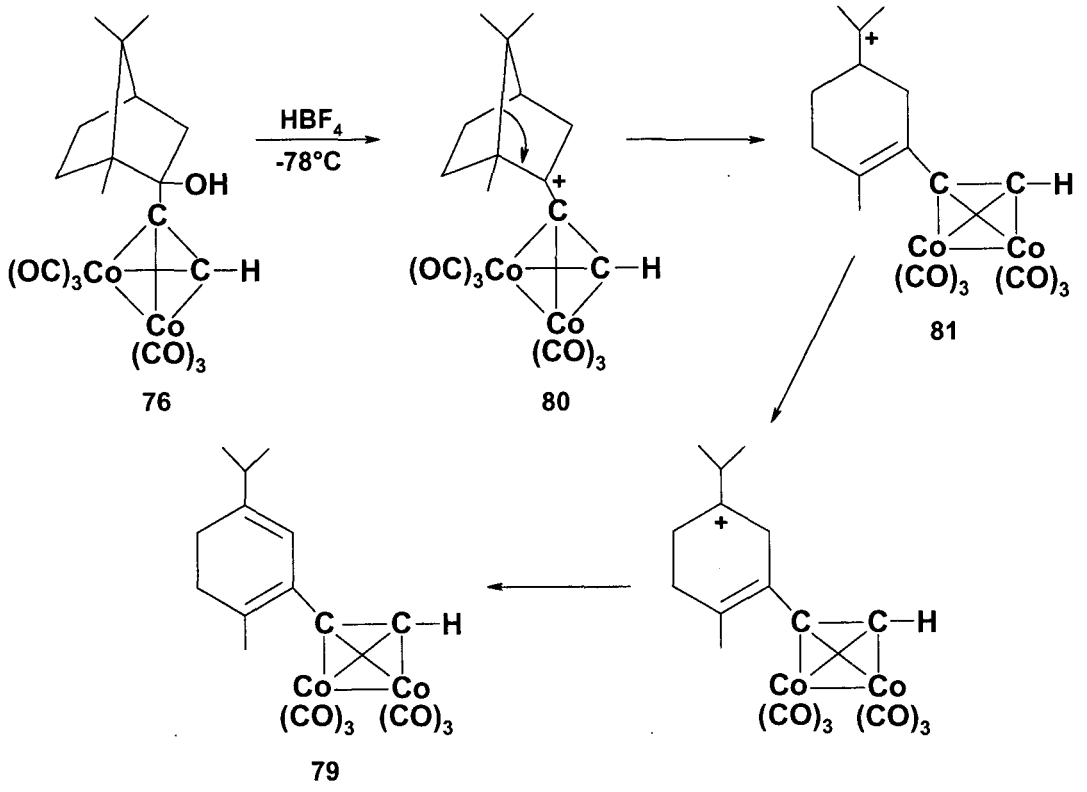

Scheme 3.8 Ring-opening and rearrangement of **76**.

Ring opening of the dimethyl bridge in cation **80** to yield the tertiary cation **81** is favored by the anti-periplanar alignment of the C(1)-C(7) linkage with the *endo*-C(2)-Co bond. A 1,2-hydride shift, to generate the isopropyl group, and subsequent elimination leads directly to the conjugated diene-yne complex **79**.[94]

A literature search revealed that this is the first metal complexed ring-opening of a bornyl entity. However, these ring openings are not unknown in purely organic systems, as they can be traced back to more than a century ago, where camphor was found to undergo a ring opening to produce 3,4-dimethylacetophenone and carvenone upon reaction with sulfuric acid.[100] An elegant illustration of this phenomenon involves 2-*endo*-bornylamine, **82**, which furnishes, upon diazotization, the bridge-opened products **83** and **84**.[101] In complete contrast, 2-*exo*-bornylamine, **85**, is perfectly aligned for a

Wagner-Meerwein rearrangement and gives **86** and **87**, as shown in Scheme 3.9. Currently, bornyl ring openings are induced efficiently through substitution of bromine on the *anti* apical methyl, and treatment with an acid or sodium salt, in natural product syntheses.[102]

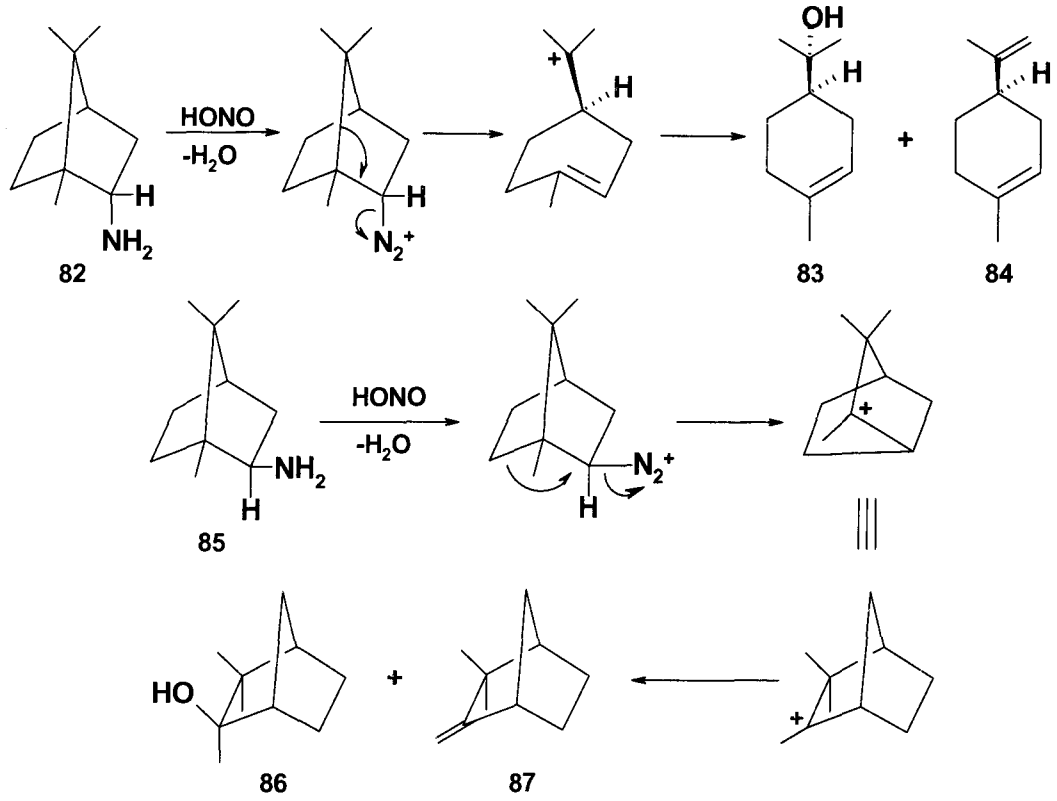

Scheme 3.9 Rearrangements of *endo* and *exo* bornyl diazonium ions.

One can now appreciate how the fenchyl cluster **65** might yield a plethora of products, not merely via generation and rearrangement of a terminal alkyne cluster, but also through Wagner-Meerwein skeletal rearrangements of the terpene skeleton, which are known to be very extensive in fenchol itself.[100a,103]

These results, while rationalizing the observed products, do not explain the failure of the bornyl-allylsilane dicobalt complex, **63**, to undergo an allyl migration, and one should consider steric effects that might hinder formation of the crucial seven-membered

ring cationic intermediate, **88**. To this end, the structure of this intermediate has been modelled[83] (Figure 3.2), and it can be seen that the presence of the spiro-C(2) centre brings about unfavourable interactions between the allyl unit and one of the methyl groups attached to C(7).[94] Presumably, this effect hinders the allyl transfer process, which makes the terpene skeletal rearrangements and the cluster transformations more competitive.

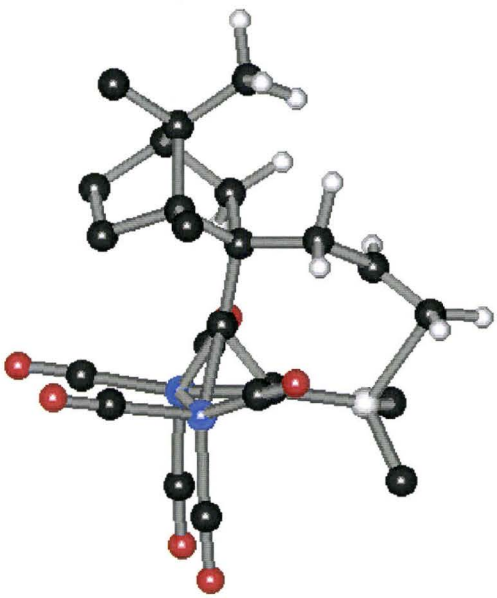

Figure 3.2. Semi-empirically derived model of **88** (PM3 Hamiltonian), showing only pertinent hydrogen interactions.[83]

3.3 Tricobalt Clusters

3.3.1 Background

Currently, the most widely used route to alkylidyne-tricobalt nonacarbonyl clusters involves the reaction of the appropriate trichloromethyl precursor, $RCCl_3$, with $Co_2(CO)_8$.[104] However, the first trinuclear cobalt cluster, CH_3-$CCo_3(CO)_9$, was prepared serendipitously in 1958 by Cotton and coworkers, from reflux of the parent compound, $(HC{\equiv}CH)Co_2(CO)_6$, with aqueous sulfuric acid in methanol.[95] Krüerke and Hübel

initially identified the compound spectroscopically, and used chemical degradation studies to propose a tetrahedral structure comprised of one apical carbon σ-bonded symmetrically to three cobalt atoms in a triangular plane,[96] which Dahl later confirmed with X-ray crystallography.[97] Since then, it has been well established that tricobalt clusters are generated from their corresponding dicobalt acetylenic precursors upon addition of a strong acid,[104] and subsequently, Pauson has used this reaction (Scheme 3.10) to convert terminal alkynes into the corresponding esters.[105]

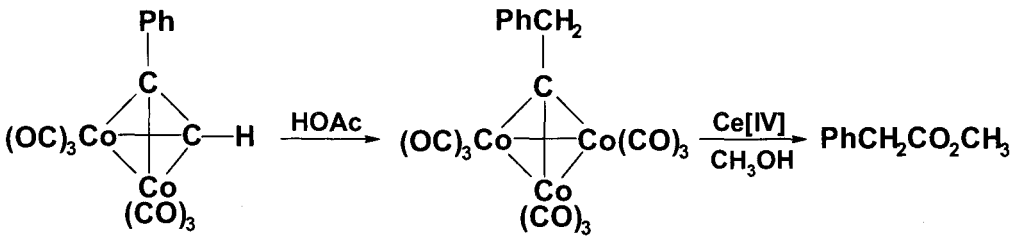

Scheme 3.10 Conversion of [phenylacetylene]$Co_2(CO)_6$ to methyl phenylacetate.

3.3.2 Mechanistic Investigation

Although it was initially postulated that migration of an acetylenic hydrogen must be involved in this transformation,[96] the origin of the methylene hydrogens have never been precisely resolved, and therefore, any mechanistic description must first determine the source of these hydrogens in the final product. Morawietz[94,106] readily accomplished this by reaction of (PhC≡C**D**)$Co_2(CO)_6$ with acetic acid which furnished Ph-C**HD**-$CCo_3(CO)_9$, **89**; likewise, treatment of (PhC≡C**H**)$Co_2(CO)_6$ with deuterated acetic acid also led to **89**, as seen in Scheme 3.11.[94] Figure 3.3 shows the ^{13}C NMR resonance of the -CHD- linkage in **89,** which appears as a deuterium-coupled triplet at 62.9 ppm.[106] These experiments established unequivocally that one of the methylene hydrogens was originally bonded to the terminal alkyne carbon, while the acid provides its partner.

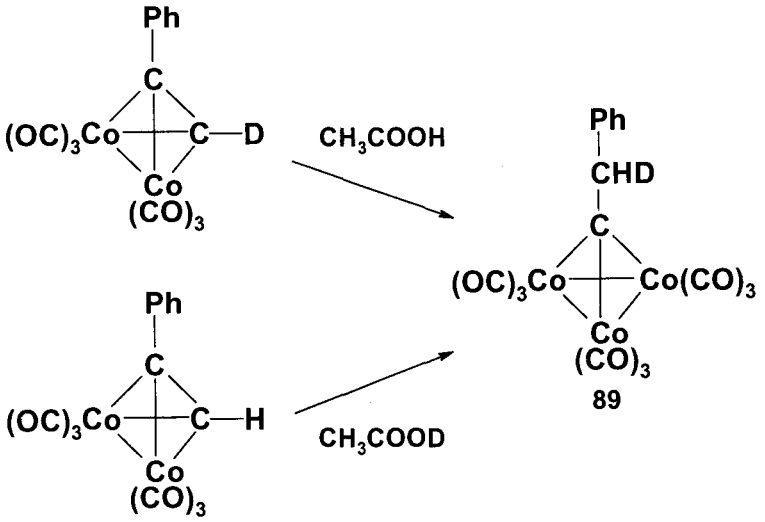

Scheme 3.11 Dual synthesis of the mono-deuterated tricobalt species, **89**.[106]

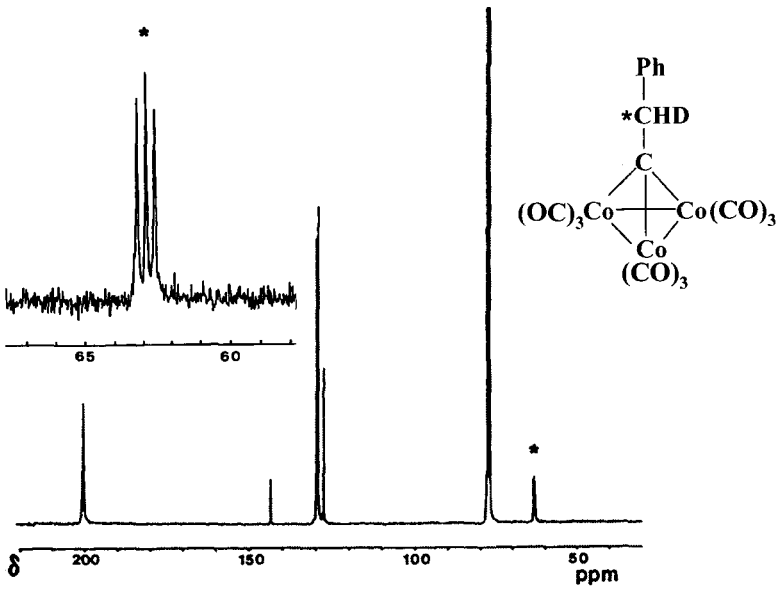

Figure 3.3. ^{13}C NMR spectrum of **89** in $CDCl_3$.

An important observation made independently by Curtis[107] and by Knox[108] must be noted, whereby protonation of the terminal dimolybdenum-alkyne clusters, $Cp_2Mo_2(CO)_4(RC{\equiv}CH)$ generates the μ-η^1,η^3-vinyl complex **90**. Curtis also indicated that in all cases studied, the vinyl units have the *E* configuration thus implying that the

initial site of attack by the proton was at the metal-metal bond, with subsequent migration to the coordinated alkyne.[107] This assertion is greatly strengthened by Stone's isolation of $[Cp_2W_2(CO)_4(\mu\text{-}H)(RC{\equiv}CR)]^+$, **91**, in which the hydrogen bridges the tungsten vertices.[109] Moreover, Stone has also characterized $Cp_2W_2(CO)_4[Et(\mu\text{-}H)B{\equiv}CMe]$, **92**, whereby the hydrogen bridges the tungsten-boron bond, as shown in Figure 3.4.[110]

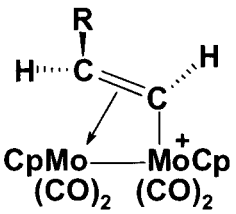

90

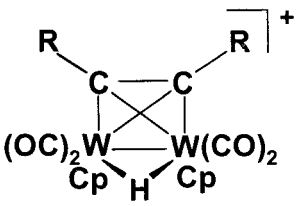

R = Me or p-tolyl

91

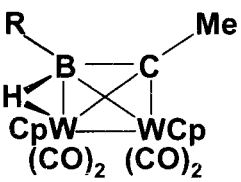

92

Figure 3.4 Molecules **90-92**

A hypothesis may now be ventured based upon these observations, which, when taken together with the isolobal analogy,[33] lend themselves to a viable mechanistic proposal. Scheme 3.12 presents a series of sequential steps for attaining a tricobalt cluster from its dicobalt-complexed terminal alkyne involving: (a) initial protonation across a cobalt-cobalt bond, as in **93**; (b) bridging and then transfer of this hydrogen to the *internal* carbon of the alkyne linkage, **94** → **95**; (c) migration of the *terminal* hydrogen so as to generate the required methylene group, thus placing the cationic charge on either a metal vertex, as in **96**, or on the bridging carbon atom. However, a more attractive resonance structure would regard this species as a Hückel-type 2π aromatic cyclopropenium cation, **97**, in which two of the CH units have been replaced by isolobal $Co(CO)_3$ vertices.[33]

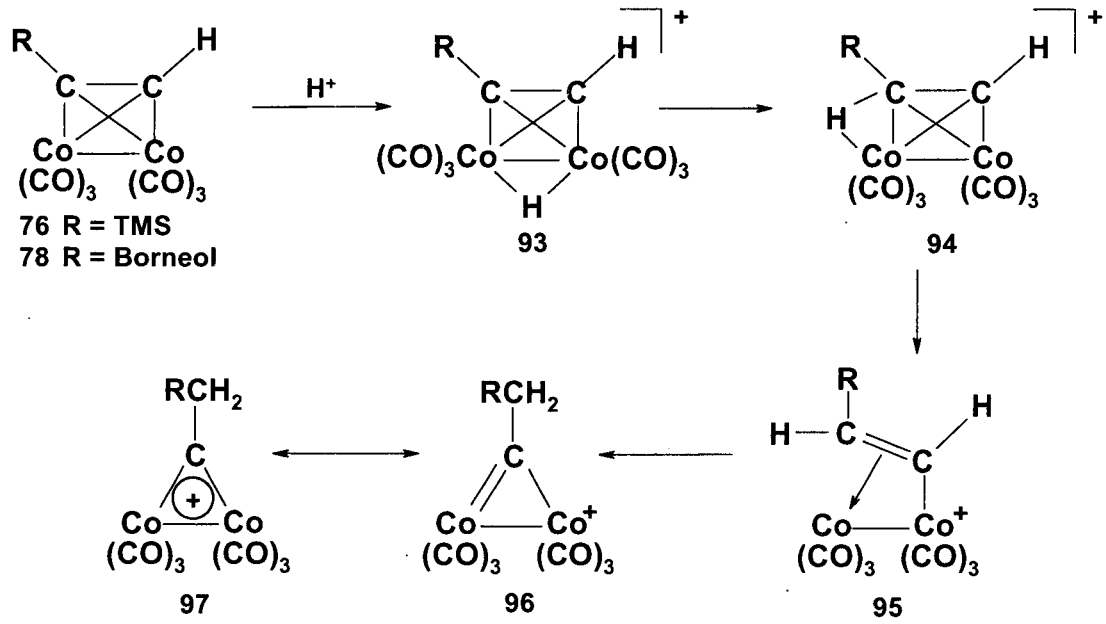

Scheme 3.12 Proposed mechanism for acid-promoted rearrangement of terminal alkynl dicobalt complexes.[95]

It is particularly noteworthy that the previously mentioned $[(\mu\text{-}\eta^1,\eta^3\text{-}CH{=}CH_2)Mo_2(CO)_4Cp_2]^+$ complex, **90**, is fluxional whereby the cyclopentadienyl environments, and also the geminal vinylic protons, undergo site exchange. Knox has suggested a mirror-symmetric transition state, **98**, such that the vinyl fragment bridges the molybdenum-molybdenum bond.[108] We note that an intermediate of this type would facilitate migration of the unique hydrogen and lead directly to the dimetallacyclopropenium structure, **99**, as depicted in Scheme 3.13.[94]

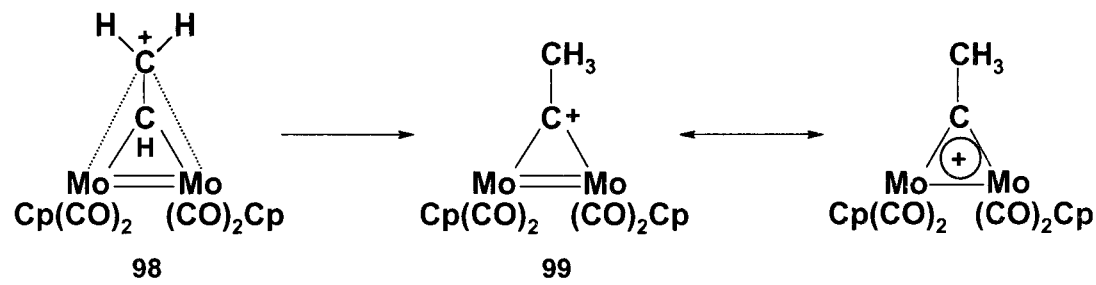

Scheme 3.13 Proposed route to a dimetallacyclopropenium intermediate.

It should be noted that this mechanistic proposal applies to the origination of tricobalt clusters from terminal alkynyl precursors, and the formation of trinuclear species from alkynyl silanes via initial cleavage of the silicon group to produce the corresponding terminal alkyne. However, due to the ease of this transformation, one cannot ignore the possibility of a concerted process, whereby desilylation affords a dimetalla-methylenecyclopropene, **100**, which subsequently undergoes protonation to produce the resonance stabilized cyclopropenium ion, **97**, as illustrated in Scheme 3.14.

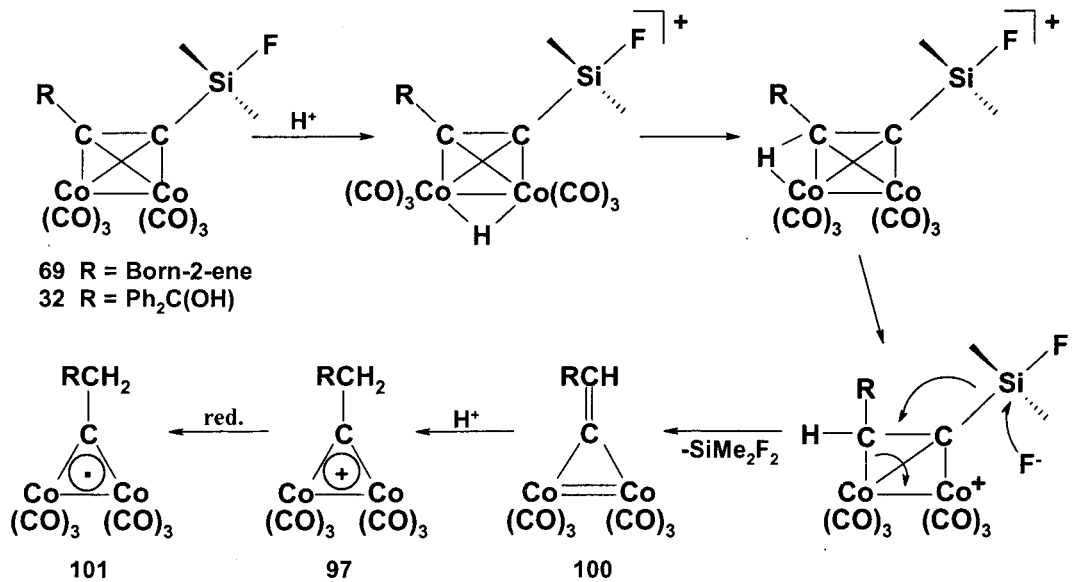

Scheme 3.14 Proposed mechanism for acid-promoted rearrangement of alkynylsilane dicobalt complexes.

It is freely admitted that this is merely a proposed mechanistic pathway for the dicobalt system, but it is important to note that several of the intermediates invoked, in particular **93**, **94** and **95**, have been unequivocally characterized where the $Co(CO)_3$ vertices have been replaced by other isolobal metal vertices such as $(C_5H_5)Mo(CO)_2$ or $(C_5H_5)W(CO)_2$, in **91**, **92** and **90**, respectively. The final step whereby the third metal is incorporated to generate the tetrahedral cluster remains unclear at present, and may either

involve addition of $HCo(CO)_4$ across **100**, or reduction of the dimetallacyclopropenium cation, **97**, to the corresponding radical, **101**, and subsequent coupling with $(CO)_4Co\bullet$ or a related species.

Although it is believed that $[Co(CO)_4]^-$ is the active reagent in generation of tricobalt complexes from the aforementioned reaction of trihalo compounds with octacarbonyldicobalt,[104a] it should be acknowledged that several early reports suggested that $HCo(CO)_4$ was involved in the generation of trinuclear cobalt clusters by direct reaction of octacarbonyldicobalt with terminal alkynes. It was proposed that the cobalt-complexed alkyne is formed initially and subsequently reacts with any excess free alkyne, serving as the acid. However, these ideas appear to have been discounted by the failure to detect any trinuclear species upon the addition of $HCo(CO)_4$ to $[PhC{\equiv}CH]Co_2(CO)_6$.[111] Therefore, it is perhaps more likely that a radical species is involved in the final step with regards to formation of tricobalt species.

3.4 Summary

It is now apparent that (propargyl alcohol)$Co_2(CO)_6$ terpenoidal systems derived from terminal alkynes can exhibit a wide variety of reactivity patterns, such as ring-openings and formation of trinuclear clusters, in addition to the Wagner-Meerwein rearrangements characteristic of the uncomplexed systems. Moreover, one might hope that the mechanistic speculations concerning the acid-promoted conversion of $(RC{\equiv}CH)Co_2(CO)_6$ complexes into alkylidyne- nonacarbonyltricobalt clusters, RCH_2-$CCo_3(CO)_9$, have offered some enlightenment into this fascinating transformation.

Chapter Four: Cobalt-Complex Mediated Radical Products

4.1 Radicals

4.1.1 Background

Atoms or molecular fragments with unpaired electrons are classified as radicals, and generally are extremely reactive. Whereas ions result from the heterolytic fragmentation of molecules, radicals result from a symmetrical cleavage of a covalent bond, whereby one electron remains with each newly formed species. Radicals are often formed under mild conditions and can provide an efficient method of generating carbon-carbon bonds in a wide variety of organic syntheses.[112] Radical chemistry has been studied for over a century, starting with the initial investigation by Gomberg of the triphenylmethyl radical and its reactive properties.[113] Nearly three decades later, Paneth elegantly demonstrated that radicals were also manifested in less stable alkyl systems, through studies in the gaseous phase.[114] More notably, radicals were shown to be involved in homolytic aromatic substitutions and the anti-Markovnikov addition of hydrogen bromide to olefins.[115] The formation, structure, reactions,[116] and absolute rate constants[117] of general radical systems were later compiled.

Radicals are implicated in explosions, combustions, pyrolyses, and many reactions of industrial importance such as the thermal cracking of petroleum, various polymerizations from the formation of synthetic rubber from styrene and butadiene to more recent productions of neoprene, polyethylene, and other plastics. Radicals are also

characterized intermediates in several vital processes, including respiration and photosynthesis.[118]

Bond cleavage to afford radicals may be accomplished by photolysis, thermolysis, radiation or oxidation/reduction of a molecule, and in organic syntheses, typically involve an initiator to induce formation. Although radical initiators range from azo compounds to peroxides, organoboranes and inorganic metal halides, AIBN (2,2′-azobisisobutyronitrile), shown in Scheme 4.1, is the most widely applied reagent for this purpose, as it is has an easily surmountable bond dissociation energy, and a half-life of one hour at 81°C.[118]

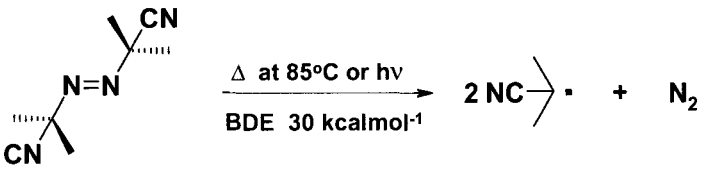

Scheme 4.1: Dissociation of the radical initiator AIBN.

The formation of radicals can be catalytic in that only a small amount of radical initiator is required for initiation of the active species, which may then undergo several cycles of propagation before the existing radical is terminated by combination or disproportionation, as shown in Scheme 4.2 for the chlorination of a hydrocarbon, RH.[119]

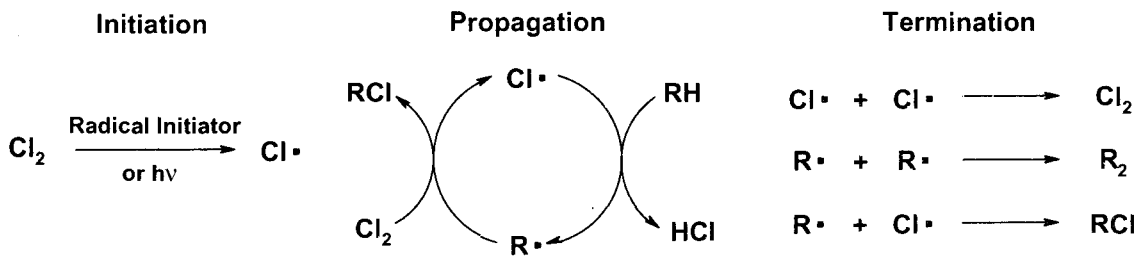

Scheme 4.2: Radical chain reaction for the chlorination of a hydrocarbon.

4.1.2 Introduction

Although radicals have been recognized for approximately a century, radical chemistry has been less developed in organometallic systems. Specifically, with regard to this dissertation, it has been previously established that cobalt-stabilized cations derived from (propargyl alcohol)$Co_2(CO)_6$ clusters such as **102**, are well-characterized and have been extensively exploited for synthetic purposes.[44] However, the corresponding radical chemistry has been less well studied,[120] and has generally involved the addition of a radical initiator, or a reducing metal such as zinc.[121] This is exemplified in Scheme 4.3, where Nicholas and Melikyan[122] have generated coupling products via zinc reduction of the initially generated propargyl cation.

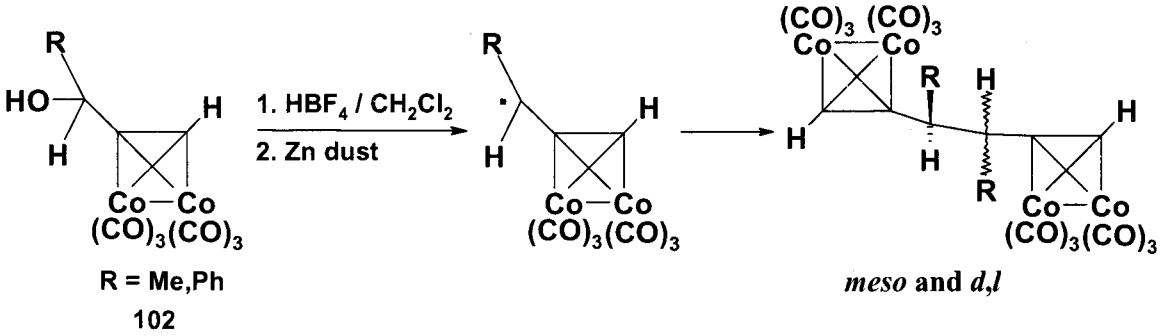

Scheme 4.3 Formation of radical products through protonation in the presence of zinc.

More recently, Melikyan[123] has noted that formation of cobalt-stabilized cations in certain solvents, notably THF or ether, induces a similar electron transfer, thereby yielding the identical coupling products as were afforded by zinc reduction. Furthermore, Melikyan proposed that cobalt stabilized propargyl cations generated *in situ* will undergo either single electron transfer (SET) or hydride ion transfer (HIT) in several other solvents.[123a] Efficient hydride ion donor solvents such as 1,4-cyclohexadiene and tributyl

tin result primarily in hydride abstraction, whereas dimerization is promoted in the presence of a milder hydride ion donor via a one electron reduction. THF and 1,3-dioxolane are found to be the most prolific reducing solvents, however several sulfur-containing radical mediators are also efficient, including tetrahydrothiophene and 1,3-dithiane.[123b] In accordance with these studies, Melikyan concluded that there are two possibilites for formation of these radicals: (i) donation of a single electron from a heteratom (O, S) to the carbocationic centre (Path A), or (ii) electrophilic attack of the α-C-H bond of the solvent by the empty p-orbital of the cation (Path B). The former may be discounted for several reasons, including the reduced reactivity in the presence of diethyl ether, the variation in reaction time for different O-containing solvents, and the lack of acceleration observed in the less electronegative S-containing species.[123b] In addition, it has been well established that the interaction of oxygen-, sulfur-, nitrogen- and phosphorus-containing nucleophiles with cobalt stabilized cations results in various solvolysis products without any evidence of dimerization.[124] Therefore, it is highly probable that a three-centre-two-electron transition state similar to **103**, will lead either to hydride abstraction (HIT) or a single electron transfer (SET) with subsequent dimerization, as shown in Scheme 4.4. The final state of tetrahydrofuran is not known, however, it is probable that the resulting derivative of THF is likely a dimeric or oligomeric species that is sufficiently volatile to be removed during roto-evaporation.

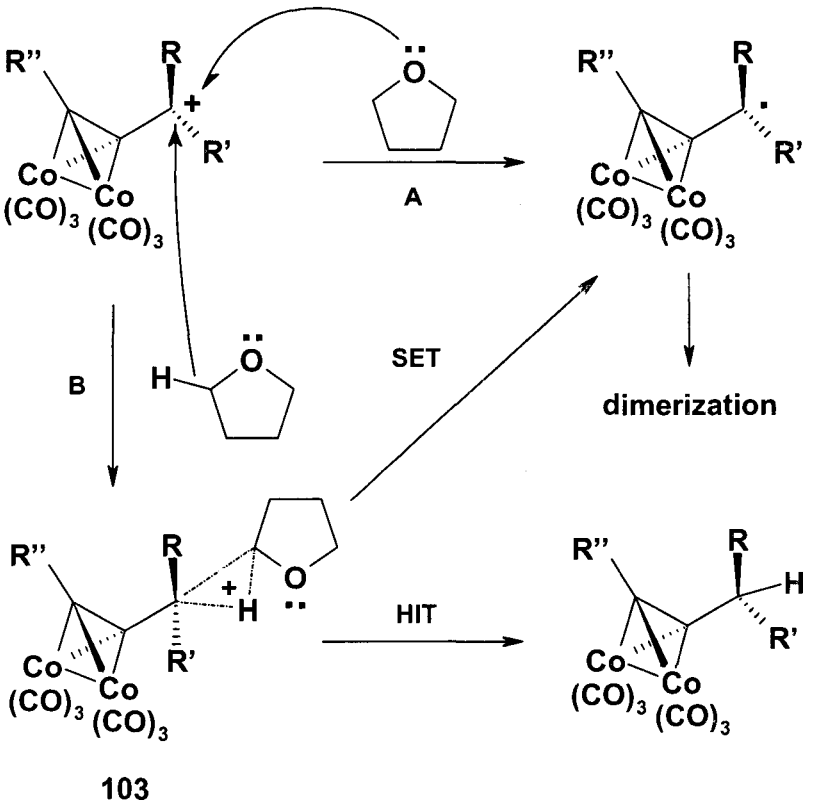

Scheme 4.4 Mechanistic interpretation for the generation of cobalt-mediated propargyl radicals in tetrahydrofuran.

One should note that these reductions only occur with cobalt-complexed propargyl alcohols, as the initial heterolysis of the free-standing alkynol is severely retarded in the absence of the metal cluster. It must also be emphasized that this fascinating and facile transformation using homogeneous radical initiators is markedly superior to the previously used, and somewhat tedious, methods involving heterogeneous and air-sensitive reducing agents. Moreover, initial investigations suggest that compatibility with nearly all functional groups is evident.[123]

4.1.3 Objective

Intrigued by these reports of radical intermediates in cobalt cluster chemistry, this methodology was implemented into our sterically encumbered systems, in order to understand the chemical variation provided by differing solvents. Initially, the radical $(Co_2(CO)_6)[HC{\equiv}C\text{-}CPh_2\cdot]$, **104**, was prepared to see whether it would couple to yield the corresponding symmetrical ethane, **105**, or rather mimic the classic behavior[125] of the triphenylmethyl radical, **106**, which for steric reasons yields the unsymmetrical dimer **107**, as in Scheme 4.5.

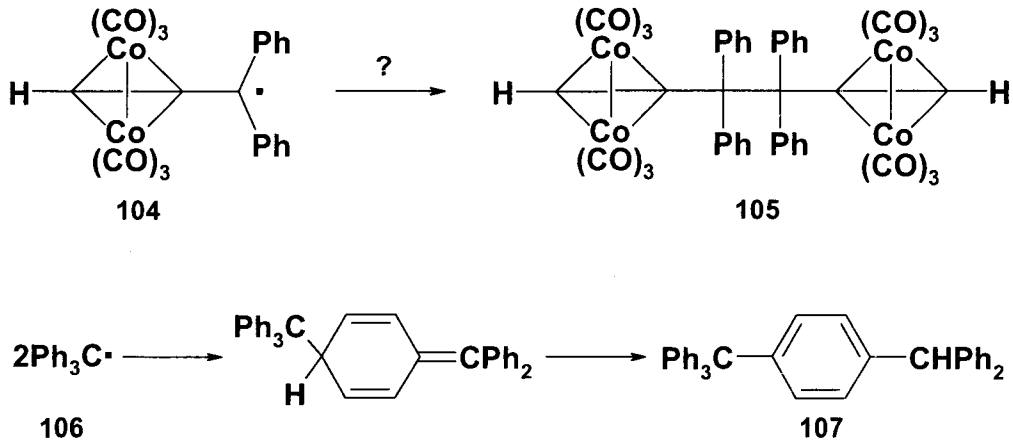

Scheme 4.5 Attempted correlation of diphenyl-cobalt and triphenylmethyl radicals.

4.2 Results and Discussion

4.2.1 Diphenyl System

Since the organic alkynyl precursor **30**, had already been prepared, addition of octacarbonyldicobalt readily afforded $(Co_2(CO)_6)[HC{\equiv}C\text{-}CPh_2OH]$, **108.** Treatment of **108**, with HBF_4 in SO_2 yields the isolable cation $(Co_2(CO)_6)[HC{\equiv}C\text{-}CPh_2]^+$.[52a] In contrast, an earlier report by Hagihara on the protonation of $(Co_2(CO)_6)[HC{\equiv}C\text{-}CPh_2OH]$

with concentrated sulfuric acid suggests that the major product is the tricobalt cluster **109**. This product was characterized by microanalysis, but no spectroscopic data were given.[126,127] As previously mentioned, it has been well established that terminal alkyne complexes of the type $[RC{\equiv}CH](Co_2(CO)_6)$ rearrange in acid media to yield the corresponding $RCH_2\text{-}CCo_3(CO)_9$ clusters[95,97,105] (Scheme 4.6). One might therefore have anticipated the formation of the alcohol **110**, or its elimination product **33**, rather than the saturated cluster **109**. Indeed, we find that treatment of $(Co_2(CO)_6)[HC{\equiv}C\text{-}CPh_2OH]$ with HBF_4 in dichloromethane at -78 °C does yield the alkenyl cluster **33**, which had been previously prepared by desilylation of the corresponding allylsilane (Section 2.8). Suitable crystals of **33** were isolated and its X-ray crystal structure appears as Figure 4.1.[128]

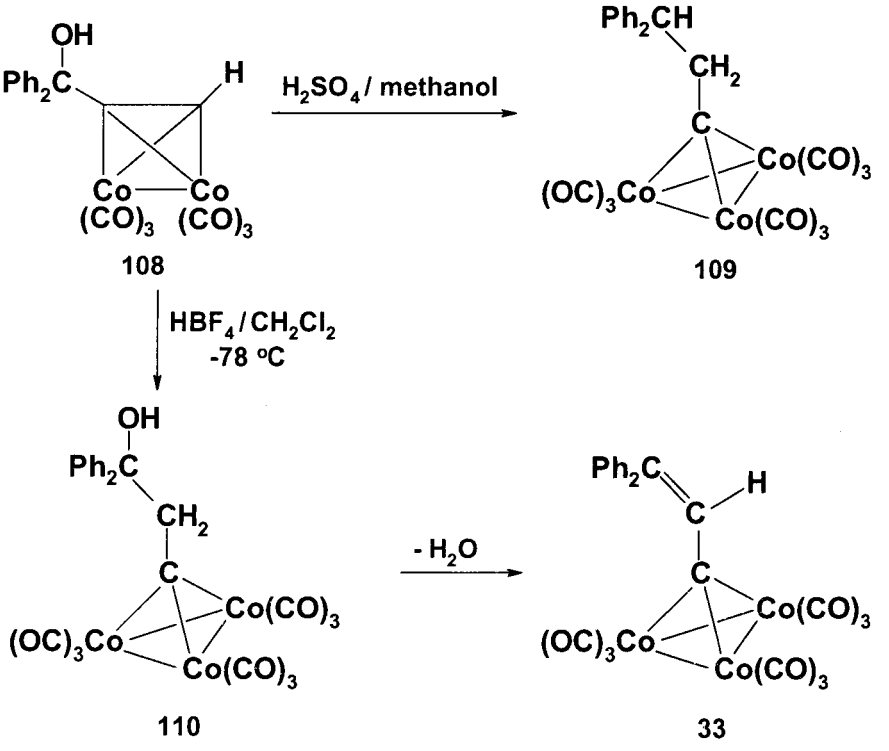

Scheme 4.6 The formation of various tricobalt species from **108**.

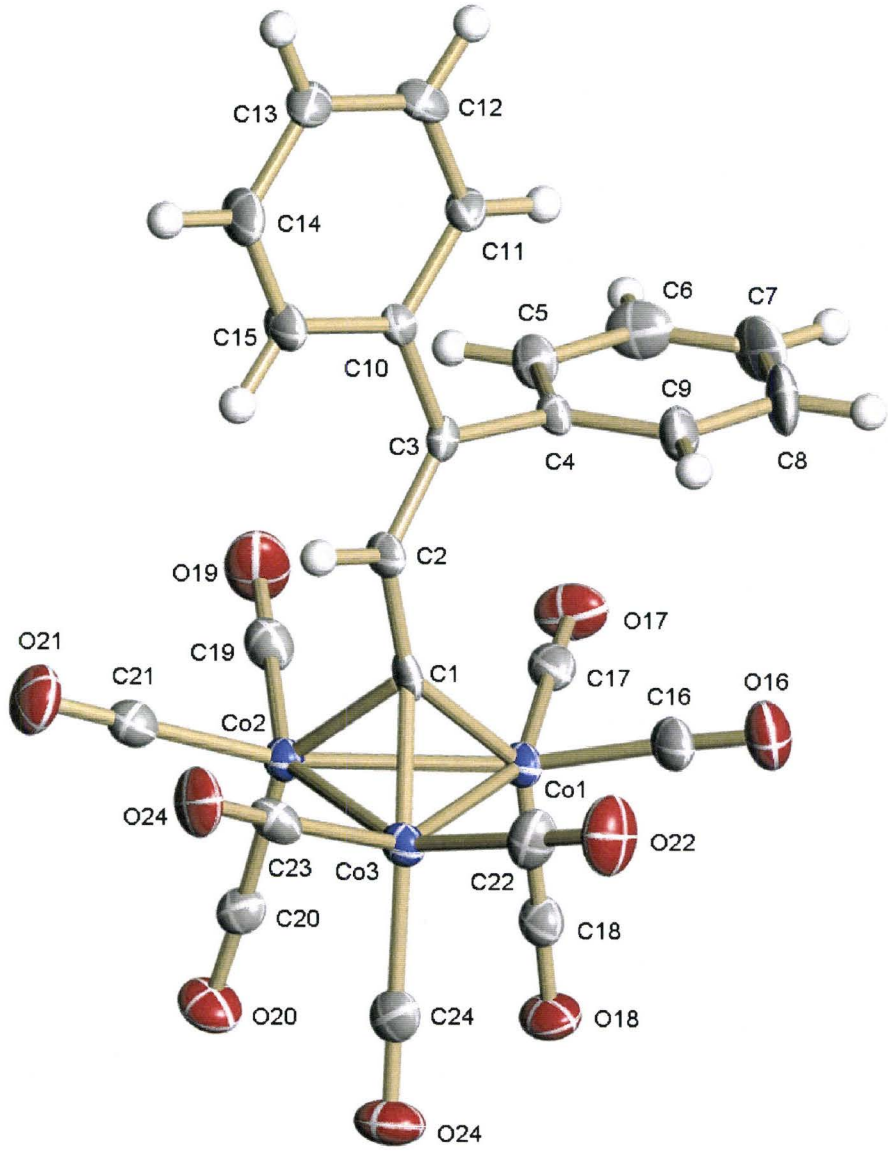

Figure 4.1 Molecular structure of **33**, with thermal ellipsoids at 30%.

However, returning to our stated objective of generating the radical **104**, the precursor alcohol, **108**, was treated with HBF_4 in THF at -78 °C and the mixture slowly allowed to warm to room temperature before quenching with water. Chromatographic separation yielded three products: the alkenyl tricobalt cluster **33** (18%), (ethynyldiphenylmethane)$Co_2(CO)_6$, **111**, (8%), and a bright yellow material **112** (20%).

The cluster **33** has already been discussed, and **111** is readily envisaged as arising either through hydrogen abstraction by the intermediate radical, or hydride transfer to the initially generated cation, as in Scheme 4.7.[128]

The bright yellow compound exhibited a strong infrared absorption at 1703 cm^{-1}, and ^{1}H and ^{13}C NMR resonances typical of carbonyl, phenyl and alkene fragments. The parent peak in the mass spectrum at *m/z* 410, together with the observed breakdown pattern, corresponded to a molecule containing two Ph_2C-C-CH moieties plus a carbonyl group. Comparison of these data with those of related systems[129,130] suggested that the yellow compound, **112**, was 2,5-bis-(diphenylmethylene)cyclopent-3-en-1-one, and this assignment was confirmed by X-ray crystallography (Figure 4.2).[128]

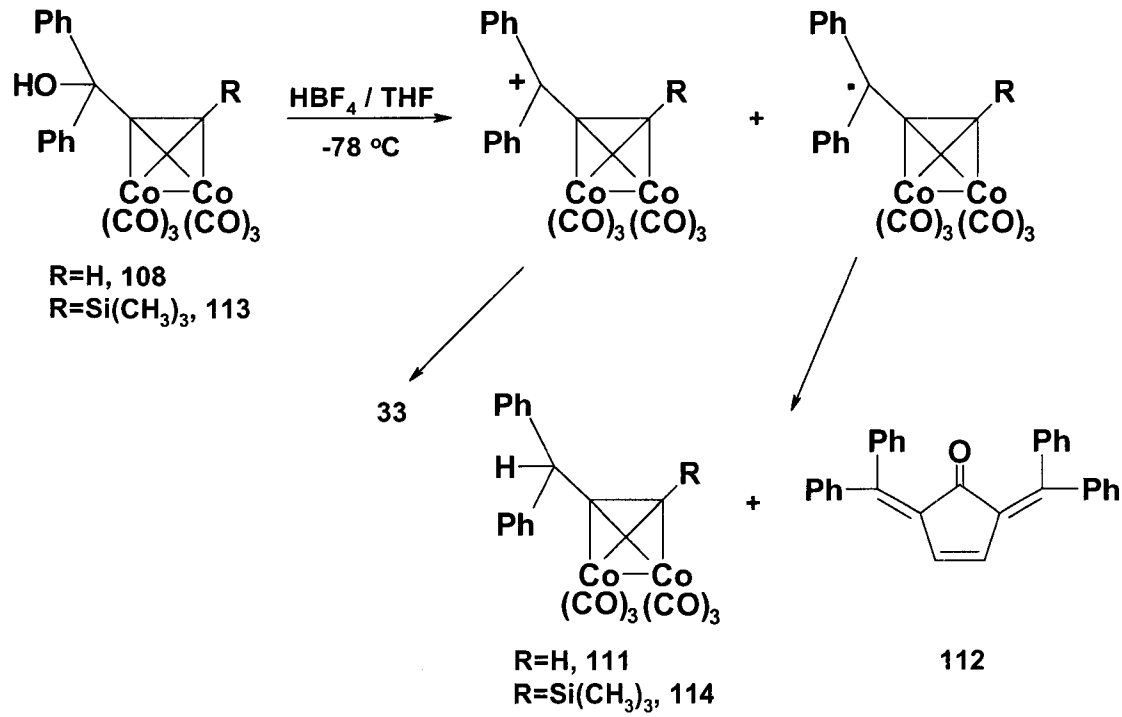

Scheme 4.7 Radical products observed from protonation of **108** and **113** in THF.

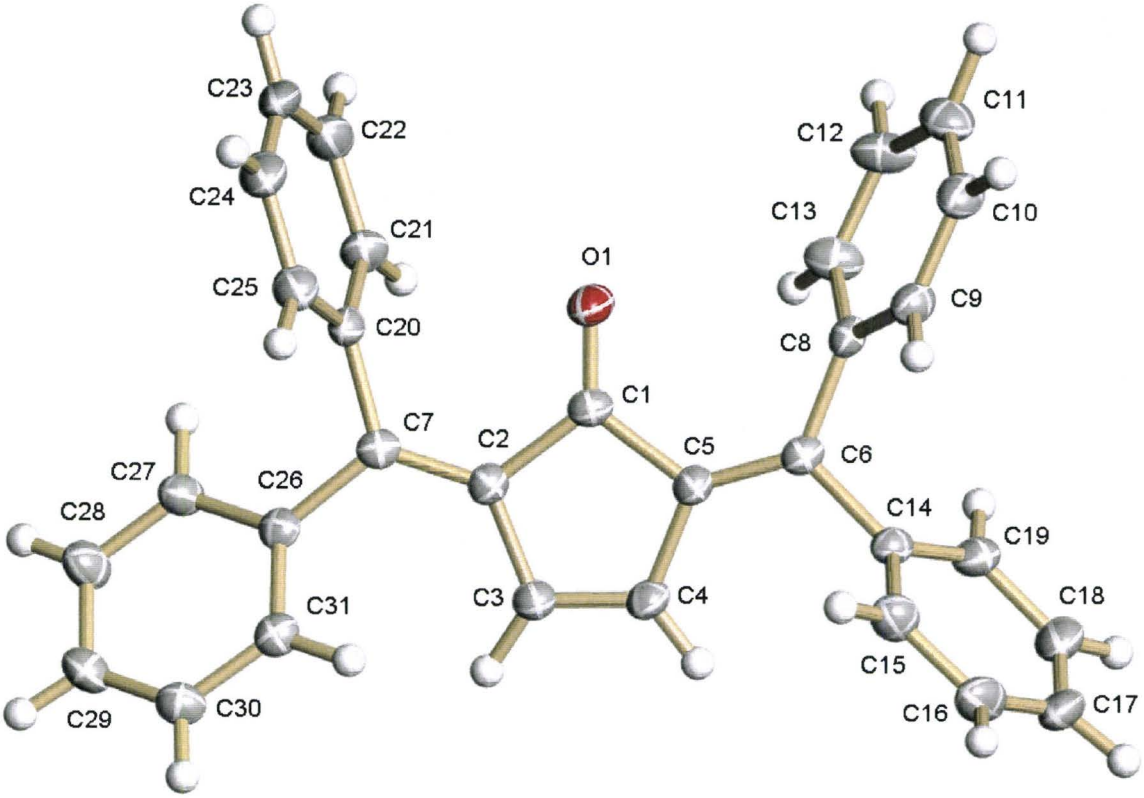

Figure 4.2 Molecular structure of **112**, with thermal ellipsoids at 30%.

One might speculate that, since coupling of the diphenylmethyl radicals to give **104** is presumably sterically disfavored, coupling of the methyne termini followed by a carbonyl insertion process could lead to the observed product. The precise nature of the cobalt center in Scheme 4.8 remains unknown at present, and requires further assessment.

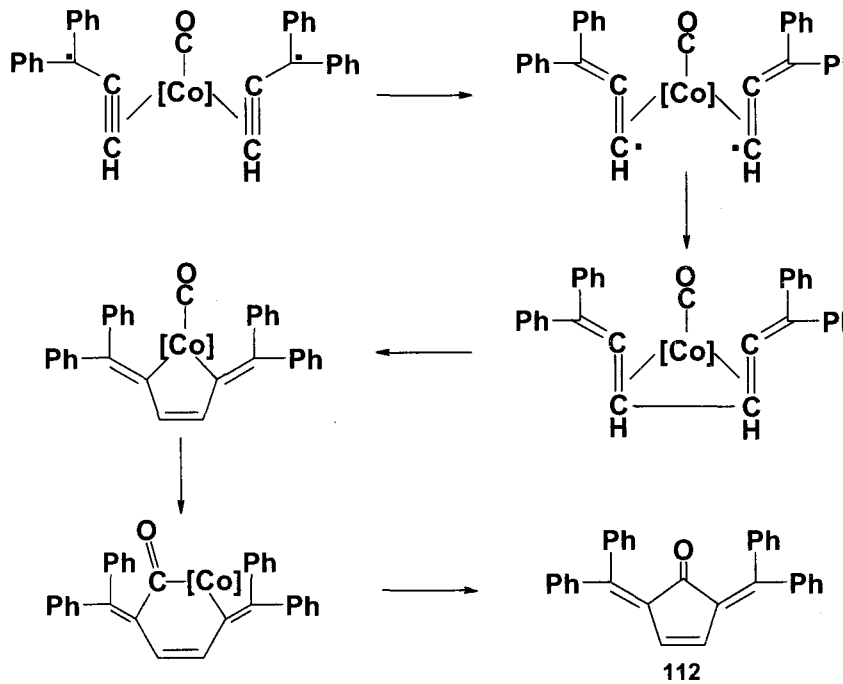

Scheme 4.8 Proposed mechanism for the formation of **112**.

In seeking precedents for such a process, we note Eaton's elegant [4+1] iron-catalyzed cycloaddition of conjugated diallenes and a carbon monoxide to produce five-membered rings.[131] However, in those examples, one must first synthesize the diallene either (a) by dibromocarbene addition to an appropriate butadiene followed by debromination with methyllithium,[132a] or (b) by palladium-catalyzed coupling of a propargyl bromide and an allenyl-zinc reagent.[132b] In the present case, it is apparent that the coupling, cyclization and carbonylation processes are all cobalt-mediated in a one-pot synthesis.

Interestingly, protonation of the analogous trimethylsilyl protected cobalt-complexed alkynol, **113**, in THF, affords only the hydrogen abstraction product, **114**, shown in Scheme 4.7.[20] The dimeric cyclized product is presumably not generated because of the steric interference invoked by the trimethylsilyl group.

4.2.2 Fluorenyl System

In an attempt to explore the generality of this process, the corresponding deprotected fluorenyl system, **115**, was protonated initially in dichloromethane, and diethyl ether, and latterly in tetrahydrofuran. The former reaction yielded only a single product, the tricobalt cluster **116**. In contrast, protonation in diethyl ether, which would be expected to generate radicals, yields a reduced quantity of the tricobalt cluster **116,** along with the hydrogen abstraction product, **117**, while utilizing THF afforded **117** as the major product (Scheme 4.9).[128] It is surmised that **118**, the fluorenyl analogue of **112**, would suffer severe steric problems and that the fluorenyl moieties would need to be noticeably twisted out of plane as depicted in the AM1 HyperChem model[83,133] in Figure 4.3.

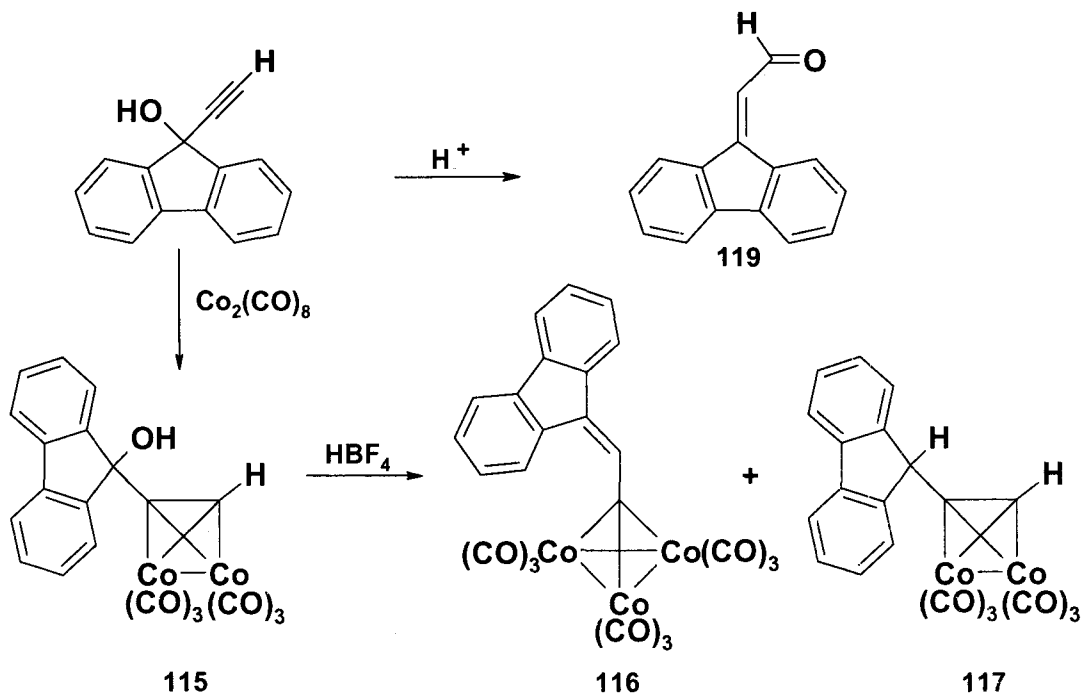

Scheme 4.9 Fluorenyl products formed upon protonation.

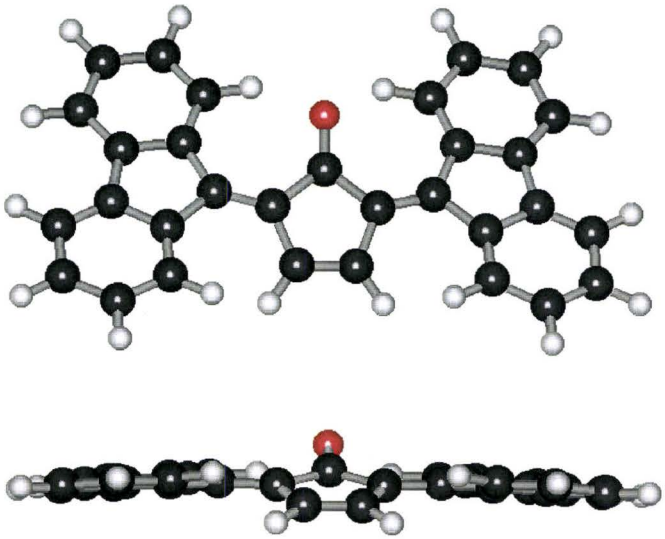

Figure 4.3 Optimized Structural Model of **118** at the AM1 level.[83,133]

These results contrast markedly with the behavior of the free ligands 1,1-diphenyl-2-propyn-1-ol and 9-ethynyl-fluoren-9-ol which undergo the Meyer-Schuster (rather than the Rupe)[134] rearrangement to 3,3-diphenylacrolein and 9*H*-fluoren-9-ylideneacetaldehyde, **119**, respectively, under acidic conditions (Scheme 4.9).[135]

4.2.3 Migrations Revisited

As a result of our success with generating novel radical products merely from alternating the protonation solvent, we decided to redirect our focus to the previously investigated cobalt complexed silanes.

As was alluded to in Chapter 2, protonation of the cobalt-complexed fluorenyl vinyl and benzyl silanes, **53** and **54** respectively, with HBF_4 in dichloromethane at -78 °C, did not afford any desirable migration products. In fact, protonation of the vinyl analogue **53** in the migratory solvent of choice, dichloromethane, furnished a novel

trinuclear species, **120**. This product, whose molecular structure appears as Figure 4.4, was almost certainly obtained through initial hydrogen abstraction and ensuing rearrangement to a trinuclear complex. Intriguingly, formation of **120** confirms the earlier report by Hagihara[126] of generating a saturated tricobalt cluster from its parent alkynol, suggesting that hydride abstraction is also achievable in various other solvents.

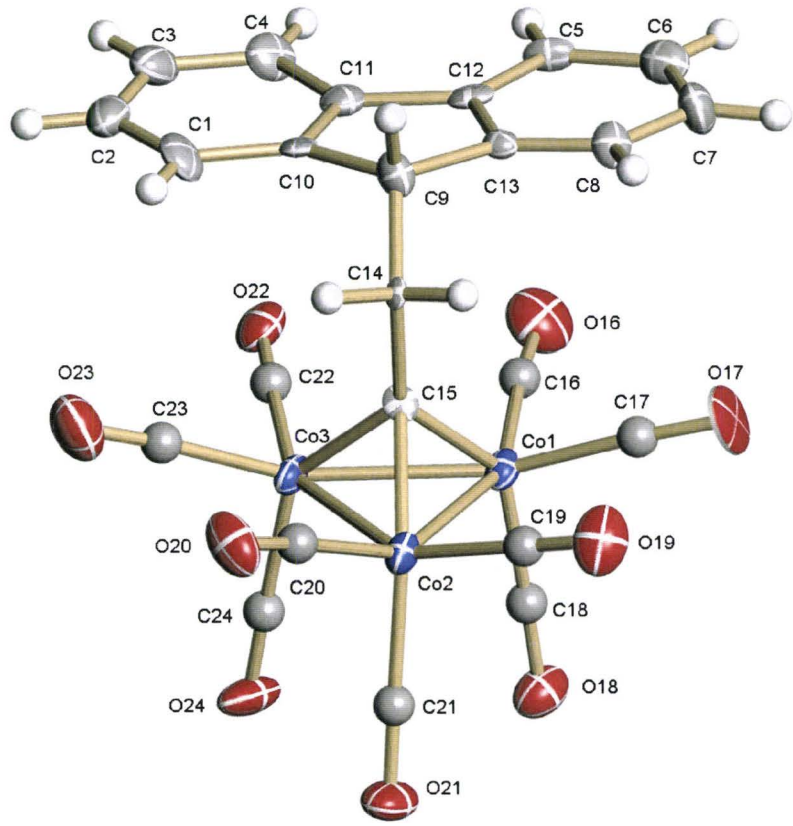

Figure 4.4 Molecular structure of **120**, whereby 30% anisotropic thermal probability ellipsoids were established for all atoms except the carbonyl carbon atoms.

Replication of this reaction in dichloromethane using the analogous benzylsilane, also gave rise to **120**, and additionally afforded a second previously unknown product (Scheme 4.10). The colour of this compound suggested that it was a cobalt complex; this was supported by a preliminary ^{13}C NMR spectrum that exhibited two resonances above

200 ppm, one of which was diagnostic for the presence of cobalt carbonyls. However after several hours there was noticeable decomposition, and further NMR analysis of the resulting product implicated an unsymmetrical dimer containing an uncomplexed alkyne. A single ^{13}C resonance above 200 ppm remained, suggesting the presence of an unusual unsaturated carbon. Infrared spectroscopy revealed a signal at 1915 cm^{-1}, indicative of an allene. Successful isolation of single crystals indeed revealed an uncomplexed allenic dimer, **121**, illustrated in Figure 4.5. This was unambiguously identified by the linear hybridization of the central allene carbon with bond lengths of 1.310(15) Å and 1.287(9) Å for C9-C14 and C14-C15, respectively.

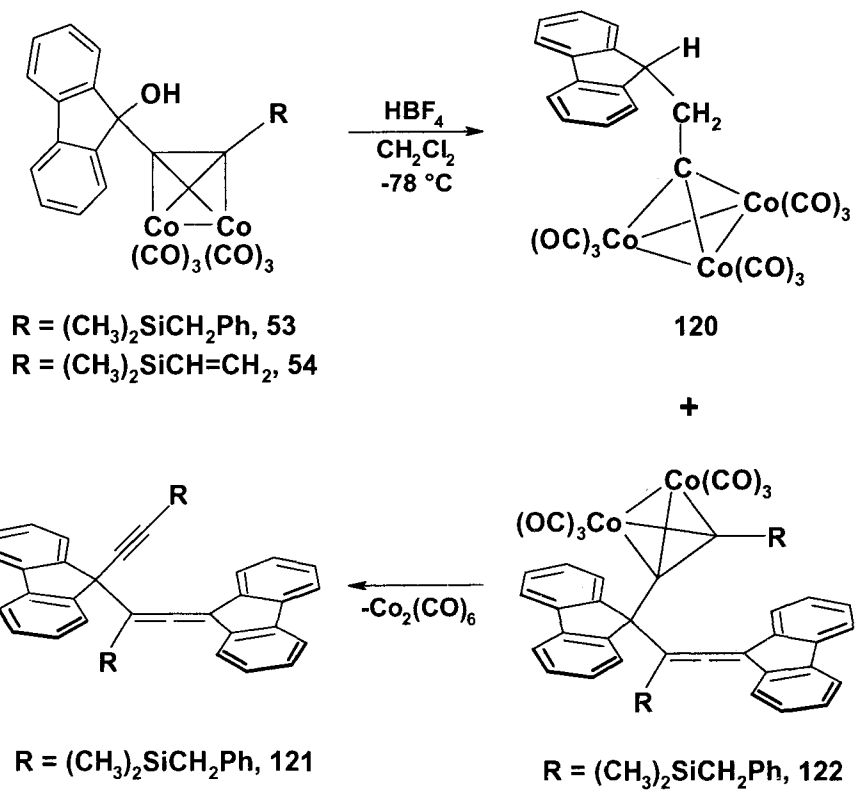

Scheme 4.10 Products isolated from the protonation of cobalt-complexed fluorenyl-vinyl and –fluorenyl-benzyl alkynylsilanes, in dichloromethane.

(a)

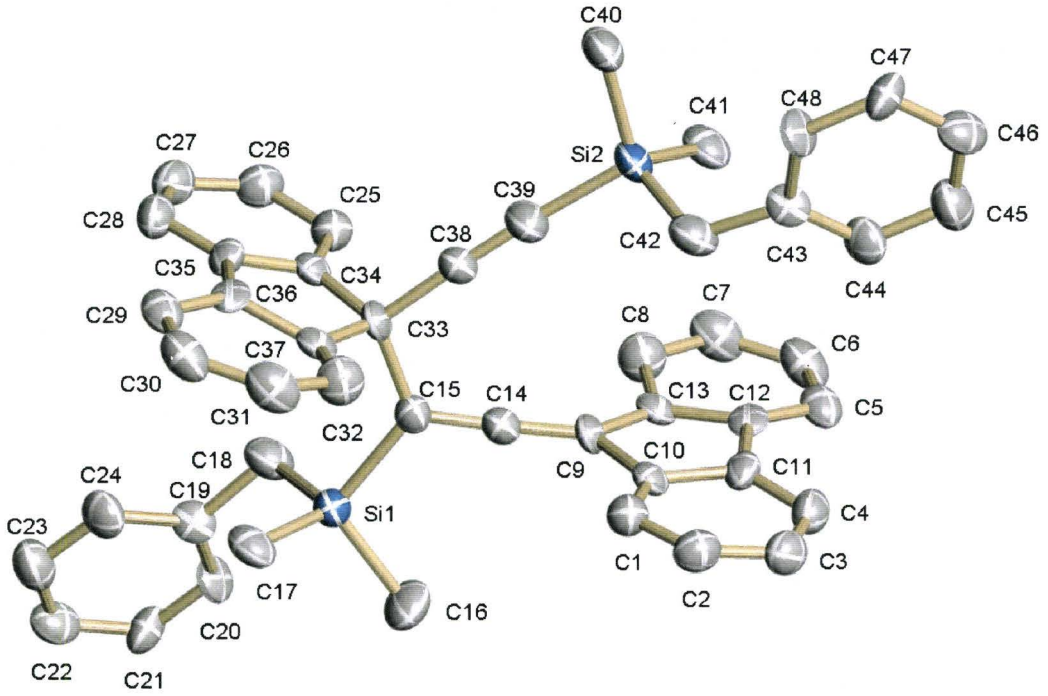

(b)

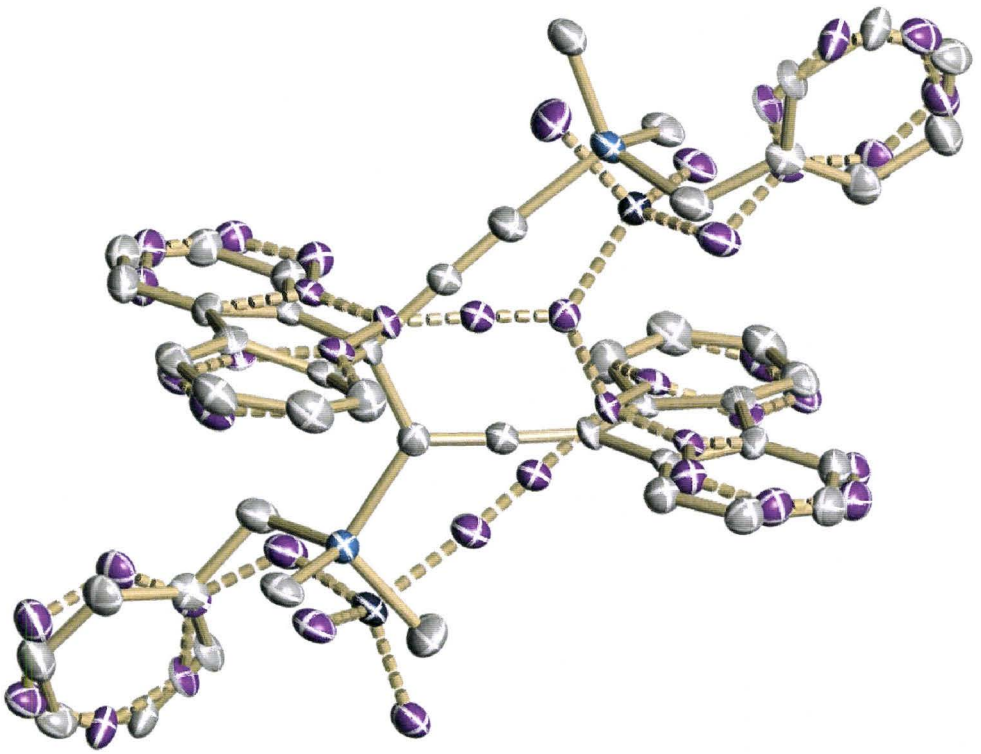

Figure 4.5 a) Molecular structure of **121** with 30% thermal probability ellipsoids, omitting hydrogen atoms for clarity. b) Identical view showing the extensive overlap of both partially occupied models of the molecule.

The two-fold disorder in the molecule, evident in Figure 4.5b, was effectively modeled, whereby the unit cell consists of two molecular orientations with 50% occupancy of each. It is quite remarkable that the thermal paramaters are congruent considering the 180° rotational disorder, which causes the fluorenyl and silyl substituents of the alkyne in one molecule to overlap with the corresponding fluorenyl and silyl substituents of the allene in its complementary molecule.

It is worth noting that, although the vinyl analogue of **121** was not isolated, it may not be discounted, as there were other minor unidentifiable products present. A literature search for precedence revealed a similar trimethysilyl substituted dimer identified merely by ^{13}C NMR and IR. This dimer was obtained under markedly different anionic, reflux conditions, upon treatment of a purely organic, bromo-substituted fluorenylidene-ethene precursor with alkanethiolate ions in diethyl ether.[136]

The allene, **122**, was undoubtedly formed prior to decomplexation of the metal moiety, as the second NMR resonance at 202 ppm in the initial compound is representative of the central allene carbon.[136] It is inconceivable that dimerization occurs through a cationic intermediate, as the site of addition implies a potential transition state involving a positive charge alpha to silicon, which is hyperconjugatively disfavoured, and would require subsequent elimination of $(OH)^+$. Therefore the most reasonable method of formation involves generation of a fluorenyl radical, decomplexation of cobalt and rearrangement to an allenic radical, and subsequent head-to-tail coupling with another cobalt complexed fluorenyl radical, **123**, with final removal of hexacarbonyldicobalt, thereby producing the observed dimerization product, **121**, as illustrated in Scheme 4.11.

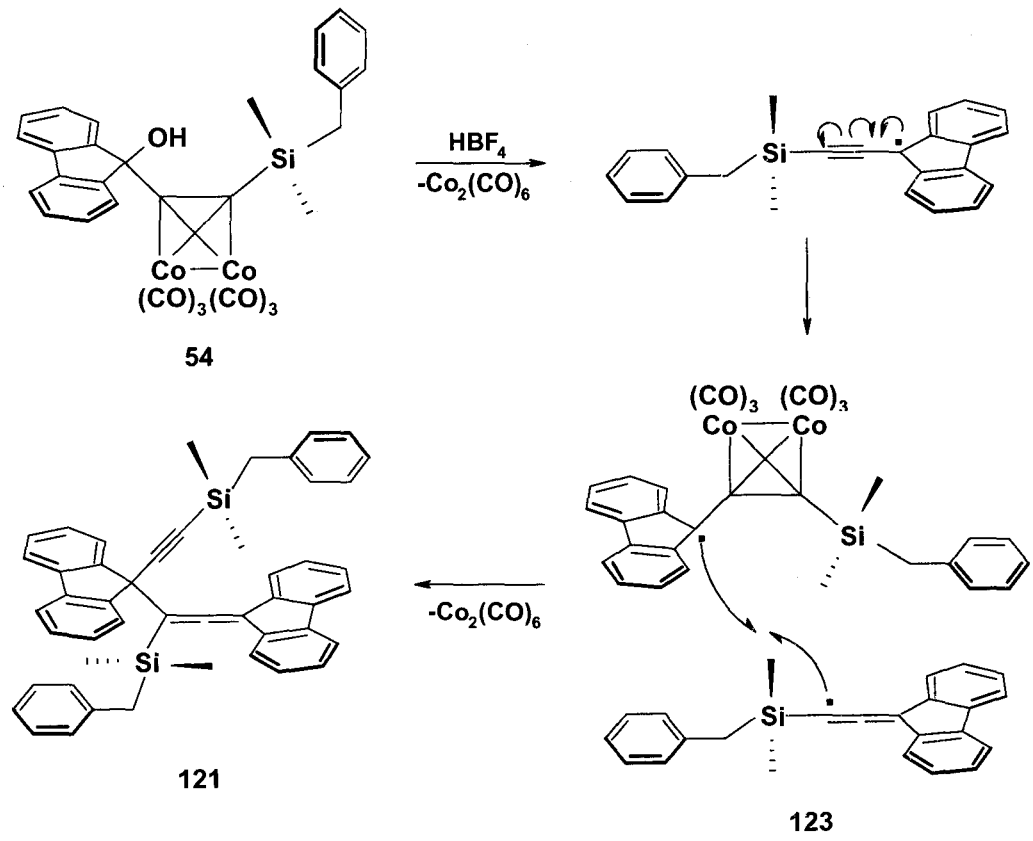

Scheme 4.11 Mechanistic proposal for the formation of **121**, involving radical intermediates.

Since dicholoromethane is not considered an electron-donating solvent, it is highly improbable that it initiated formation of the fluorenyl radical. However, this anomaly may be attributed to a single electron transfer from a cobalt radical fragment, inferred by the presence of the trinuclear complex, **120**, since it is believed to be essential in the final step of formation of tricobalt clusters, as described in Section 3.3.2. Therefore it is not unrealistic that formation of a radical product in dichloromethane may occur when an independently generated radical mediator is present. Furthermore, in this particular scenario, the impossibility of migration, or of any other simple rearrangement, along with the instability of the initially generated fluorenyl cation of **54**, presumably facilitates its one-electron reduction.

4.2.4 Peroxides

In order to contrast the aforementioned products to those generated in a radical enhancing medium, the benzylsilane, **54**, was treated with HBF_4 at -78 °C in tetrahydrofuran, thereby affording a novel product, **124**. NMR spectroscopy of the sole isolable compound revealed resonances very similar to the starting material, except for the absence of the alcoholic proton signal. Mass spectrometry indicated the formation of a dimeric product, yet its identification was not conclusive. It was initially assumed that the unknown compound was in all probability an ether complex, as such dimerizations of propargylic cobalt silanes have been previously reported.[137] However, isolation of single crystals and careful crystallographic analysis unveiled a fascinating new product; a peroxide, **124**, whose molecular structure appears as Figure 4.6a. An interesting crystallographic feature is presented in Figure 4.6b, where each of the fluorenyl ligands is distorted, as each six-membered ring deviates from planarity by approximately 7 degrees, thereby adopting a "Star Wars TIE Fighter" type geometry.

(a)

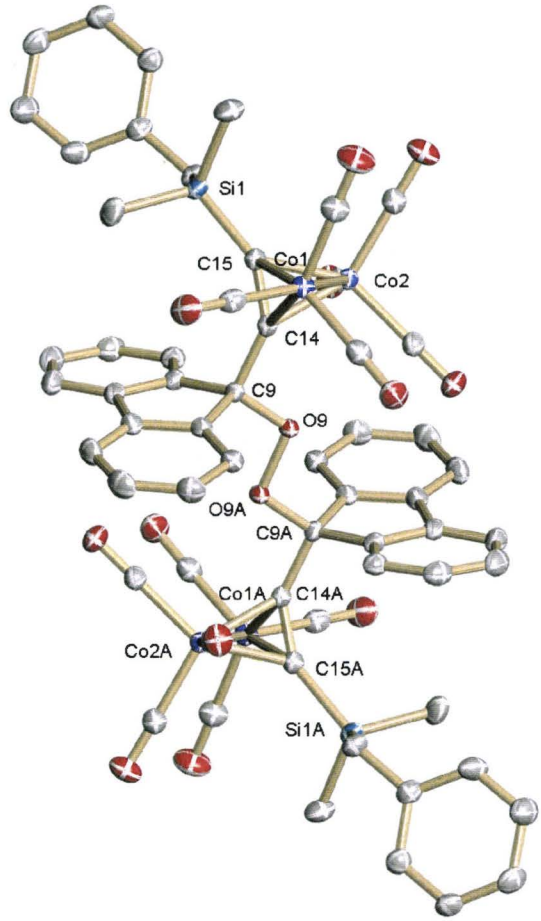

(b)

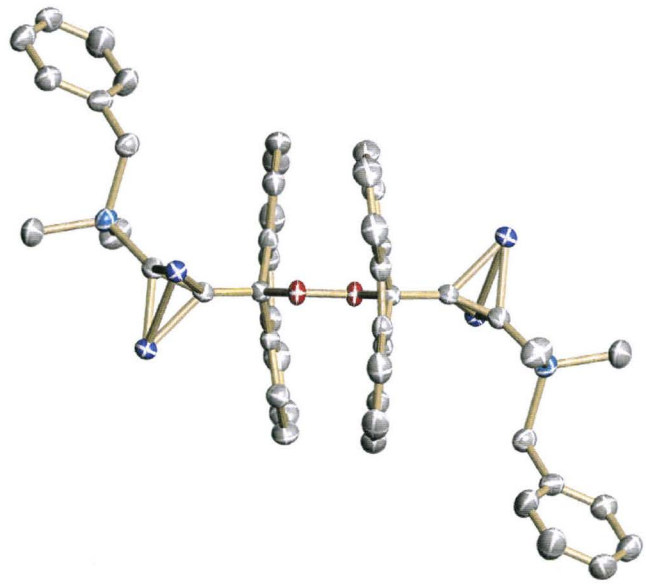

Figure 4.6 (a) Molecular structure of **124** with 30% thermal probability ellipsoids, hydrogen atoms have been excluded for clarity. (b) Perpendicular view of **124**, without carbonyl atoms, emphasizing the curved nature of the fluorenyl ligands.

One might now appreciate the difficulty in distinguishing the peroxide from the potential formation of an ether complex, as the NMR spectra would be virtually identical. Moreover, without the presence of a distinct molecular ion in the mass spectrum, the fragmentation pattern would otherwise be very similar, since it is appararent that the first major dissociation is that of the oxygen-oxygen linkage.

The fluorenyl-vinylsilane was protonated under identical conditions, and also afforded the analogous peroxide, **125**, as the only isolable product, shown in Scheme 4.12. Weakly diffracting crystals were obtained for **125**, thus confirming this result by establishing the atom connectivity of the molecule presented in Figure 4.7. It is worth noting that the fluorenyl ligands deviate merely 3.5 degrees from planarity, less than was seen in the benzyl analgoue, likely due to a reduction in packing influences afforded by the smaller vinyl substituents. Repetition of both peroxide-generating reactions in diethyl ether produced similar results, as these peroxides were the major and only identifiable products.

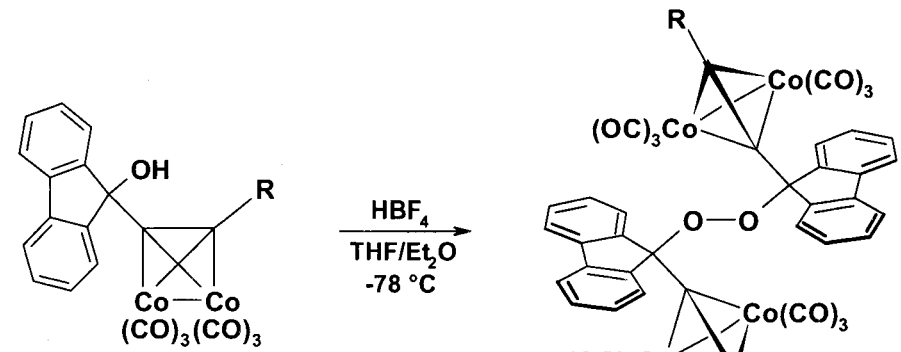

R = $(CH_3)_2SiCH_2Ph$, 54
R = $(CH_3)_2SiCH{=}CH_2$, 53

R = $(CH_3)_2SiCH_2Ph$, 124
R = $(CH_3)_2SiCH{=}CH_2$, 125

Scheme 4.12 Formation of cobalt clustered peroxides from the protonation of cobalt-complexed fluorenyl-vinyl and -benzyl silanes, in tetrahydrofuran or diethyl ether.

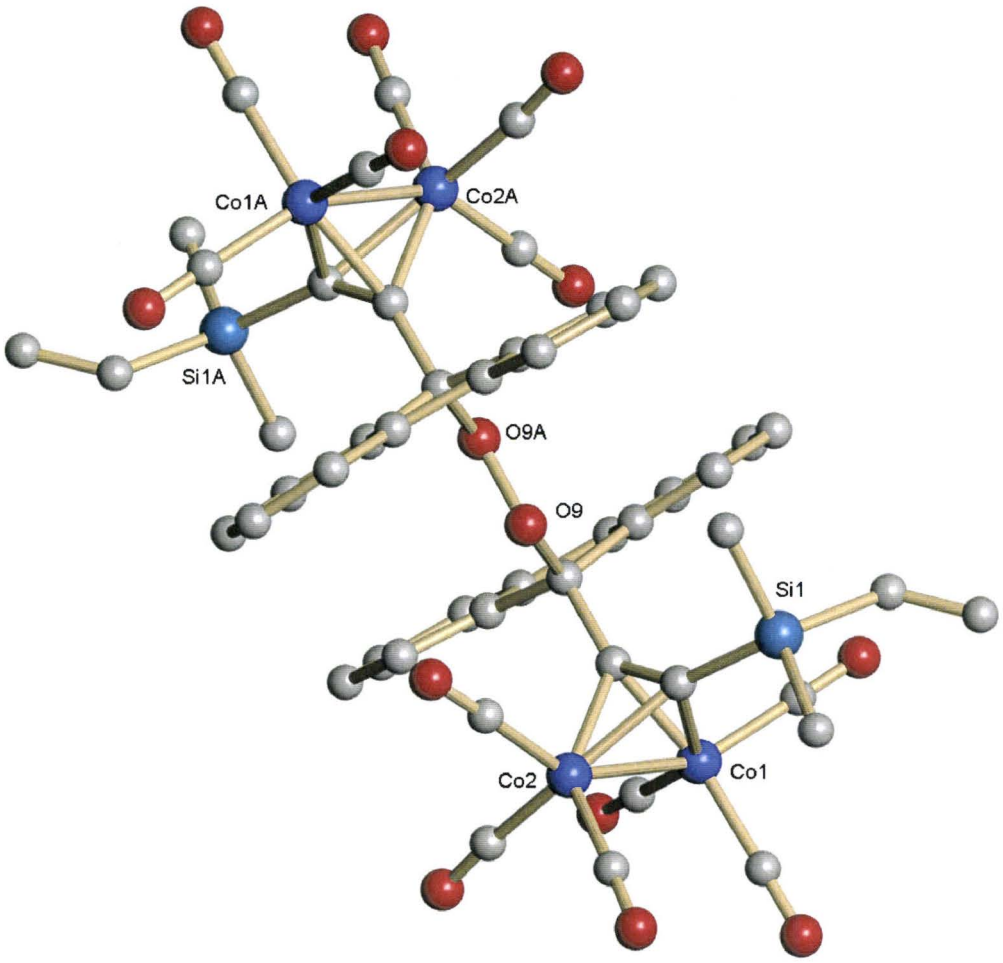

Figure 4.7 Molecular structure of **125**; fluorenyl hydrogen atoms have been excluded for clarity.

It is worth noting that mechanistic investigations have not been accomplished on these systems, but it is clear that either diethyl ether or THF can serve as the radical initiator. Furthermore, one may speculate that although removal of a hydrogen radical from the alcohol with subsequent oxygen radical coupling cannot be excluded, it is much more probable that the fluorenyl radical is initially generated and reacts with atmospheric oxygen in a combination process, as shown in Scheme 4.13.

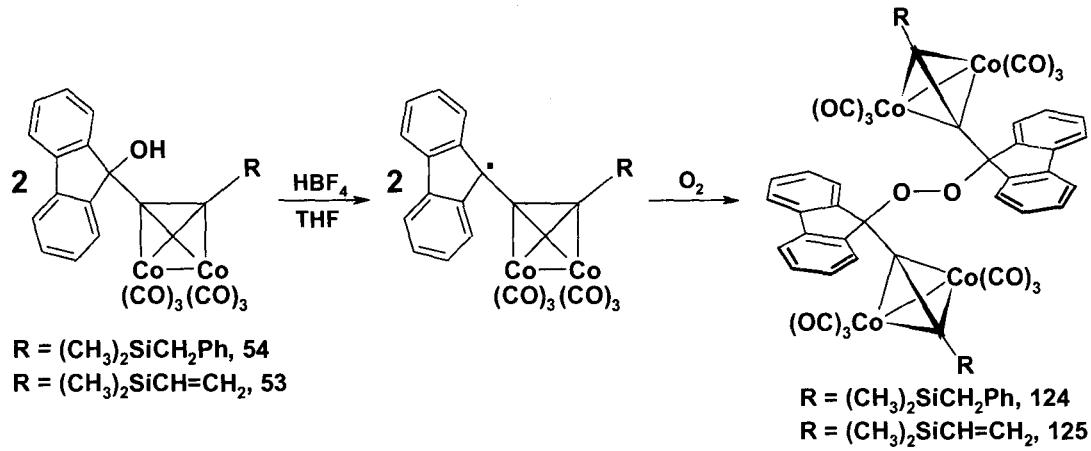

Scheme 4.13 Mechanistic proposal for the formation of the cobalt containing peroxides, **124** and **125**, from radical intermediates and atmospheric oxygen.

Although protonation of the allysilane, **38**, in diethyl ether or THF has not been accomplished, it is postulated that allyl transfer would still be competitive, and likely the major product, due to the efficiency of migration observed in dichloromethane. Furthermore, adaptation of these radical mediated reactions to the diphenyl analogues of **53** and **54** could perhaps bring about steric restrictions invoked by the less rigid phenyl rings, which may hinder such a coupling reaction. Moreover, this was previously evidenced in Figure 4.7, as protonation of the terminal alkyne, **30**, and trimethylsilyl substituted, **113**, analogues in THF, did not afford any peroxide-like products.[128]

Interestingly, peroxides are generally formed by autoxidation or radical formation through addition of an initiator, or by thermolysis, or photolysis in the presence of oxygen gas.[138] Although these are, to our knowledge, the first metal-complexed fluorenyl peroxides to have been synthesized, there are several known metal-free dimers, including phenyl,[139] isopropyl,[140] and benzyl[141] substituted systems.

It must be emphasized that organometallic peroxides are rare because peroxides usually are not sufficiently stable to survive complexation of the ligand by a metal, and

until now there have not been any widely applicable or practical methods of generating peroxides of complexes already containing transiiton metals. In fact, examples predominantly consist of numerous mercuric peroxides,[142] and transition metal containing porphyrins.[143] The very first organometallic peroxide, and perhaps the most similarly prepared to our systems, involved a cobaltocene,[144] whereby oxygen gas was passed through a solution of cobaltocene in diethyl ether at -78 °C, thereby formulating a dimeric peroxide adduct, unbeknownst to the authors that diethyl ether was a radical inducing solvent. The only other examples of metallocene peroxide derivatives, are primarily ferrocenyl systems,[145] which may be biologically applicable,[146] and also a rhodenocene.[147] However, these systems are prepared either from coordination of dioxygen to cationic complexes of the metal in the absence of any radical initiating solvents, or nucleophilic addition of the metal complex to a preformed peroxide.

4.3 Summary

Therefore, it cannot be over-emphasized that by simply altering the protonation solvent, an entirely new discipline in cobalt alkynyl chemistry has presented itself. Also, these unexpected results obtained from cobalt-cluster propargyl radicals, to our knowledge, provide the first examples of bimetallic centered peroxides. Furthermore, it is believed that this innovative technique of initiating a radical with tetrahydrofuran and subsequent exposure to atmospheric oxygen, readily provides a novel, efficient, and controlled synthetic methodology which may potentially be applied to the generation of an almost limitless array of transition metal peroxides.

Chapter Five: $Co_2(CO)_6$ as a Conformational Switch

5.1 Cyclohexyl Systems

5.1.1 Background

Cyclohexane has been a known molecule since the early nineteenth century. However it was not until 1890 that a German chemist, Ulrich Sachse, proposed a puckered ring geometry, and suggested that it existed in more than one form. Since there was no experimental evidence during this period, Sachse's hypothesis was not verified until the middle of the twentieth century, when in 1943 a Norwegian chemist, Odd Hassel, employed electron diffraction to demonstrate the chair conformation of cyclohexane in the gas phase. Hassel later was awarded the Nobel Prize in Chemistry in 1969 in conjunction with Sir Derek Barton for his work in conformational analysis.[148]

Cyclohexane is now known to have three primary geometric forms; chair, **126a**, boat, **126b**, and twist-boat, **126c**, as illustrated in Figure 5.1. Several years ago, there was much debate over which conformation, boat or twist-boat, was the intermediary conformer in the chair-to-chair interconversion process of cyclohexane.[149] Since then computational analysis has established that the chair conformation, by far the most common, has the highest stability, while the boat and twist-boat forms, which are less frequent, decrease in stability by 6.9 and 5.5 kcal mol^{-1},[150] respectively, indicating that the twist-boat is in all actuality the more likely transitional form. In fact there are no isolated examples of cyclohexyl derivatives with ideal boat geometries, and relatively

few characterized examples of twist-boats, which will be thoroughly discussed later in this chapter.

126a **126b** **126c**

Figure 5.1 Most common conformations of cyclohexane.

5.1.2 Introduction

Although the ability of the alkynyl dicobalt hexacarbonyl moiety to stabilize a neighboring carbocationic site has been well established,[44] as previously disclosed in chapter one, its use as a stereocontrol element has been less widely exploited. Melikyan and Nicholas have rationalized the $Mn(OAc)_3$-mediated oxidative cycloaddition of β-dicarbonyl compounds with $Co_2(CO)_6$-complexed 1-alken-3-ynes in terms of a transition state whereby the bulky cluster unit is disposed pseudo-equatorially; this favors a pseudo-axial approach by the incoming nucleophile.[120a] Similarly, the stereospecificity of the Friedel-Crafts cyclization of cobalt-stabilized propargyl cations onto suitably activated arenes[151] has been explained by invoking a transition state in which the $(-C{\equiv}CH)Co_2(CO)_6$ fragment adopts the less hindered pseudo-equatorial site.[152] It is also worth noting that Isobe has reported the facile epimerization of a series of $Co_2(CO)_6$-complexed alkynyl sugars such that the cluster adopts an equatorial rather than an axial site.[153]

5.1.3 Objective

Several years ago, Malisza *et al.*[152] reported the X-ray crystal structures of 2-methyl-1-(phenylethynyl)cyclopentanol, **127**, and of the corresponding dicobalt hexacarbonyl adduct, **128**. In the former case, the alkynyl anion attacks the precursor ketone in a pseudo-axial fashion, cis to the methyl group. Addition of the $Co_2(CO)_6$ unit brings about a conformational flip such that the methyl and hydroxyl substituents become pseudo-axial and the cluster occupies a pseudo-equatorial position, as in Scheme 5.1.

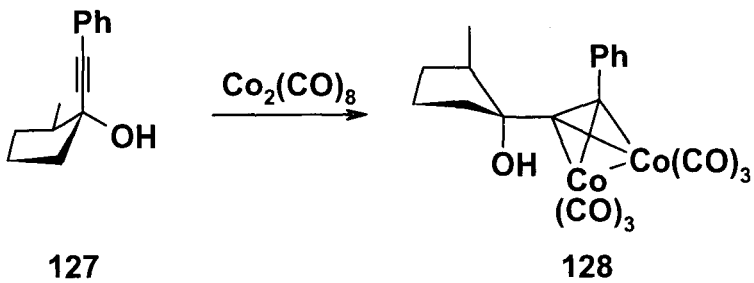

127 **128**

Scheme 5.1 Conformational flip in cyclopentyl upon cobalt complexation.

Our goal was to establish an extension of this concept, by treating several cyclohexanones with alkynyl anions of increasing steric demand, and comparing the structures of these alkynols with the conformations of the corresponding dicobalt hexacarbonyl complexes by using X-ray crystallography.

5.2 Results and Discussion

5.2.1 Conformational Changes

The conformation adopted by a cyclohexane ring — whether it be a chair, twist-boat, etc. — is critically dependent on the steric interplay between the substituents.[150] The proclivity for a particularly bulky group, such as tert-butyl, to occupy an equatorial

site and thus "lock in" a given conformation is well-known.[154] In contrast, a needle-like substituent, such as an alkynyl moiety imposes minimal steric interactions within the system, and thus offers little opportunity for conformational control. As previously noted, treatment of the alkynylcyclopentanol, **127**, with dicobalt octacarbonyl yields the cluster complex **128**, in which the formerly pseudo-axial alkyne linkage now occupies a pseudo-equatorial site.[152] However, the conformational flexibility of 5-membered rings[154a,155] is much greater than is found in cyclohexane systems for which the chair is generally favoured.

When cyclohexanone was allowed to react with (trimethylsilylethynyl)lithium, and then hydrolysed, the resulting alkynol, **129**, was characterized by NMR spectroscopy as the conformer in which the entering nucleophile occupies an axial site.[156] After identification of all the proton and carbon resonances by use of standard ^{1}H-^{1}H COSY and ^{1}H-^{13}C shift-correlated techniques, observation of nuclear Overhauser interactions between the hydroxyl proton and the hydrogens at C-2 and C-6 clearly established the equatorial positioning of the OH group. Subsequent incorporation of the $Co_2(CO)_6$ unit yielded the complex **130**, in which the cyclohexane ring has flipped to allow the cluster fragment to occupy the equatorial position, as illustrated in Scheme 5.2. The structure of **130** was unequivocally determined by X-ray diffraction, and is shown in Figure 5.2.[157]

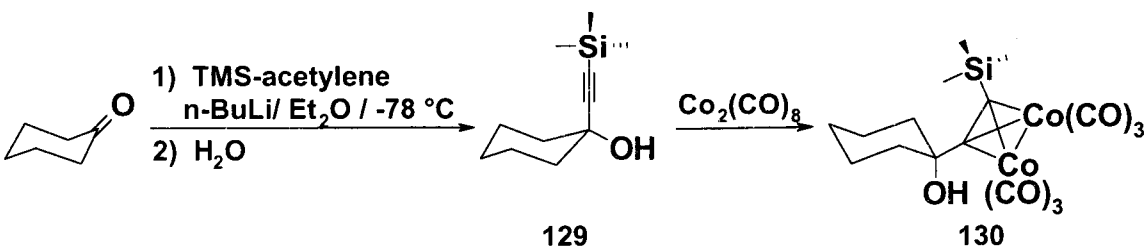

129 130

Scheme 5.2 Axial substitution of trimethylsilylacetylene and further complexation of hexacarbonyldicobalt.

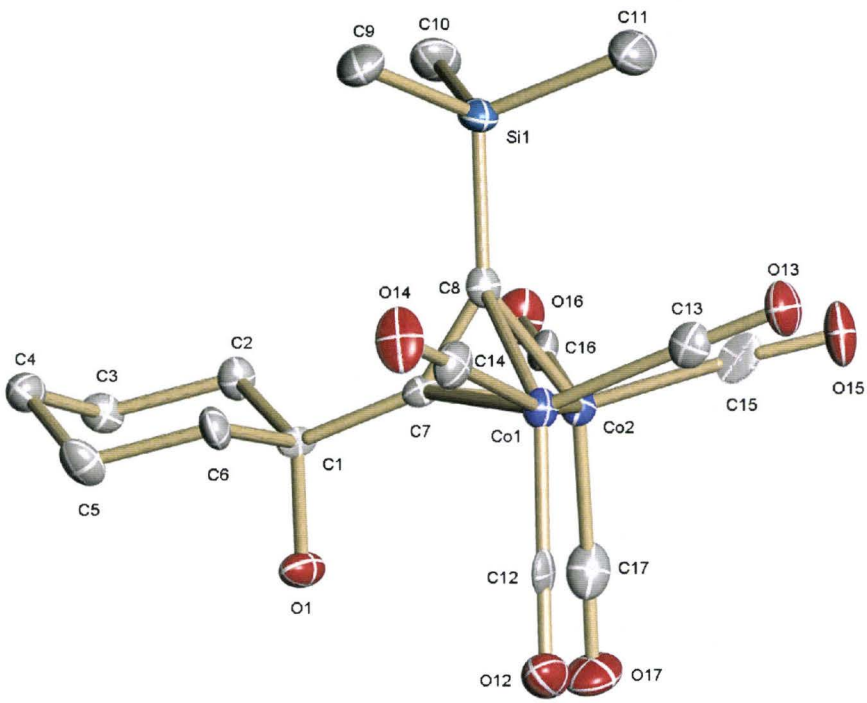

Figure 5.2 A 30% Thermal Ellipsoid Plot of **130**.

It is clearly relevant to note that Braga and co-workers have reported the X-ray crystal structures of both 1-(tert-butylethynyl)cyclohexan-1-ol, **131**, and of the nickel and platinum complexes **132a**,**b**, shown in Scheme 5.3. As with the conversion of **129** to **130**, the alkynyl substituent in **5** has moved from an axial to an equatorial site in **132**; however, the authors made no mention of this conformational change since their primary focus was on the intermolecular hydrogen bonding patterns in the crystal lattice.[158]

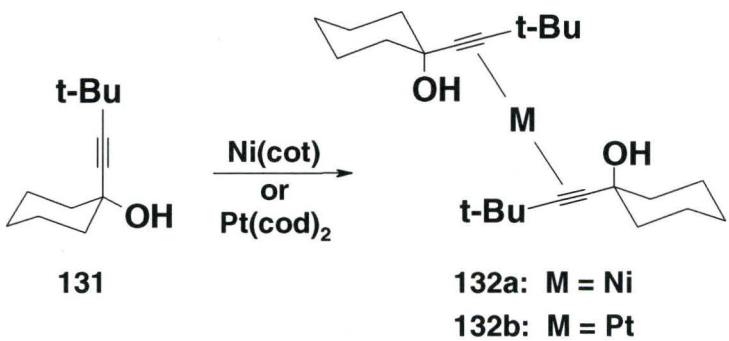

Scheme 5.3 Nickel and platinum complexes of 1-(tert-butylethynyl)cyclohexan-1-ol.

5.2.2 Alkynols Derived from 4-tert-Butylcyclohexanone

The next question concerns the relative ability of a tert-butyl versus an $(RC{\equiv}C)Co_2(CO)_6$ substituent to maintain its equatorial alignment. To this end, Lock treated trans-4-tert-butyl-1-(phenylethynyl)cyclohexan-1-ol, with $Co_2(CO)_8$ to furnish its complexed alkynol, whose solid state structure indicates that the tert-butyl group continues to control the ring conformation.[159]

In an attempt to increase the steric bulk of the alkynyl substituent, 4-tert-butylcyclohexanone was treated with (trimethylsilylethynyl)lithium; subsequent hydrolysis yielded two alkynols that were readily separable by column chromatography on silica gel. The isomers with axial and equatorial alkynyl groups, **133** and **134** respectively, were formed in a 5:2 ratio (Scheme 5.4).

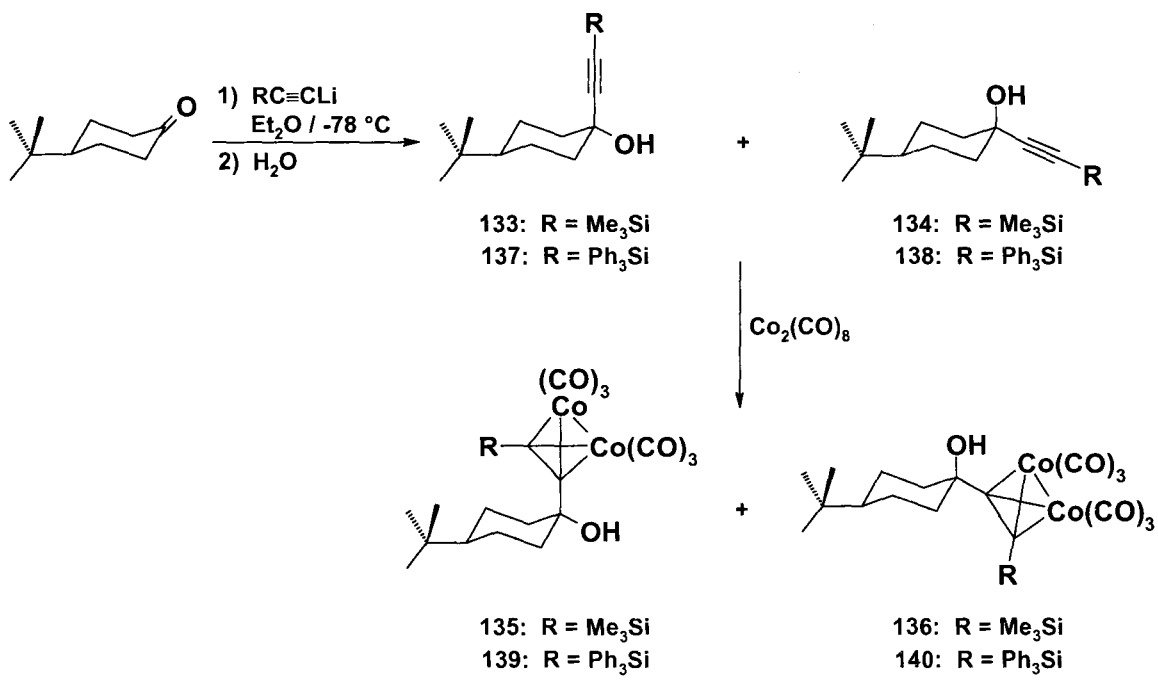

Scheme 5.4 Generation of axial and equatorial substituted alkynes in 4-tert-butylcyclohexyl systems.

The direction of attack by alkynyl anions on alkyl-substituted 5- and 6-membered ring systems (initially investigated by Cadiot and Chodkiewicz[160]) cannot be predicted simply from Cram's Rule.[161] The torsional strain transition state model proposed by Felkin,[162] and subsequently supported by Anh and Eisenstein,[163] has been used to rationalize the experimentally observed stereoselectivities of nucleophilic additions to cyclic ketones. In this model, it is suggested that the direction of nucleophilic attack is controlled not only by steric effects but also by the torsional strain imposed on the system in the transition state. In the case of cyclohexanones, this involves a distorted chair conformation whereby the axial transition state is perfectly staggered, whereas equatorial attack proceeds through a transition state that affords partial eclipsing.[164]

The solid state structures of the dicobalt hexacarbonyl clusters **135** and **136**, derived from **133** and **134**, respectively, appear as Figures 5.3a and 5.3b. Although the conformations of the cyclohexane rings in these complexes are not markedly perturbed, the data allow for comparison of the solid state structures of these isomers. They reveal that the conformation of the cyclohexane chair at the tert-butyl end of the molecule remains reasonably constant; the angle between the planes defined by C(3)-C(4)-C(5) and C(2)-C(3)-C(5)-C(6) is 53° ± 0.5°. There is slightly more variation at the cluster end whereby the interplanar angle between C(2)-C(1)-C(6) and C(2)-C(3)-C(5)-C(6) ranges from 44° to 47°.[157]

(a)

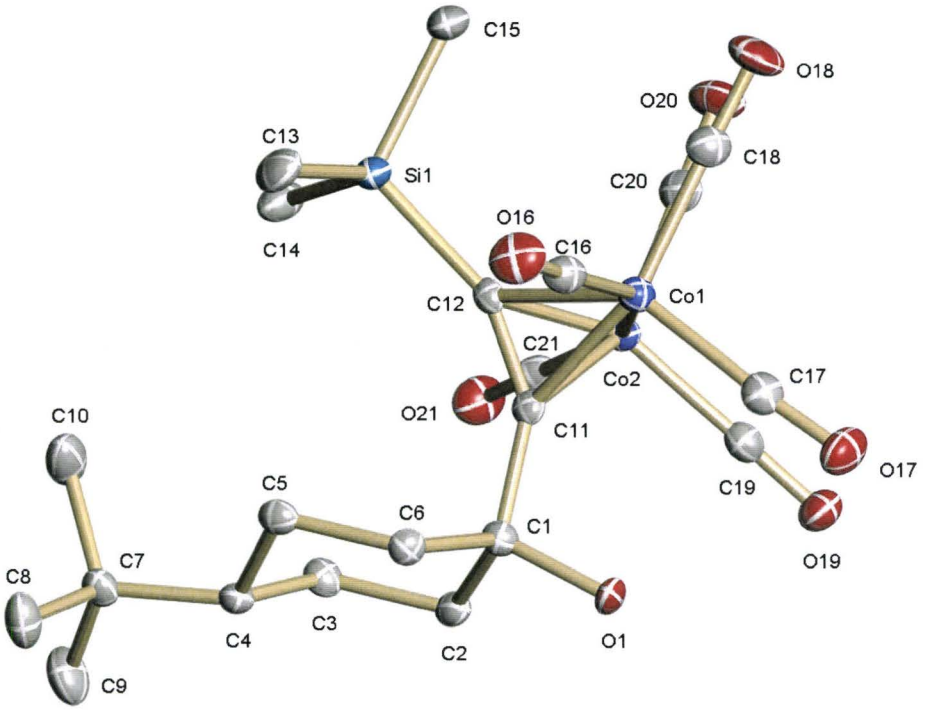

(b)

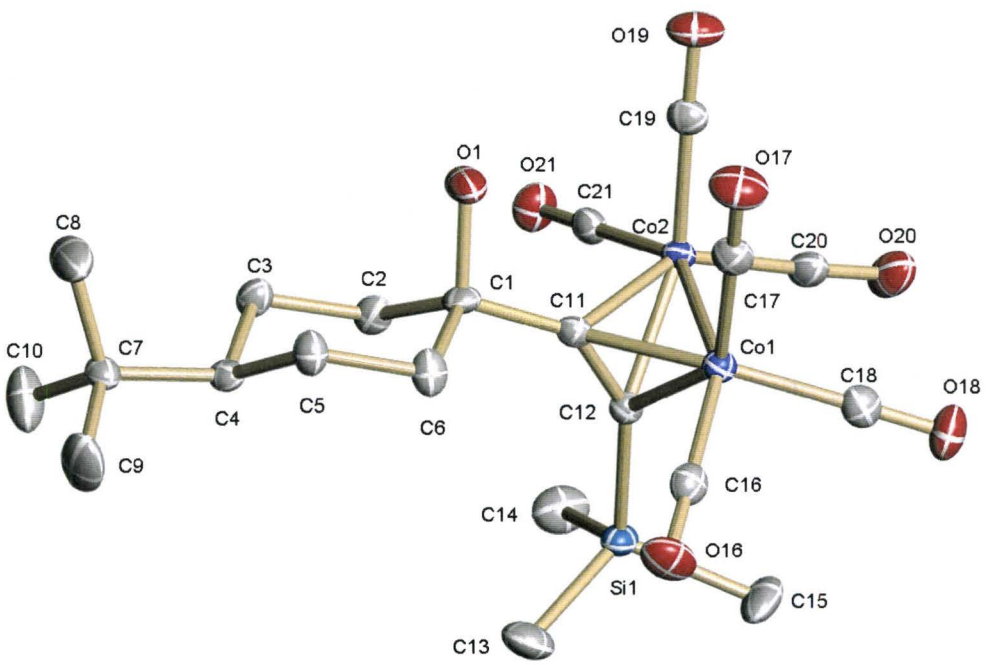

Figure 5.3 50% Thermal Ellipsoid Plots of (a) **135**, and (b) **136**.

The X-ray crystallographic characterizations of the cobalt clusters **135** and **136** allowed for the unequivocal assignment of their precursors **133** and **134** as possessing, axial and equatorial alkynyl substituents, respectively. The ^{13}C NMR spectra of the alkynols show clear chemical shift differences: in **133**, the C(1) absorption is found at δ 69.7, while in **134** the C(1) peak occurs δ 66.0, suggesting that for systems of this type the C(1) resonance of the isomer with the equatorial alkynyl moiety is approximately 4 ppm more shielded than its axial counterpart.

Replacement of the trimethylsilylethynyl substituent by a triphenylsilylethynyl group again yields a mixture of 4-tert-butyl-(1-alkynyl)cyclohexan-1-ols; in this case, the axial isomer, **137**, is more favored than its equatorial partner, **138**, by a 4:1 ratio.[157] These assignments are based on the C(1) NMR absorptions which again differ by approximately 4 ppm. Although both **137** and **138** yield crystalline complexes (**139** and **140**, respectively) when treated with $Co_2(CO)_8$, it has not yet proven possible to acquire acceptable X-ray data sets on these cobalt clusters. Nevertheless, it is evident that increasing the bulk of the attacking nucleophile disfavors the formation of axial isomers.

5.2.3 Alkynols Derived from Cyclohexan-1,4-dione

The observation that a triphenylsilylethynyl group could adopt either an axial or an equatorial position when a bulky substituent was already present at C(4) suggested that both cis and trans isomers of 1,4-bis(triphenylsilylethynyl)cyclohexan-1,4-diol might be readily available. Assuming that the initial attack occurred at an axial site, to give **141**, the second alkynyl unit could then adopt either an axial, **142**, or an equatorial, **143**, orientation, as depicted in Scheme 5.5. Treatment of cyclohexan-1,4-dione with two

equivalents of (triphenylsilylethynyl)lithium yielded three products; the trans di-alkynol, **142**, was obtained as colourless crystals and characterized by X-ray crystallography. The solid state structure of **142** is shown in Figure 4a and illustrates clearly the diaxial nature of the alkynyl substituents.[157] The molecule has an inversion center, the crystal packing is apparently dominated by the bulk of the triphenylsilyl groups, and hydrogen bonding does not seem to play a significant role in this particular case.

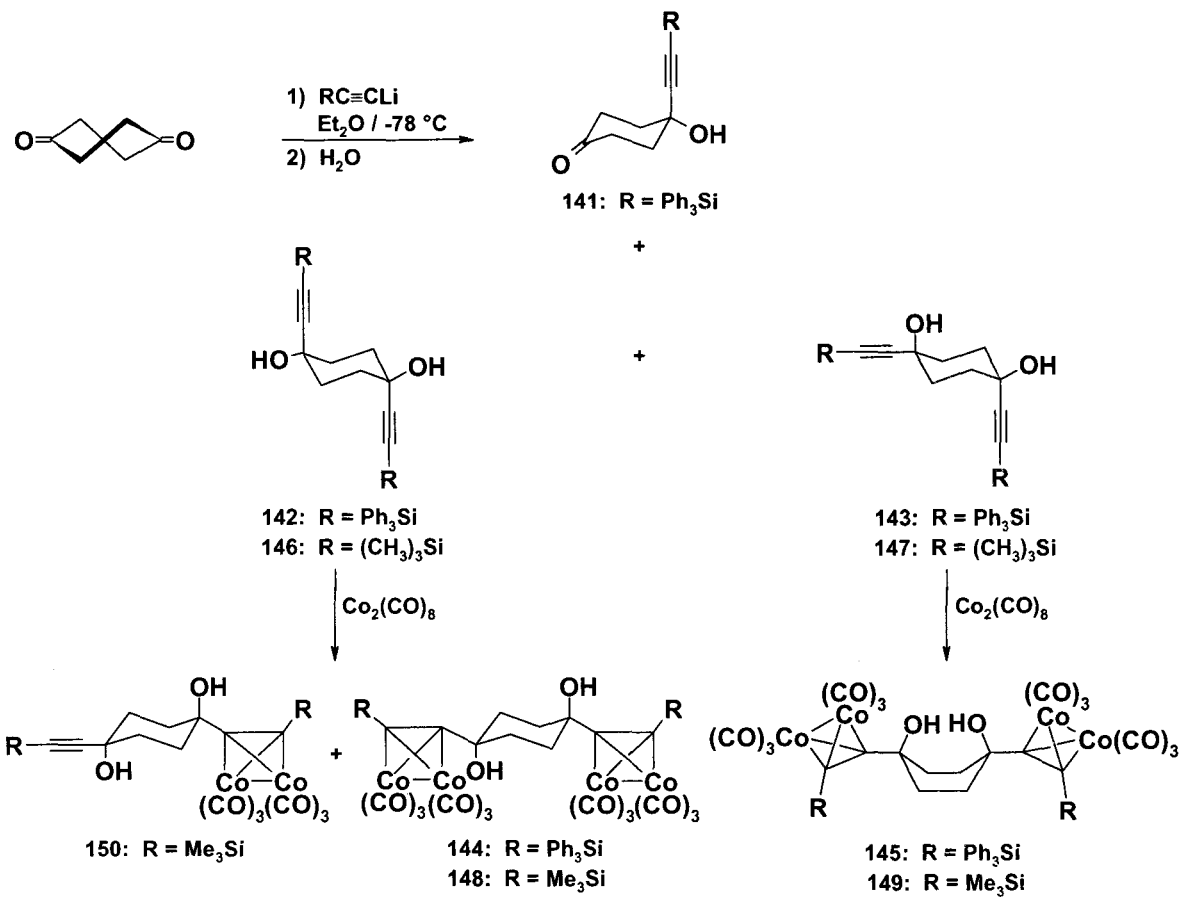

Scheme 5.5 Synthesis of *cis*- and *trans*-cyclohexan-1,4-diols.

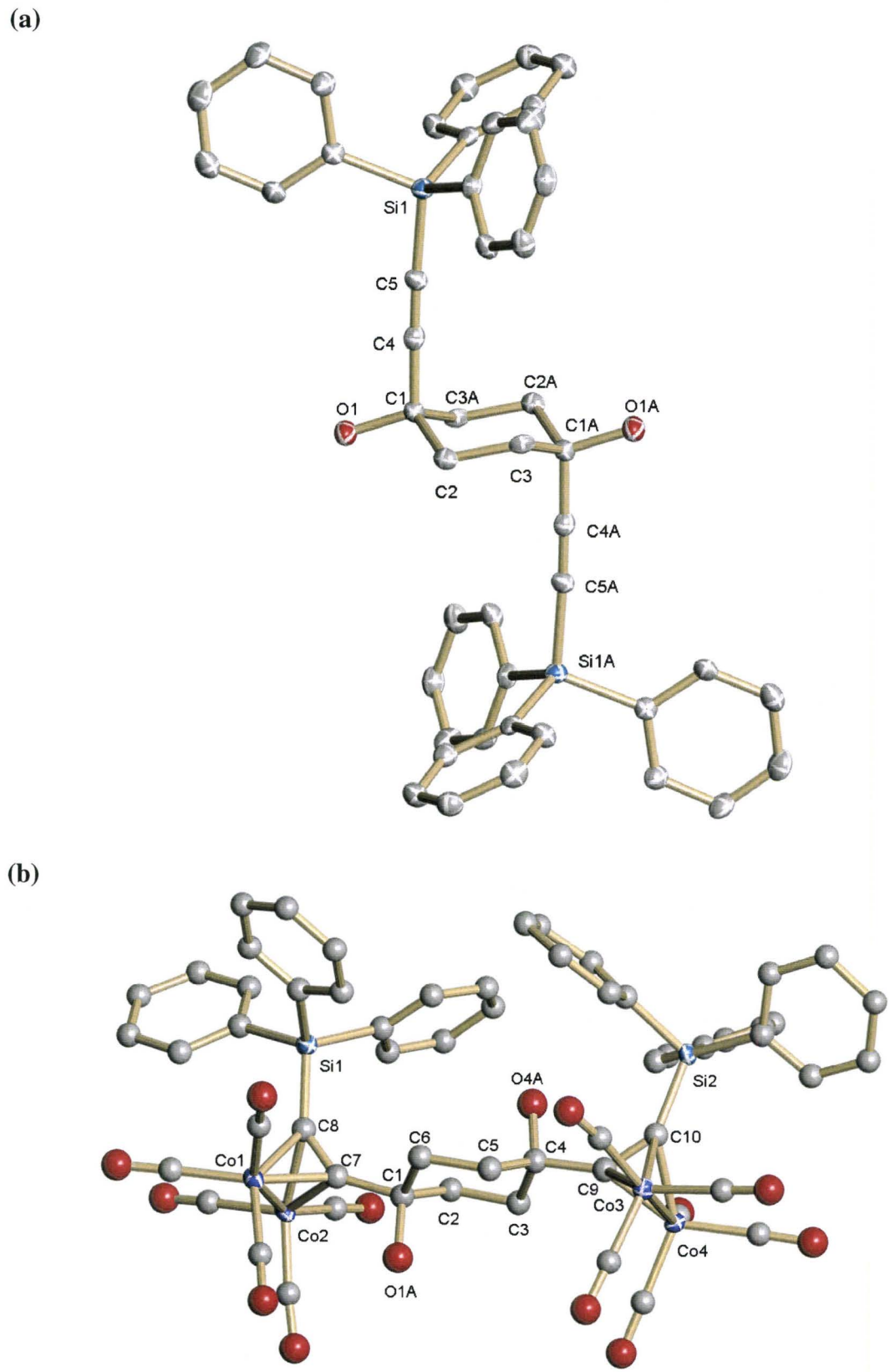

Figure 5.4 30% Thermal Ellipsoid Plots of (a) **142** and (b) **144**, excluding hydrogens.

The other two products from this reaction were identified spectroscopically as the isomeric di-substituted material **143**, along with a small quantity of the mono-alkyne **141**. However, since these latter two materials could not be cleanly separated by chromatography, they were treated with dicobalt octacarbonyl and the separation achieved at the cluster stage. Similarly, the diaxial isomer **142**, was allowed to react with $Co_2(CO)_8$ to give the corresponding trans-cluster, **144**, whose solid state structures are shown in Figure 5.4.[157] The most obvious result is that the cyclohexane ring has undergone a conformational flip whereby addition of a dicobalt hexacarbonyl moiety to each of the axial alkynyl units in **142** has resulted in the formation of the diequatorial isomer, **144**. Interestingly, in the solid state, the molecule no longer possesses an inversion center, but instead packs such that the phenyl groups form rows along the c axis of the unit cell, as depicted in Figure 5.5.

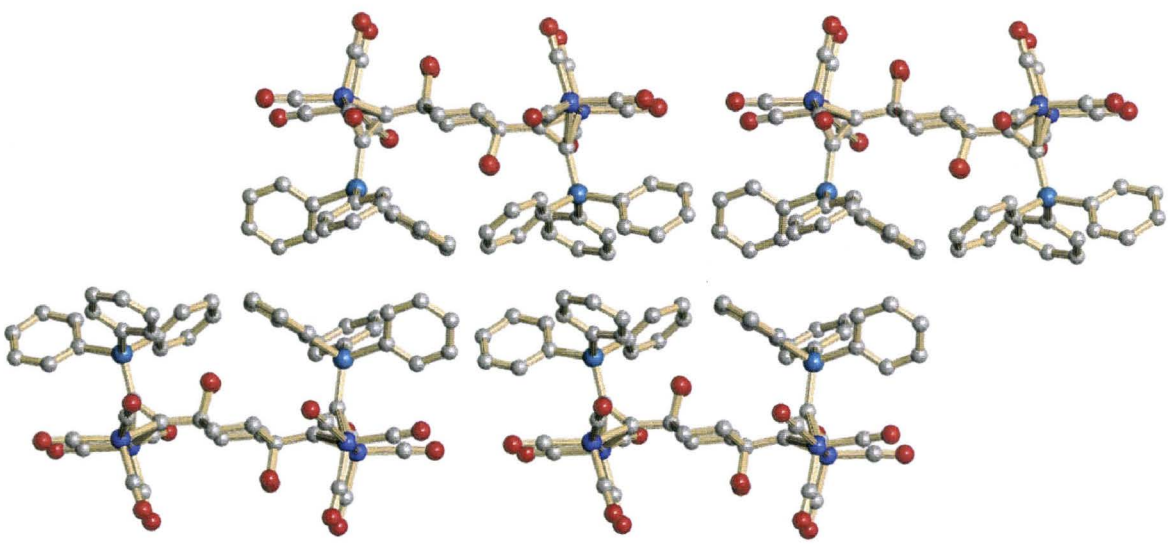

Figure 5.5 Packing Diagram along the c-axis of **144**.

The most dramatic effects are found for the cis complex **145**, the X-ray structure of which appears as Figure 5.6. The molecule adopts a well-defined twist-boat conformation with overall C_2 molecular symmetry. The angle between the C(2)-C(1)-C(3) and C(2)-C(3)-C(2A)-C(3A) planes is ≈ 33°, and the distance between O(1) and O(1A) is 2.705(10) Å.[158] The net result of converting two alkyne substituents into cobalt clusters has been to provide a convenient route to a twist-boat cyclohexane-1,4-diol, while decomplexation with iodine allows facile reversal of this conformational change.

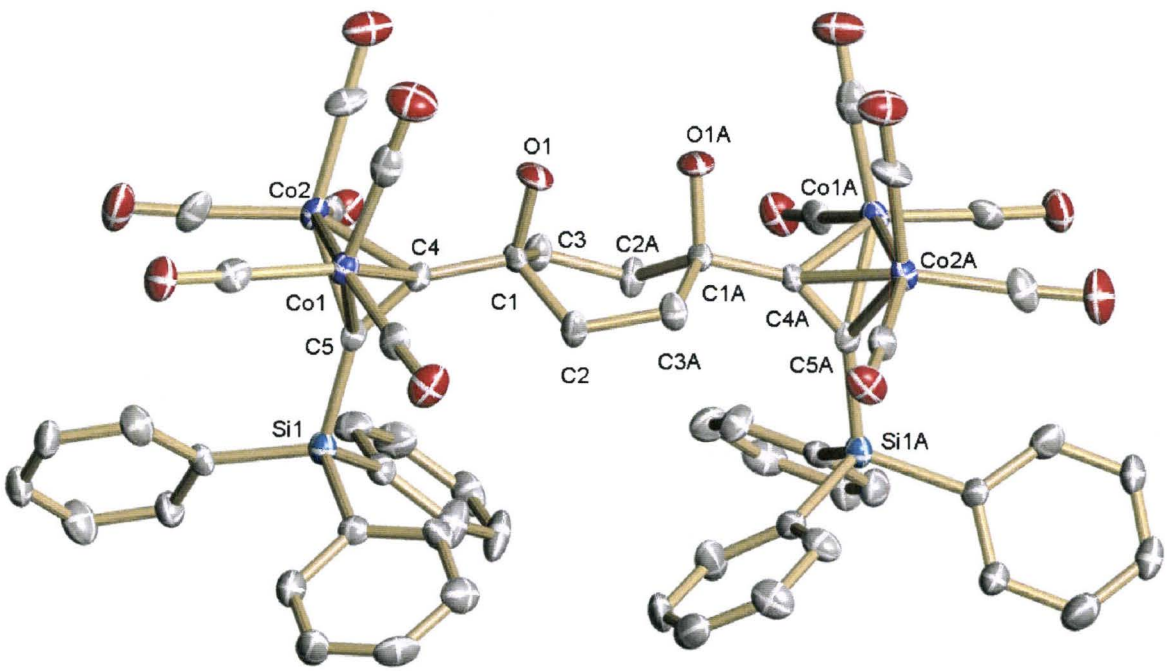

Figure 5.6 A 30% Thermal Ellipsoid Plot of **145**, without hydrogen atoms.

The analogous reaction of cyclohexan-1,4-dione with two equivalents of (trimethylsilylethynyl)lithium again afforded the trans- and cis-di-alkynols, **146** and **147**, and after treatment with $Co_2(CO)_8$: the bis-complexed trans- and cis-di-alkynols, **148** and **149** respectively, and a small quantity of the mono-complexed trans di-alkynol **150**,

which was also characterized by X-ray crystallography (Figure 5.7). The ring-flipped nature of complex **150** further illustrates the tendency of the cluster moiety to favour an equatorial position.[157]

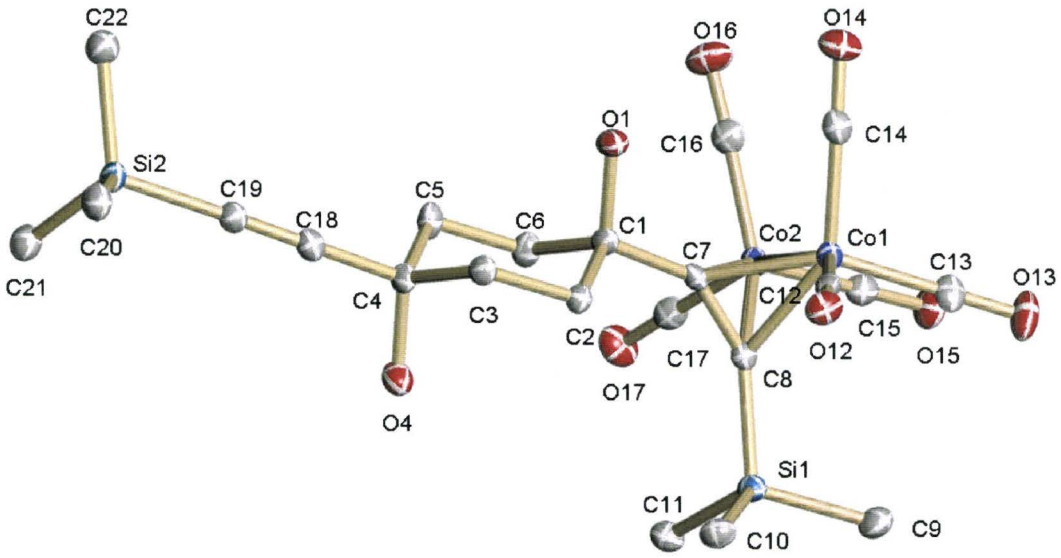

Figure 5.7 A 50% Thermal Ellipsoid Plot of **150**, with hydrogens removed for clarity.

Gratifyingly, the bis-cluster complex, **149**, derived from the cis-di-alkynol also yielded a twist-boat conformation with overall C_2 molecular symmetry, as shown in Figure 5.8. In contrast to the triphenylsilylated twist-boat, **145**, the O(1)···O(4) distance in **149** is now 3.099(12) Å, probably too long to support intra-molecular hydrogen bonds. However, in the solid state the molecules of **149** pack in pairs (Figure 5.9) such that the four oxygens are in a pseudo-tetrahedral arrangement with intermolecular O···O distances of approximately 2.776(11) Å, indicative of hydrogen bonding.[157]

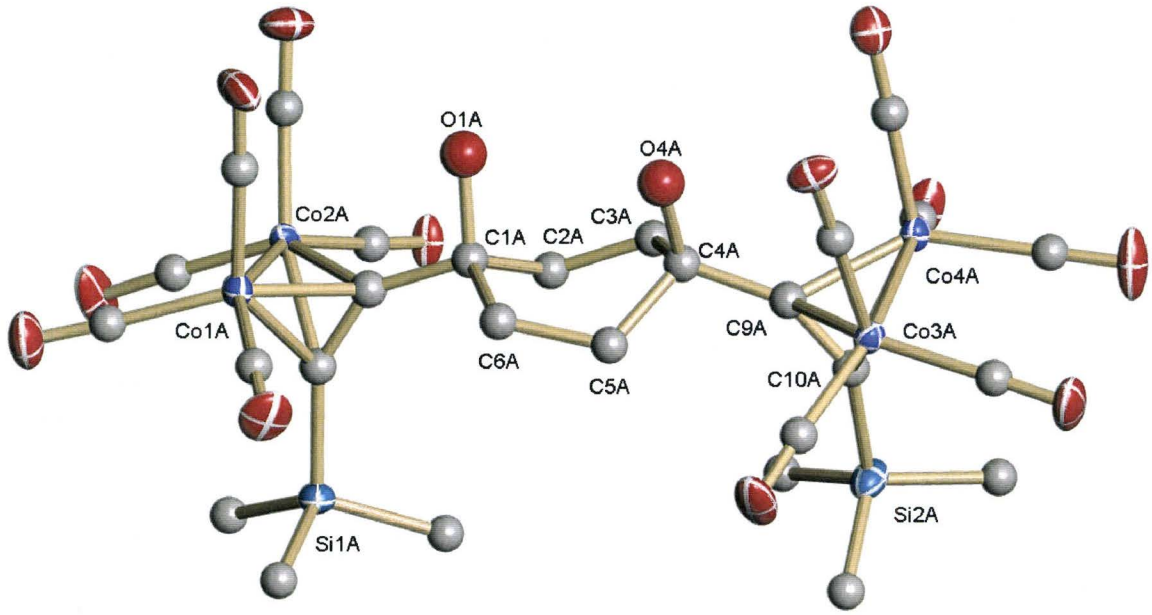

Figure 5.8 A 30% Thermal Ellipsoid Plot of **149** without hydrogen atoms.

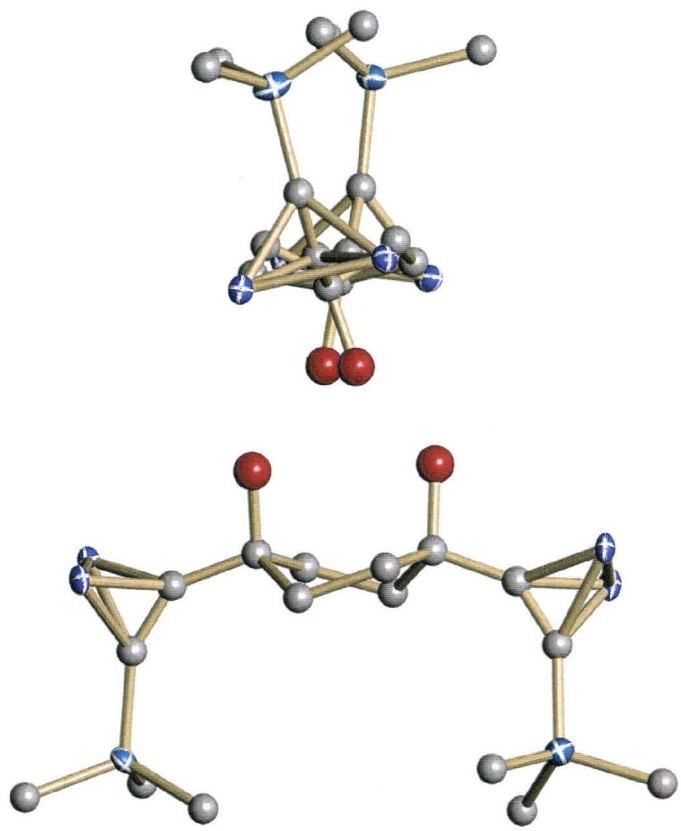

Figure 5.9 Illustration of the intermolecular interactions between the crystallographically independent molecules of **149**; cobalt carbonyls excluded for clarity.

One can readily envision silicon, germanium, or a transition metal occupying such a tetrahedral coordination site. Furthermore, decomplexation of the twist-boat complexes, **145** and **149**, would undoubtedly cause reversion back to the chair conformations, however, connection of the proximal alcohols via a heteroatom prior to decomplexation would presumably maintain the twist-boat geometries. Unfortunately, preliminary attempts to occupy this site by coordinating a silane between the diol have failed. Treatment of **149** with two equivalents of triethylamine in dichloromethane, and addition of diphenyldichlorosilane and 5% imidazole at 0 °C, according to literature procedures,[165] afforded the cyclohexenol, **151**, exclusively (Scheme 5.6). Single crystal diffraction analysis verified the identity of the complex, and revealed the predicted[166] pseudo 'half-chair' conformation of the cyclohexene ligand, illustrated in Figure 5.10. Intriguingly, the cobalt clusters maintain their equatorial positioning, while the trimethylsilyl substituents realign parallel with one another in opposing directions.

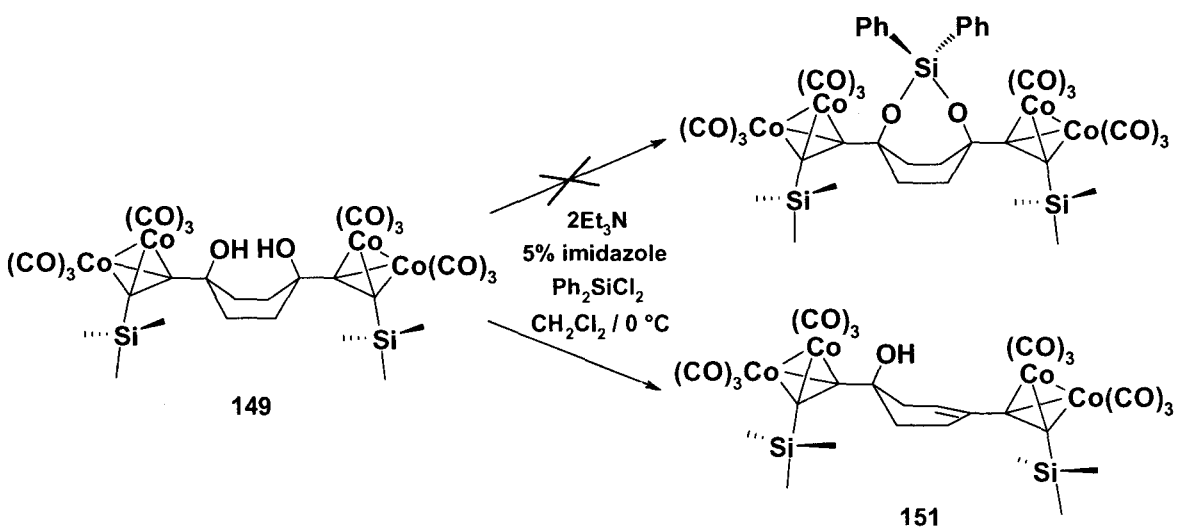

Scheme 5.6 Formation of a cyclohexenol in an attempt to bridge the twist-boat alcohols.

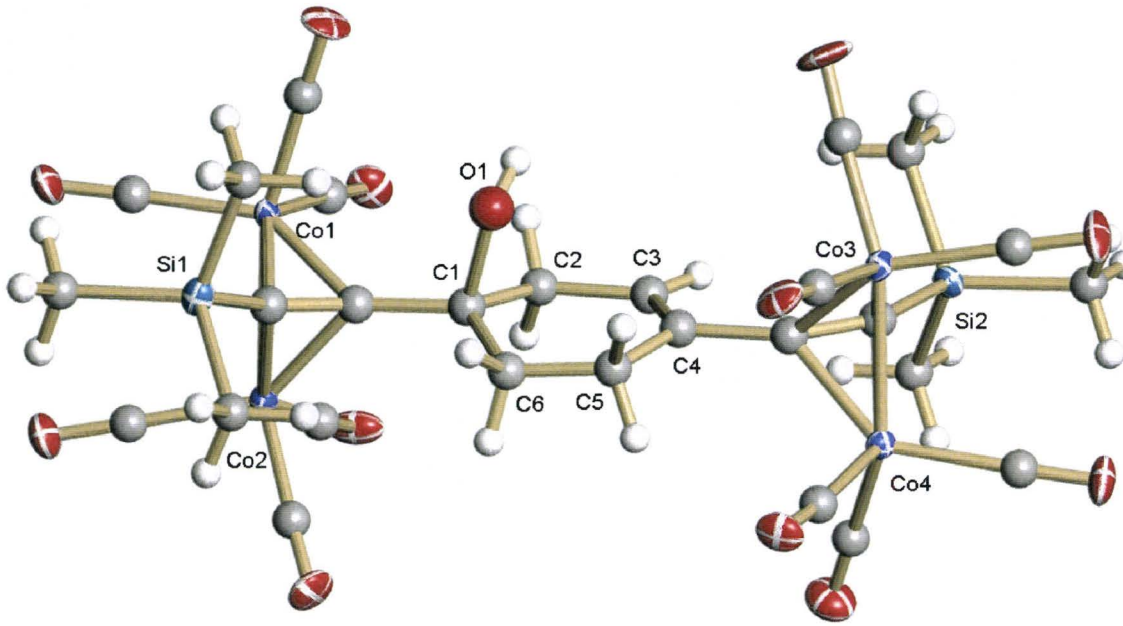

Figure 5.10 A 30% Thermal Ellipsoid Plot of **151**, whereby cyclohexyl hydrogen atoms are excluded for clarity.

It must be emphasized that crystallographically characterized cyclohexane twist-boats are relatively rare. Twenty-five years ago, Berti *et al.* reported the structure of 2,3-dibromo-4-tert-butyl-cyclohexyl para-nitrobenzoate,[167] and Biali has recently described two other cases, cis,trans,trans-1,2,3,4- and cis,syn,cis-1,2,4,5-tetracyclohexyl-cyclohexane.[168,169] There are also several examples in the Cambridge Crystallographic Database of metal complexes containing multiple polycyclohexyl-phosphines or –silanes in which severe crowding gives rise to the occasional maverick non-chair cyclohexyl ring. To our knowledge, the only crystallographically characterized 1,4-disubstituted twist-boat cyclohexane possesses both a porphyrin ring and a 2-methyl-1,4-naphthoquinone.[170] In that system, the torsion angles within the cyclohexane ring differ quite substantially from those expected for an idealized twist-boat geometry.[154c] It is indeed fascinating that **145** is the closest reported example of an idealized twist boat, evident in Table 5.1, for which a statistical comparison of the torsion angles of the

aforementioned twist-boats, and the cobalt-containing ones, **145** and **149**, is made. It should be noted that the two sets of values for **149** correspond to the two cystallographically independent molecules present within the unit cell.

Table 5.1 A comparison of torsional angles in known twist-boats.

	Idealized	Berti	Dieks	Biali (1,2,3,4)	Biali (1,2,4,5)	**145**	**149**
C(6)-C(1)-C(2)-C(3)	+65	+63.5	+61.8	+60.1	+64.5	+61.2	+57.8 +58.2
C(1)-C(2)-C(3)-C(4)	-31	-36.5	-42.4	-28.5	-24.7	-29.4	-37.8 -38.0
C(2)-C(3)-C(4)-C(5)	-31	-20.6	-17.5	-24.0	-37.1	-30.2	-17.6 -21.3
C(3)-C(4)-C(5)-C(6)	+65	+61.8	+61.8	+48.8	+64.5	+61.2	+56.1 +60.0
C(4)-C(5)-C(6)-C(1)	-31	-37.6	-42.3	-16.4	-24.7	-29.4	-37.1 -40.1
C(5)-C(6)-C(1)-C(2)	-31	-25.4	-17.8	-37.2	-36.9	-30.2	-20.9 -18.5

In principle, the accessibility of a boat conformer of cis-cyclohexan-1,4-diol can be turned into a synthetic advantage. For example, it has been reported that treatment of cis-cyclohexan-1,4-diol with dibutyldichlorogermane yields a mixture of cyclic germanoxane polymers, as depicted in Scheme 5.7; however, under conditions of very high dilution, small quantities of the cyclic dimer are obtained.[171] In contrast, use of cis-2,5-di-tert-butylcyclohexan-1,4-diol (for which infrared data indicate strong intramolecular hydrogen bonding, consistent with a twist-boat conformation[172]) furnishes the monomer, **152**, in 75% yield. Nevertheless, the product still contains bulky alkyl groups that would be difficult to remove, whereas use of cobalt carbonyl clusters to effect

a temporary augmentation of the steric bulk of an appropriately positioned substituent can be used for stereochemical control.

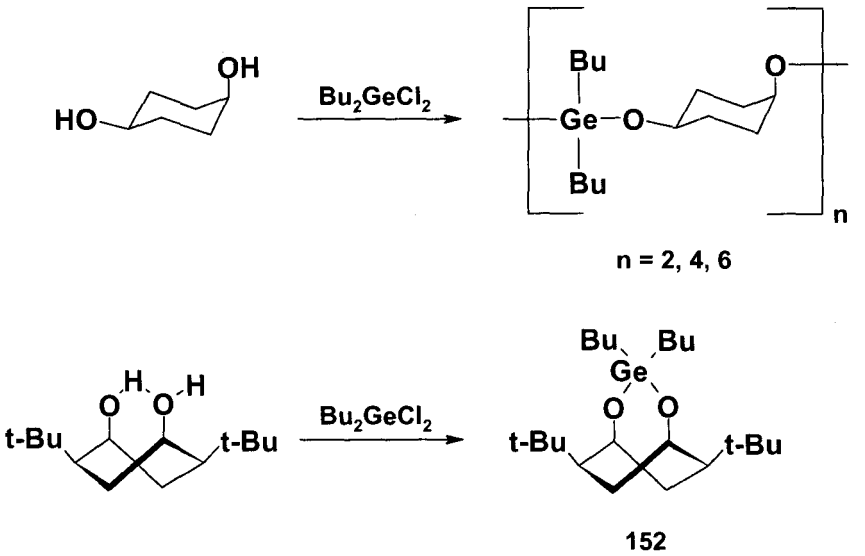

Scheme 5.7 Germanium-complexed twist-boat.[173]

5.4 Summary

Therefore, to our knowledge, the present examples are the only ones in which the chair–twist-boat interconversion can be controlled by incorporation of a readily removable functionality. Furthermore, this approach, whereby a dicobalt hexacarbonyl moiety can function as a conformational switch, illustrates the versatility of alkynyl cobalt-clusters, and has considerable potential for the selective manipulation of other ring systems.

Chapter Six: Future Work

6.1 Summary

The versatility of cobalt alkynyl clusters has been illustrated throughout this thesis, as an alkynyl protecting group, as a sterically demanding fragment useful for conformational control, and as a geometric modifier of linear alkynes that can engender migrations and other rearrangements. Furthermore, the inherent ability of cobalt clusters to provide stability to neighbouring cations facilitates unique transformations that may otherwise be unavailable, such as ring openings in terpenes, formation of tricobalt clusters, and conversion of these cations into their corresponding radical species.

6.2 Migrations

In order to further explore our original intention of taking advantage of the bend angle resulting from the complexation of a hexacarbonyldicobalt unit to a linear alkyne, it seems reasonable to investigate other substituents with the potential to migrate via cyclic intermediates of various sizes. Although Green's work[59a] and the efficiency of the aforementioned allyl migrations have thoroughly established the feasibility of cyclizations with seven-membered systems, the viability of smaller rings remains in question. As discussed in Section 2.3.1, it is possible that the incorporation of a silicon atom, with its enhanced size relative to carbon, will help relieve some ring strain in these smaller cycles. Even though our initial attempts of using a simple vinylsilane have not

succeeded thus far in demonstrating the viability of this reaction, preliminary calculations, shown in Figure 2.6, have indicated that this may in fact be sterically possible, as formation of the five-membered ring was presumably disfavored by the instability of the potentially generated intermediate cation. Perhaps, this electronic deterrence may be corrected by slightly modifying the vinyl substituent. For example, one could use (2-methylpropenyl)chlorodimethylsilane, **153**,[173] attach an appropriate propynol ligand, and subsequently complex with dicobalt hexacarbonyl to form **154**, which upon protonation would lead to the generation of a much more stable tertiary cation within the five-membered ring intermediate, **155**, and thus enhance the probability of migration, as illustrated in Scheme 6.1. Furthermore, this idea could be extended to six-membered rings by using 2-methylpropenyl(chloromethyl)dimethylsilane, **156**, as the starting silane, to form **157**, thus inserting a methylene spacer between the silane and the alkyne (Scheme 6.1). One could also contrast the stability of a secondary cation positioned β to silicon versus that of the tertiary one by initially using the commercially available silanes, **158** and **159**. Furthermore the alcohol can be altered while keeping in mind that a sterically non-demanding propargyl alcohol is preferable for a migration. Therefore, the fluorenyl ligand seems to be ideal, and cannot be ignored in these systems. However, several other planar ligands could be employed, including cyclopenta-phenanthren-4-one or a 2,3-disubstituted indenone, such as the dimethyl or diphenyl derivatives. Moreover, one could investigate the electronic effects endowed upon the initial cation by choosing hexafluoroacetone as the starting ketone. It would be interesting to see how the electron-withdrawing nature of the CF_3 groups would combat the stabilizing effects of the cobalt cluster on the cation. Several potential candidates for

alkynol ligands are presented in Figure 6.1 along with the various silanes that could be attached.

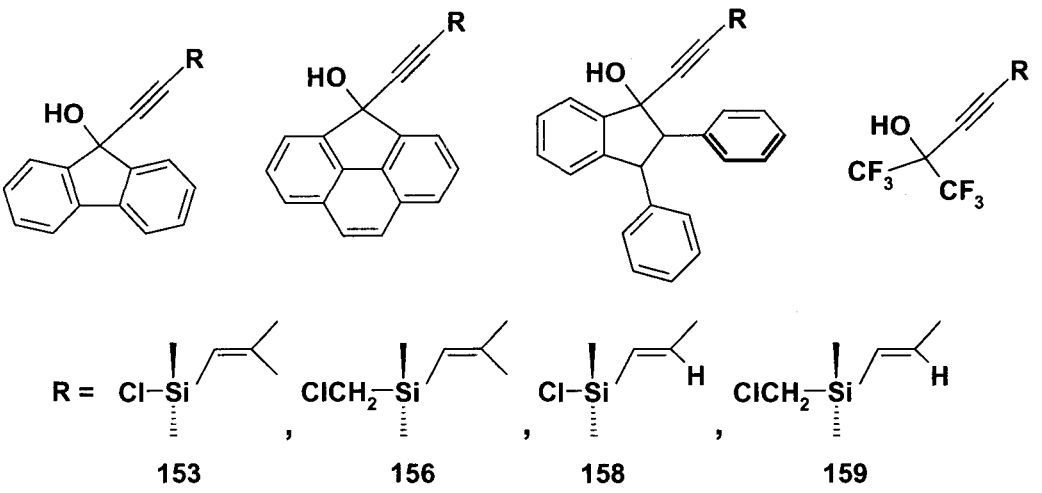

Figure 6.1 Potential ligands for migration reactions.

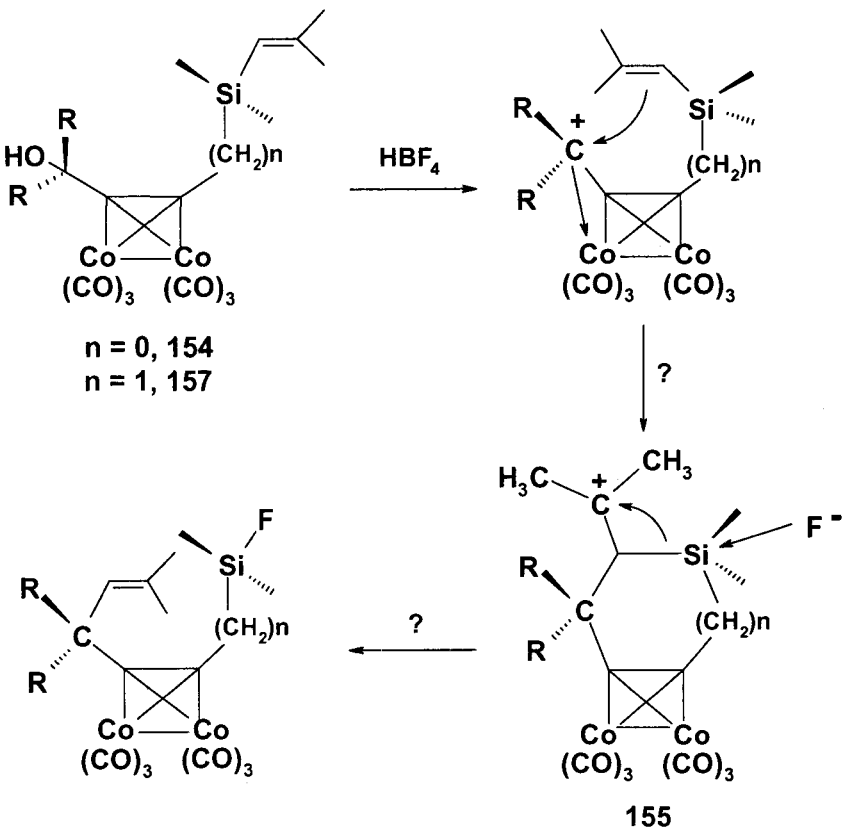

Scheme 6.1 Proposed route to other possible migration products via a 5- or 6-membered ring transition state.

6.3 Twist-Boats

The effects of cobalt complexed alkynes on cyclohexane conformations, and the fact that the chair to twist-boat interconversion can be controlled simply by addition or removal of the metal moiety is indeed quite remarkable. To reiterate, ideally one would like to maintain the distorted geometry induced by the cobalt carbonyls, even after their removal. It is hypothesized that this may be readily accomplished by tethering the axially positioned alcohols in these systems prior to detaching the metal fragments. Although we have not yet succeeded in our attempts to position a metal between the alcohols in either prepared twist-boat, **145** or **149**, it is thought that altering the coordination species by using an electron deficient transition metal, such as titanium, may facilitate bridging between the oxygens. Therefore, with the use of a reagent such as dichloro-bis(cyclo-pentadienyl)titanium (Cp_2TiCl_2), according to literature procedures,[174] it is thought that it might be possible to link the alcohols. Furthermore use of tetrachlorotitanium ($TiCl_4$),[175] may in fact permit the reaction of two twist-boat molecules, such that the titanium is situated in a tetrahedral environment as shown in Scheme 6.2. Subsequent removal of the cobalt carbonyls will not only maintain the twist-boat geometries, but allow further manipulation of the alkynyl substituents.

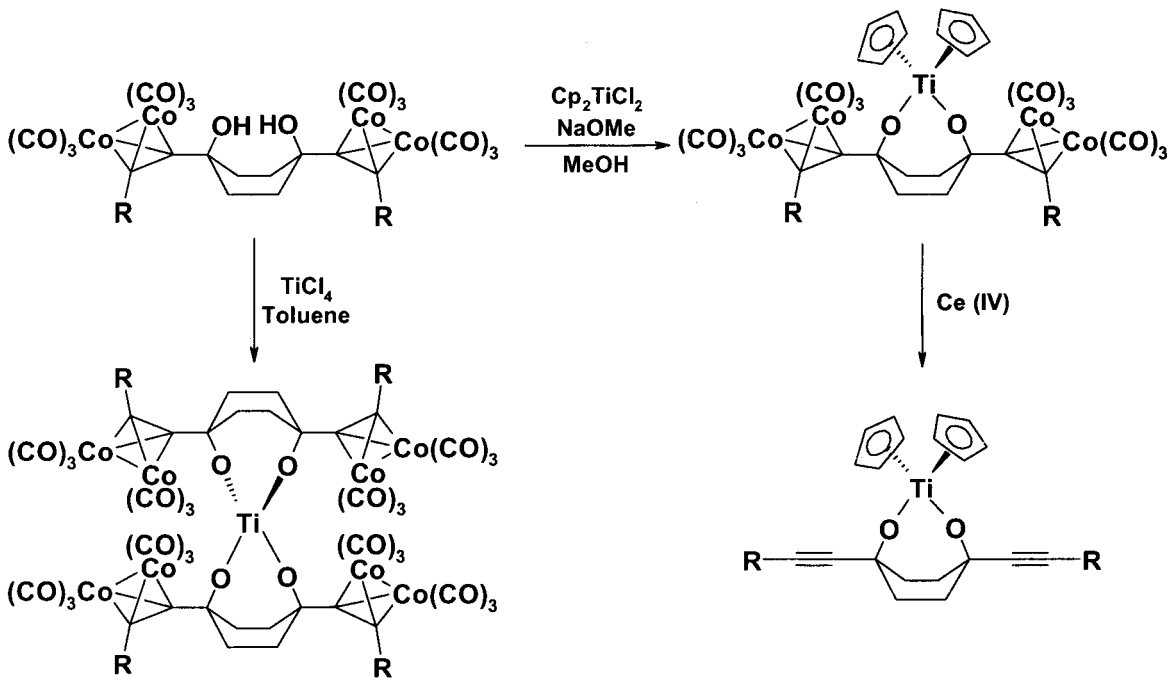

Scheme 6.2 Proposed method of maintaining the twist-boat conformation upon removal of the cobalt cluster.

6.4 Radicals

Considering all the unique reactions afforded by cobalt-clusters presented in this thesis, the radical preparations have by far the greatest potential to be widely applicable. The use of tetrahydrofuran as the solvent mediating protonation of cobalt-complexed propargyl alcohols, has opened the door to a plethora of possibilities. In particular, since very few metal peroxides are known, and consist primarily of metallocene derivatives, the synthesis of bimetallic transition metal peroxides may be extended to numerous other organometallic systems. An intriguing comparison can be made between tetrahedral dicobalt complexes and other similar clusters containing molybdenum, and tungsten. It is commonly acknowledged that molybdenum and tungsten have a greater stabilization effect on propargyl alcohols than does cobalt; so much that several complementary molybdenum cationic systems have been successfully isolated and characterized by x-ray

crystallography.[46c,91,107,176] Therefore, addition of $Cp_2M_2(CO)_4$ (M = Mo or W) to the fluorenylalkynyl-vinyl and -benzylsilanes, will afford the corresponding complexes **160** and **161** which, upon protonation in THF or diethyl ether, should generate the first molybdenum and tungsten peroxides (Scheme 6.3). Furthermore, it is worth noting that manipulation of the propargyl ligand and variation of the substituents on the metals, could yield an almost endless number of possibilities of dimetallic peroxides.

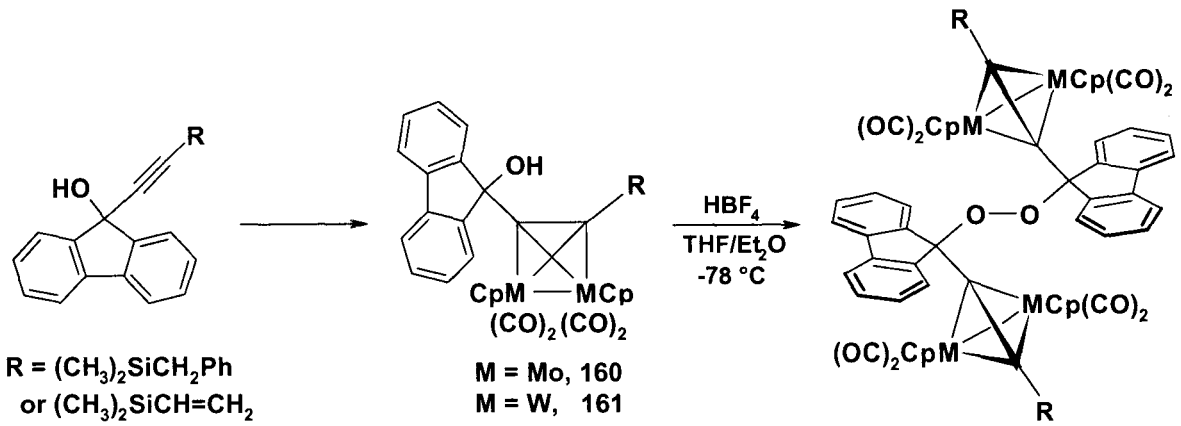

Scheme 6.3 A synthetic route to novel molybdenum and tungsten peroxides.

6.5 Conclusion

In closing, this thesis describes our attempts to expand the chemistry of cobalt clusters, and in particular the applicability of propargyl cation and radical systems for synthetic purposes. Nevertheless, these contributions in an expanding field only serve to underscore the many promising research avenues which may be pursued in the future.

Chapter Seven: Experimental

7.1 General Procedures

All syntheses were carried out under a dry nitrogen atmosphere in an enclosed round bottom flask, with constant stirring. All reactants and products were weighed in a glove bag. Solvents were dried and distilled according to standard procedures.[177] All chemicals were purchased and used as supplied by the Aldrich Chemical Company, with the exception of dicobalt octacarbonyl, obtained from Strem Chemicals Inc, allydimethylchlorosilane, vinyldimethylchlorosilane and benzyldimethylchlorosilane, which were acquired from Gelest Inc. Silica gel, 230-400 mesh, was used for flash column chromatography. Melting points (uncorrected) were determined with a Thomas-Hoover Unimelt capillary melting point apparatus. Elemental analyses are from Guelph Chemical Laboratories, Guelph, Ontario.

7.2 NMR Spectra

^{1}H and ^{13}C solution NMR spectra were acquired on Bruker DRX-500, AC-300 or AC-200/AV-200 spectrometers; spectra were recorded at ambient temperatures and referenced to the residual proton or ^{13}C solvent signal. The nOe experiments for **129** were accomplished using a non-spinning sample, on a Bruker DRX 500 spectrometer. One-dimensional ^{1}H, ^{13}C, ^{13}C DEPT, and two-dimensional ^{1}H-^{1}H COSY, ^{1}H-^{13}C shift-correlated and long range ^{1}H-^{13}C shift-correlated experiments recorded on the Bruker

DRX-500 spectrometer were measured on non-spinning samples that were prepared by filtering the dissolved compound through a small glass pipette containing glass wool and silica gel.

7.3 IR Spectra

IR spectra were obtained using dicholromethane solutions of individual samples, on a Bio-Rad FTS-40 FT-IR spectrometer using 0.1 mm NaCl windows.

7.4 Mass Spectra

All low resolution mass spectra were acquired acquired with a Finnigan EI/CI mass spectrometer system, using Direct Electron Impact (DEI) and Chemical Ionization (CI) methods. Chemical ionization was induced using NH_3 as the collision gas. High resolution mass spectra (HRMS) were obtained using a Micromass GCT, GC Time-of-Flight mass spectrometer. Electrospray Ionization (ESI) methods were used to acquire the mass spectra for compounds **139**, **140**, **142**, **144**, **145**, **147**, **148**, **149**, **150** and **151**, employing a Quattro LC triple quadrupole mass spectrometer (Micromass Canada Inc.).

7.5 X-ray Crystallography

X-ray crystallographic data were collected from single crystal samples of **33**, **39**, **42**, **43**, **77**, **112**, **120**, **121**, **124**, **125**, **130**, **135**, **136**, **142**, **144**, **145**, **149**, **150** and **151** mounted on a glass fibers. Data were collected using a P4 Bruker diffractometer, equipped with a Bruker SMART 1K charge coupled device (CCD) area detector, using the program SMART,[178] and a rotating anode, using graphite-monochromated Mo-Kα

radiation (λ = 0.71073 Å). The crystal-to-detector distance was 4.987 cm for all samples, and the data collection was carried out in 512 x 512 pixel mode, utilizing 2 x 2 pixel binning. The initial unit cell parameters were determined by a least-squares fit of the angular settings of the strong reflections, collected by a 12° scan in 40 frames over three different sections of reciprocal space (120 frames in total). Almost a complete sphere of data was collected, to better than 0.8 Å resolution at 148 K. Upon completion of the data collection, the first 50 frames were recollected in order to improve the decay correction analyses. Data reduction was carried out using the program SAINT,[179] which applied Lorentz and polarization corrections to the three-dimensionally integrated diffraction spots. The program SADABS,[180] was utilized for the scaling of diffraction data, the application of a decay correction, and an empirical absorption correction based on redundant reflections for all data sets except the twinned sample **144**, for which no absorption correction was applied. The structures were solved by using the direct-methods procedure in the Bruker SHELXTL program library,[181] and refined by full-matrix least squares methods on F^2 with anisotropic thermal parameters for all non-hydrogen atoms in **33**, **39**, **42**, **43**, **112**, **121**, **124**, **130**, **135**, **136**, **142**, **145**, and **150**.

The bridging methylene carbon, cluster carbon, carbonyl and cobalt atoms for **77**, were all successfully refined anisotropically, but a slight rotational disorder of the borneol ligand prevented such for this functionality.

Only the carbonyl carbons of **120** could not be refined anisotropically, however, as a result of the weak intensity of the data the fluorenyl moieties were restrained to simulate isotropic behaviour to provide a better model.

A partial twist-disorder of the silyl groups in **125**, modeled so that the major component consisted of 57%, did not allow for anisotropic refinement of the silicon methyls and vinyl group.

A small slip-disorder of one of the hydrogen-bonded fluorenyl ligands in **42**, containing 73% occupancy of the major fragment, required a partial restraining of these ligands to optimize the model.

As previously discussed in section 4.2.3, **121** contained a two-fold rotational disorder, whereby the fluorenyl ligands and the silyl substituents of the alkyne and allene in the two equally occupied molecular orientations, overlap with one another.

All carbon and oxygen atoms in **144**, and all carbons and the alcohol oxygens in **149**, had to be refined isotropically due to an insufficient amount of diffraction data available from the crystal samples. The crystal of **144** exhibited non-merohedral twinning, which was solved using the program GEMINI.[182] It was necessary to include a large number of partially overlapped diffraction spots to complete the refinement. There was a twist-disorder in the position of the chair. The hydroxides were modeled accordingly, but the disorder in the carbons could not be resolved.

PLATON[183] was used to subtract the diffractional contribution of a disordered cyclohexane solvent molecule from the intensity data of **149**; however, it could not be used for the disordered methylene chloride molecule found in **144** due to the twinning, and therefore the CH_2Cl_2 moiety was partially modeled.

An out-of-plane rotational disorder of the cyclohexyl ring was evident from a weakly diffracting crystal of **151**, whereby four of the six ring carbons were fully occupied, while the remaining two carbons and the oxygen of the alcohol were partially

occupied. Subsequently, anisotropic refinement was only possible for the cobalt, silicon, and carbonyl oxygen atoms.

Hydrogen atoms were added as fixed contributors at calculated positions with isotropic thermal parameters, based on the carbon atom to which they were bonded for **33**, **42**, **77**, **120**, **121**, **125**, **149**, **151**, the trimethylsilyl group of **130**, and the triphenyl silyl group of **145**. Hydrogen atoms were assigned from the difference map for the remaining samples. The symmetry disordered, intermolecular hydrogen bonding in **135** was modeled by fixing three hydrogens on the alcohol oxygens (H1a, H1b, H1c) whereby H1a has an occupancy of 50%, while H1b and H1c each have an occupancy of 25%.

121, **124**, **125**, **142** and **145** all sit on 2-fold rotation axes or inversion centers; therefore only half of each molecule was refined, and the other half was generated by the symmetry element listed in each respective Table 3 of the Appendix. **42**, **77**, **149**, and **151** crystallized with two crystallographically unrelated molecules in the unit cell; **120** and **130**, contained three and four crystallographically inequivalent molecules in the unit cell, respectively, while the remainder of structures consisted of one molecule in the asymmetric unit.

A full crystallographic appendix for **33**, **39**, **42**, **43**, **77**, **112**, **120**, **121**, **124**, **125**, **130**, **135**, **136**, **142**, **144**, **145**, **149**, **150** and **151**, containing all atomic coordinates, bond lengths, bond angles, thermal parameters, and any hydrogen bonds are listed in tables on the compact disc provided.

7.6 Synthesis and Characterization

1,1-Diphenyl-3-allyldimethylsilylpropynol, 31

Benzophenone (1.5 g, 8.2mmol) was added to a mixture of trimethylsilylacetylene (1.2 mL, 8.2 mmol), and n-butyllithium (8.2 mmol) in diethyl ether (30 mL) at -78 °C in a dry ice / isopropanol bath, affording after hydrolysis and flash chromatography with a 2:1 mixture of CH_2Cl_2/hexanes as eluent, 1,1-diphenyl-3-trimethylsilylpropynol[184] (2.1 g, 7.5 mmol, 92%), as a white solid. Treatment with tetra-n-butylammonium fluoride (4.7 mL, 7.5 mmol) in diethyl ether (30 mL) yielded, after flash chromatography with a 2:1 mixture of CH_2Cl_2/hexanes as eluent, 1,1-diphenylpropyn-1-ol (87%), as a yellow oil. Two equivalents of nBuLi (11.0 ml of a 1.6 M hexanes solution, 17.6 mmol) were added slowly to a solution of 1,1-diphenylpropyn-1-ol (1.83 g, 8.8 mmol) in anhydrous diethyl ether (20 mL), and left to react for 4 hours at low temperature. A solution of vinyldimethylchlorosilane (1.1 mL, 8.8 mmol) in anhydrous diethyl ether (20 mL) was then added dropwise and allowed to gradually warm to room temperature. The final mixture was quenched with 10 mL of $NaHCO_3$, and the product was extracted with diethyl ether, dried using $MgSO_4$, filtered, and isolated in vacuo. The product, **31**, a yellow oil, was purified using a silica gel chromatography column with a 50:50 mixture of CH_2Cl_2/hexanes, and recovered in 73% yield. ^{1}H NMR (200 MHz, $CDCl_3$): δ 7.53-7.60 (4H, m, Ph's), 7.12-7.37 (6H, m, Ph's), 5.78 (1H, m, CH=C), 4.86 (2H, m, C=CH_2), 3.02 (1H, s, OH), 1.67 (2H, d, CH_2), 0.19 (6H, s, $Si(CH_3)_2$). ^{13}C NMR (50 MHz): δ 144.7 (Ar C), 133.7 (*C*H=CH_2), 128.1, 127.5, 125.9 (Ar C's), 114.1 (CH=*C*H_2), 90.2 (*C*CSi), 74.5 (COH), 23.7 (CH_2), -2.4 ($Si(CH_3)_2$). MS (DEI, m/z (%)): 305 (1) $[(M-H)]^+$, 265 (33) $[(M-C_3H_5)]^+$, 247 (12) $[(M-C_3H_5-H-OH)]^+$, 232 (11) $[(M-C_3H_5-H-OH-CH_3)]^+$,

205 (12) $[(M-H-(C_3H_5)Si(CH_3)_2]^+$, 183 (100) $[(Ph_2COH)]^+$. (CI, NH_3, m/z (%)): 289 (46) $([M-OH]^+)$, 265 (13) $([M-C_3H_5]^+)$. HRMS: *m/z* calcd for $C_{20}H_{21}OSi$ 305.1327 $([M-H]^+)$, found 305.1362. HRMS: *m/z* calcd for $C_{17}H_{17}OSi$ 265.0999 $([M-C_3H_5]^+)$, found 265.1049.

1,1-Diphenyl-3-allyldimethylsilylpropynol[$Co_2(CO)_6$], 32. Dark red solid, (82%). Treatment of **31** with an equimolar quantity of $Co_2(CO)_8$ in THF at room temperature for 12 hours, gave **32** after chromatographic separation with hexanes. ^1H NMR (200 MHz, $CDCl_3$): δ 7.59-7.63 (4H, m, Ph's), 7.20-7.35 (6H, m, Ph's), 5.83 (1H, m, CH=C), 4.97 (2H, m, $C=CH_2$), 2.70 (1H, s, OH), 1.88 (2H, d, CH_2, ^2JH-H = 8.0 Hz), 0.39 (6H, s, $Si(CH_3)_2$). ^{13}C NMR (50 MHz): δ 199.6 (6CO's), 146.5 (Ar C), 133.7 ($CH=CH_2$), 128.0, 127.7, 126.4 (Ar C's), 121.9 ($CCSi$), 114.8 ($CH=CH_2$), 80.6 (COH), 76.7 ($CCSi$), 25.5 (CH_2), -0.5 ($Si(CH_3)_2$). MS (DEI, m/z (%)): 536 (1) $([M-2CO]^+)$, 508 (1) $([M-3CO]^+)$, 480 (5) $([M-4CO]^+)$, 452 (4) $([M-5CO]^+)$, 424 (10) $([M-6CO]^+)$, 382 (2) $([M-6CO-H-C_3H_5]^+)$, 265 (38) $([M-Co_2(CO)_6-C_3H_5]^+)$. (CI, NH_3, m/z (%)): 575 (4) $([M-OH]^+)$, 547 (3) $([M-OH-CO]^+)$, 519 (20) $([M-OH-2CO]^+)$, 491 (8) $([M-OH-3CO]^+)$, 480 (13) $([M-4CO]^+)$, 463 (6) $([M-OH-4CO]^+)$, 452 (8) $([M-5CO]^+)$, 435 (4) $([M-OH-5CO]^+)$, 424 (21) $([M-6CO]^+)$, 407 (3) $([M-OH-6CO]^+)$, 289 (90) $([M-OH-Co_2(CO)_6]^+)$, 183 (100) $[(Ph_2COH)]^+$. HRMS: *m/z* calcd for $C_{27}H_{22}OSi_2Co_2$ 535.9883 $([M-2CO]^+)$, found 535.9900.

A solution of **32** (0.9 g, 1.5 mmol) in 30 mL of THF was treated with 1.5 equivalents of HBF_4 at -78 °C in a dry ice / isopropanol bath, and monitored to completion using thin layer chromatography, before allowing to warm to room temperature and quenching with

H_2O. Removal of the solvent and chromatographic separation with hexanes afforded the trinuclear complex **33** (65%), and the hydrogen abstraction product **34** (12%).

Ph_2C=CHC$Co_3(CO)_9$, 33: Dark red solid, (65%), m.p. 132-133 °C. ^{1}H NMR (200 MHz, $CDCl_3$): δ 8.25 (1H, s, C=CH), 7.21-7.40 (10H, m, Ph's). ^{13}C NMR (50 MHz, $CDCl_3$): δ 199.8 (9CO's), 149.1, 142.7, 139.5, 136.6, 130.2, 128.8, 128.5, 127.9, 127.8, 127.6. MS (DEI, m/z (%)): 536 (23) ([M-3CO]$^+$), 452 (25) ([M-6CO]$^+$), 368 (42) ([M-9CO]$^+$), 191 (42) ([M-$Co_3(CO)_9$]$^+$). (CI, NH_3, *m/z* (%)): 621 (25) ([M+H]$^+$), 192 (100) ([M+H-C-$Co_3(CO)_9$]$^+$). Anal. Calc. for $C_{24}H_{11}O_9Co_3$: C 46.48; H 1.79. Found: C 46.08; H 1.90.

Ph_2CHCC-SiMe_2Allyl[$Co_2(CO)_6$], 34. Dark red oily solid, (12%). ^{1}H NMR (200 MHz, $CDCl_3$): δ 7.18-7.49 (10H, m, Ph's), 5.83 (1H, m, CH=C), 5.36 (1H, s, Ph_2CH), 4.98 (2H, m,C=CH_2), 1.81 (2H, d, CH_2, ^{2}JH-H = 8.0 Hz), 0.34 (6H, s, Si(CH_3)$_2$). ^{13}C NMR (50.13 MHz): δ 200.1 (6CO's), 143.8 (Ar C), 133.9 (*C*H=CH_2), 128.6, 128.2 and 127.3 (Ar C's), 114.5 (CH=*C*H_2), 78.2 (*C*CSi), 59.5 (Ph_2CH), 25.3 (CH_2), -0.9 (Si(CH_3)$_2$). MS (ESI (+ve, CH_3OH), *m/z* (%)): 560 (20) [(M-H-CH_3)]$^+$, 519 (11) [(M-H-2CO)]$^+$, 491 (8) [(M-H-3CO)]$^+$, 464 (18) [(M-4CO)]$^+$, 436 (15) [(M-5CO)]$^+$, 393 (100) [(M-CH_3-6CO)]$^+$. (DEI, *m/z* (%)): 520 (2) [(M-2CO)]$^+$, 464 (6) [(M-4CO)]$^+$, 436 (6) [(M-5CO)]$^+$, 408 (28) [(M-6CO)]$^+$, 349 (7) [(M-Co-6CO)]$^+$, 290 (10) ([M-$Co_2(CO)_6$]$^+$), 249 (100) ([M-$Co_2(CO)_6$-C_3H_5]$^+$), 167 (43) [(Ph_2CH)]$^+$.

Allyldimethylsilylethynylfluoren-9-ol, 37

37 was prepared analogously to **31** and was isolated as a yellow oil in 74% yield.

^{1}H NMR (200.13 MHz, $CDCl_3$): δ 7.25-7.97 (8H, m, fluorenyl), 5.79 (1H, m, CH=C),

4.90 (2H, m, C=CH_2), 2.79 (1H, s, OH), 1.64 (2H, d, CH_2, ^{2}JH-H = 7.3 Hz), 0.17 (6H, s, $Si(CH_3)_2$). ^{13}C NMR (50.13 MHz): δ 146.9, 139.1 (Ar C's), 133.7 (*C*H=CH_2), 129.5, 128.4, 124.3, 120.1 (Ar C's), 113.9 (CH=*C*H_2), 105.8 (*C*CSi), 86.6 (C*C*Si), 74.9 (COH), 23.7 (CH_2), -2.5 ($Si(CH_3)_2$). MS (DEI, *m/z* (%)): 304 (15) $[(M)]^+$, 287 (30) $[(M-OH)]^+$, 263 (76) $[(M-C_3H_5)]^+$. (CI, NH_3, *m/z* (%)): 304 (43) $[(M)]^+$, 287 (100) $[(M-OH)]^+$, 263 (24) $[(M-C_3H_5)]^+$, 247 (6) $[(M-OH-C_3H_5)]^+$.

Allyldimethylsilanylethynylfluoren-9-ol[$Co_2(CO)_6$], 38

Addition of octacarbonyldicobalt to **37**, at room temperature in THF yielded **38** after purification. Dark red oily solid, (86%). ^{1}H NMR (200 MHz, $CDCl_3$): δ 7.53-7.60 (4H, m, fluorenyl), 7.24-7.35 (4H, m, fluorenyl), 5.65 (1H, m, CH=C), 4.84 (2H, m, C=CH_2), 2.57 (1H, s, OH), 1.46 (2H, d, CH_2, ^{3}JH-H = 7.2 Hz), 0.00 (6H, s, $Si(CH_3)_2$). ^{13}C NMR (50 MHz): δ 199.9 (6CO's) 150.3, 138.8 (Ar C's), 134.2 (*C*H=CH_2), 129.5, 127.6, 124.3, 120.2 (Ar C's), 117.8 (*C*CSi), 114.0 (CH=*C*H_2), 83.3 (COH), 24.6 (CH_2), -1.7 ($Si(CH_3)_2$). MS (DEI, *m/z* (%)): 534 (21) $[(M-2CO)]^+$, 506 (10) $[(M-3CO)]^+$, 478 (43) $[(M-4CO)]^+$, 450 (42) $[(M-5CO)]^+$, 422 (100) $[(M-6CO)]^+$, 380 (30) $[(M+H-C_3H_5-6CO)]^+$. (DCI, NH_3, m/z (%)): 573 (100) $[(M-OH)]^+$, 545 (60) $[(M-OH-CO)]^+$, 517 (48) $[(M-OH-2CO)]^+$, 489 (13) $[(M-OH-3CO)]^+$, 478 (7) $[(M-4CO)]^+$, 450 (6) $[(M-5CO)]^+$, 422 (7) $[(M-6CO)]^+$, 304 (10) $[(M-Co_2(CO)_6)]^+$, 287 (13) $[(M-OH-Co_2(CO)_6)]^+$, 181 (12) $[(C_{13}H_8OH)]^+$.

Treatment of **38** (0.6 g, 1.0 mmol) with an equimolar amount of HBF_4 in dichloromethane at -78 °C, after column chromatography using hexanes, gave **39** and **40**.

(9-Allylfluorenylethynyl)dimethylfluorosilane[$Co_2(CO)_6$], 39: Dark red solid, (60%), m.p. 96 °C. ^{1}H NMR (200 MHz, $CDCl_3$): δ 7.72 (2H, m, fluorenyl), 7.58 (2H, m,

fluorenyl), 7.29-7.42 (4H, m, fluorenyl), 4.65-5.10 (3H, m, CH=CH_2), 3.17 (2H, d, CH_2, ^{3}JH-H = 6.6 Hz), 0.57 (6H, d, $Si(CH_3)_2$, ^{3}JH-F = 6.9 Hz). ^{13}C NMR (50 MHz): δ 199.0 (6CO's) 149.9, 140.2 (Ar C's), 132.9 (*C*H=CH_2), 128.3, 127.3, 124.3, 119.6 (Ar C's), 118.2 (CH=*C*H_2), 57.8 (C quat.), 45.0 (CH_2), 0.9 ($Si(CH_3)_2$, ^{2}JC-F = 16.8 Hz). MS (DEI, *m/z* (%)): 536 (10) $[(M-2CO)]^+$, 508 (18) $[(M-3CO)]^+$, 452 (26) $[(M-5CO)]^+$, 424 (25) $[(M-6CO)]^+$, 265 (32) $[(M-C_3H_5-Co_2(CO)_6)]^+$. (DCI, NH_3, *m/z* (%)): 610 (25) $[(M+NH_4)]^+$, 582 (56) $[(M+NH_4-CO)]^+$, 554 (24) $[(M+NH_4-2CO)]^+$, 537 (34) $[(M+NH_4-OH-2CO)]^+$, 509 (12) $[(M+NH_4-OH-3CO)]^+$, 469 (44) $[(M+NH_4-H-5CO)]^+$, 424 (100) $[(M-6CO)]^+$, 324 (30) $[(M-C_3H_5-Co-6CO)]^+$, 265 (12) $[(M-C_3H_5-Co_2(CO)_6)]^+$.

(9-Allylfluorenylethynyl)dimethylsilanol[$Co_2(CO)_6$], 40: Dark red solid, (20%), m.p. 67 °C. ^{1}H NMR (200 MHz, $CDCl_3$): δ 7.66-7.74 (4H, m, fluorenyl), 7.33-7.40 (4H, m, fluorenyl), 4.66-5.13 (3H, m, CH=CH_2), 3.24 (2H, d, CH_2, ^{3}JH-H = 6.6 Hz), 0.48 (6H, s, $Si(CH_3)_2$). ^{13}C NMR (50 MHz): δ 199.5 (6CO's) 150.1, 140.2 (Ar C's), 133.0 (*C*H=CH_2), 128.2, 127.2, 124.4, 120.1 (Ar C's), 118.1 (CH=*C*H_2), 78.3 (C*C*Si), 57.8 (C quat.), 44.7 (CH_2), 1.9 ($Si(CH_3)_2$). MS (DEI, m/z (%)): 534 (15) $[(M-2CO)]^+$, 506 (14) $[(M-3CO)]^+$, 478 (7) $[(M-4CO)]^+$, 450 (100) $[(M-5CO)]^+$, 422 (68) $[(M-6CO)]^+$, 322 (21) $[(M-C_3H_5-Co-6CO)]^+$. (DCI, NH_3, *m/z* (%)): 608 (24) $[(M+NH_4)]^+$, 580 (66) $[(M+NH_4-CO)]^+$, 552 (12) $[(M+NH_4-2CO)]^+$, 535 (100) $[(M+NH_4-OH-2CO)]^+$, 507 (32) $[(M+NH_4-OH-3CO)]^+$, 496 (36) $[(M+NH_4-4CO)]^+$, 467 (30) $[(M+NH_4-H-5CO)]^+$, 450 (83) $[(M-5CO)]^+$, 422 (50) $[(M-6CO)]^+$, 322 (24) $[(M-C_3H_5-Co-6CO)]^+$, 263 (15) $[(M-C_3H_5-Co_2(CO)_6)]^+$

Addition of octacarbonyldicobalt (0.150 g) to the minor fraction (0.105 g) obtained from the preparation of **37,** afforded **41**, **42**, and **43**.

(9-Allyldimethylsiloxyfluorenylethynyl)-9-allyldimethylsilane[$Co_2(CO)_6$], **41**: Dark red oily solid, (0.055 g). ^{1}H NMR (200 MHz, $CDCl_3$): δ 7.53-7.66 (4H, m, fluorenyl), 7.27-7.42 (4H, m, fluorenyl), 5.63 (2H, m, CH=C), 4.82 (4H, m, C=CH_2), 1.46 and 1.36 (2H each, d, CH_2, ^{3}JH-H = 7.8 Hz), 0.01 and –0.25 (6H each, s, $Si(CH_3)_2$). ^{13}C NMR (50 MHz): δ 200.2 (6CO's) 150.2, 138.9 (Ar C's), 134.1 and 133.9 (*C*H=CH_2), 129.5, 127.4, 125.2, 120.2 (Ar C's), 113.9 and 113.6 (CH=*C*H_2), 85.0 (*C*CSi), 25.6 and 24.6 (CH_2), -1.1 and –1.8 ($Si(CH_3)_2$). MS (DEI, *m/z* (%)): 632 (5) $[(M-2CO)]^+$, 576 (10) $[(M-4CO)]^+$, 548 (14) $[(M-5CO)]^+$, 520 (100) $[(M-6CO)]^+$, 478 (10) $[(M-C_3H_5-H-6CO)]^+$. (DCI, NH_3, *m/z* (%)): 573 (100) $[(M-OSi(CH_3)_2(C_3H_5))]^+$, 548 (60) $[(M-5CO)]^+$, 520 (85) $[(M-6CO)]^+$.

Fluorenylethynyldimethyl-2-hydroxypropylsilane[$Co_2(CO)_6$], **42**: Dark red solid, (0.030 g), m.p. 130-132 °C. ^{1}H NMR (200 MHz, $CDCl_3$): δ 7.65-7.72 (4H, m, fluorenyl), 7.32-7.40 (4H, m, fluorenyl), 4.10 (1H, s, SiOH), 2.63 (1H, s, OH), 1.36 (2H, broad, CH_2), 1.20 (3H, broad, CH_3), 0.19 and 0.15 (3H, s, $Si(CH_3)$). ^{13}C NMR (50 MHz): δ 199.4 (6CO's) 150.6, 139.2, 129.2, 127.4, 124.2, 120.0 (Ar C's), 117.8 (*C*CSi), 83.4 (C*C*Si), 66.5 (COH), 37.2 28.3, 27.6, 0.9 and –0.1 ($Si(CH_3)_2$). MS (DEI, *m/z* (%)): 608 (3) $[(M)]^+$, 552 (10) $[(M-2CO)]^+$, 496 (12) $[(M-4CO)]^+$, 468 (41) $[(M-5CO)]^+$, 440 (30) $[(M-6CO)]^+$, 380 (15) $[(M+H-Co-6CO)]^+$, 321 (10) $[(M+H-Co_2(CO)_6)]^+$. (DCI, NH_3, *m/z* (%)): 591 (52) $[(M-OH)]^+$, 563 (35) $[(M-OH-CO)]^+$, 535 (22) $[(M-OH-2CO)]^+$, 507 (20) $[(M-OH-3CO)]^+$, 479 (20) $[(M-OH-4CO)]^+$, 468 (21) $[(M-5CO)]^+$, 399 (18) $[(M+NH_4-Co-6CO)]^+$, 305 (54) $[(M-OH-Co_2(CO)_6)]^+$, 181 (70) $[(C_{13}H_8OH)]^+$.

3-Hydroxyl-3-methyl-but-1-ynyl-fluoren-9-ol[$Co_2(CO)_6$], 43: Dark red solid, (0.086 g), m.p. 120-121 °C. ^{1}H NMR (200 MHz, $CDCl_3$): δ 7.71-7.84 (4H, m, fluorenyl), 7.36-7.53 (4H, m, fluorenyl), 4.09 and 3.03 (1H, s, OH), 1.58 (6H, s, $C(CH_3)_2$). ^{13}C NMR (50 MHz): δ 199.1 (6CO's) 150.1, 138.8, 129.4, 127.6, 124.5, 120.1 (Ar C's), 106.9 and 102.6 (CC-cluster), 83.5 and 73.4 (COH), 32.9 (CH_2). MS (DEI, *m/z* (%)): 522 (4) $[(M-CO)]^+$, 494 (3) $[(M-2CO)]^+$, 466 (12) $[(M-3CO)]^+$, 438 (11) $[(M-4CO)]^+$, 410 (8) $[(M-5CO)]^+$, 382 (48) $[(M-6CO)]^+$, 364 (50) $[(M-H-OH-6CO)]^+$, 324 (12) $[(M+H-Co-6CO)]^+$. (DCI, NH_3, *m/z* (%)): 533 (35) $[(M-OH)]^+$, 505 (34) $[(M-H-2OH)]^+$, 449 (12) $[(M-OH-3CO)]^+$, 438 (32) $[(M-4CO)]^+$, 410 (16) $[(M-5CO)]^+$, 382 (24) $[(M-6CO)]^+$, 364 (16) $[(M-H-OH-6CO)]^+$, 247 (13) $[(M-OH-Co_2(CO)_6)]^+$, 230 (11) $[(M-2OH-Co_2(CO)_6)]^+$,181 (100) $[(C_{13}H_8OH)]^+$.

$(H_3C)_2C(OH)C{\equiv}CSi(CH_3)_2(CH{=}CH_2)$, 45. Two equivalents of nBuLi (14.77 mL of a 1.6 M hexanes solution, 23.64mmol) were added slowly to a solution of 2-methyl-3-butyn-2-ol (1.15 mL, 11.82 mmol) in anhydrous diethyl ether (20 mL), and left to react for 4 hours at low temperature. A solution of vinyldimethylchlorosilane (1.43 g, 11.82 mmol) in anhydrous diethyl ether (20 mL) was then added dropwise. The solution was allowed to gradually warm up to room temperature, and the final mixture was quenched with 10 mL of $NaHCO_3$. **45** was extracted with diethyl ether, dried using $MgSO_4$, filtered, isolated in vacuo, purified using a silica gel column with a 50:50 mixture of CH_2Cl_2/hexanes, and recovered as a yellow oil in 87% yield. ^{1}H NMR (200 MHz, $CDCl_3$): δ 5.61-6.30 (3H, m, vinyl), 1.47 (6H, s, $(CH_3)_2COH$), 0.17 (6H, s, $(CH_3)_2Si$). ^{13}C NMR (50 MHz): δ 138.8 ($CH{=}CH_2$), 132.4 ($CH{=}CH_2$), 88.8 ($CCSi$), 70.0 ($CCSi$), 32.8 ($CH_3)_2COH$), -0.4 ($CH_3)_2Si$). MS (DEI, *m/z* (%)): 168 (37) $[(M)]^+$, 153 (71) [(M-

$CH_3)]^+$, 151 (27) $[(M\text{-}OH)]^+$, 85 (42) $[((CH_3)_2SiCH{=}CH_2)]^+$. (DCI, NH_3, *m/z* (%)): 186 (19) $[(M{+}NH_4)]^+$, 168 (51) $[(M)]^+$, 151 (42) $[(M\text{-}OH)]^+$.

$(H_3C)_2C(OH)C{\equiv}CSi(CH_3)_2(CH{=}CH_2)[Co_2(CO)_6]$, **46**. Dark red oily solid, (91%). A solution of **45** (0.49 g, 2.94 mmol) in anhydrous THF (15 mL) was added dropwise to octacarbonyldicobalt (1.02 g, 2.98 mmol) dissolved in anhydrous THF (40 mL). The mixture was left to react for 12 hours at room temperature. The solvent was removed in vacuo and the product was purified using column chromatography with a hexanes solution. ^{1}H NMR (500 MHz, CD_2Cl_2): δ 6.30 (1H, d of d, C*H*=CH_2, ^{2}JH-H = 20.3 Hz, ^{3}JH-H = 14.6 Hz), 6.07 (1H, d of d, CH=C*H*$_2$, ^{3}JH-H = 14.6 and 3.4 Hz), 5.89 (1H, d of d, CH=C*H*$_2$, ^{2}JH-H = 20.3 Hz, ^{3}JH-H = 3.4 Hz), 1.81 (1H, s, OH), 1.58 (6H, s, (C*H*$_3$)$_2$COH), 0.41 (6H, s, $(CH_3)_2$Si). ^{13}C NMR (125.7 MHz): δ 138.0 (*C*H=CH_2), 133.5 (CH=*C*H$_2$), 105.7 (*C*C-Si), 73.3 (C*C*-Si), 33.6 (*C*H$_3$)$_2$COH), -0.9 $(CH_3)_2$Si). MS (DEI, *m/z* (%)): 454 (18) $[(M)]^+$, 398 (100) $[(M\text{-}2CO)]^+$, 342 (65) $[(M\text{-}4CO)]^+$, 286 (91) $[(M\text{-}6CO)]^+$, 258 (52) $[(M\text{-}6CO\text{-}C_2H_4)]^+$. (DCI, NH_3, *m/z* (%)): 437 (76) $[(M\text{-}OH)]^+$, 409 (60) $[(M\text{-}OH\text{-}CO)]^+$, 381 (60) $[(M\text{-}OH\text{-}2CO)]^+$, 353 (65) $[(M\text{-}OH\text{-}3CO)]^+$, 342 (100) $[(M\text{-}4CO)]^+$, 325 (49) $[(M\text{-}OH\text{-}4CO)]^+$, 314 (18) $[(M\text{-}5CO)]^+$, 286 (30) $[(M\text{-}6CO)]^+$, 227 (16) $[(M\text{-}Co\text{-}6CO)]^+$, 168 (21) $[(M\text{-}Co_2(CO)_6)]^+$.

$(H_3CC{=}CH_2)C{\equiv}CSi(CH_3)_2(CH{=}CH_2)[Co_2(CO)_6]$, **47**. Dark red solid, (72%), m.p. (dec.) > 151 °C. HBF_4 (0.18 mL, 1.21 mmol) was added dropwise to **46** (0.55 g, 1.21 mmol) dissolved in 25 mL of CH_2Cl_2, at -78 °C, and the mixture was left to gradually warm to room temperature. The solution was quenched with 10 mL of $NaHCO_3$, dried with $MgSO_4$, filtered and isolated in vacuo. The compound was purified

chromatographically using a 50:50 mixture of CH_2Cl_2/hexanes and identified as **47**. ^1H NMR (500 MHz, CD_2Cl_2): δ 6.30 (1H, d of d, C*H*=CH_2 (vinyl), ^{2}JH-H = 20.3 Hz, ^{3}JH-H = 14.6 Hz), 6.06 (1H, d of d, CH=C*H*$_2$ (vinyl), ^{3}JH-H = 14.6 and 3.4 Hz), 5.86 (1H, d of d, CH=C*H*$_2$ (vinyl), ^{2}JH-H = 20.3 Hz, ^{3}JH-H = 3.4 Hz), 5.41 (1H, m, CH_3C=C*H*$_2$, ^{4}JH-H = 0.7 Hz), 5.27 (1H, m, CH_3C=C*H*$_2$, ^{4}JH-H = 1.4 Hz), 2.11 (3H, d, C*H*$_3$C=CH_2, ^{4}JH-H = 0.7 Hz), 0.42 (3H, s, CH_3Si), 0.08 (3H, s, CH_3Si). ^{13}C NMR (125.7 MHz): δ 200.9 (6CO's), 142.2 (CH_3*C*=CH_2), 137.8 (*C*H=CH_2 vinyl), 133.3 (CH=*C*H$_2$ vinyl), 117.6 (CH_3C=*C*H$_2$), 24.7 (*C*H$_3$C=CH_2), -1.0 ((CH_3)$_2$Si). MS (DEI, *m/z* (%)): 380 (100) [(M-2CO)]$^+$, 352 (32) [(M-3CO)]$^+$, 324 (17) [(M-4CO)]$^+$, 296 (42) [(M-5CO)]$^+$, 268 (18) [(M-6CO)]$^+$, 209 (15) [(M-Co-6CO)]$^+$. (DCI, NH_3, *m/z* (%)): 437 (60) [(M+H)]$^+$, 409 (48) [(M+H-CO)]$^+$, 381 (42) [(M+H-2CO)]$^+$, 353 (48) [(M+H-3CO)]$^+$, 342 (100) [(M+NH_4-4CO)]$^+$, 325 (36) [(M+H-4CO)]$^+$, 314 (55) [(M+NH_4-5CO)]$^+$, 269 (8) [(M+H-6CO)]$^+$.

All benzyl syntheses were identical to the corresponding vinyl syntheses, using benzyldimethylchlorosilane instead of vinyldimethylchlorosilane.

(H_3C)$_2$C(OH)C≡CSi(CH_3)$_2$(CH_2Ph), **50**. Yellow oil, (81%). ^1H NMR (200 MHz, $CDCl_3$): δ 7.02-7.25 (5H, m, Ph), 2.17 (2H, s, CH_2), 1.48 (6H, s, (CH_3)$_2$COH), 0.11 (6H, s, (CH_3)$_2$Si). ^{13}C NMR (50 MHz): δ 139.0 (ipso), 128.4 (2 x ortho or meta), 128.1 (2 x meta or ortho), 124.3 (para), 31.2 ((CH_3)$_2$COH), -2.1 (CH_3)$_2$Si). MS (DEI, *m/z* (%)): 232 (12) [(M)]$^+$, 231 (43) [(M-H)]$^+$, 215 (6) [(M-OH)]$^+$, 149 (42) [((CH_3)$_2$SiCH_2Ph)]$^+$, 91 (100) [(CH_2Ph)]$^+$. (DCI, NH_3, *m/z* (%)): 215 (100) [(M-OH)]$^+$, 149 (11) [((CH_3)$_2$SiCH_2Ph)]$^+$, 91 (26) [(CH_2Ph)]$^+$.

$(H_3C)_2C(OH)C{\equiv}CSi(CH_3)_2(CH_2Ph)[Co_2(CO)_6]$, 51. Dark red oily solid, (88%). ^1H NMR (200 MHz, $CDCl_3$): δ 7.03-7.24 (5H, m, Ph), 2.36 (2H, s, CH_2), 1.81 (1H, s, OH), 1.58 (6H, s, $(CH_3)_2COH$), 0.25 (6H, s, $(CH_3)_2Si$). ^{13}C NMR (50 MHz): δ 200.2 (CO's), 138.6 (ipso), 128.4 (2 x ortho or meta), 128.3 (2 x meta or ortho), 124.6 (para), 121.8 (*C*CSi), 76.4 (C*C*Si), 72.9 (C-OH), 33.4 ($(CH_3)_2COH$), 27.5 (CH_2), -1.1 ($(CH_3)_2Si$). MS (DEI, *m/z* (%)): 434 (33) $[(M-3CO)]^+$, 378 (28) $[(M-4CO)]^+$, 350 (30) $[(M-6CO)]^+$, 291 (24) $[(M-Co-6CO)]^+$, 273 (58) $[(M-H_2O-Co-6CO)]^+$, 59 (31) $[((CH_3)_2COH)]^+$. (DCI, NH_3, *m/z* (%)): 501 (22) $[(M-OH)]^+$, 473 (16) $[(M-OH-CO)]^+$, 417 (33) $[(M-OH-3CO)]^+$, 389 (13) $[(M-OH-4CO)]^+$, 350 (17) $[(M-6CO)]^+$, 250 (38) $[(M+NH_4-Co_2(CO)_6)]^+$, 232 (31) $[(M-Co_2(CO)_6)]^+$, 215 (100) $[(M-OH-Co_2(CO)_6)]^+$, 91 (34) $[(CH_2Ph)]^+$.

$(H_3CC{=}CH_2)C{\equiv}CSi(CH_3)_2(CH_2Ph)[Co_2(CO)_6]$, 52. Dark red solid, (66%), m.p. (dec.) > 112 °C. ^1H NMR (200 MHz, $CDCl_3$): δ 7.04-7.24 (5H, m, Ph), 5.37 and 5.26 (1H each, broad, $C{=}CH_2$), 2.36 (2H, s, CH_2), 2.05 (3H, s, CH_3), 0.25 (6H, s, $(CH_3)_2Si$). ^{13}C NMR (50 MHz): δ 200.0 (6CO's), 141.6 ($CH_3C{=}CH_2$), 138.8 (ipso), 128.4 (2 x ortho or meta), 128.3 (2 x meta or ortho), 124.6 (para), 117.6 ($CH_3C{=}CH_2$), 108.3 (*C*CSi), 78.6 (C*C*Si), 27.3 (CH_2), 24.6 ($CH_3C{=}CH_2$), -1.3 ($(CH_3)_2Si$). MS (DEI, *m/z* (%)): 416 (42) $[(M-3CO)]^+$, 388 (15) $[(M-4CO)]^+$, 360 (21) $[(M-5CO)]^+$, 332 (37) $[(M-6CO)]^+$, 273 (100) $[(M-Co-6CO)]^+$, 123 (90) $[(CH_2C(CH_3)C{\equiv}CSi(CH_3)_2)]^+$, 91 (31) $[(CH_2-Ph)]^+$. (DCI, NH_3, *m/z* (%)): 501 (5) $[(M+H)]^+$, 473 (14) $[(M-OH)]^+$, 417 (50) $[(M+H-3CO)]^+$, 389 (73) $[(M+H-4CO)]^+$, 332 (37) $[(M-6CO)]^+$, 273 (100) $[(M-Co-6CO)]^+$, 233 (22) $[(M+H-Co_2(CO)_6)]^+$.

All syntheses involving borneol ligands were prepared analogously to the 1,1-diphenyl-3-allyldimethylsilylpropynyl systems, **31** and **32**, using (1R)-(+)-camphor as the starting ketone, unless otherwise stated.

(2-Endo-allyldimethylsilyl)ethynylborneol, 67. Yellow oil, (76%). ^{1}H NMR (200 MHz, $CDCl_3$): δ 5.77 (1H, d of d of t, $SiCH_2CH{=}CH_2$, ^{3}JH-H = 16.4, 10.5 and 8.1 Hz), 4.91 and 4.87 (1H each, m, $SiCH_2CH{=}CH_2$), 2.17 (1H, d of d of d, H_3, ^{2}JH-H = 13.4 Hz, ^{3}JH-H = 3.7 and 3.7 Hz), 2.03 (1H, s, OH), 1.53-1.88 (6H, m), 1.42 (1H, m), 1.09 (1H, m), 1.01 and 0.83 (3H each, s, $Me_{8,9}$) 0.90 (3H, s, Me10), 0.12 (6H, s, $SiMe_2$). ^{13}C NMR (50 MHz): δ 133.9 ($SiCH_2CH{=}CH_2$), 113.7 ($SiCH_2CH{=}CH_2$), 111.1 (*C*CSi), 85.5 (C_2), 77.9 (C*C*Si), 53.3 (C_1), 48.2 (C_3), 47.7 (C_7), 45.3 (C_4), 32.3 (C_6), 26.7 (C_5), 24.0 ($SiCH_2CH{=}CH_2$), 21.2 and 20.9 ($Me_{8/9}$), 10.2 (Me_{10}), -2.3 ($SiMe_2$). MS (DEI, *m/z* (%)): 276 (3) $[(M)]^+$, 259 (25) $[(M\text{-}OH)]^+$, 235 (7) $[(M\text{-}C_3H_5)]^+$, 217 (6) $[(M\text{-}H_2O\text{-}C_3H_5)]^+$, 159 (7) $[(M\text{-}H_2O\text{-}(CH_3)_2SiCH_2CH{=}CH_2)]^+$. (DCI, NH_3, m/z (%)): 277 (4) $[(M+H)]^+$, 276 (14) $[(M)]^+$, 259 (60) $[(M\text{-}OH)]^+$, 235 (5) $[(M\text{-}C_3H_5)]^+$, 217 (3) $[(M\text{-}H_2O\text{-}C_3H_5)]^+$. HRMS: *m/z* calcd for $C_{17}H_{28}OSi$ 276.1909 $[(M)]^+$, found 276.1899.

(2-Endo-allyldimethylsilyl)ethynylborneol[$Co_2(CO)_6$], 63. Dark red solid, (88%), m.p. 96-97 °C. ^{1}H NMR (500 MHz, $CDCl_3$): δ 5.81 (1H, m, $SiCH_2CH{=}CH_2$), 4.97 and 4.93 (1H each, m, $SiCH_2CH{=}CH_2$), 2.41 (1H, m, H_3, ^{2}JH-H = 12.2 Hz,), 1.98 (1H, s, OH), 1.84 (2H, m, $SiCH_2CH{=}CH_2$), 1.83 (1H, m, H_4), 1.82 (1H, m, H_5), 1.60 (1H, m, H_3), 1.57 (1H, m, H_6), 1.43 (1H, m, H_6), 1.28 (1H, m, H_5), 1.17 and 0.91 (3H each, s, $Me_{8,9}$), 0.94 (3H, s, Me_{10}), 0.35 (6H, s, $SiMe_2$). ^{13}C NMR (125.7 MHz): δ 195.0 (6CO's), 133.8 ($SiCH_2CH{=}CH_2$), 122.0 (*C*C-cluster), 114.7 ($SiCH_2CH{=}CH_2$), 83.3 (C_2), 78.6 (C*C*-

cluster), 54.0 (C_1), 53.8 (C_3), 51.0 (C_7), 45.4 (C_4), 30.6 (C_6), 27.7 (C_5), 25.3 ($SiCH_2CH=CH_2$), 21.7 and 21.5 ($Me_{8/9}$), 10.7 (Me_{10}), -0.8 ($SiMe_2$). MS (DEI, *m/z* (%)): 506 (2) $[(M-2CO)]^+$, 478 (3) $[(M-3CO)]^+$, 450 (11) $[(M-4CO)]^+$, 422 (5) $[(M-5CO)]^+$, 394 (14) $[(M-6CO)]^+$, 352 (15) $[(M-6CO-C_3H_6)]^+$. (DCI, NH3, *m/z* (%)): 545 (100) $[(M-OH)]^+$, 517 (52) $[(M-OH-CO)]^+$, 489 (41) $[(M-OH-2CO)]^+$, 461 (33) $[(M-OH-3CO)]^+$, 450 (94) $[(M-4CO)]^+$, 433 (52) $[(M-OH-4CO)]^+$, 394 (43) $[(M-6CO)]^+$, 352 (46) $[(M-6CO-C_3H_6)]^+$, 335 (27) $[(M-Co-6CO)]^+$, 276 (58) $[(M-Co_2(CO)_6)]^+$, 259 (85) $[(M-OH-Co_2(CO)_6)]^+$, 217 (3) $[(M-Co_2(CO)_6-H_2O-C_3H_5)]^+$. Anal. Calc. For $C_{23}H_{28}O_7Co_2Si$: C 49.12; H 5.02. Found: C 49.70; H 5.61.

Protonation of **63** with an equimolar amount of HBF_4 at -78 °C, and subsequent chromatographic separation using hexanes, yielded **68** and **69**.

(2-Allyldimethylsilyl)ethynylborn-2-ene[$Co_2(CO)_6$], 68. Dark red oily solid, (45%). ^{1}H NMR (200 MHz, $CDCl_3$): δ 6.25 (1H, broad, H_3), 5.82 (1H, m, $SiCH_2CH=CH_2$), 4.98 (2H, m, $SiCH_2CH=CH_2$), 1.21-2.48 (7H, broad), 1.10 (3H, s, Me), 0.86 (6H, s, 2Me), 0.35 (6H, s, $SiMe_2$). ^{13}C NMR (50 MHz): δ 200.7 (6CO's), 145.8 (C_2), 139.9 (C_3), 134.0 ($SiCH_2CH=CH_2$), 114.4 ($SiCH_2CH=CH_2$), 79.7 and 78.2 (CCSi), 57.4 (C_1), 56.6 (C_7), 52.4 (C_4), 31.9 (C_6), 29.7 (C_5), 25.4 ($SiCH_2CH=CH_2$), 19.6 ($Me_{8/9}$), 2.9 (Me_{10}), -0.8 and -0.9 ($SiMe_2$). MS (DEI, *m/z* (%)): 488 (1) $[(M-2CO)]^+$, 432 (3) $[(M-4CO)]^+$, 404 (6) $[(M-5CO)]^+$, 376 (21) $[(M-6CO)]^+$, 317 (4) $[(M-Co-6CO)]^+$, 217 (4) $[(M-Co_2(CO)_6-C_3H_5)]^+$. (DCI, NH_3, *m/z* (%)): 545 (2) $[(M+H)]^+$, 517 (2) $[(M+H-CO)]^+$, 489 (2) $[(M+H-2CO)]^+$, 461 (4) $[(M+H-3CO)]^+$, 450 (20) $[(M+NH_4-4CO)]^+$, 433 (11) $[(M+H-4CO)]^+$, 376 (7) $[(M-6CO)]^+$, 317 (5) $[(M-Co-6CO)]^+$, 276 (12) $[(M+NH_4-Co_2(CO)_6)]^+$, 259 (27) $[(M+H-$

$Co_2(CO)_6)]^+$, 99 (52) $[(Me_2SiCH_2CH{=}CH_2)]^+$.

(2-Dimethylfluorosilyl)ethynylborn-2-ene[$Co_2(CO)_6$], 69. Dark red oily solid, (36%). ^1H NMR (200.13 MHz, $CDCl_3$): δ 6.36 (1H, broad, H_3), 1.22-2.49 (5H, broad), 1.11 and 0.87 (3H and 6H, s, $Me_{8,9,10}$), 0.55 (6H, s, $SiMe_2$). ^{13}C NMR (50.13 MHz): δ 200.1 (6CO's), 145.9 (C_2), 140.9 (C_3), 97.0 (CCSi), 78.3 (CCSi), 57.4 (C_1), 56.7 (C_7), 52.5 (C_4), 31.8 (C_6), 25.3 (C_5), 19.6 and 19.4 ($Me_{8/9}$), 12.3 (Me_{10}), 0.8 and 0.4 ($SiMe_2$). MS (DEI, *m/z* (%)): 438 (1) $[(M\text{-}3CO)]^+$, 410 (3) $[(M\text{-}4CO)]^+$, 382 (4) $[(M\text{-}5CO)]^+$, 354 (3) $[(M\text{-}6CO)]^+$, 236 (6) $[(M\text{-}Co_2(CO)_6)]^+$, 221 (12) $[(M\text{-}Co_2(CO)_6\text{-}Me)]^+$. (DCI, NH_3, *m/z* (%)): 523 (2) $[(M+H)]^+$, 495 (1) $[(M+H\text{-}CO)]^+$, 456 (2) $[(M+NH_4\text{-}3CO)]^+$, 428 (8) $[(M+NH_4\text{-}4CO)]^+$, 237 (25) $[(M+H\text{-}Co_2(CO)_6)]^+$.

(2-Norbornylidene)CHC$Co_3(CO)_9$, 70. Method 1 A five-fold excess of HBF_4 in ether was added dropwise to **63**, (0.11 g, 0.20 mmol) in an NMR tube at -78 °C and allowed to warm gradually to room temperature over 12 hours. Chromatographic separation yielded a dark red solid (19%), m.p. 47-48 °C. Method 2 **76**, (1.95 g, 4.37 mmol) was heated at reflux in acetone (30 ml) for 36 hours and, after flash chromatography, yielded **70** (38%). ^1H NMR (500 MHz, $CDCl_3$): δ 7.37 (1H, s, C=CH), 2.39 (1H, m, H_3), 2.36 (1H, m, H_3), 1.88 (1H, m, H_4), 1.80 (1H, m, H_5), 1.70 (1H, m, H_6, $^2JH\text{-}H$ = 11.5), 1.28 (1H, m, H_6), 1.18 (1H, m, H_5, $^3JH\text{-}H$ = 8.9 Hz), 0.99 (3H, s, Me_{10}), 0.92 and 0.75 (3H each, s, $Me_{8/9}$). ^{13}C NMR (125.7 MHz): δ 200.5 (9CO's), 152.4 (*C*=CH), 139.5 (C=*C*H), 53.1 (C_1), 48.2 (C_7), 45.2 (C_4), 38.0 (C_3), 29.7 (C_6), 27.6 (C_5), 19.6 and 19.0 ($Me_{8/9}$), 12.9 (Me_{10}). MS (DEI, *m/z* (%)): 562 (3) $[(M\text{-}CO)]^+$, 534 (1) $[(M\text{-}2CO)]^+$, 506 (1) $[(M\text{-}3CO)]^+$, 478 (4) $[(M\text{-}4CO)]^+$, 450 (4) $[(M\text{-}5CO)]^+$, 422 (4) $[(M\text{-}6CO)]^+$, 394 (2) $[(M\text{-}7CO)]^+$, 366 (3) [(M-

8CO)]$^+$, 338 (3) [(M-9CO)]$^+$. (DCI, NH_3, *m/z* (%)): 591 (6) [(M+H)]$^+$, 563 (4) [(M+H-CO)]$^+$, 535 (3) [(M+H-2CO)]$^+$. Anal. Calc. for $C_{21}H_{17}O_9Co_3 \cdot (C_2H_5)_2O$: C 45.20; H 4.10. Found: C 45.42; H 3.63. HRMS: *m/z* calcd for $C_{21}H_{17}O_9Co_3$ 589.8869 [(M)]$^+$, found 589.8884.

(2-Endo-trimethylsilyl)ethynylborneol[$Co_2(CO)_6$]. Dark red solid, (89%), m.p. 77-78 °C. ^{1}H NMR (500 MHz, $CDCl_3$): δ 2.40 (1H, m, H_3), 1.98 (1H, s, OH), 1.82 (2H, m), 1.67 (1H, m), 1.62 (1H, m), 1.45 (1H, m), 1.26 (1H, m), 1.18 (3H, s, Me), 0.94 (3H, s, Me), 0.91 (3H, s, Me), 0.37 (9H, s, $SiMe_3$). ^{13}C NMR (125.7 MHz): δ 200.6 (6CO's), 121.9 (*C*CSi), 83.2 (C_2), 80.3 (C*C*Si), 54.0 (C_1), 53.7 (C_3), 51.0 (C_7), 45.4 (C_4), 30.6 (C_6), 27.7 (C_5), 21.7 and 21.5 ($Me_{8/9}$), 10.7 (Me_{10}), 1.5 (Me_3Si). MS (DEI, *m/z* (%)): 368 (3) [(M-6CO)]$^+$, 233 (2) [(M-OH-$Co_2(CO)_6$)]$^+$. (DCI, NH_3, *m/z* (%)): 519 (2) [(M-OH)]$^+$, 424 (8) [(M-4CO)]$^+$, 250 (4) [(M-$Co_2(CO)_6$)]$^+$, 233 (100) [(M-OH-$Co_2(CO)_6$)]$^+$, 153 (17) [(M-$C_2Co_2(CO)_6$-$SiMe_3$)]$^+$. HRMS: *m/z* calcd for $C_{21}H_{26}O_7SiCo_2$ 536.0112 [(M)]$^+$, found 536.0106.

(2-Trimethylsilyl)ethynylborn-2-ene[$Co_2(CO)_6$]. Dark red solid, (81%), m.p. 46-47 °C. Protonation of the precursor alcohol, yielded the elimination product, [2-(trimethylsilyl)ethynylborn-2-ene]$Co_2(CO)_6$, exclusively. Reflux of the alcohol in acetone resulted primarily in decomposition, with 37% yield of the elimination product. ^{1}H NMR (200.13 MHz, $CDCl_3$): δ 6.29 (1H, broad s, H_3), 2.40 (1H, broad s), 1.92 (1H, m), 1.61 (1H, m), 1.42 (1H, m), 1.24 (1H, m), 1.09 (3H, s, Me), 0.82 (6H, s, 2Me), 0.34 (9H, s, $SiMe_3$). ^{13}C NMR (50.13 MHz): δ 200.6 (6CO's), 146.0 (*C*CSi), 139.8 (C_3), 99.2 (C_2), 81.3 (C*C*Si), 57.3 (C_1), 56.6 (C_7), 52.3 (C_4), 31.8 (C_6), 25.4 (C_5), 19.6 and 19.4

($Me_{8/9}$), 12.7 (Me_{10}), 1.4 (Me_3Si). MS (DEI, *m/z* (%)): 490 (1) $[(M-CO)]^+$, 462 (4) $[(M-2CO)]^+$, 434 (4) $[(M-3CO)]^+$, 406 (9) $[(M-4CO)]^+$, 378 (17) $[(M-5CO)]^+$, 350 (7) $[(M-6CO)]^+$, 291 (3) $[(M-Co-6CO)]^+$, 232 (20) $[(M-Co_2(CO)_6)]^+$, 217 (33) $[(M-Co_2(CO)_6-CH_3)]^+$, 73 (79) $[SiMe_3)]^+$. (DCI, NH_3, *m/z* (%)): 519 (8) $[(M+H)]^+$, 491 (6) $[(M+H-CO)]^+$, 480 (4) $[(M+NH_4-2CO)]^+$, 452 (3) $[(M+NH_4-3CO)]^+$, 424 (11) $[(M+NH_4-4CO)]^+$, 233 (54) $[(M+H-Co_2(CO)_6)]^+$, 177 (13) $[(M+NH_4-Co_2(CO)_6-SiMe_3)]^+$. HRMS: *m/z* calcd for $C_{21}H_{24}O_6SiCo_2$ 536.0006 $[(M)]^+$, found 536.0016.

Trimethylsilyl(allyldimethylsilyl)ethyne[$Co_2(CO)_6$], 71 was prepared according to the method of Ruffolo et al.[185] and protonated, thereby affording **72**,[185] and, **73**. The latter was apparently produced during purification of **72** by column chromatography.

$Me_3SiC{\equiv}CSiMe_2F[Co_2(CO)_6]$, 72. Dark red oily solid, (72%). ^1H NMR (200 MHz, $CDCl_3$): δ 0.48 (6H, d, $SiMe_2F$, $^3JH\text{-}F$ = 6.8 Hz), 0.30 (9H, s, $SiMe_3$). ^{13}C NMR (50 MHz): δ 200.1 (6CO's), 0.9 ($SiMe_3$), 0.4 ($SiMe_2F$), $^2JC\text{-}F$ = 16.3 Hz). MS (DEI, *m/z* (%)): 432 (53) $[(M-CO)]^+$, 404 (22) $[(M-2CO)]^+$, 376 (24) $[(M-3CO)]^+$, 348 (26) $[(M-4CO)]^+$, 320 (46) $[(M-5CO)]^+$, 292 (48) $[(M-6CO)]^+$, 233 (50) $[(M-Co-6CO)]^+$. (DCI, NH_3, *m/z* (%)): 478 (2) $[(M+NH_4)]^+$, 441 (1) $[(M-F)]^+$, 433 (3) $[(M+H-CO)]^+$, 410 (11) $[(M-HF-2CH_3)]^+$, 383 (15) $[(M-SiMe_2F)]^+$, 354 (27) $[(M-H-SiMe_2F-CO)]^+$, 326 (43) $[(M-H-SiMe_2F-2CO)]^+$, 250 (58) $[(M+NH_4-Co-6CO)]^+$. HRMS: *m/z* calcd for $C_{13}H_{15}O_6FSi_2Co_2$ 459.9055 $[(M)]^+$, found 459.9046.

$Me_3C{\equiv}CSiMe_2OH[Co_2(CO)_6]$, 73. Dark red oily solid, (10%). ^1H NMR (200 MHz, $CDCl_3$): δ 2.46 (1H, broad s, OH), 0.39 (6H, s, $SiMe_2OH$), 0.29 (9H, s, $SiMe_3$). ^{13}C NMR (50 MHz): δ 200.7 (6CO's), 91.7 and 90.2 (C≡C), 1.6 ($SiMe_2OH$), 0.9 ($SiMe_3$).

MS (DCI, NH_3, *m/z* (%)): 476 (10) $[(M+NH_4)]^+$, 459 (26) $[(M+H)]^+$, 431 (15) $[(M+H-CO)]^+$, 410 (20) $[(M-H_2O-2CH_3)]^+$, 392 (51) $[(M+NH_4-3CO)]^+$, 382 (16) $[(M-H-SiMe_2OH)]^+$, 364 (47) $[(M+NH_4-4CO)]^+$, 354 (55) $[(M-H-SiMe_2OH-CO)]^+$, 326 (100) $[(M-H-SiMe_2OH-2CO)]^+$, 248 (94) $[(M+NH_4-Co-6CO)]^+$, 190 (31) $[(M+NH_4-Co_2(CO)_6)]^+$.

Protonation of **72**, with HBF_4 in diethyl ether -78 °C gave **$Me_3SiC{\equiv}CH[Co_2(CO)_6]$**, **74**,[186] in 32% yield.

Me_3SiCH_2-$CCo_3(CO)_9$, 75.[187] Dark red solid, (12%), m.p. 37 °C (lit.[187] 36-37 °C). When **74** was heated at reflux in acetone for 36 hours, **75** was afforded. ^1H NMR (200.13 MHz, $CDCl_3$): δ 3.81 (2H, s, CH_2CCo_3), 0.20 (9H, s, $SiMe_3$). ^{13}C NMR (50 MHz): δ 200.6 (9CO's), 56.9 (CH_2CCo_3), -1.0 ($SiMe_3$). MS (DEI, *m/z* (%)): 528 (11) $[(M)]^+$, 500 (84) $[(M-CO)]^+$, 472 (41) $[(M-2CO)]^+$, 444 (39) $[(M-3CO)]^+$, 416 (55) $[(M-4CO)]^+$, 388 (98) $[(M-5CO)]^+$, 360 (100) $[(M-6CO)]^+$, 332 (60) $[(M-7CO)]^+$, 304 (38) $[(M-8CO)]^+$, 276 (71) $[(M-9CO)]^+$, 217 (22) $[(M-Co-9CO)]^+$.

2-Endo-ethynylborneol[$Co_2(CO)_6$], 76. Dark red solid, (90%), m.p. 53-54 °C. ^1H NMR (200 MHz, $CDCl_3$): δ 6.09 (1H, s, CCH), 2.46 (1H, m, H_3), 2.40 (1H, m, H_3), 1.90 (1H, s, OH), 1.79 (2H m,), 1.55 (1H m,), 1.52 (1H m,), 1.45 (1H m,), 1.17 (3H, s, Me), 0.92 (3H, s, Me), 0.89 (3H, s, Me). ^{13}C NMR (50 MHz): δ 199.8 (6CO's), 105.6 (*C*CH), 82.8 (C*C*H), 74.5 (C2), 54.7 (C_3), 53.7 (C_1), 51.0 (C_7), 45.4 (C_4), 30.4 (C_6), 27.7 (C_5), 21.5 and 21.3 ($Me_{8/9}$), 10.6 (Me_{10}). MS (DEI, *m/z* (%)): 408 (1) $[(M-2CO)]^+$, 380 (3) $[(M-3CO)]^+$, 324 (4) $[(M-5CO)]^+$, 296 (11) $[(M-6CO)]^+$. (DCI, NH_3, *m/z* (%)): 447 (13) $[(M-OH)]^+$, 419 (3) $[(M-OH-CO)]^+$, 408 (3) $[(M-2CO)]^+$, 352 (9) $[(M-4CO)]^+$, 296 (1)

$[(M\text{-}6CO)]^+$, 237 (2) $[(M\text{-}Co\text{-}6CO)]^+$, 161 (40) $[(M\text{-}OH\text{-}Co_2(CO)_6)]^+$. Anal. Calc. for $C_{18}H_{18}O_7Co_2 \cdot 1/2(C_2H_5)_2O$: C 47.92; H 4.62. Found: C 48.35; H 4.81. HRMS: *m/z* calcd for $C_{17}H_{18}O_6Co_2$ 435.9767 $[(M\text{-}CO)]^+$, found 435.9754.

[2-(2-Hydroxybornyl)]$CH_2CCo_3(CO)_9$, 77. Dark red solid, (24%), m.p. (dec.) > 88 °C. The synthesis and purification of this product were identical to method 2 for **70**. ^{1}H NMR (500 MHz, $CDCl_3$): δ 4.00 (1H, d, CH_2CCo_3, ^{2}JH-H = 16.6 Hz), 3.81 (1H, d, CH_2CCo_3, ^{2}JH-H = 16.5 Hz), 2.12 (1H, m, H_3, ^{2}JH-H = 13.1 Hz), 1.83 (1H, m, H_4, ^{3}JH-H = 6.3 Hz), 1.80 (1H, m, H_3), 1.75 (1H, m, H_5), 1.59 (1H, s, OH), 1.51 (1H, m, H_6), 1.47 (1H, m, H_6), 1.13 and 0.90 (3H each, s, $Me_{8/9}$), 1.07 (1H, m, H_5), 0.92 (3H, s, Me_{10}). ^{13}C NMR (125.7 MHz): δ 200.4 (9CO's), 81.1 (C_2), 64.7 (CH_2CCo_3), 53.8 (C_1), 48.6 (C_7), 46.0 (C_3), 45.4 (C_4), 30.1 (C_6), 27.0 (C_5), 21.6 and 21.0 ($Me_{8/9}$), 10.1 (Me_{10}). MS (DEI, *m/z* (%)): 478 (3) $[(M\text{-}H_2O\text{-}4CO)]^+$, 450 (4) $[(M\text{-}H_2O\text{-}5CO)]^+$, 422 (4) $[(M\text{-}H_2O\text{-}6CO)]^+$, 304 (13) $[(M\text{-}H_2O\text{-}Co_2(CO)_6)]^+$, 276 (22) $[(M\text{-}H_2O\text{-}CO\text{-}Co_2(CO)_6)]^+$. (DCI, NH_3, *m/z* (%)): 591 (9) $[(M\text{-}OH)]^+$, 563 (5) $[(M\text{-}OH\text{-}CO)]^+$, 535 (3) $[(M\text{-}OH\text{-}2CO)]^+$, 395 (100) $[(M\text{-}OH\text{-}7CO)]^+$. Anal. Calc. For $(C_{21}H_{18}O_9Co_3)_2O$: C 42.10; H 3.03. Found: C 42.10; H 3.20. (Loss of water from the alcohol to form the ether). HRMS: *m/z* calcd for $C_{20}H_{19}O_9Co_3$ 579.9025 $[(M\text{-}CO)]^+$, found 579.9095.

Protonation of **76** at -78 °C yielded **78**, (53%), and **79**, (32%). Repetition at room temperature also afforded **78** (74%) and **79** (13%).

2-Ethynyl-2-bornene[$Co_2(CO)_6$], 78. Dark red solid, m.p. 41-43 °C. ^{1}H NMR (200 MHz, $CDCl_3$): δ 6.38 (1H, broad, H_3), 6.21 (1H, s, CCH), 2.41 (1H, m), 1.47-1.93 (4H, m), 1.05 (3H, s, Me), 0.80 (6H, s, 2Me). ^{13}C NMR (50 MHz): δ 200.1 (6CO's), 145.7

(C_2), 141.1 (C_3), 83.4 (*C*CH), 73.4 (C*C*H), 57.3 (C_1), 56.4 (C_7), 52.6 (C_4), 31.6 (C_6), 25.1 (C_5), 19.6 and 19.4 ($Me_{8/9}$), 12.0 (Me_{10}). MS (DEI, *m/z* (%)): 446 (3) $[(M)]^+$, 418 (15) $[(M-CO)]^+$, 390 (35) $[(M-2CO)]^+$, 362 (25) $[(M-3CO)]^+$, 334 (46) $[(M-4CO)]^+$, 306 (41) $[(M-5CO)]^+$, 278 (18) $[(M-6CO)]^+$. (DCI, NH_3, *m/z* (%)): 447 (100) $[(M+H)]^+$, 419 (40) $[(M+H-CO)]^+$, 380 (10) $[(M+NH_4-3CO)]^+$, 352 (27) $[(M+NH_4-4CO)]^+$, 178 (11) $[(M+NH_4-Co_2(CO)_6)]^+$, 161 (19) $[(M+H-Co_2(CO)_6)]^+$. Anal. Calc. for $C_{18}H_{16}O_6Co_2 \cdot (C_2H_5)_2O$: C 50.79; H 5.04. Found: C 50.84; H 4.91.

2-Ethynyl-4-isopropyl-1-methylcyclohexa-1,3-diene[$Co_2(CO)_6$], 79. Dark red oily solid. ^1H NMR (500 MHz, $CDCl_3$): δ 6.34 (1H, s, CCH), 5.40 (1H, s, H_3), 2.87 (m, 2H, H_5), 2.74 (2H, m, H_6), 2.30 (1H, m, H_7), 1.87 (3H, broad, Me_{10}), 1.06 and 1.05 (6H, broad, 2Me). ^{13}C NMR (125.7 MHz): δ 200.1 (6CO's), 141.4 (C_4), 133.4 (C_1), 123.0 (C_2), 114.7 (C_3), 89.6 (*C*CH), 74.7 (C*C*H), 35.2 (C_6), 34.3 (C_7), 33.9 (C_5), 21.1 (2Me), 21.0 (Me). MS (DEI, *m/z* (%)): 446 (4) $[(M)]^+$, 418 (9) $[(M-CO)]^+$, 390 (6) $[(M-2CO)]^+$, 362 (5) $[(M-3CO)]^+$, 334 (8) $[(M-4CO)]^+$, 306 (18) $[(M-5CO)]^+$, 278 (21) $[(M-6CO)]^+$. (DCI, NH_3, *m/z* (%)): 447 (100) $[(M+H)]^+$, 419 (7) $[(M+H-CO)]^+$, 391 (4) $[(M-H-2CO)]^+$, 380 (5) $[(M+NH_4-3CO)]^+$, 352 (5) $[(M+NH_4-4CO)]^+$, 161 (13) $[(M+H-Co_2(CO)_6)]^+$.

Treatment of 1,1-diphenylpropyn-1-ol[$Co_2(CO)_6$], **108**,[126,127] (1.00 g, 2.02 mmol) in CH_2Cl_2 (40 mL) with HBF_4 (0.4 mL, 2.71 mmol) at -78 °C in a dry ice / isopropanol bath, afforded **33** (41%, 0.34 g, 0.55 mmol). The analogous reaction in Et_2O (40 mL) gave **33** (34%, 0.28 g, 0.45 mmol) and **111** (2%, 0.02 g, 0.04 mmol), while in THF (40 mL), the products were **33** (18%, 0.15 g, 0.24 mmol), **111** (8%, 0.08 g, 0.16 mmol) and 2,5-bis(diphenylmethylene)-3-cyclopentenone, **112**,[132] (28%, 0.12 g, 0.28 mmol).

Ethynyldiphenylmethane[$Co_2(CO)_6$], 111. Dark red solid, m.p. 121-122 °C. ^{1}H NMR (200 MHz, $CDCl_3$): δ 7.18-7.46 (10H, m, Ph's), 6.40 (1H, s, CCH), 5.32 (1H, s, Ph_2CH). ^{13}C NMR (50 MHz, $CDCl_3$): δ 199.7 (6CO's), 144.0, 128.7, 127.9, 127.2 (Ar C's), 73.4 (C*C*H), 57.8 (Ph_2CH). MS (DEI, *m/z* (%)): 450 (39) $[(M-CO)]^+$, 394 (100) $[(M-3CO)]^+$, 310 (44) $[(M-6CO)]^+$, 251 (37) $[(M-Co-6CO)]^+$. (CI, NH_3, *m/z* (%)): 451 (47) $[(M+H-CO)]^+$, 310 (36) $[(M-6CO)]^+$, 192 (31) $[(M-Co_2(CO)_6)]^+$. Anal. Calc. for $C_{21}H_{12}O_6Co_2 \cdot H_2O$: C 50.83; H 2.84. Found: C 50.82; H 2.86.

Trimethylsilyl(1,1-diphenyl-2-propyn-1-ol)[$Co_2(CO)_6$], 113. Dark red solid (88%). Addition of $Co_2(CO)_8$ (1.83 g, 5.4 mmol) to trimethylsilyl(1,1-diphenyl-2-propyn-1-ol)[184,188] (1.50 g, 5.4 mmol) in 40 mL of tetrahydrofuran afforded **113**. ^{1}H NMR (200 MHz, $CDCl_3$): δ 7.63-7.68 (4H, m, Ph's), 7.19-7.35 (6H, m, Ph's), 2.71 (1H, s, OH) 0.45 (9H, s, $SiCH_3)_3$). ^{13}C NMR (50 MHz, $CDCl_3$): δ 199.8 (6CO's), 146.6, 128.0, 127.6, 126.3 (Ar C's), 80.6 (COH), 78.3 (C*C*Si), 1.8 ($(CH_3)_3Si$). MS (DEI, *m/z* (%)): 538 (3) $[(M-CO)]^+$, 398 (17) $[(M-6CO)]^+$, 280 (14) $[(M-Co_2(CO)_6)]^+$, 263 (91) $[(M-OH-Co_2(CO)_6)]^+$. (CI, NH_3, *m/z* (%)): 522 (4) $[(M+H-OH-CO)]^+$, 455 (4) $[(M+H-4CO)]^+$, 398 (5) $[(M-6CO)]^+$, 263 (100) $[(M-OH-Co_2(CO)_6)]^+$.

(Trimethylsilylethynyldiphenylmethane)$Co_2(CO)_6$, 114. Black solid, (65%), m.p. 91-93 °C. Treatment of **113**, (1.55g, 2.74mmol) with HBF_4 (0.4mL, 2.94mmol) in tetrahydrofuran (40mL) afforded, **114**. ^{1}H NMR (300 MHz, $CDCl_3$): δ 7.55-7.58 (4H, m, Ph's), 7.30-7.41 (6H, m, Ph's), 5.46 (1H, s, Ph_2CH), 0.47 (9H, s, $Si(CH_3)_3$). ^{13}C NMR (75 MHz, $CDCl_3$): δ 200.0 (6CO's), 143.9, 128.6, 128.2, 127.3 (Ar C's), 115.4 (*C*CSi), 78.7 (C*C*H), 59.8 (Ph_2CH), 1.4 ($(CH_3)_3Si$). MS (DEI, *m/z* (%)): 466 (10) $[(M-3CO)]^+$,

382 (13) $[(M-6CO)]^+$, 264 (4) $[(M-Co_2(CO)_6)]^+$. (CI, NH3, *m/z* (%)): 383 (3) $[(M+H-6CO)]^+$, 265 (23) $[(M+H-Co_2(CO)_6)]^+$.

Fluorenylidene=CHCCo$_3$(CO)$_9$, 116. Black solid (38%), m.p. 141-142 °C. Treatment of 1-fluorenylpropyn-1-ol$[Co_2(CO)_6]$, **115**,[189] (1.00 g, 2.03 mmol) with HBF_4 (0.4 mL, 2.71 mmol) in dichloromethane (40 mL) yielded the fluorenylidene-tricobalt cluster, **116**. ^{1}H NMR (200 MHz, $CDCl_3$): δ 8.94 (1H, s, C=CH), 8.11 (1H, d, ^{3}JH-H = 7.5 Hz, Ar), 7.70-7.77 (3H, m, Ar), 7.29-7.45 (4H, m Ar). ^{13}C NMR (50 MHz, $CDCl_3$): δ 199.8 (9CO's), 148.4, 141.3, 140.4, 139.2, 136.3, 129.7, 128.8, 128.4, 128.3, 127.2, 126.0, 120.3, 120.1. MS (DEI, *m/z* (%)): 590 (1) $[(M-CO)]^+$, 450 (7) $[(M-6CO)]^+$, 178 (100) $[(M-C-Co_3(CO)_9)]^+$. (CI, NH_3, *m/z* (%)): 619 (5) $[(M+H)]^+$, 591 (3) $[(M+H-CO)]^+$, 366 (10) $([M-9CO]^+)$, 179 (100) $([M+H-C-Co_3(CO)_9]^+)$.

Repetition of this reaction in 40mL of diethyl ether afforded **116** (23%, 0.19 g, 0.31 mmol), and **9-Ethynylfluorene[Co$_2$(CO)$_6$], 117**, as a dark red solid (7%, 0.07 g, 0.14 mmol), m.p. 98 °C. ^{1}H NMR (500 MHz, $CDCl_3$): δ 7.69-7.78 (4H, d of d, ^{3}JH-H = 11.9 and 7.2 Hz, Ar), 7.34-7.45 (4H, m Ar), 6.38 (1H, s, CCH), 5.13 (1H, s, C*H*CCH). ^{13}C NMR (125.7 MHz, $CDCl_3$): δ 199.3 (6CO's), 146.7, 140.6, 128.2, 127.4, 125.1, 120.2 (Ar C's), 98.6 (*C*CH), 74.9 (C*C*H), 49.7 (Ar-CH). MS (DEI, *m/z* (%)): 308 (100) $[(M-6CO)]^+$, 249 (25) $[(M-Co-6CO)]^+$. (CI, NH_3, *m/z* (%)): 449 (42) $[(M+H-CO)]^+$, 308 (100) $[(M-6CO)]^+$, 249 (13) $[(M-Co-6CO)]^+$. Addition of HBF_4 (0.4 mL, 2.71 mmol) to **115** (1.0 g, 2.03 mmol) in THF (40 mL), afforded **116** (10%, 0.08 g, 0.13 mmol) and **117** (30%, 0.29 g, 0.61 mmol).

Vinyldimethylsilylfluoren-9-ol was prepared analogously to **45**, using fluorenone as the starting ketone and isolated in 74% yield as a yellow oil. ^{1}H NMR (200 MHz, $CDCl_3$): δ 7.53-7.68 (4H, m, fluorenyl), 7.29-7.36 (4H, m, fluorenyl), 5.76-6.15 (3H, m, $CH{=}CH_2$), 3.42 (1H, s, OH), 0.19 (6H, s, $Si(CH_3)_2$). ^{13}C NMR (50 MHz): δ 146.9, 139.0 (Ar C's), 136.1 (*C*H=C), 133.0 (C=*C*H_2), 129.4, 128.3, 124.2, 119.9, (Ar C's), 106.3 (*C*CSi), 85.6 (C*C*Si), 74.7 (COH), –1.8 ($Si(CH_3)_2$). MS (DEI, m/z (%)): 290 (97) $[(M)]^+$, 275 (65) $[(M\text{-}CH_3)]^+$. (CI, NH_3, *m/z* (%)): 290 (10) $[(M)]^+$, 273 (100) $[(M\text{-}OH)]^+$.

Vinyldimethylsilylfluoren-9-ol[$Co_2(CO)_6$], 53. Dark red solid, (71%), m.p. 71-72 °C. ^{1}H NMR (200 MHz, $CDCl_3$): δ 7.58-7.63 (4H, m, fluorenyl), 7.26-7.38 (4H, m, fluorenyl), 5.70-6.06 (3H, m, $CH{=}CH_2$), 2.58 (1H, s, OH), 0.16 (6H, s, $Si(CH_3)_2$). ^{13}C NMR (50 MHz): δ 199.8 (6CO's), 150.3, 138.9 (Ar C's), 137.4 (*C*H=C), 132.8 (C=*C*H_2), 129.5, 127.6, 124.3, 117.4, (Ar C's), 118.2 (*C*CSi), 83.4 (C*C*Si), 78.2 (COH), –1.3 ($Si(CH_3)_2$). MS (DEI, *m/z* (%)): 520 (10) $[(M\text{-}2CO)]^+$, 492 (5) $[(M\text{-}3CO)]^+$, 464 (30) $[(M\text{-}4CO)]^+$, 436 (34) $[(M\text{-}5CO)]^+$, 408 (100) $[(M\text{-}6CO)]^+$, 290 (8) $[(M\text{-}Co_2(CO)_6)]^+$. (DCI, NH_3, *m/z* (%)): 559 (100) $[(M\text{-}OH)]^+$, 531 (94) $[(M\text{-}OH\text{-}CO)]^+$, 503 (18) $[(M\text{-}OH\text{-}2CO)]^+$, 464 (25) $[(M\text{-}4CO)]^+$, 408 (32) $[(M\text{-}6CO)]^+$.

Benzyldimethylsilylfluoren-9-ol was prepared analogously to **50**, using fluorenone as the starting ketone, and isolated in 68% yield as a white solid, m.p. 87-88 °C . ^{1}H NMR (200 MHz, $CDCl_3$): δ 7.62-7.74 (4H, m, fluorenyl), 7.39-7.44 (4H, m, fluorenyl), 7.03-7.21 (5H, m, Ph), 2.69 (1H, s, OH), 2.21 (2H, s, CH_2), 0.17 (6H, s, $Si(CH_3)_2$). ^{13}C NMR (50 MHz): δ 146.7, 139.0, 138.7, 129.6, 128.4, 128.3, 128.0, 124.3, 120.1 (Ar C's), 106.2 (*C*CSi), 86.5 (C*C*Si), 74.9 (COH), 25.9 (CH_2), –2.3 ($Si(CH_3)_2$). MS (DEI, *m/z*

(%)): 354 (53) $[(M)]^+$, 336 (20) $[(M\text{-}H\text{-}OH)]^+$, 263 (100) $[(M\text{-}CH_2Ph)]^+$.

Benzyldimethylsilylfluoren-9-ol[$Co_2(CO)_6$], 54. Dark red solid, (71%), m.p. 99 °C. ^1H NMR (200 MHz, $CDCl_3$): δ 7.55-7.69 (4H, m, fluorenyl), 6.90-7.44 (9H, m, fluorenyl and Ph), 2.59 (1H, s, OH), 1.90 (2H, s, CH_2), -0.09 (6H, s, $Si(CH_3)_2$). ^{13}C NMR (50 MHz): δ 200.0 (6CO's), 150.4, 139.1, 138.9, 129.6, 128.3, 128.2, 127.7, 124.3, 120.2 (Ar C's), 83.3 (COH), 26.6 (CH_2), –1.9 ($Si(CH_3)_2$). MS (DEI, *m/z* (%)): 612 (1) $[(M\text{-}CO)]^+$, 556 (22) $[(M\text{-}3CO)]^+$, 528 (8) $[(M\text{-}4CO)]^+$, 500 (20) $[(M\text{-}5CO)]^+$, 472 (95) $[(M\text{-}6CO)]^+$, 354 (18) $[(M\text{-}Co_2(CO)_6)]^+$, 263 (55) $[(M\text{-}CH_2Ph\text{-}Co_2(CO)_6)]^+$, 181 (88) $[(C_{13}H_8OH)]^+$, 149 (90) $[(Si(CH_3)_2CH_2Ph)]^+$. (DCI, NH_3, *m/z* (%)): 181 (100) $[(C_{13}H_8OH)]^+$. HRMS: *m/z* calcd for $C_{29}H_{22}O_6SiCo_2$ 611.9850 ($[M\text{-}CO]^+$), found 611.9664.

Treatment of **54 (1.0 g, 1.5 mmol)** with 1.5 equivalents of HBF_4 (0.33 mL, 2.3 mmol) in dicholoromethane, and subsequent purification with a silica column using 1:1 dichloromethane/hexanes as eluent afforded the tricobalt-hydride, **120**, and a cobalt complexed allene, **122**, which quickly decomposed to the uncomplexed allene, **121**.

Fluorenyl-$CH_2CCo_3(CO)_9$, 120. Dark red solid, (32%). ^1H NMR (200 MHz, $CDCl_3$): δ 7.10-7.69 (8H, m, fluorenyl), 5.15 (1H, s, CH), 3.34 (2H, CH_2). ^{13}C NMR (50 MHz, $CDCl_3$): δ 199.8 (9CO's), 146.8, 140.7, 128.6, 126.9, 125.7, 120.1, 58.7, 50.5.

9-[Benzyldimethylsilylethynyl]-9-[1-benzyldimethylsilyl-2-fluoren-9-ylidene-vinyl]-9H-fluorene[$Co_2(CO)_6$], 122. Dark red solid. ^1H NMR (500 MHz, CD_2Cl_2): δ 7.05-7.91 (22H, m, Ar), 6.74 (4H, m, Ar), 1.75 and 1.66 (2H each, s, CH_2), -0.38 and –0.43 (6H

each, s, $Si(CH_3)_2$). ^{13}C NMR (125.7 MHz, CD_2Cl_2): δ 206.3 (allene =C=), 200.6 (6CO's), 152.5, 147.7, 141.6, 141.0, 139.2, 138.8, 129.5, 129.0, 128.9, 128.8, 128.6, 128.5, 128.0, 127.7, 126.4, 123.2, 121.0, 120.9 (Ar C's), 26.7 and 26.2 (CH_2's), -2.1 and –2.6 ($Si(CH_3)_2$).

9-[Benzyldimethylsilylethynyl]-9-[1-benzyldimethylsilyl-2-fluoren-9-ylidene-vinyl]-9H-fluorene, 121. Yellow solid, (42%), m.p. 169-170 °C. IR, (s): 2168 cm^{-1} (C≡C), 1915 cm^{-1} (=C=). ^1H NMR (200 MHz, CD_2Cl_2): δ 7.82-7.91 (8H, m, Ar), 7.45-7.58 (8H, m, Ar), 7.05-7.14 (6H, m, Ar) 6.71-6.74 (4H, m, Ar), 1.72 and 1.67 (2H each, s, CH_2), -0.40 and –0.43 (6H each, s, $Si(CH_3)_2$). ^{13}C NMR (125.7 MHz, CD_2Cl_2): δ 205.6 (allene =C=), 147.0, 140.4, 139.0, 138.8, 138.5, 138.1, 128.8, 128.2, 128.0, 127.8, 127.3, 127.0, 125.7, 124.1, 123.9, 122.4, 120.2, 110.5, 106.1, 105.7, 86.0 (*C*CSi), 54.2 (C-quat.), 26.1 and 25.7 (CH_2's), -2.6 and –3.1 ($Si(CH_3)_2$). MS (DEI, *m/z* (%)): 674 (4) $[(M-H)]^+$, 337 (100) $[(C_{13}H_8CCSi(CH_3)_2CH_2Ph)]^+$, 149 (81) $[(Si(CH_3)_2CH_2Ph)]^+$. (CI, NH_3, *m/z* (%)): 674 (10) $[(M-H)]^+$, 337 (100) $[(C_{13}H_8CCSi(CH_3)_2CH_2Ph)]^+$, 149 (47) $[(Si(CH_3)_2CH_2Ph)]^+$. HRMS: *m/z* calcd for $C_{48}H_{42}Si_2$ 674.2836 ($[M]^+$), found 674.2825.

Benzyldimethyl-[9-(9-benzyldimethylsilylalk-1-ynyl-9H-fluoren-9-ylperoxy)-9H-fluoren-9-ylethynyl]silane$[Co_2(CO)_6]_2$, 124. Dark red solid, m.p. 137-138 °C. Treatment of **54 (0.5 g, 0.8 mmol)** with an equimolar amount of HBF_4 (0.11 mL, 0.8 mmol) in diethyl ether and THF afforded **124** in 56% and 63% respectively, upon purification with a silica column using a 50:50 dichloromethane/hexanes solution as eluent. ^1H NMR (200 MHz, $CDCl_3$): δ 7.58 (4H, d, Ar, ^3JH-H = 7.4 Hz), 7.08-7.42 (18H, m, Ar), 6.85 (4H, d, Ar, ^3JH-H = 7.0 Hz), 1.71 (4H, s, CH_2's), -0.26 (12H, s,

$2Si(CH_3)_2$). ^{13}C NMR (50 MHz): δ 199.0 (12CO's), 147.3, 139.7, 139.2, 129.5, 128.3, 128.1, 127.1, 125.1, 124.2, 120.1 (Ar C's), 26.6 (CH_2), –1.9 ($Si(CH_3)_2$). MS (ESI (-ve, CH_3OH), *m/z* (%)): 639 (35) $[(M\text{-}C_{13}H_8OC_2Co_2(CO)_6Si(CH_3)_2Ph)]^+$.

Vinyldimethyl-[9-(9-vinyldimethylsilylalk-1-ynyl-9H-fluoren-9-ylperoxy)-9H-fluoren-9-ylethynyl]silane$[Co_2(CO)_6]_2$, 125. Dark red solid, m.p. 144-145 °C. Treatment of **53 (0.5 g, 0.9 mmol)** with an equimolar amount of HBF_4 (0.12 mL, 0.9 mmol) in diethyl ether and THF afforded **125** in 52% and 60% respectively, upon purification with a silica column using a 50:50 dichloromethane/hexanes solution as eluent. ^1H NMR (200 MHz, $CDCl_3$): δ 7.59 (4H, d, $^3JH\text{-}H$ = 6.9, Ar), 7.20-7.39 (12H, m, Ar), 5.50-5.82 (6H, m, $CH{=}CH_2$), -0.09 (12H, s, $2Si(CH_3)_2$). ^{13}C NMR (50 MHz): δ 198.8 (12CO's), 147.4, 139.7 (Ar C's), 137.6 (*C*H=C), 132.4 (C=*C*H_2), 129.3, 127.0, 125.2, 119.9 (Ar C's), –1.5 ($Si(CH_3)_2$). MS (ESI (-ve, CH_3OH), *m/z* (%)): 559 (10) $[(C_{13}H_8C_2Co_2(CO)_6Si(CH_3)_2C_3H_5)]^+$, 273 (20) $[(C_{13}H_8CCSi(CH_3)_2C_3H_5)]^+$.

All cyclohexanols were prepared analogously to **31** using 2 equivalents of trimethylsilylacetylene for disubstitution, unless otherwise stated.

1-(Trimethylsilylethynyl)cyclohexan-1-ol, 129. Colourless crystals, (70%), m.p. 72-73 °C. ^1H NMR (500 MHz, DMSO-d^6): δ 3.29 (1H, s, OH), 1.70 (2H, m, $H_{2,6\text{-}ax}$) 1.57 (2H, m, $H_{3,5\text{-}eq}$), 1.35-1.48 (5H, m, $H_{2,6\text{-}eq,4\text{-}eq,3,5\text{-}ax}$), 1.16 (1H, m, $H_{4\text{-}ax}$), 0.13 (9H, s, $Si(CH_3)_3$). ^{13}C NMR (125 MHz, DMSO-d^6): δ 112.0 (*C*CSi), 86.1 (C*C*Si), 66.8 (C_1), 39.7 ($C_{2,6}$), 24.9 (C_4), 22.7 ($C_{3,5}$), 0.1 ($Si(CH_3)_3$). MS (DEI, *m/z* (%)): 181 (14) $([M\text{-}CH_3]^+)$.

1-(Trimethylsilylethynyl)cyclohexan-1-ol[$Co_2(CO)_6$], 130. Dark red crystals, (79%), m.p. 104-105 °C. ^{1}H NMR (200 MHz, $CDCl_3$): δ 1.57–1.85 (11H, m, $[CH_2]_5$ and OH), 0.31 (9H, s, $Si(CH_3)_3$). ^{13}C NMR (50 MHz, $CDCl_3$): δ 200.5 (6CO's), 122.8 (*C*CSi), 73.5 (C_1), 42.1 ($C_{2,6}$), 25.7 (C_4), 22.6 ($C_{3,5}$), 1.1 ($Si(CH_3)_3$). MS (DEI, *m/z* (%)): 426 (5) ([M-2CO]$^+$), 398 (8) ([M-3CO]$^+$), 370 (10) ([M-4CO]$^+$), 342 (12) ([M-5CO]$^+$), 314 (10) ([M-6CO]$^+$). (CI, NH_3, *m/z* (%)): 465 (50) ([M+H-H_2O]$^+$), 437 (14) ([M+H-H_2O -CO]$^+$), 179 (67) ([M+H-H_2O-$Co_2(CO)_6$]$^+$).

***trans*-4-t-Butyl-1-(trimethylsilylethynyl)cyclohexan-1-ol, 133**. Colourless crystals, (62%), m.p. 145 °C (lit.[190] 145-147 °C). ^{1}H NMR (200 MHz, $CDCl_3$): δ 2.60 (1H, broad s, OH), 1.95-1.32 (9H, m, $[CH_2]_{2,3,5,6}$ and H_4), 0.84 (9H, s, $C(CH_3)_3$), 0.14 (9H, s, $Si(CH_3)_3$). ^{13}C NMR (50 MHz, $CDCl_3$): δ 109.1 (*C*CSi), 89.6 (C*C*Si), 69.7 (C_1), 46.8 (C_4), 40.2 ($C_{2,6}$), 32.2 ($C(CH_3)_3$), 27.5 ($C(CH_3)_3$), 24.7 ($C_{3,5}$), 0.0 ($Si(CH_3)_3$). MS (DEI, *m/z* (%)): 237 (11) [(M-CH_3)]$^+$, 195 (5) [(M-$C(CH_3)_3$)]$^+$, 179 (12) [(M-$Si(CH_3)_3$)]$^+$, 57 (100) [($C(CH_3)_3$)]$^+$. (CI, NH_3, *m/z* (%)): 252 (8) [M]$^+$, 237 (39) [(M-CH_3)]$^+$, 235 (100) [(M+H-H_2O)]$^+$, 195 (15) [(M-$C(CH_3)_3$)]$^+$, 179 (23) [(M-$Si(CH_3)_3$)]$^+$.

***cis*-4-t-Butyl-1-(trimethylsilylethynyl)cyclohexan-1-ol, 134**. Colourless crystals, (24%), m.p. 68-69 °C. ^{1}H NMR (200 MHz, $CDCl_3$): δ 2.15 (1H, broad s, OH), 1.20-2.02 (9H, m, $[CH_2]_{2,3,5,6}$ H_4), 0.82 (9H, s, $C(CH_3)_3$), 0.12 (9H, s, $Si(CH_3)_3$). ^{13}C NMR (50 MHz, $CDCl_3$): δ 111.4 (*C*CSi), 85.8 (C*C*Si), 66.0 (C_1), 47.2 (C_4), 39.3 ($C_{2,6}$), 32.4 ($C(CH_3)_3$), 27.4 ($C(CH_3)_3$), 21.8 ($C_{3,5}$), 0.0 ($Si(CH_3)_3$). MS (DEI, *m/z* (%)): 237 (11) [(M-CH_3)]$^+$, 195 (4) [(M-$C(CH_3)_3$)]$^+$, 179 (9) [(M-$Si(CH_3)_3$)]$^+$, 57 (100) [($C(CH_3)_3$)]$^+$. (CI, NH_3, *m/z* (%)): 252 (9) [M]$^+$, 237 (40) [(M-CH_3)]$^+$, 235 (100) [(M+H-H_2O)]$^+$, 195 (10)

$[(M\text{-}C(CH_3)_3)]^+$, 179 (14) $[(M\text{-}Si(CH_3)_3)]^+$.

***trans*-4-t-Butyl-1-(trimethylsilylethynyl)cyclohexan-1-ol[$Co_2(CO)_6$], 135.**[191] Dark red crystals, (63%), m.p. 89-90 °C. ^{1}H NMR (200 MHz, $CDCl_3$): δ 3.71 (1H, broad s, OH), 1.82-1.92 (5H, m, $[CH_2]_{2,6}$ and H_4), 1.19-1.23 (4H, m, $[CH_2]_{3,5}$), 0.88 (9H, s, $C(CH_3)_3$), 0.31 (9H, s, $Si(CH_3)_3$). ^{13}C NMR (50 MHz, $CDCl_3$): δ 200.6 (6CO's), 120.9 (*C*CSi), 79.3 (C*C*Si), 74.3 (C_1), 47.9 (C_4), 42.8 ($C_{2,6}$), 32.5 ($C(CH_3)_3$), 28.0 ($C(CH_3)_3$), 24.5 ($C_{3,5}$), 1.6 ($Si(CH_3)_3$). MS (DEI, *m/z* (%)): 510 (10) $[(M\text{-}CO)]^+$, 482 (8) $[(M\text{-}2CO)]^+$, 454 (40) $[(M\text{-}3CO)]^+$, 426 (32) $[(M\text{-}4CO)]^+$, 398 (38) $[(M\text{-}5CO)]^+$, 370 (35) $[(M\text{-}6CO)]^+$. (CI, NH_3, *m/z* (%)): 521 (15) $[(M+H\text{-}H_2O)]^+$, 482 (8) $[(M+H\text{-}C(CH_3)_3)]^+$.

***cis*-4-t-Butyl-1-(trimethylsilylethynyl)cyclohexan-1-ol[$Co_2(CO)_6$], 136.**[191] Dark red crystals, (58%), m.p. 105-106 °C. ^{1}H NMR (200 MHz, $CDCl_3$): δ 3.72 (1H, broad s, OH), 1.49–1.89 (9H, m, $[CH_2]_{2,3,5,6}$ and H_4), 0.87 (9H, s, $C(CH_3)_3$), 0.30 (9H, s, $Si(CH_3)_3$). ^{13}C NMR (50 MHz, $CDCl_3$): δ 200.5 (6CO's), 122.61 (*C*CSi), 73.14 (C_1), 47.8 (C_4), 42.5 ($C_{2,6}$), 32.4 ($C(CH_3)_3$), 27.5 ($C(CH_3)_3$), 23.5 ($C_{3,5}$), 1.1 ($Si(CH_3)_3$). MS (DEI, *m/z* (%)): 510 (5) $[(M\text{-}CO)]^+$, 482 (4) $[(M\text{-}2CO)]^+$, 454 (25) $[(M\text{-}3CO)]^+$, 426 (22) $[(M\text{-}4CO)]^+$, 398 (24) $[(M\text{-}5CO)]^+$, 370 (45) $[(M\text{-}6CO)]^+$. (CI, NH_3, *m/z* (%)): 521 (35) $[(M+H\text{-}H_2O)]^+$, 482 (8) $[(M+H\text{-}C(CH_3)_3)]^+$.

***trans*-4-t-Butyl-1-(triphenylsilylethynyl)cyclohexan-1-ol, 137.** Colourless crystals, (58%), m.p. 121-122 °C. ^{1}H NMR (200 MHz, $CDCl_3$): δ 7.26-7.69 (15H, m, $Si(C_6H_5)_3$), 1.34-2.18 (9H, m, $[CH_2]_{2,3,5,6}$ and H_4), 0.88 (9H, s, $C(CH_3)_3$). ^{13}C NMR (50 MHz, CDCl3): δ 135.5 (meta-C's), 133.5 (para-C's), 129.9 (ipso-C's), 127.9 (ortho-C's), 113.8 (*C*CSi), 84.4 (C*C*Si), 70.1 (C_1), 47.2 (C_4), 40.3 ($C_{2,6}$), 32.3 ($C(CH_3)_3$), 27.6 ($C(CH_3)_3$),

24.4 ($C_{3,5}$). MS (DEI, *m/z* (%)): 284 (6) $[(CCSiPh_3)]^+$, 155 (100) $[(M\text{-}CCSiPh_3)]^+$. (CI, NH_3, *m/z* (%)): 456 (100) $[(M+H+NH_3)]^+$, 438 (14) $[M]^+$, 421 (25) $[(M+H\text{-}H_2O)]^+$.

***cis*-4-t-Butyl-1-(triphenylsilylethynyl)cyclohexan-1-ol, 138.** Colourless crystals, (14%), m.p. 187-188 °C. ^{1}H NMR (200 MHz, $CDCl_3$): δ 7.26-7.69 (15H, m, $Si(C_6H_5)_3$), 1.28-2.17 (9H, m, $[CH_2]_{2,3,5,6}$ and H_4), 0.89 (9H, s, $C(CH_3)_3$). ^{13}C NMR (50 MHz, $CDCl_3$): δ 135.5 (meta-C's), 133.5 (para-C's), 129.9 (ipso-C's), 127.9 (ortho-C's), 116.1 (*C*CSi), 81.1 (C*C*Si), 66.4 (C_1), 47.2 (C_4), 39.3 ($C_{2,6}$), 32.4 ($C(CH_3)_3$), 27.3 ($C(CH_3)_3$), 21.8 ($C_{3,5}$). MS (DEI, *m/z* (%)): 284 (5) $[(C{\equiv}CSiPh_3)]^+$, 155 (27) $[(M\text{-}C{\equiv}CSiPh_3)]^+$. (CI, NH_3, m/z (%)): 456 (100) $[(M+H+NH_3)]^+$, 438 (36) $[M]^+$, 421 (62) $[(M+H\text{-}H_2O)]^+$.

***trans*-4-t-Butyl-1-(triphenylsilylethynyl)cyclohexan-1-ol[$Co_2(CO)_6$], 139.** Dark red crystals, (50%), m.p. 103-104 °C. ^{1}H NMR (200 MHz, $CDCl_3$): δ 7.26-7.77 (15H, m, $Si(C_6H_5)_3$), 1.25-1.97 (9H, m, $[CH_2]_{2,3,5,6}$ and H_4), 1.04 (9H, s, $C(CH_3)_3$). ^{13}C NMR (50 MHz, $CDCl_3$): δ 200.1 (6CO's), 136.4 (meta-C's), 134.0 (para-C's), 130.0 (ipso-C's), 127.9 (ortho-C's), 122.9 (*C*CSi), 74.2 (C*C*Si), 45.0 (C_4), 41.2 ($C_{2,6}$), 32.7 ($C(CH_3)_3$), 27.7 ($C(CH_3)_3$), 23.5 ($C_{3,5}$). MS (ESI (-ve, CH_3CN), *m/z* (%)): 723 (100) $[(M\text{-}H)]^-$, 667 (30) $[(M\text{-}H\text{-}2CO)]^-$, 639 (30) $[(M\text{-}H\text{-}3CO)]^-$.

***cis*-4-t-Butyl-1-(triphenylsilylethynyl)cyclohexan-1-ol[$Co_2(CO)_6$], 140.** Dark red crystals, (80%), m.p. 150-152 °C. ^{1}H NMR (200 MHz, $CDCl_3$): δ 7.29-7.75 (15H, m, $Si(C_6H_5)_3$), 1.28-1.83 (9H, m, $[CH_2]_{2,3,5,6}$ and H_4), 0.86 (9H, s, $C(CH_3)_3$). ^{13}C NMR (50 , $CDCl_3$): δ 200.6 (6CO's), 136.3 (meta-C's), 134.0 (para-C's), 130.0 (ipso-C's), 127.9 (meta-C's), 73.1 (C_1), 47.4 (C_4), 41.6 ($C_{2,6}$), 32.3 ($C(CH_3)_3$), 27.5 ($C(CH_3)_3$), 23.3 (C3,5). MS (ESI (-ve, CH_3CN), *m/z* (%)): 723 (100) $[(M\text{-}H)]^-$, 667 (4) $[(M\text{-}H\text{-}2CO)]^-$.

Addition of cyclohexane-1,4-dione to triphenylsilylacetylene and n-butyllithium in Et_2O gave a mixture of **141**, **142**, and **143**. The dialkynol **142** was separated from the mixture by flash column chromatography on silica gel, whereas **141**, was only partially isolated, and was predominantly co-eluted with **143** from the column.

Cis-1,4-bis(triphenylsilylethynyl)cyclohexane-1,4-diol, **143** was not isolated from the mixture but was treated directly with $Co_2(CO)_8$.

4-Hydroxy-4-(triphenylsilylethynyl)cyclohexanone, **141**. White solid, m.p. 154 °C. ^{1}H NMR (200 MHz, $CDCl_3$): δ 7.34-7.66 (15H, m, $Si(C_6H_5)_3$), 2.12-2.62 (9H, m, $[CH_2]_4$ and OH). ^{13}C NMR (50 MHz, $CDCl_3$): δ 135.4 (meta-C's), 132.9 (para-C's), 130.1 (ipso-C's), 128.1 (ortho-C's), 111.9 (*C*CSi), 85.1 (C*C*Si), 66.8 ($C_{1,4}$), 38.8 (CH_2), 37.3 (CH_2). MS (DEI, *m/z* (%)): 396 (5) $[M]^+$, 259 (4) $[(Si(Ph)_3)]^+$. (CI, NH_3, *m/z* (%)): 414 (100) $[(M+H+NH_3)]^+$, 379 (14) $[(M+H-H_2O)]^+$, 319 (11) $[(M-Ph)]^+$, 259 (4) $[(Si(Ph)_3)]^+$.

***trans*-1,4-Bis(triphenylsilylethynyl)cyclohexane-1,4-diol**, **142**. Colourless crystals, (37%), m.p. 225-226 °C. ^{1}H NMR (200 MHz, $CDCl_3$): δ 7.34-7.67 (30H, m, $Si(C_6H_5)_3$), 2.01-2.19 (10H, m, $[CH_2]_4$ and $[OH]_2$). ^{13}C NMR (50 MHz, $CDCl_3$): δ 135.5 (meta-C's), 133.2 (para-C's), 130.0 (ipso-C's), 128.0 (ortho-C's), 113.3 (*C*CSi), 84.2 (C*C*Si), 67.9 ($C_{1,4}$), 36.1 ($C_{2,3,5,6}$). MS (ESI (-ve, NH_4OAc), *m/z* (%)): 739 (100) $[(M+OAc)]^-$.

***trans*-1,4-Bis(triphenylsilylethynyl)cyclohexane-1,4-diol$[Co_2(CO)_6]_2$**, **144**. Dark red crystals, (82%), m.p. (dec.) > 192 °C. ^{1}H NMR (200 MHz, $CDCl_3$): δ 7.36-7.78 (30H, m, $Si(C_6H_5)_3$), 1.50-2.09 (10H, m, $[CH_2]_4$ and $[OH]_2$). ^{13}C NMR (50 MHz, $CDCl_3$): δ 199.8 (12CO's), 136.4 (meta-C's), 133.9 (para-C's), 130.0 (ipso-C's), 127.9 (ortho-C's), 92.6

($C_{1,4}$), 37.1 ($C_{2,3,5,6}$). MS (ESI (-ve, CH_3CN), *m/z* (%)): 1251 (100) $[(M-H)]^-$, 1195 (10) $[(M-H-2CO)]^-$.

4-hydroxy-4-(triphenylsilylethynyl)cyclohexanone[$Co_2(CO)_6$]. A small quantity of the mono-substituted complexed alkyne, 4-hydroxy-4-(triphenylsilylethynyl)cyclohexanone[$Co_2(CO)_6$], was also isolated as a dark red oil. ^1H NMR (200 MHz, $CDCl_3$): δ 7.44-7.73 (15H, m, $Si(C_6H_5)_3$), 1.50-2.76 (9H, m, $[CH_2]_{2,3,5,6}$ and [OH]). ^{13}C NMR (50 MHz, $CDCl_3$): δ 210.6 (C_1), 199.8 (Co-CO's), 136.2 (meta-C's), 133.9 (para-C's), 130.4 (ipso-C's), 128.1 (ortho-C's), 72.1 (C_4), 40.2 ($C_{2,6}$), 37.3 ($C_{3,5}$). MS (ESI (-ve, CH_3CN), *m/z* (%)): 681 (100) $[(M-H)]^-$, 625 (18) $[(M-H-2CO)]^-$.

***cis*-1,4-Bis(triphenylsilylethynyl)cyclohexane-1,4-diol[$Co_2(CO)_6$]$_2$, 145**. Dark red crystals, m.p. (dec.) > 150 °C. ^1H NMR (200 MHz, $CDCl_3$): δ 7.33-7.72 (30H, m, $Si(C_6H_5)_3$), 1.55-1.91 (8H, m, $[CH_2]_4$). ^{13}C NMR (50 MHz, $CDCl_3$): δ 199.8 (12CO's), 136.3 (meta-C's), 133.9 (para-C's), 130.2 (ipso-C's), 128.0 (ortho-C's), 72.9 ($C_{1,4}$), 37.3 ($C_{2,3,5,6}$). MS (ESI (-ve, CH_3CN), *m/z* (%)): 1251 (68) $[(M-H)]^-$, 1223 (100) $[(M-H-CO)]^-$, 1195 (27) $[(M-H-2CO)]^-$.

***trans*-1,4-Bis(trimethylsilylethynyl)cyclohexane-1,4-diol, 146**. Colourless crystals, (56%), m.p. 188-190 °C. ^1H NMR (200 MHz, $CDCl_3$): δ 1.89-2.10 (10H, m, $[CH_2]_4$ and $[OH]_2$), 0.16 (18H, s, $2Si(CH_3)_3$). ^{13}C NMR (50 MHz, $CDCl_3$): δ 108.5 (*C*CSi), 89.0 (C*C*Si), 68.0 ($C_{1,4}$), 36.5 ($C_{2,3,5,6}$), -0.1 ($Si(CH_3)_3$). MS (CI, NH_3, *m/z* (%)): 326 (5) $[(M+H+NH_3)]^+$, 308 (40) $[M]^+$, 291 (23) $[(M+H-H_2O)]^+$, 73 (22) $[(Si(CH_3)_3)]^+$.

***cis*-1,4-Bis(trimethylsilylethynyl)cyclohexane-1,4-diol, 147.** Colourless crystals, (21%), m.p. 146-147 °C. ^{1}H NMR (200 MHz, $CDCl_3$): δ 2.58 (2H, broad s, $[OH]_2$), 1.87 (8H, broad s, $[CH_2]_4$), 0.12 (18H, s, $2Si(CH_3)_3$). ^{13}C NMR (50 MHz, $CDCl_3$): δ 109.1 and 108.7 (*C*CSi), 88.8 and 88.0 (C*C*Si), 67.8 and 66.8 ($C_{1,4}$), 36.4 and 35.7 ($C_{2,3,5,6}$), -0.1 ($Si(CH_3)_3$). MS (ESI (-ve, NH_4OAc), *m/z* (%)): 367 (20) $[(M+OAc)]^-$.

***trans*-1,4-Bis(trimethylsilylethynyl)cyclohexane-1,4-diol$[Co_2(CO)_6]_2$, 148.** Dark red crystals, (80%), m.p. (dec.) > 165 °C. ^{1}H NMR (200 MHz, $CDCl_3$): δ 2.21 (4H, broad d, ^{3}JH-H = 8.9 Hz, $[CH_2]_4$), 1.76 (4H, broad d, ^{3}JH-H = 8.7 Hz, $[CH_2]_4$), 1.36 (2H, s, OH), 0.36 (18H, s, $2Si(CH_3)_3$). ^{13}C NMR (50 MHz, $CDCl_3$): δ 200.3 (12CO's), 121.5 (*C*CSi), 72.9 ($C_{1,4}$), 38.2 ($C_{2,3,5,6}$), 1.1 ($Si(CH_3)_3$). MS (ESI (-ve, CH_3OH), m/z (%)): 656 (10) $[(M-8CO)]^-$, 628 (11) $[(M-9CO)]^-$, 593 (100) $[(M-H-Co_2(CO)_6)]^-$. (DEI, *m/z* (%)): 566 (1) $[(M-Co_2(CO)_6-CO)]^+$, 538 (3) $[(M-Co_2(CO)_6-2CO)]^+$, 510 (2) $[(M-Co_2(CO)_6-3CO)]^+$, 482 (4) $[(M-Co_2(CO)_6-4CO)]^+$, 454 (3) $[(M-Co_2(CO)_6-5CO)]^+$, 426 (3) $[(M-Co_2(CO)_6-6CO)]^+$, 73 (100) $[(Si(CH_3)_3)]^+$. (CI, NH_3, *m/z* (%)): 577 (75) $[(M+H-H_2O-Co_2(CO)_6)]^+$, 521 (28) $[(M+H-H_2O-Co_2(CO)_6-2CO)]^+$, 308 (84) $[(M-2Co_2(CO)_6)]^+$.

***cis*-1,4-Bis(trimethylsilylethynyl)cyclohexane-1,4-diol$[Co_2(CO)_6]_2$, 149.** Dark red crystals, (53%), m.p. (dec.) > 129 °C. ^{1}H NMR (200 MHz, $CDCl_3$): δ 2.75 (2H, s, $[OH]_2$), 1.80-2.25 (8H, m, $[CH_2]_4$), 0.34 (18H, s, $2Si(CH_3)_3$). ^{13}C NMR (50 MHz, $CDCl_3$): δ 200.2 (12CO's), 120.4 (*C*CSi), 78.8 (C*C*Si), 73.2 ($C_{1,4}$), 38.0 ($C_{2,3,5,6}$), 1.1 $Si(CH_3)_3$). MS(ESI (-ve, NH_4OAc), *m/z* (%)): 879 (100) $[(M-H)]^-$, 823 (19) $[(M-H-2CO)]^-$, 795 (7) $[(M-H-3CO)]^-$, 593 (10) $[(M-H-Co_2(CO)_6)]^-$.

***trans*-1,4-bis(trimethylsilylethynyl)cyclohexane-1,4-diol[$Co_2(CO)_6$], 150.** Dark red crystals, (18%), m.p. (dec.) > 154 °C. ^{1}H NMR (200 MHz, $CDCl_3$): δ 1.38-2.12 (10H, m, $[CH_2]_4$ and $[OH]_2$), 0.32 (9H, s, $Si(CH_3)_3$), 0.16 (9H, s, $Si(CH_3)_3$). ^{13}C NMR (50 MHz, $CDCl_3$): δ 200.2 (6CO's), 121.7 (*C*CSi), 110.1, 87.1, 72.5 and 65.7 (C_{1and4}), 36.6 and 35.0 ($C_{2,6,and3,5}$), 1.0 and -0.1 ($2Si(CH_3)_3$). MS(ESI (-ve, CH_3OH), *m/z* (%)): 593 (100) [(M-H)]$^-$, 537 (19) [(M-H-2CO)]$^-$, 509 (27) [(M-H-3CO)]$^-$.

1,4-Bis(trimethylsilylethynyl)cyclohex-3-ene-1-ol[$Co_2(CO)_6$]$_2$, 151. Dark red crystals, (90%), m.p. (dec.) > 180 °C. Treatment of **149** (0.26g, 0.30mmol) with 2 equivalents of triethylamine, 5% imidazole, and subsequent additon of diphenyldichlorosilane (0.1 mL) in dicholormethane, afforded **151** after chromatographic purification with a 50:50 mixture of dichloromethane/hexanes. ^{1}H NMR (200 MHz, $CDCl_3$): δ 6.12 (1H, broad, C=CH), 1.94-2.89 (6H, m, $[CH_2]_3$), 1.81 (1H, s, OH), 0.37 (9H, s, $Si(CH_3)_3$), 0.36 (9H, s, $Si(CH_3)_3$). ^{13}C NMR (50 MHz, $CDCl_3$): δ 200.2 (12CO's), 72.1 (COH), 43.5, 37.9 and 28.7 (CH_2's), 1.1 and 0.88 ($2Si(CH_3)_3$). MS (ESI (-ve, CH_3OH), *m/z* (%)): 861 (100) [(M-H)]$^-$, 834 (5) [(M-CO)]$^-$, 750 (5) [(M-4CO)]$^-$.

References

1. Coates, G.E.; Green, M.L.H.; Wade, K. *Organometallic Compounds Vol. 1 & 2*, Methuen & Co. Ltd., London, **1968**.

2. Parkins, A.W.; Poller, R.C. *An Introduction to Organometallic Chemistry*, Oxford Univ. Press, New York, **1986**, p.21.

3. Davenport, D. *ChemMatters* **1984**, *2*, 14.

4. (a) Frankland, E. *Experimental Researches in Pure, Applied, and Physical Chemistry*, London, **1877**. (b) Seyferth, D. *Organometallics*, **2001**, *20*, 2940-55.

5. Yamamoto, A. *Organotransition Metal Chemistry: Fundamental Concepts and Applications*, John Wiley & Sons, Inc., New York, **1986**, p. 1-4.

6. Wilkinson, G. *J. Organomet. Chem.* **1975**, *100*, 273-8.

7. (a) Fischer, E.O.; Hafner, W. *Z. Naturforsch. B* **1955**, *10*, 665-8. (b) Seyferth, D. *Organometallics*, **2002**, *21*, 2800-20.

8. (a) Wilkinson, G.; Rosenblum, M.; Whiting, M.C.; Woodward, R.B. *J. Am. Chem. Soc.* **1952**, *74*, 2125-6. (b) Fischer, E.O.; Pfab, W. *Z. Naturforsch. B* **1952**, *7*, 377-

9. (a) Seyferth, D. *Organometallics*, **2001**, *20*, 2-6. (b) *ibid.*, 1488-98. (c) *ibid.*, 2940-55. (d) *ibid.*, 4978-92. (e) Seyferth, D. *Organometallics*, **2002**, *21*, 1520-30. (f) Seyferth, D. *Organometallics*, **2003**, *22*, 2-20. (g) *ibid.*, 2346-57. (h) Pauson, P.L. *J. Organomet. Chem.* **2001**, *637-9*, 3-6. (i) Fischer, E.O.; Jira, R. *Organomet. Chem.* **2001**, *637-9*, 7-12. (j) Rosenblum, M. *Organomet. Chem.* **2001**, *637-9*, 13-15. (k) Whitig, M.C. *Organomet. Chem.* **2001**, *637-9*, 16-17. (l) Cotton, F.A. *Organomet. Chem.* **2001**, *637-9*, 18-26.

10. (a) Sidgwick, N.V. *The Electronic Theory of Valency*, Oxford Univ. Press **1927**. (b) Sidgwick, N.V. *Chem.* and *Ind.* **1927**, *46*, 799-807. (c) Sidgwick, N.V. *Z. Elektrochem.* **1928**, *34*, 445-50.

11. (a) Lewis, G.N. *J. Am. Chem. Soc.* **1916,** *38*, 762-85. (b) Lewis, G.N. *Valence and the Structure of Atoms and Molecules*, New York, Chemical Catalogue Company, **1923**.

12. Crabtree, R.H., *The Organometallic Chemistry of the Transition Metals 2nd ed.* John Wiley and Sons Inc., New York, **1994**, p.13-17.

13. Young, R.S., *Cobalt Its Chemistry, Metallurgy, and Uses*, New York, Reinhold Publishing Corporation, **1960**.

14. Mellor, J.W., *A Comprehensive Treatise on Inorganic and Theoretical Chemistry Vol. XIV*, Longmans, Green & Co., London, **1935**.

15. Goldschmidt, V.M. *J. Chem. Soc.* **1937**, 655-73.

16. Young, R.S. *The Analytical Chemistry of Cobalt*, Pergamon Press, Oxford, **1966**, p.4.

17. Infoplease.com: *http://www.infoplease.com/ce6/sci/A0824719.html* Pearson Education, **2003**.

18. (a) Szabó, P.; Markó, L.; Bor, G. *Chem. Tech. (Liepzig, Germany)* **1961**, *13*, 549-50. (b) King, R.B. *Organometallic. Synthesis Vol. 1: Transition Metal Compounds*, Academic Press, New York, **1965**, p. 98.

19. (a) Sumner, G.G.; Klug, H.P., Alexander, L.E. *Acta Crystallogr.* **1964**, *17*, 732-42. (b) Leung, P.; Coppens, P. *Acta Crystallogr., Sect. B* **1983**, *39*, 535-42.

20. (a) Noack, K. *Spectrochim. Acta* **1963**, *19*, 1925-31. (b) Bor, G. *Spectrochim. Acta* **1963**, *19*, 2065-73. (c) Noack, K. *Helv. Chim. Acta* **1964**, *47*, 1064-7.

21. (a) Bor, G.; Noack, K. *J. Organomet. Chem.* **1974**, *64*, 367-72. (b) Bor, G.; Dietler, U.K.; Noack, K. *J. Chem. Soc., Chem. Commun.* **1976**, 1914-6. (c) Sweany, R.L.; Brown, T.L. *Inorg. Chem.* **1977**, *16*, 415-21.

22. Onaka, S.; Shriver, D.F. *Inorg. Chem.* **1976**, *15*, 915-8.

23. Aullón, G.; Alvarez, S. *Eur. J. Inorg. Chem.* **2001**, 3031-8.

24. (a) Whyman, R. *Chem. Commun.* **1970**, 1194-5. (b) Whyman, R. *J. Chem. Soc., Dalt. Trans.* **1972**, 1375-81. (c) Hanlan, L.A.; Ozin, G.A. *J. Am. Chem. Soc.* **1974**, *96*, 6324-9. (d) Hanlan, A.J.L.; Ozin, G.A.; Gray, H.B. *Inorg. Chem.* **1979**, *18*, 1790-2.

25. Hanlan, A.J.L.; Ozin, G.A. *J. Organomet. Chem.* **1979**, *179*, 57-64.

26. Sternberg, H.W.; Greenfield, H.; Friedel, R.A., Wotiz, J., Markby, R., Weder, I. *J. Am. Chem. Soc.* **1956**, *78*, 120-4.

27. Sternberg, H.W.; Greenfield, H.; Friedel, R.A., Wotiz, J., Markby, R., Weder, I. *J. Am. Chem. Soc.* **1954**, *76*, 1457-8.

28. Sly, W.G. *J. Am. Chem. Soc.* **1959**, *81*, 18-20.

29. Dickson, R.S.; Fraser, P.J. *Adv. Organomet. Chem.* **1976**, *12*, 323-77.

30. (a) Nicholas, K.M.; Petit, R. *Tetrahedron Lett.* **1971**, *37*, 3475-8. (b) Melikyan, G.G.; Vostrowsky, O.; Bauer, W.; Bestmann, H.J.; Khan, M.: Nicholas, K.M. *J. Org. Chem.* **1994**, *59*, 222-9.

31. Seyferth, D.; Wehman, A.T. *J. Am. Chem. Soc.* **1970**, *92*, 5520-2.

32. (a) Cetini, G.; Gambino, O.; Rosetti, R.; Sappa, E. *J. Organomet. Chem.* **1967**, *8*, 149-54. (b) Krüerke, U.; Hübel, W. *Chem. Ber.* **1961**, *94*, 2817-20. (c) Hübel, W.; Merényi, R. *Chem. Ber.* **1963**, *96*, 930-43.

33. (a) Hoffmann, R. *Science* **1981**, *211*, 995-1002. (b) Hoffmann, R. *Angew. Chem. Int. Ed. Engl.* **1982**, *21*, 711-24.

34. Ege, S.N. *Organic Chemistry* 2nd ed.; D.C. Heath and Company: Toronto, **1989**, p. 121.

35. Olah, G.A. *Angew. Chem.* **1973**, *85*, 183-225.

36. Winstein, S.; Trifan, D.S. *J. Am. Chem. Soc.* **1949**, *71*, 2953. (a) Myhre, P.C.; Webb, G.G.; Yannoni, C.S. *J. Am. Chem. Soc.* **1990**, *112,* 8991-2. (b) Johnson, S.A.; Clark, D.T. *J. Am. Chem. Soc.* **1988**, *110,* 4112-7. (c) Schleyer, P.v.R.; Sieber, S. *Angew. Chem. Int. Ed.* **1993**, *32*, 1604-6.

37. Olah, G.A.; Liang, G. *J. Am. Chem. Soc.* **1975**, *97*, 6803-6 and references therein.

38. Bethell, D.; Gold, V. *Carbonium Ions: An Introduction*, Academic Press, New York, **1967**.

39. Wieting, R.D.; Staley, R.H.; Beauchamp, J.L. *J. Am. Chem. Soc.* **1974**, *96*, 7552-4.

40. Morrison, R.T.; Boyd, R.N. *Organic Chemistry* 4th ed., Allyn and Bacon, Boston, **1983**, p.495-6.

41. (a) Olah, G.A.; Svoboda, J.J.; Ku, A.T. *Synthesis* **1973**, *8*, 492-3. (b) Hogeveen, H. *Rec. Trav. Chim.* **1967**, 86, 1061-2.

42. Hollenstein, S.; Laube, T. *J. Am. Chem. Soc.* **1993**, *115*, 7240-5.

43. (a) Olah, G.A.; Westerman, P.W.; Nishimura *J. Am. Chem. Soc.* **1974**, *96*, 3548-59. (b) Olah, G.A.; Westerman, P.W *J. Am. Chem. Soc.* **1973**, *95*, 7530-1.

44. (a) Cais, M.; *Organomet. Chem. Rev.* **1966**, *1*, 435-54. (b) Caffyn, A.J.M.; Nicholas, K.M. in *Comprehensive Organometallic Chemistry II*; Wilkinson, G.; Stone, F.G.A.; Abel, E.W., Eds.; Pergamon Press: Oxford, **1995**; Vol. 12, Chapter 7.1, p 685-702. (c) El Amouri, H.; Gruselle, M. *Chem. Rev.* **1996**, *96*, 1077-103.

(c) Hill, E.A.; Wiesner, R.; *J. Am. Chem. Soc.* **1969**, *91*, 509-10. (d) Gleiter, R.; Seeger, R.; Binder, H.; Fluck, E.; Cais, M. *Angew. Chem. Int. Ed. Engl.* **1972**, *11*, 1028-30.

45. (a) Nicholas, K.M. *Acc. Chem. Res.* **1987**, *20*, 207-14. (a) O'Boyle J.E.; Nicholas, K.M. *Tetrahedron Lett.* **1980**, *21*, 1595-8.

46. (a) Schreiber, S.L.; Sammakia, T.; Crowe, W.E. *J. Am. Chem. Soc.* **1986**, *108*, 3128-30.
(b) Takano, S.; Sugihara, T.; Ogasawara, K. *Synlett.* **1992**, 70-2. (c) McGlinchey, M.J.; Girard, L.; Ruffolo, R. *Coord. Chem. Rev.* **1995**, *143*, 331-81. (d) El Amouri, H.; Gruselle, M. *Chem. Rev.* **1996**, *96*, 1077-1103.

47. (a) Schilling, B.E.R.; Hoffmann, R. *J. Am. Chem. Soc.* **1978**, *100*, 6274. (b) Hoffman, D.M.; Hoffmann, R.; Fisel, C.R. *J. Am. Chem. Soc.* **1982**, *104*, 3858-75.

48. Osella, D.; Dutto, G.; Jaouen, G.; Vessières, A.; Raithby, P.R.; De Benedetto, L.; McGlinchey, M.J. *Organometallics* **1993**, *12*, 4545-52.

49. Dunn, J.A.; Hunks, W.J.; Ruffolo, R.; Rigby, S.S.; Brook, M.A.; McGlinchey, M.J. *Organometallics* **1999**, *18*, 3372-82.

50. Padmanabhan, S.; Nicholas, K.M. *J. Organomet. Chem.* **1983**, *268*, C23-7.

51. Edidin, R.T.; Norton, J.; Mislow, K. *Organometallics* **1982**, *1*, 561-2.

52. (a) Connor, R.E.: Nicholas, K.M. *J. Organomet. Chem.* **1977**, *125*, C45-8. (b) Nicholas, K.M.; Pettit, R. *J. Organomet. Chem.* **1972**, *44*, C21-4.

53. Schreiber, S.L.; Klimas, M.T.; Sammakia, T. *J. Am. Chem. Soc.* **1987**, *109*, 5749-59.

54. Pfletschinger, A.; Koch, W.; Schmalz, H.-G. *Chem. Eur. J.* **2001**, *7*, 5325-32.

55. Victor, R. *J. Organomet. Chem.* **1977**, *127*, C25-8.

56. Melikyan, G.G; Bright, S.; Monroe, T.; Hardcastle, K.I.; Ciurash, J. *Angew. Chem. Int. Ed.* **1998**, *37*, 161-4.

57. Troitskaya, L.L.; Sokolov, V.I.; Bakhmutov, V.I.; Reutov, O.A.; Gruselle, M.; Cordier, C.; Jaouen, G. *J. Organomet. Chem.* **1989**, *364*, 195-206.

58. Ruffolo, R., Ph.D. Thesis, McMaster University, Hamilton, Ontario, **1997**, p 14.

59. (a) Green, J.R. *Curr. Org. Chem.* **2001**, *5*, 809-26. (b) Teobald, B.J. *Tetrahedron* **2002**, *58*, 4133-70. (c) Went, M.J. *Adv. Organomet. Chem.* **1997**, *41*, 69-125. (d) Wojcicki, A.; Shuchart, C.E. *Coord. Chem. Rev.* **1990**, *105*, 35-60.

60. Seyferth, D.; Wehman, A.T. *J. Am. Chem.* Soc. **1970**, *92*, 5520-2.

61. (a) Magnus, P.; Becker, D.P. *J. Chem. Soc. Chem Commun.* **1985**, 640-2. (b) Shvo, Y.; Hazum, E. *J. Chem. Soc. Chem Commun.* **1974**, 336-7.

62. Sugihara, T.; Ban, H.; Yamaguchi, M. *J. Organomet. Chem.* **1998**, *554*, 163-6.

63. Magnus, P; Lewis, R.T.; Huffman, J.C. *J. Am. Chem.* Soc. **1988**, *110*, 6921-3.

64. Mukai, C.; Moharram, S.M.; Kataoka, O.; Hanaoka, M. *J. Chem. Soc. Perkin Trans. 1* **1995**, 2849-54.

65. Mukai, C.; Katuoka, O.; Hanaoka, M. *J. Org. Chem.* **1993**, *58*, 2946-52.

66. Saha, M.; Bagby, B.; Nicholas, K.M. *Tetrahedron Lett.* **1986**, *27*, 915-8.

67. Jacobi, P.A.; Rajeswari, S. *Tetrahedron Lett.* **1992**, *33*, 6231-4.

68. Henrick, C.A. *Tetrahedron* **1977**, *33*, 1845-89.

69. (a) Kienzle, F. *Pure Appl. Chem.* **1976**, *47*, 183-90. (b) Makin, S.M. *Pure Appl. Chem.* **1976**, *47*, 173-81.

70. Schegolev, A.A.; Smit, W.A.; Kalyan, Y.B.; Krimer, M.Z.; Caple, R. *Tetrahedron Lett.* **1982**, *23*, 4419-22.

71. Pauson, P.L. *Tetrahedron* **1985**, *41*, 5855-60.

72. Schreiber, S.L.; Sammakia, T.; Crowe, W.E. *J. Am. Chem. Soc.* **1986**, *108*, 3128-30.

73. (a) Gilbert, J.C.; Hou, D.-R.; Grimme, J.W. *J. Org. Chem.* **1999**, *64*, 1529-1534. (b) Gilbert, J.C.; McKinley, E.G.; Hou, D.-R. *Tetrahedron* **1997**, *53*, 9891-9902. (c) Gilbert, J.C.; Baze, M.E. *J. Am. Chem. Soc.* **1983**, *24*, 664-665. (d) Fitjier, L.; Modaressi, S. *Tetrahedron Lett.* **1983**, *24*, 5495-5498. (e) Fitjier, L.; Kliebisch, V.; Wehle, D.; Modaressi, S. *Tetrahedron Lett.* **1982**, *23*, 1661-1664. (f) Wentrup, C.; Blanch, R.; Briehl, H.; Gross, G. *J. Am. Chem. Soc.* **1988**, *110*, 1874-1880. (g) Bottini, A.T.; Frost, K.A., II; Anderson, B.R.; Dev, V. *Tetrahedron* **1973**, *29*, 1975-1981. (h) Montegomery, L.K.; Applegate, L.E. *J. Am. Chem. Soc.* **1967**, *89*, 5305-5307.

74. Bloomquist, A.T.; Liu, L.H. *J. Am. Chem. Soc.* **1953**, *75*, 2153-2154.

75. (a) Magnus, P.; Pitterna, T. *J. Chem. Soc. Chem. Commun.* **1991**, 541-543. (b) Magnus, P.; Carter, R.; Davies, M.; Elliott, J.; Pitterna, T. *Tetrahedron* **1996**, *52*, 6283-6306.

76. Chisolm, M.H.; Folting, K.; Huffman, J.C.; Lucas, E.A. *Organometallics* **1991**, *10*, 535-537.

77. Green, J.R. *Chem. Commun.* **1998**, 1751-2.

78. Patel, M.M.; Green, J.R. *Chem. Commun.* **1999**, 509-10.

79. Soleilhavoup, M.; Maurette, L.; Lamirand, C.; Donnadieu, B.; McGlinchey, M.J.; Chauvin, R. *Eur. J. Org. Chem.* **2003**, 1652-60.

80. Ruffolo, R.; Brook, M.A.; McGlinchey, M.J. *Organometallics*, **1998**, *17*, 4992-6.

81. Goldberg, S.I. *J. Org. Chem.* **1960**, *25*, 482-3.

82. Lukasser, J.; Angleitner, H.; Schottenberger, H.; Kopacka, H.; Schweiger, M.; Bildstein, B.; Ongania, K.-H.; Wurst, K. *Organometallics* **1995**, *14*, 5556-5578.

83. Hyperchem Pro Version 5.1, Heypercube Inc., 1114 NQ 4th Street, Gainsville, FL 32601, 1997.

84. (a) Gaus, C.; Veghini, D.; Orama, O.; Berke, H. *J. Organomet. Chem.* **1997**, *541*, 19-38. (b) Berke, H.; Haerter, P.; Huttner, G.; Zsolnai, L. *Chem. Ber.* **1984**, *117*, 3423-31. (c) Toda, F.; Tanaka, K.; Watanabe, M.; Tamura, K.; Miyahara, I.; Nakai, T.; Hirotsu, K. *J. Org. Chem.* **1999**, *64*, 3102-5.

85. Bradley, D.H.; Khan, M.A.; Nicholas, K.M. *Organometallics* **1989**, *8*, 554-6.

86. (a) Brook, M.A. *Silicon in Organic, Organometallic, and Polymer Chemistry* John Wiley & Sons, New York, **2000**, p. 32. (b) Takimoto, K.; Miura, M. *Bull. Chem. Soc. Jpn.* **1971**, *44*, 1534-8 and references therein.

87. King, J.F.; De Mayo, P. *Molecular Rearrangements*; De Mayo, P., Ed.; Wiley-Interscience: New York, **1964**.

88. (a) Morris, D.G.; Shepherd, A.G.; Walker, M.F.; Jemison, R.W. *Aust. J. Chem.* **1982**, *35*, 1061-4. (b) Kagawa, M. *Chem. Pharm. Bull.* **1959**, *7*, 306-15.

89. D'Agostino, M.F.; Frampton, C.S.; McGlinchey, M.J. *J. Organomet. Chem.* **1990**, *394*, 145-66.

90. Gruselle, M.; El Hafa, H.; Nikolski, M.; Jaouen, G.; Vaissermann, J.; Li, L.; McGlinchey, M.J. *Organometallics* **1993**, *12*, 4917-25.

91. Kondratenko, M.; El Hafa, H.; Gruselle, M.; Vaissermann, J.; Jaouen, G.; McGlinchey, M. J. *J. Am. Chem. Soc.* **1995**, *117*, 6907-13.

92. Capmau, M-L.; Chodkiewicz, W.; Cadiot, P.; Fayet, A.-M. *Bull. Chim. Soc. Fr.* **1968**, 3233-8.

93. (a) Chodkiewicz, W.; Capmau, M-L.; Boissard-Gerde M. *C. R. Acad. Sci.* **1968**, *267C*, 911-4. (b) Gosselin, P.; Joulain, D.; Laurin, P.; Rouessac, F. *Tetrahedron Lett.* **1990**, *31*, 3151-4.

94. Kaldis, J.H.; Morawietz, P.; McGlinchey, M.J. *Organometallics* **2003**, *22*, 1293-1301.

95. Markby, R.; Wender, I., Friedel, R.A.; Cotton, F.A.; Sternberg, H.W. *J. Am. Chem. Soc.* **1958**, *80*, 6529-6533.

96. Krüerke, U.; Hübel, W. *Chem. Ind.* **1960**, 1264.

97. Sutton, P.W.; Dahl, L.F. *J. Am. Chem. Soc.* **1967**, *89*, 261-268.

98. Beck, J.A.; Knox, S.A.R.; Stansfield, R.F.D.; Stone, F.G.A.; Winter, M.J.; Woodward, P. *J. Chem. Soc. Dalton Trans.* **1982**, 195-200.

99. The ^{13}C NMR spectra of **22** match closely with the data for 1-isopropyl-4-methylcyclohexa-1,3-diene (α-terpinene): Bohlmann, F.; Zeisberg, R.; Klein, E. *Org. Magn. Reson.* **1975**, *7*, 426-32.

100. (a)Lutz, R.P.; Roberts, J.D. *J. Am. Chem. Soc.* **1962**, *84*, 3715-21. (b) Armstrong, H.E.; Kipping F.S.; *J. Chem. Soc.* **1893**, *63*, 75-99. (c) Bredt, J.; Rochussen, F.; Monheim, J. *Justus Liebigs Ann. Chem.* **1901**, *314*, 369.

101. (a) Banthorpe, D.V.; Morris, D.G.; Bunton, C.A. *J. Chem. Soc. B* **1971**, 687-91. (b) Hückel, W.; Kern, H.J. *Justus Liebigs Ann. Chem.* **1969**, *728*, 49-55. (c) Edwards, O.E.; Lesage, M. *Can. J. Chem.* **1963**, *41*, 1592-1605.

102. (a) Vaillancourt, V.; Agharahimi, M.R.; Sundram, U.N.; Richou, O.; Faulkner, J.F.; Albizati, K.F *J. Org. Chem.* **1991**, *56*, 378-387. (b) Richou, O.; Vaillancourt, V.; Faulkner, D.J.; Albizati, K.F. *J. Org. Chem.* **1989**, *54*, 4729-4730. (c) Hutchinson, J.H.; Money, T.; Piper, S.E *Can. J. Chem.* **1986**, *64*, 854-860. (d) Money, T. *Natur. Prod. Rep.* **1985**, *2*, 253-89. (e) Harnon, D.P.G.; Taylor, G.F.; Young, R.N. *Synthesis* **1975**, 428-430. (f) Baker, K.M.; Davis, B.R. *Tetrahedron* **1968**, *24*, 1655-1662.

103. Sorensen, T. S. *Acc. Chem. Res.* **1976**, *9*, 257-65.

104. (a) Seyferth, D. *Adv. Organomet. Chem.* **1976**, *14*, 97-144. (b) Bor, G.; Markó, L.; Markó, B. *Chem. Ber.* **1962**, *95*, 333-40. (c) Dent, W.T.; Duncanson, L.A.; Guy, R.G.; Reed, H.W.B.; Shaw, B.L. *Proc. Chem. Soc.* **1961**, 169.

105. Khand, I.U.; Knox, G.R.; Pauson, P.L.; Watts, W.E. *J. Organomet. Chem.* **1974**, *73*, 383-388.

106. Morawietz, P., M. Sc. Thesis, McMaster University, Hamilton, Ontario, **1989**.

107. Gerlach, R.F.; Duffy, D.N.; Curtis, M.D. *Organometallics* **1983**, *2*, 1172-8.

108. Beck, J.A.; Knox, S.A.R.; Riding, G.H.; Taylor, G.E.; Winter, M.J. *J. Organomet. Chem.* **1980**, *202*, C49-52.

109. Jeffery, J.C.; Laurie, J.C.V.; Moore, I; Stone, F.G.A. *J. Organomet. Chem.* **1983**, *258*, C37-40.

110. Carriedo, G.A.; Elliot, G.P.; Howard, J.A.K.; Lewis, D.B.; Stone, F.G.A. *J. Chem. Soc., Chem. Commun.* **1984**, 1585-6.

111. Dickson, R.S.; Tailby, G.R. *Aust. J. Chem.* **1970**, *23*, 229-242.

112. Giese, B. *Radicals in Organic Synthesis: Formation of Carbon-Carbon Bonds* Pergamon Press, Oxford, **1986**, p. 1-11.

113. Gomberg, M. *J. Am. Chem. Soc.* **1900**, *22*, 757-71. (b) Gomberg, M. *Chem. Ber.* **1900**, *33*, 3150.

114. Paneth, F.; Hofeditz, W. *Chem. Ber.* **1929**, *62*, 1335.

115. Kharasch, M.S.; Margolis, E.T.; Mayo, F.R. *J. Org. Chem.* **1937**, *2*, 393-404.

116. Kochi, J.K. (ed.) *Free Radicals*, Wiley, NewYork, **1973**.

117. Fishcer, H. (ed.) *Landoldt-Börnstein, New Series, Vol. 13*, Springer, Berlin, **1983**.

118. Renaud, P.; Sibi, M.P. (eds.) *Radicals in Organic Synthesis* Vol.1, Wiley-VCH, Toronto, **2001**.

119. Pryor, W.A. *Free Radicals*, McGraw Hill Inc., New York, **1986**, p.4-10, 58-65, 232-246.

120. (a) Melikyan, G.G.; Vostrowsky, G.; Bauer, W.; Bestmann, H.J.; Khan, M.; Nicholas, K.M. *J. Org. Chem.* **1994**, *59*, 222-9, and references cited therein. (b) Melikyan, G.G.; Khan, M.A.; Nicholas, K.M. *Organometallics* **1995**, *14*, 2170-2. (c) Salazar, K.L.; Khan, M.A.; Nicholas, K.M. *J. Am. Chem. Soc.* **1997**, *119*, 9053-4. (d) Salazar, K.L.; Nicholas, K.M. *Tetrahedron* **2000**, *56*, 2111-24.

121. Pályi, G.; Ungváry, F; Galamb, V.; Markó, L. *Coord. Chem. Rev.* **1984**, *53*, 37-53.

122. Melikyan, G.G.; Combs, R.C.; Lamirand, J.; Khan, M.; Nicholas, K.M. *Tetrahedron Lett.* **1994**, *35*, 363-6.

123. (a) Melikyan, G.G.; Deravakian, A. *J. Organomet. Chem.* **1997**, *544*, 143-5. (b) Melikyan, G.G.; Deravakian, A.; Myer, S.; Yadegar, S.; Hardcastle, K.I.; Ciurash, J.; Toure, P. *J. Organomet. Chem.* **1999**, *578*, 68-75. (c) Toure, P.; Myer, S.; Melikyan, G.G. *J. Phys. Chem. A* **2001**, *105*, 4579-84.

124. (a) Gruselle, M.; Philomin, V.; Chaminant, F.; Jaouen, G.; Nicholas, K.M. *J. Organomet. Chem.* **1990**, *399*, 317-26. (b) Saha, M.; Nicholas, K.M. *J. Am. Chem. Soc.* **1984**, *49*, 417. (c) Roth, K.D.; Muller U. *Tetrahedron Lett.* **1993**, *34*, 2919-22. (d) Gelling, A.; Mohmand, F.; Jeffrey, J.C.; Went, M.J. *J. Chem. Soc., Dalt. Trans.* **1993**, 1857-62. (e) Kuhn, O.; Rau, D.; Mayr, H. *J. Am. Chem. Soc.* **1998**, *120*, 900-7. (f) Gruselle, M.; Malezieux, B.; Baissermann, J.; Amouri, H. *Organometallics* **1998**, *17*, 2337-43.

125. (a) Eğe, S. *Organic Chemistry*; Heath and Co.: Lexington, Mass., 1984; p 612. (b) Gomberg, M. *J. Chem. Ed.* **1932**, *9*, 439. (c) Neumann, W.P.; Uzick, W.; Zarkadis, A.K. *J. Am. Chem. Soc.* **1986**, *108*, 3762-70.

126. Kim, P-J.; Hagihara, N. *Bull. Chem. Soc. Jpn.* **1968**, *41*, 1184-7.

127. One could envisage initial formation of the alkene **33,** which is subsequently hydrogenated to the alkane **109** by reaction of the acid with cobalt-containing decomposition products.

128. Kaldis, J.H.; McGlinchey, M.J. *Tetrahedron Lett.* **2002**, *43*, 4049-53.

129. (a) Kishan, K.V.R.; Desiraju, G.R. *Indian J. Chem.* **1988**, *27B*, 953-4. (b) Desiraju, G.R.; Bernstein, J.; Kishan, K.V.R.; Sarma, J.A.R.P. *Tetrahedron Lett.* **1989**, *30*, 3029-32.

130. Kawase, T.; Muro, S.; Oda, M. *Tetrahedron Lett.* **1992**, *33*, 5961-4.

131. Eaton, B.E.; Rollman, B.; Kaduk, J.A. *J. Am. Chem. Soc.* **1992**, *114*, 6245-6.

132. (a) Kleveland, K.; Skattebøl, L. *Acta Chem. Scand. B* **1975**, *29*, 191-6. (b) Ruitenberg, K.; Kleijn, H.; Elsevier, C.J.; Meijer, J.; Vermeer, P. *Tetrahedron Lett.* **1981**, *22*, 1451-2.

133. Dewar, M.J.S.; Zoebisch, E.G.; Healy, E.F.; Stewart, J.J.P. *J. Am. Chem. Soc.* **1985**, *107*, 3902-9.

134. Harwood, L.M. *Polar Rearrangements*, Oxford University Press, Oxford, UK, **1992**, p. 86-87.

135. (a) Hennion, G.F.; Fleck, B.R. *J. Am. Chem. Soc.* **1955**, *77*, 3253-8. (b) Rauss-Godineau, J.; Barralis, J.; Chodkiewicz, W.; Cadiot, P. *Bull. Soc. Chim. Fr.* **1968**, 193-200. (c) Bharathi, P.; Periasamy, M. *Org. Lett.* **1999**, *1*, 857-9.

136. Toda, T.; Kuwana, M.; Ohhashi, Y.; Yoshida, M. *Chem. Lett.* **1997**, 21-2.

137. Ruffolo, R.; Decken, A.; Girard, L.; Gupta, H.K.; Brook, M.A.; McGlinchey, M.J. *Organometallics*, **1994**, *13*, 4328-35.

138. (a) Renaud, P.; Sibi, M.P. (eds.) *Radicals in Organic Synthesis* Vol. 2, Wiley-VCH, Toronto, 2001, p.455-84. (b) Waters, W.A. *The Chemistry of Free Radicals*, Oxford University Press, London, 1946, p. 232-45.

139. (a) Pilati, T.; Simonetta, M.; Quici, S. *Cryst. Struc. Commun.* **1982**, *11*, 1027. (b) Baum, G.; Shechter, H. *J. Org. Chem.* **1976**, *41*, 2120-4. (c) Van Tamelen, E.E.; Cole, T.M.Jr. *J. Am. Chem. Soc.* **1971**, *93*, 6158-66. (d) Takeuchi, K.; Kitagawa, T.; Miyabo, A.; Fujii, H.; Okazaki, T.; Mori, T.; Matsudou, M. Sugie, T. *J. Org. Chem.* **1997**, *62*, 888-892.

140. Robinson, P.D.; Hou, Y.; Myers, C.Y. *Acta Crystallogr. Sect. C. Cryst. Struc. Commun.* **1999**, *55*, 9900147.

141. Cadogan, J.I.G.; Hey, D.H.; Sanderson, W.A. *J. Chem. Soc.* **1960**, *82*, 3203-10.

142. (a) Nixon, J.R.; Cudd, M.A.; Porter, N.A. *J. Org. Chem.* **1978**, *43*, 4048-52. (b) Halfpenny, J.; Small, R.W.H. *Chem. Commun.* **1979**, 879. (c) Dussault, P.; Davies, D.R. *Tetrahedron Lett.* **1996**, *37*, 463-6. (d) Bloodworth, A.J.; Johnson, K.A. *Tetrahedron Lett.* **1994**, *35*, 8057-60. (e) Bloodworth, A.J.; Curtis, R.J.; Spencer, M.; Tallant, N.A. *Tetrahedron* **1993**, *49*, 2729-50. (f) Bloodworth, A.J.; Shah, A. *J. Chem. Soc., Chem. Commun.* **1991**, 947-8.

143. Copper: (a) Dietrich-Buchecker, C.O.; Sauvage, J.P.; Weiss, J. *Tetrahedron Lett.* **1986**, *27*, 2257-60. (b) Besancon, J.; Top, S.; Tirouflet, J.; Gautheron, B.; Dusausoy, Y. *J. Organomet. Chem.* **1975**, *94*, 35-46. Cobalt: (c) Kohno, M. *Bull. Chem. Soc. Jpn.* **1988**, *61*, 1509-15. (d) Buckingham, D.A.; Dekkers, J.; Sargeson, A.M. *J. Am. Chem. Soc.* **1973**, *95*, 4173-9. Iron: (e) Kalish, H.; Lee, H.M.; Olmstead, M.M.; Latos-Grazynski, L.; Rath, S.P.; Balch, A.L. *J. Am. Chem. Soc.* **2003**, *125*, 4674-4675. (f) Haraldsson, G.G.; Baldwin, J.E.; Jones, J.G.; Debernardis, J. *Polyhedron* **1993**, *12*, 2453-58. (g) Gold, A.; Ivey, W.; Toney, G.E.; Sangaiah, R. *Inorg. Chem.* **1984**, *23*, 2932-5. Paladium: (h) Freyer, W.; Flatau, S. *Tetrahedron Lett.* **1996**, *37*, 5083-6. (i) Freyer, W.; Stiel, H.; Hild, M.; Teuchner, K.; Leupold, D. *Photochem. and Photobio.* **1997**, *66*, 596-604.

144. Kojima, H.; Takahashi, S.; Hagihara, N. *J. Chem. Soc., Chem. Commun.* **1973**, *7*, 230-1.

145. (a) Dikusar, E.A.; Shirokii, V.L.; Yuvchenko, A.P.; Bazhanov, A.V.; Moiseichuk, K.L.; Khrustalev, V.N.; Antipin, M.Yu. *Zh. Obshch. Khim.* (Russ. J. Gen. Chem.) **1999**, *69*, 1315. (b) Stepin, S.G.; Stepina, O.S.; Dikusar, E.A.; Shirokii, V.L. *Zhum. Prik. Khim.* (Sankt-Petersburg, Russian Federation) **2000**, *73*, 1519-22. (c) Hamon, J.R.; Astruc, D. *Organometallics* **1988**, *7*, 1036-46.

146. (a) Delhaes, L.; Biot, C.; Berry, L.; Maciejewski, L.A.; Camus, D.; Brocard, J.S.; Dive, D. *Bioorg. & Med. Chem.* **2000**, *8*, 2739-2745. (b) Paitayatat, S.; Tarnchompoo, B.; Thebtaranonth, Y.; Yuthavong, Y. *J. Med Chem.* **1997**, *40*, 633-638.

147. (a) Jeffery, J.; Mawby, R.J.; Hursthouse, M.B.; Walker, N.P.C. *J. Chem. Soc., Chem. Commun.* **1982**, 1411-2. (b) Jeffery, J.; Probitts, E.J.; Mawby, R.J. *J. Chem. Soc., Dalt. Trans.: Inorg. Chem.* **1984**, *21*, 2423-7.

148. Eğe, S. *Organic Chemistry*; Heath and Co.: Lexington, Mass., **1984**; p 166-7.

149. Kellie, G.M.; Riddell, F.G. *Top. Stereochem.* **1974**, *8*, 225-69.

150. Weiser, J.; Golan, O.; Fiyjer, L.; Biali, S.E. *J. Org. Chem.* **1996**, *61*, 8277-84, and references therein.

151. (a) Grove, D.D.; Miskevich, F.; Smith, C.C.; Corte, J.R. *Tetrahedron Lett.* **1990**, 6277-80. (b) Grove, D.D.; Corte, J.R.; Spencer, R.P.; Pauly, M.E.; Rath, N.P. *J. Chem. Soc., Chem. Commun.* **1994**, 49-50.

152. Malisza, K.L.; Girard, L.; Hughes, D.W.; Britten, J.F.; McGlinchey, M.J. *Organometallics* **1995**, *14*, 4676-84.

153. (a) Tanaka, S.; Tsukiyama, T.; Isobe, M. *Tetrahedron Lett.* **1993**, *34*, 5757-60. (b) Tanaka, S.; Isobe, M. *Tetrahedron* **1994**, *50*, 5633-44.

154. (a) Eliel, E.L. *Stereochemistry of Carbon Compounds*, McGraw-Hill: New York, 1962, pp 208-21, 248-52. (b) Kellie, G.M.; Riddell, F.G. *Top. Stereochem.* **1974**, *8*, 224-269. (c) Bucourt, R. *Top. Stereochem.* **1974**, *8*, 159-224.

155. Malloy, T.B., Jr.; Bauman, L.E *Top. Stereochem.* **1979**, *11*, 97-185.

156. The synthesis of 1-(trimethylsilylethynyl)cyclohexan-1-ol has been reported previously, but no NMR data are available: Iritani, K.; Yanagihara, N.; Utimoto, K. *J. Org. Chem.* **1986**, *51*, 5499-501.

157. Deschamps, N.M.; Kaldis, J.H.; Lock, P.E.; Britten, J.F.; McGlinchey, M.J. *J. Org. Chem.* **2001**, *66*, 8585-91.

158. Braga, D.; Grepioni, F.; Walther, D.; Heubach, K.; Schmidt, A.; Imhof, W.; Görls, H.; Klettke, T. *Organometallics* **1997**, *16*, 4910-19.

159. Lock P.E. Ph.D. Thesis, 2001, p. 111-2.

160. (a) Battioni, J-P.; Chodkiewicz, W.; Cadiot, P. *C. R. Seances Acad. Sci. Ser. C* **1967**, *264*, 991-4. (b) Battioni, J-P.; Capmau, M-L.; Chodkiewicz, W. *Bull. Soc. Chim. Fr.* **1969**, 976-81. (c) Battioni, J-P.; Chodkiewicz, W. *Bull. Soc. Chim. Fr.* **1969**, 981-4.

161. Cram, D.J.; Abd Elhafez, F.A. *J. Am. Chem. Soc.* **1952**, *74*, 5828-35.

162. (a) Cherest, M.; Felkin, H.; Prudent, N. *Tetrahedron Lett.* **1968**, 2199-204. (b) Cherest, M.; Felkin, H. *Tetrahedron Lett.* **1968**, 2205-8.

163. (a) Anh, N.T.; Eisenstein, O. *Nouv. J. Chim.* **1977**, *1*, 61-70. (b) Anh, N.T. *Top. Curr. Chem.* **1980**, *88*, 145-62.

164. For more recent analyses of this concept, see: (a) Wu, Y-D.; Tucker, J.A.; Houk, K.N. *J. Am. Chem. Soc.* **1991**, *113*, 5018-27. (b) Frenking, G.; Köhler, K.F.; Reetz, M.T. *Angew. Chem., Int. Ed. Engl.* **1991**, *30*, 1146-9. (c) Wu, Y-D.; Houk, K.N. *Angew. Chem., Int. Ed. Engl.* **1992**, *31*, 1019-21.

165. (a) Brook, M.A. *Silicon in Organic, Organometallic, and Polymer Chemistry* John Wiley & Sons, New York, 2000, p. 198-203. (b) Williams, R.V.; Gadgil, V.R.; Kamlesh, C. *J. Org. Chem.* **1998**, *63*, 3302-9. (c) Jenner, M.R.; Khan, R. *J. Chem. Soc., Chem. Commun.* **1980**, 50-1

166. For examples of free-standing cyclohexenol X-ray crystal structures see: (a) Knapp, S.; Sebastian, M.J.; Ramanathan, H.; Bharaduraj, P.; Potenza, J.A. *Tetrahedron*, **1986**, *42*, 3405-10. (b) Roush, W.R.; Brown, B.B. *J. Org. Chem.* **1993**, *58*, 2151-61. (c) Metz, P.; Meiners, U.; Froehlich, R.; Grehl, M. *J. Org. Chem.* **1994**, *59*, 3687-9. (d) Magnus, P.; Tavares, F.; Westwood, N. *Tetrahedron Lett.* **1997**, *38*, 1341-4. (e) Kohrt, J.T.; Gu, J.-X.; Johnson, C.R. *J. Org. Chem.* **1998**, *63*, 5088-93. (f) Batey, R.A.; Thadani, A.N.; Lough, A.J. *J. Am. Chem. Soc.* **1999**, *121*, 450-1.

167. Bellucci, G.; Berti, G.; Colapietro, M.; Spagna, R.; Zambonelli, L. *J. Chem. Soc. Perkin Trans. 2* **1976**, 1213-8.

168. Columbus, I.; Hoffman, R.E.; Biali, S.E. *J. Am. Chem. Soc.* **1996**, *118*, 6890-6.

169. Golan, O.; Cohen, S.; Biali, S.E. *J. Org. Chem.* **1999**, *64*, 6505-7.

170. Dieks, H.; Senge, M. O.; Kirste, B.; Kurreck, H. *J. Org. Chem.* **1997**, *62*, 8666-80.

171. Sara, A.N. *J. Organomet. Chem.* **1973**, *47*, 331-6.

172. Stolow, R.D. *J. Am. Chem. Soc.* **1961**, *83*, 2592-3.

173. Petrov, A.D.; Nikishin, G.I. *Zhurn. Obshch. Khim.* **1956**, *26*, 1233-9.

174. Wen, T.-B.; Kang, B.-S.; Su, C.-Y.; Wu, D.-X.; Wang, L.-G.; Liao, S.; Liu, H.-Q. *Bull. Chem. Soc. Jpn.* **1998**, *71*, 2339-43.

175. (a) Tsukasa, M.; Hiroyuki, A.; Masahiro, S. *J. Chem. Soc., Dalt. Trans.* **2002**, 2536-40. (b) Gomez-Carrera, A.; Mena, M.; Royo, P.; Serrano, R. *J. Organomet. Chem.* **1986**, *315*, 329-35.

176. (a) El Amouri, H; Vaissermann, J.; Besace, Y.; Vollhardt, K.P.C.; Bell, G.E. *Organometallics*, **1993**, *12*, 605-9. (b) Meyer, A.; McCabe, D.J.; Curtis, M.D. *Organometallics* **1987**, *6*, 1491-8. (c) Barinov, I.V.; Reutov, O.A.; Polyakov, A.V.; Yanovsky, A.I.; Struchkov, Yu.T. *J. Organomet. Chem.* **1991**, *418*, C24-7. (d) El Amouri, H.; Besace, Y.; Vaissermann, J.; Jaouen, G.; McGlinchey, M.J. *Organometallics*, **1994**, *13*, 4426-30.

177. Perrin, D.D.; Armarego, W.L.F.; Perrin, D.R. In *Purification of Laboratory Chemicals, 2nd Ed.*, Permagon Press, Elmsford, New York, **1980**.

178. SMART, Release 5.611, Bruker AXS Inc., Madison, WI 53711, 2000.

179. SAINT, Release 6.02a, Bruker AXS Inc., Madison, WI 53711, 2000.

180. Sheldrick, G.M. SADABS, Bruker AXS Inc., Madison, WI 53711, 2000.

181. Sheldrick, G.M. SHELXTL, Version 5.1, Bruker AXS Inc., Madison, WI 53711, 1998.

182. Sparks, R. *GEMINI* Autoindexing Program for Twinned Crystals, version 1.01, Bruker AXS Inc., Madison WI 53711, 1999.

183. Spek, A.L. *PLATON*, Program for the Automated Analysis of Molecular Geometry, Version 200296, University of Utrecht, Netherlands, 1996.

184. Olah, G.A.; Berrier, A.L.; Field, L.D.; Prakash, G.K.S. *J. Am. Chem. Soc.* **1982**, *104*, 1349-55.

185. Ruffolo, R.; Kainz, S.; Gupta, H.K.; Brook, M.A.; McGlinchey, M.J. *J. Organomet Chem.* **1997**, *547*, 217-226.

186. Krüerke, U.; Hübel, W.; Vanhee, G. *Chem. Ber.* **1961**, *94*, 2829-56.

187. Previously synthesized from heating $Hg(CHBrSiMe_3)_2$ and $HCCo_3(CO)_9$ in benzene at reflux, and characterized by ^1H NMR, melting point and elemental analysis: Seyferth, D.; Hallgren, J.E.; Spohn, R.J.; Williams, G.H.; Nestle, M.O.; Hung, P.L.K. *J. Organomet. Chem.* **1974**, *65*, 99-118.

188. Cooper, M.A.; Lucas, M.A.; Taylor, J.M.; Ward, D.; Williamson, N.M. *Synthesis* **2001**, *4*, 621-5.

189. a) Buchmeiser, M.; Schottenberger, H. *Organometallics* **1993**, *12*, 2472-7. b) Schottenberger, H.; Wurst, K.; Buchmeiser, M. *J. Organomet. Chem.* **1999**, *584*, 301-9.

190. Yoshimatsu, M.; Fuseya, T. *Chem. Pharm. Bull.* **1996**, *44*, 1954-7.

191. The clusters **11** and **12** have been reported previously, but no spectroscopic or structural data are available: Daly, S.M.; Armstrong, R.W. *Tetrahedron Lett.* **1989**, *30*, 5713-6.

Appendix: X-ray Crystallographic Data

Table A1: Crystal data and structure refinement for **33**.

Empirical formula	C24 H11 Co3 O9	
Formula weight	620.12	
Temperature	197(2) K	
Wavelength	0.71073 Å	
Crystal system	Monoclinic	
Space group	C2/c	
Unit cell dimensions	a = 16.793(4) Å	α= 90°.
	b = 7.874(2) Å	β= 96.923(4)°.
	c = 36.834(8) Å	γ= 90°.
Volume	4834.6(19) $Å^3$	
Z	8	
Density (calculated)	1.704 Mg/m^3	
Absorption coefficient	2.086 mm^{-1}	
F(000)	2464	
Crystal size	.08 x .28 x .34 mm^3	
θ range for data collection	1.11 to 24.99°.	
Index ranges	$-20\leq h\leq 21$, $-10\leq k\leq 10$, $-46\leq l\leq 47$	
Reflections collected	16663	
Independent reflections	4236 [R(int) = 0.1102]	
Absorption correction	SADABS	
Refinement method	Full-matrix least-squares on F^2	
Data / restraints / parameters	4195 / 0 / 326	
Goodness-of-fit on F^2	1.008	
Final R indices [$I>2\sigma(I)$]	R1 = 0.0612, wR2 = 0.1294	
R indices (all data)	R1 = 0.1109, wR2 = 0.1546	
Extinction coefficient	0.00078(12)	
Largest diff. peak and hole	0.715 and -0.581 $e.Å^{-3}$	
Ratio of min/max apparent transmission	0.503387	

Table B1: Crystal data and structure refinement for **39**.

Empirical formula	C26 H19 Co2 F O6 Si	
Formula weight	592.36	
Temperature	173(2) K	
Wavelength	0.71073 Å	
Crystal system	Monoclinic	
Space group	P2(1)/n	
Unit cell dimensions	a = 8.624(2) Å	α= 90°.
	b = 20.573(5) Å	β= 95.017(4)°.
	c = 14.556(4) Å	γ= 90°.
Volume	2572.6(11) $Å^3$	
Z	4	
Density (calculated)	1.529 Mg/m^3	
Absorption coefficient	1.382 mm^{-1}	
F(000)	1200	
Crystal size	0.10 x 0.16 x 0.28 mm^3	
θ range for data collection	1.72 to 27.00°.	
Index ranges	$-11 \le h \le 11$, $-23 \le k \le 26$, $-18 \le l \le 17$	
Reflections collected	22551	
Independent reflections	5615 [R(int) = 0.0608]	
Completeness to θ = 27.00°	100.0 %	
Absorption correction	Empirical (SADABS)	
Refinement method	Full-matrix least-squares on F^2	
Data / restraints / parameters	5615 / 0 / 402	
Goodness-of-fit on F^2	1.010	
Final R indices [$I>2\sigma(I)$]	R1 = 0.0389, wR2 = 0.0658	
R indices (all data)	R1 = 0.0718, wR2 = 0.0742	
Extinction coefficient	0.00005(15)	
Largest diff. peak and hole	0.368 and -0.278 $e.Å^{-3}$	
Ratio of min/max apparent transmission	0.878006	

Table C1: Crystal data and structure refinement for **42**.

Empirical formula	C26 H22 Co2 O8 Si	
Formula weight	608.39	
Temperature	173(2) K	
Wavelength	0.71073 Å	
Crystal system	Monoclinic	
Space group	P2(1)/c	
Unit cell dimensions	a = 20.445(7) Å	α= 90°.
	b = 10.233(3) Å	β= 105.938(5)°.
	c = 27.202(9) Å	γ= 90°.
Volume	5472(3) $Å^3$	
Z	8	
Density (calculated)	1.477 Mg/m^3	
Absorption coefficient	1.302 mm^{-1}	
F(000)	2480	
Crystal size	.03 x .17 x .20 mm^3	
θ range for data collection	1.04 to 23.75°.	
Index ranges	$-23 \le h \le 21$, $-11 \le k \le 11$, $-30 \le l \le 30$	
Reflections collected	35492	
Independent reflections	8346 [R(int) = 0.1443]	
Completeness to θ = 23.75°	100.0 %	
Absorption correction	Empirical (SADABS)	
Refinement method	Full-matrix least-squares on F^2	
Data / restraints / parameters	8346 / 243 / 834	
Goodness-of-fit on F^2	0.975	
Final R indices [$I>2\sigma(I)$]	R1 = 0.0607, wR2 = 0.0762	
R indices (all data)	R1 = 0.1486, wR2 = 0.0945	
Extinction coefficient	0.00020(4)	
Largest diff. peak and hole	0.425 and -0.377 $e.Å^{-3}$	
Ratio of min/max apparent transmission	0.797769	

Table D1: Crystal data and structure refinement for **43**.

Empirical formula	C24 H16 Co2 O8	
Formula weight	550.23	
Temperature	197(2) K	
Wavelength	0.71073 Å	
Crystal system	Tetragonal	
Space group	P-42(1)c	
Unit cell dimensions	a = 22.489(5) Å	α= 90°.
	b = 22.489(5) Å	β= 90°.
	c = 9.846(3) Å	γ= 90°.
Volume	4980(2) $Å^3$	
Z	8	
Density (calculated)	1.468 Mg/m^3	
Absorption coefficient	1.376 mm^{-1}	
F(000)	2224	
Crystal size	.02 x .04 x .25 mm^3	
θ range for data collection	1.28 to 24.99°.	
Index ranges	$-26 \le h \le 26$, $-26 \le k \le 26$, $-11 \le l \le 11$	
Reflections collected	37626	
Independent reflections	4385 [R(int) = 0.1088]	
Completeness to θ = 24.99°	100.0 %	
Absorption correction	Empirical (SADABS)	
Refinement method	Full-matrix least-squares on F^2	
Data / restraints / parameters	4385 / 0 / 372	
Goodness-of-fit on F^2	1.077	
Final R indices [$I>2\sigma(I)$]	R1 = 0.0394, wR2 = 0.0686	
R indices (all data)	R1 = 0.0856, wR2 = 0.0835	
Absolute structure parameter	0.00(2)	
Extinction coefficient	0.00036(7)	
Largest diff. peak and hole	0.328 and -0.311 $e.Å^{-3}$	
Ratio of min/max apparent transmission	0.866793	

Table E1: Crystal data and structure refinement for **77**.

Empirical formula	C21 H19 Co3 O10	
Formula weight	608.15	
Temperature	299(2) K	
Wavelength	0.71073 Å	
Crystal system	Triclinic	
Space group	P1	
Unit cell dimensions	a = 7.761(4) Å	α= 90.486(14)°.
	b = 12.739(7) Å	β= 106.479(12)°.
	c = 13.332(8) Å	γ= 91.064(18)°.
Volume	1263.6(13) $Å^3$	
Z	2	
Density (calculated)	1.598 Mg/m^3	
Absorption coefficient	1.996 mm^{-1}	
F(000)	612	
Crystal size	.03 x 0.1 x .17 mm^3	
θ range for data collection	1.59 to 25.00°.	
Index ranges	$-9 \leq h \leq 8$, $-15 \leq k \leq 15$, $-15 \leq l \leq 15$	
Reflections collected	9539	
Independent reflections	6746 [R(int) = 0.0656]	
Completeness to θ = 25.00°	99.6 %	
Absorption correction	Empirical (SADABS)	
Refinement method	Full-matrix least-squares on F^2	
Data / restraints / parameters	6746 / 69 / 425	
Goodness-of-fit on F^2	0.988	
Final R indices [$I>2\sigma(I)$]	R1 = 0.0567, wR2 = 0.0872	
R indices (all data)	R1 = 0.1439, wR2 = 0.1105	
Absolute structure parameter	0.08(4)	
Largest diff. peak and hole	0.492 and -0.424 $e.Å^{-3}$	
Ratio of min/max apparent transmission	0.892549	

Table F1: Crystal data and structure refinement for **112**.

Empirical formula	C31 H22 O	
Formula weight	410.49	
Temperature	197(2) K	
Wavelength	0.71073 Å	
Crystal system	Orthorhombic	
Space group	P2(1)2(1)2(1)	
Unit cell dimensions	a = 5.9605(15) Å	α= 90°.
	b = 12.804(3) Å	β= 90°.
	c = 28.760(8) Å	γ= 90°.
Volume	2194.9(10) $Å^3$	
Z	4	
Density (calculated)	1.242 Mg/m^3	
Absorption coefficient	0.073 mm^{-1}	
F(000)	864	
Crystal size	.04 x .05 x .40 mm^3	
θ range for data collection	1.42 to 25.00°.	
Index ranges	$-7 \leq h \leq 7$, $-16 \leq k \leq 15$, $-35 \leq l \leq 34$	
Reflections collected	16498	
Independent reflections	3849 [R(int) = 0.0927]	
Absorption correction	SADABS	
Refinement method	Full-matrix least-squares on F^2	
Data / restraints / parameters	3835 / 0 / 378	
Goodness-of-fit on F^2	1.015	
Final R indices [$I>2\sigma(I)$]	R1 = 0.0514, wR2 = 0.0909	
R indices (all data)	R1 = 0.0960, wR2 = 0.1048	
Absolute structure parameter	1.14(275)	
Extinction coefficient	0.0229(17)	
Largest diff. peak and hole	0.193 and -0.171 $e.Å^{-3}$	
Ratio of min/max apparent transmission	0.549239	

Table G1: Crystal data and structure refinement for **120**.

Empirical formula	C24 H11 Co3 O9	
Formula weight	620.12	
Temperature	173(2) K	
Wavelength	0.71073 Å	
Crystal system	Monoclinic	
Space group	P2(1)/n	
Unit cell dimensions	a = 8.702(6) Å	α= 90°.
	b = 30.56(2) Å	β= 98.679(12)°.
	c = 26.752(19) Å	γ= 90°.
Volume	7032(9) $Å^3$	
Z	12	
Density (calculated)	1.757 Mg/m^3	
Absorption coefficient	2.151 mm^{-1}	
F(000)	3696	
Crystal size	0.35 x 0.08 x 0.03 mm^3	
θ range for data collection	1.54 to 20.25°.	
Index ranges	$-8 \le h \le 8$, $-29 \le k \le 29$, $-26 \le l \le 26$	
Reflections collected	31554	
Independent reflections	6790 [R(int) = 0.1742]	
Completeness to θ = 20.25°	99.7 %	
Absorption correction	SADABS	
Refinement method	Full-matrix least-squares on F^2	
Data / restraints / parameters	6790 / 198 / 839	
Goodness-of-fit on F^2	1.147	
Final R indices [$I>2\sigma(I)$]	R1 = 0.1098, wR2 = 0.2429	
R indices (all data)	R1 = 0.1650, wR2 = 0.2754	
Extinction coefficient	0.0106(7)	
Largest diff. peak and hole	1.867 and -1.048 $e.Å^{-3}$	
Ratio of min/max apparent transmission	0.752301	

Table H1: Crystal data and structure refinement for **121**.

Empirical formula	C48 H42 Si2	
Formula weight	675.00	
Temperature	173(2) K	
Wavelength	0.71073 Å	
Crystal system	Monoclinic	
Space group	P2(1)/c	
Unit cell dimensions	a = 13.467(6) Å	α= 90°.
	b = 16.297(7) Å	β= 95.692(8)°.
	c = 8.923(4) Å	γ= 90°.
Volume	1948.7(14) $Å^3$	
Z	2	
Density (calculated)	1.150 Mg/m^3	
Absorption coefficient	0.123 mm^{-1}	
F(000)	716	
Crystal size	.1 x .3 x .5 mm^3	
θ range for data collection	1.97 to 25.00°.	
Index ranges	-16≤h≤15, -19≤k≤19, -9≤l≤10	
Reflections collected	14547	
Independent reflections	3424 [R(int) = 0.0522]	
Completeness to θ = 25.00°	99.9 %	
Absorption correction	SADABS	
Refinement method	Full-matrix least-squares on F^2	
Data / restraints / parameters	3424 / 36 / 296	
Goodness-of-fit on F^2	1.020	
Final R indices [I>2σ(I)]	R1 = 0.0651, wR2 = 0.1168	
R indices (all data)	R1 = 0.1189, wR2 = 0.1388	
Extinction coefficient	0.0054(7)	
Largest diff. peak and hole	0.343 and -0.305 $e.Å^{-3}$	
Ratio of min/max apparent transmission	0.916917	

Table I1: Crystal data and structure refinement for **124**.

Empirical formula	C60 H42 Co4 O14 Si2	
Formula weight	1278.84	
Temperature	173(2) K	
Wavelength	0.71073 Å	
Crystal system	Triclinic	
Space group	P-1	
Unit cell dimensions	a = 10.516(5) Å	α= 86.312(8)°.
	b = 12.051(6) Å	β= 76.860(8)°.
	c = 12.382(6) Å	γ= 66.034(8)°.
Volume	1395.6(12) $Å^3$	
Z	1	
Density (calculated)	1.522 Mg/m^3	
Absorption coefficient	1.278 mm^{-1}	
F(000)	650	
Crystal size	0.45 x 0.40 x 0.30 mm^3	
θ range for data collection	1.69 to 27.50°.	
Index ranges	-13≤h≤12, -15≤k≤14, -16≤l≤15	
Reflections collected	12858	
Independent reflections	6305 [R(int) = 0.0315]	
Completeness to θ = 27.50°	98.3 %	
Absorption correction	SADABS	
Refinement method	Full-matrix least-squares on F^2	
Data / restraints / parameters	6305 / 0 / 446	
Goodness-of-fit on F^2	1.009	
Final R indices [I>2σ(I)]	R1 = 0.0323, wR2 = 0.0673	
R indices (all data)	R1 = 0.0536, wR2 = 0.0759	
Extinction coefficient	0.0005(4)	
Largest diff. peak and hole	0.357 and -0.313 $e.Å^{-3}$	
Ratio of min/max apparent transmission	0.842652	

Table J1: Crystal data and structure refinement for **125**.

Empirical formula	C50 H34 Co4 O14 Si2	
Formula weight	1150.67	
Temperature	173(2) K	
Wavelength	0.71073 Å	
Crystal system	Orthorhombic	
Space group	Pbca	
Unit cell dimensions	a = 22.17(4) Å	α= 90°.
	b = 13.24(3) Å	β= 90°.
	c = 16.93(3) Å	γ = 90°.
Volume	4969(17) $Å^3$	
Z	4	
Density (calculated)	1.538 Mg/m^3	
Absorption coefficient	1.426 mm^{-1}	
F(000)	2328	
Crystal size	0.20 x 0.10 x 0.02 mm^3	
θ range for data collection	1.84 to 22.50°.	
Index ranges	-23≤h≤23, -13≤k≤14, -18≤l≤17	
Reflections collected	26564	
Independent reflections	3244 [R(int) = 0.1512]	
Completeness to θ = 22.50°	100.0 %	
Absorption correction	SADABS	
Refinement method	Full-matrix least-squares on F^2	
Data / restraints / parameters	3244 / 0 / 323	
Goodness-of-fit on F^2	1.129	
Final R indices [I>2σ(I)]	R1 = 0.0847, wR2 = 0.1172	
R indices (all data)	R1 = 0.1315, wR2 = 0.1306	
Extinction coefficient	0.00021(8)	
Largest diff. peak and hole	0.383 and -0.344 $e.Å^{-3}$	
Ratio of min/max apparent transmission	0.563115	

Table K1: Crystal data and structure refinement for **130**.

Empirical formula	C68 H80 Co8 O28 Si4	
Formula weight	1929.12	
Temperature	153(2) K	
Wavelength	0.71073 Å	
Crystal system	Monoclinic	
Space group	Pc	
Unit cell dimensions	a = 11.5638(3) Å	α= 90°.
	b = 11.6426(2) Å	β= 91.52(1)°.
	c = 31.5342(4) Å	γ= 90°.
Volume	4244.05(14) $Å^3$	
Z	8	
Density (calculated)	1.510 Mg/m^3	
Absorption coefficient	1.652 mm^{-1}	
F(000)	1968	
Crystal size	0.08 x 0.20 x 0.20 mm^3	
θ range for data collection	1.29 to 24.00°.	
Index ranges	$-13 \le h \le 14$, $-13 \le k \le 14$, $-40 \le l \le 39$	
Reflections collected	28830	
Independent reflections	12353 [R(int) = 0.0806]	
Refinement method	Full-matrix least-squares on F^2	
Data / restraints / parameters	12321 / 20 / 1162	
Goodness-of-fit on F^2	0.995	
Final R indices [$I>2\sigma(I)$]	R1 = 0.0507, wR2 = 0.0632	
R indices (all data)	R1 = 0.0932, wR2 = 0.0720	
Absolute structure parameter	0.042(11)	
Extinction coefficient	0.00014(3)	
Largest diff. peak and hole	0.466 and -0.403 $e.Å^{-3}$	
Max. and Min. effective transmission	0.893893 and 0.778849	

Table L1: Crystal data and structure refinement for **135**.

Empirical formula	C21 H28 Co2 O7 Si	
Formula weight	538.38	
Temperature	148(2) K	
Wavelength	0.71073 Å	
Crystal system	Monoclinic	
Space group	$P2_1/c$	
Unit cell dimensions	a = 15.1555(4) Å	α= 90°.
	b = 11.7868(7) Å	β= 94.730(2)°.
	c = 14.1365(8) Å	γ= 90°.
Volume	2516.7(2) $Å^3$	
Z	4	
Density (calculated)	1.421 Mg/m^3	
Absorption coefficient	1.401 mm^{-1}	
F(000)	1112	
Crystal size	0.05 x 0.10 x 0.25 mm^3	
θ range for data collection	1.35 to 25.00°.	
Index ranges	$-17 \leq h \leq 19$, $-15 \leq k \leq 15$, $-18 \leq l \leq 16$	
Reflections collected	18660	
Independent reflections	4430 [R(int) = 0.0778]	
Refinement method	Full-matrix least-squares on F^2	
Data / restraints / parameters	4407 / 0 / 362	
Goodness-of-fit on F^2	0.950	
Final R indices [$I>2\sigma(I)$]	R1 = 0.0397, wR2 = 0.0590	
R indices (all data)	R1 = 0.1000, wR2 = 0.0710	
Extinction coefficient	0.00064(14)	
Largest diff. peak and hole	0.300 and -0.315 $e.Å^{-3}$	
Max. and Min. effective transmission	0.870320 and 0.753886	

Table M1: Crystal data and structure refinement for **136**.

Empirical formula	C21 H28 Co2 O7 Si	
Formula weight	538.38	
Temperature	148(2) K	
Wavelength	0.71073 Å	
Crystal system	Monoclinic	
Space group	$P2_1$	
Unit cell dimensions	a = 8.617(6) Å	α= 90°.
	b = 16.526(9) Å	β= 94.938(15)°.
	c = 8.767(6) Å	γ= 90°.
Volume	1243.8(14) $Å^3$	
Z	2	
Density (calculated)	1.438 Mg/m^3	
Absorption coefficient	1.418 mm^{-1}	
F(000)	556	
Crystal size	0.04 x 0.22 x 0.34 mm^3	
θ range for data collection	2.33 to 25.00°.	
Index ranges	$-11 \le h \le 11$, $-21 \le k \le 21$, $-11 \le l \le 11$	
Reflections collected	10317	
Independent reflections	4295 [R(int) = 0.0358]	
Refinement method	Full-matrix least-squares on F^2	
Data / restraints / parameters	4293 / 1 / 365	
Goodness-of-fit on F^2	0.974	
Final R indices [$I>2\sigma(I)$]	R1 = 0.0381, wR2 = 0.0699	
R indices (all data)	R1 = 0.0570, wR2 = 0.0751	
Absolute structure parameter	0.00(2)	
Extinction coefficient	0.0010(7)	
Largest diff. peak and hole	0.323 and -0.333 $e.Å^{-3}$	
Max. and Min. effective transmission	0.828674 and 0.653084	

Table N1: Crystal data and structure refinement for **142**.

Empirical formula	C46 H40 O2 Si2	
Formula weight	680.96	
Temperature	148(2) K	
Wavelength	0.71073 Å	
Crystal system	Triclinic	
Space group	P-1	
Unit cell dimensions	a = 9.406(4) Å	α= 79.557(9)°.
	b = 9.501(4) Å	β= 81.686(9)°.
	c = 12.006(5) Å	γ= 61.650(8)°.
Volume	926.5(7) $Å^3$	
Z	1	
Density (calculated)	1.220 Mg/m^3	
Absorption coefficient	0.134 mm^{-1}	
F(000)	360	
Crystal size	0.12 x 0.14 x 0.20 mm^3	
θ range for data collection	1.73 to 23.32°.	
Index ranges	-10≤h≤10, -10≤k≤10, -13≤l≤12	
Reflections collected	6091	
Independent reflections	2661 [R(int) = 0.0668]	
Refinement method	Full-matrix least-squares on F^2	
Data / restraints / parameters	2661 / 0 / 307	
Goodness-of-fit on F^2	0.994	
Final R indices [I>2σ(I)]	R1 = 0.0593, wR2 = 0.1278	
R indices (all data)	R1 = 0.1026, wR2 = 0.1464	
Extinction coefficient	0.0229(46)	
Largest diff. peak and hole	0.355 and -0.255 $e.Å^{-3}$	
Max. and Min effective transmission	0.982099 and 0.620956	

Table O1: Crystal data and structure refinement for **144**.

Empirical formula	C59 H42 Cl2 Co4 O14 Si2	
Formula weight	1337.73	
Temperature	148(2) K	
Wavelength	0.71073 Å	
Crystal system	Triclinic	
Space group	P-1	
Unit cell dimensions	a = 13.309(5) Å	α= 110.403(7)°.
	b = 14.193(5) Å	β= 105.961(7)°.
	c = 17.751(7) Å	γ= 100.478(8)°.
Volume	2874.5(19) $Å^3$	
Z	2	
Density (calculated)	1.546 Mg/m^3	
Absorption coefficient	1.334 mm^{-1}	
F(000)	1356	
Crystal size	0.10 x 0.20 x 0.28 mm^3	
θ range for data collection	1.32 to 21.50°.	
Index ranges	$-17 \le h \le 17$, $-18 \le k \le 18$, $-22 \le l \le 22$	
Reflections collected	19969	
Independent reflections	19969 [R(int) = 0.0000]	
Refinement method	Full-matrix least-squares on F^2	
Data / restraints / parameters	19894 / 0 / 389	
Goodness-of-fit on F^2	0.915	
Final R indices [$I>2\sigma(I)$]	R1 = 0.0856, wR2 = 0.1977	
R indices (all data)	R1 = 0.1664, wR2 = 0.2335	
Extinction coefficient	0.0060(11)	
Largest diff. peak and hole	1.092 and -0.891 $e.Å^{-3}$	

Table P1: Crystal data and structure refinement for **145**.

Empirical formula	C58 H40 Co4 O14 Si2	
Formula weight	1252.80	
Temperature	148(2) K	
Wavelength	0.71073 Å	
Crystal system	Monoclinic	
Space group	C2/c	
Unit cell dimensions	a = 17.529(19) Å	α= 90°.
	b = 21.222(23) Å	β= 119.14(2)°.
	c = 17.686(19) Å	γ= 90°.
Volume	5746.8(107) $Å^3$	
Z	4	
Density (calculated)	1.448 Mg/m^3	
Absorption coefficient	1.239 mm^{-1}	
F(000)	2544	
Crystal size	.05 x 0.10 x .23 mm^3	
θ range for data collection	1.64 to 23.26°.	
Index ranges	$-17 \le h \le 19$, $-22 \le k \le 23$, $-18 \le l \le 19$	
Reflections collected	18840	
Independent reflections	4135 [R(int) = 0.0924]	
Absorption correction	SADABS	
Refinement method	Full-matrix least-squares on F^2	
Data / restraints / parameters	4135 / 1 / 373	
Goodness-of-fit on F^2	1.023	
Final R indices [$I>2\sigma(I)$]	R1 = 0.0547, wR2 = 0.0941	
R indices (all data)	R1 = 0.1197, wR2 = 0.1125	
Extinction coefficient	0.00013(4)	
Largest diff. peak and hole	0.314 and -0.360 $e.Å^{-3}$	
Max. and Min effective transmission	0.886841 0.839571	

Table Q1: Crystal data and structure refinement for **149**.

Empirical formula	C28 H28 Co4 O14 Si2	
Formula weight	880.40	
Temperature	148(2) K	
Wavelength	0.71073 Å	
Crystal system	Triclinic	
Space group	P-1	
Unit cell dimensions	a = 15.1645(6) Å	α= 85.838(2)°.
	b = 15.2359(9) Å	β= 65.577(3)°.
	c = 17.8463(11) Å	γ= 84.452(3)°.
Volume	3734.3(4) $Å^3$	
Z	4	
Density (calculated)	1.566 Mg/m^3	
Absorption coefficient	1.870 mm^{-1}	
F(000)	1776	
Crystal size	.02 x .10 x .12 mm^3	
θ range for data collection	1.25 to 20.00°.	
Index ranges	-15≤h≤15, -15≤k≤15, -18≤l≤18	
Reflections collected	18212	
Independent reflections	6972 [R(int) = 0.1871]	
Absorption correction	None	
Refinement method	Full-matrix least-squares on F^2	
Data / restraints / parameters	6878 / 0 / 556	
Goodness-of-fit on F^2	0.960	
Final R indices [I>2σ(I)]	R1 = 0.0737, wR2 = 0.0883	
R indices (all data)	R1 = 0.2024, wR2 = 0.1194	
Extinction coefficient	0.00020(6)	
Largest diff. peak and hole	0.576 and -0.590 $e.Å^{-3}$	
Ratio of min to max apparent transmission	0.817396	

Table R1: Crystal data and structure refinement for **150**.

Empirical formula	C22 H28 Co2 O8 Si2	
Formula weight	594.48	
Temperature	148(2) K	
Wavelength	0.71073 Å	
Crystal system	Monoclinic	
Space group	$P2_1/c$	
Unit cell dimensions	a = 12.7652(6) Å	α= 90°.
	b = 11.3770(5) Å	β= 98.176(2)°.
	c = 18.4035(4) Å	γ= 90°.
Volume	2645.6(2) $Å^3$	
Z	4	
Density (calculated)	1.493 Mg/m^3	
Absorption coefficient	1.387 mm^{-1}	
F(000)	1224	
Crystal size	0.14 x 0.24 x 0.34 mm^3	
θ range for data collection	1.61 to 25.00°.	
Index ranges	-15≤h≤16, -12≤k≤14, -23≤l≤23	
Reflections collected	19761	
Independent reflections	4666 [R(int) = 0.0496]	
Refinement method	Full-matrix least-squares on F^2	
Data / restraints / parameters	4662 / 0 / 392	
Goodness-of-fit on F^2	0.929	
Final R indices [I>2σ(I)]	R1 = 0.0289, wR2 = 0.0506	
R indices (all data)	R1 = 0.0548, wR2 = 0.0553	
Extinction coefficient	0.00043(11)	
Largest diff. peak and hole	0.269 and -0.278 $e.Å^{-3}$	
Max. and Min effective transmission	0.745773 and 0.668449	

Table S1: Crystal data and structure refinement for **151**.

Empirical formula	C28 H26 Co4 O13 Si2	
Formula weight	862.39	
Temperature	173(2) K	
Wavelength	0.71073 Å	
Crystal system	Monoclinic	
Space group	P2(1)/n	
Unit cell dimensions	a = 16.825(5) Å	α= 90°.
	b = 23.538(7) Å	β= 91.089(7)°.
	c = 18.008(5) Å	γ = 90°.
Volume	7130(4) $Å^3$	
Z	8	
Density (calculated)	1.607 Mg/m^3	
Absorption coefficient	1.955 mm^{-1}	
F(000)	3472	
Crystal size	0.25 x 0.15 x 0.10 mm^3	
θ range for data collection	1.42 to 21.50°.	
Index ranges	-16≤h≤17, -24≤k≤24, -10≤l≤18	
Reflections collected	28401	
Independent reflections	8189 [R(int) = 0.1945]	
Completeness to θ = 21.50°	100.0 %	
Absorption correction	SADABS	
Refinement method	Full-matrix least-squares on F^2	
Data / restraints / parameters	8189 / 0 / 570	
Goodness-of-fit on F^2	1.026	
Final R indices [I>2σ(I)]	R1 = 0.0904, wR2 = 0.1836	
R indices (all data)	R1 = 0.1941, wR2 = 0.2226	
Extinction coefficient	0.00084(10)	
Largest diff. peak and hole	1.270 and -0.876 $e.Å^{-3}$	
Ratio of min/max apparent transmission	0.184008	